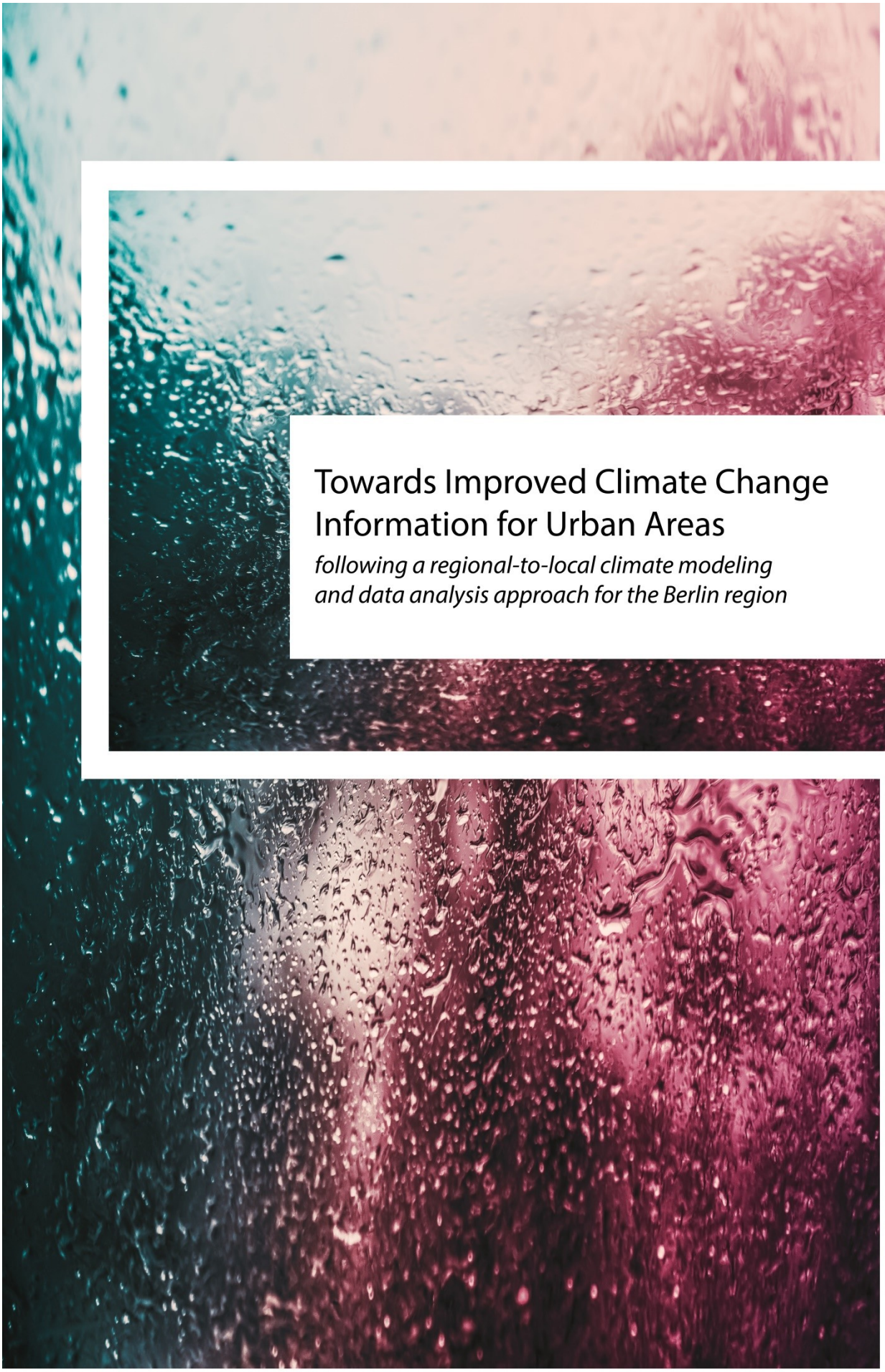

Towards Improved Climate Change Information for Urban Areas

following a regional-to-local climate modeling and data analysis approach for the Berlin region

Gaby S. Langendijk

LEUPHANA
UNIVERSITÄT LÜNEBURG

Towards Improved Climate Change Information for Urban Areas

following a regional-to-local climate modeling and data analysis approach for the Berlin region

Faculty of Sustainability
Leuphana University Lüneburg

Submitted as a requirement for the award of the title of
Doctor of natural science
- Dr. rer. nat -

Approved thesis by
Gaby Sophie Langendijk

Born 02.10.1990 in Haarlem (The Netherlands)

Submitted on: 28.09.2021

Thesis defence on: 22.07.2022

First supervisor and reviewer: Prof. Dr. Brigitte Urban
Second supervisor and reviewer: Prof. Dr. Daniela Jacob
Third reviewer: Prof. Dr. Heiko Paeth

The individual items in the cumulative thesis are published as follows:

Langendijk, G.S., Rechid, D. and Jacob, D., 2019. Urban areas and urban–rural contrasts under climate change: what does the EURO-CORDEX ensemble tell us?—Investigating near surface humidity in Berlin and its surroundings. Atmosphere, 10(12), p.730.

Langendijk, G.S., Rechid, D., Sieck, K. and Jacob, D., 2021. Added value of convection-permitting simulations for understanding future urban humidity extremes: case studies for Berlin and its surroundings. Weather and Climate Extremes, 33, p.100367.

Langendijk, G.S., Rechid, D. and Jacob, D., 2022. Improved models, improved information? Exploring how climate change impacts pollen, influenza, and mold in Berlin and its surroundings. Urban Climate, 43, p.101159.

Year of publication: 2022

Acknowledgements

Here I am, looking back at three-and-a-half years of brain gymnastics, undergoing a grand intellectual challenge: the pursuance of a PhD. It has been enjoyable, strenuous, lonely at times, and it would certainly not have been possible without the support of a core group of people, whom I wish to thank deeply.

Firstly, I want to profoundly thank my main supervisor Daniela Jacob. Foremost, you inspired me to think more creatively, and provided critical feedback on the direction of the research whenever needed, pivotal for sustained progress and the academic performance. Secondly, major thanks to Diana Rechid. Without your continuous rigorous scientific guidance, this accomplishment would not have been attainable.

A special thanks to my partner, Robin Memelink, who got to know me as a PhD candidate, and was always there with me to witness the deep valleys and the high peaks of the PhD track. Who ensured to celebrate each climbed mountain peak (we popped quite some bottles of Sekt), and who reminded me to enjoy the view, instead of to run directly to the next mountain.

I am truly thankful to my parents. You provided the basis for this accomplishment. My mother, Cokky Bentvelsen, for believing in me at all times, and for always being there for me. It means the world to me. My father, Henk Langendijk, who knows what it entails to pursue a PhD. What it means if you complete the challenge - and also what it means if you don't. With a certain worry in his eyes, he would always be there to provide helpful guidance when I needed to manage some of the finest delicate matters of the academic enterprise.

Big thanks to my beloved family, Robbie Langendijk, Barbara Langendijk, Sezayi Arslan, and Odilia Pascoal-Langendijk, Ria Peters, Gerard Memelink, Marissa Memelink, for always showing interest, and support throughout the process.

My friends in Hamburg, the Netherlands, and elsewhere spread around the world, thank you for sharing wonderful moments and for your friendships: Zita Hegger, Eva de Zeeuw, Jet Steinz, Susan Aukema, Jihye Jeong, Jana Harlos, Lianne Hulsebosch, Julien van Son, Rodrigo Valencia, Joana Kollert, Graciela Anivarro, Cristobal Reveco, Wibke Liebhart, Sabine Egerer, Floor Hofman, Francisca Wals, Robbie Parks, Eva van de Born, Tim van der Voort, Nico Perez, Mandy Warning, Joni Beintema, Julius Pröll. You made this period enjoyable – even in the midst of a pandemic.

Thank you to my band members, the music sessions always brought light and inspiration. You could make "lemon days" turn into "the land of blue skies".

A special thanks to Kim, and my boxing gloves. You were there to transform my frustration, tension, and stress into something positive. Without you, I could never have pulled through.

Big thanks to the incredible people from the Young Earth System Scientists (YESS) community, a great community of like-minded scientists with an ambition to contribute actively to shaping the world of science internationally. It has always been a pleasure working with you, as well as to share beautiful moments outside of the working environment.

Lastly, I wish to extend special thanks to Rik Leemans and Boram Lee, for their guidance during my professional career, and who encouraged me early on to conduct this "crazy" PhD.

Abstract

Urban areas are prone to climate change impacts. Simultaneously the world's population increasingly resides in cities. In this light, there is a growing need to equip urban decision makers with evidence-based climate information tailored to their specific context, to adequately adapt to and prepare for future climate change.

To construct climate information high-resolution regional climate models and their projections are pivotal, to provide a better understanding of the unique urban climate and its evolution under climate change. There is a need to move beyond commonly investigated variables, such as temperature and precipitation, to cover a wider breath of possible climate impacts. In this light, the research presented in this thesis is centered around enhancing the understanding about regional-to-local climate change in Berlin and its surroundings, with a focus on humidity. More specifically, following a regional climate modelling and data analysis approach, this research aims to understand the potential of regional climate models, and the possible added value of convection-permitting simulations, to support the development of high-quality climate information for urban regions, to support knowledge-based decision-making.

The first part of the thesis investigates what can already be understood with available regional climate model simulations about future climate change in Berlin and its surroundings, particularly with respect to humidity and related variables. Ten EURO-CORDEX model combinations are analyzed, for the RCP8.5 emission scenario during the time period 1970–2100, for the Berlin region. The results are the first to show an urban-rural humidity contrast under a changing climate, simulated by the EURO-CORDEX ensemble, of around 6 % relative humidity, and a robust enlarging urban drying effect, of approximately 2– 4 % relative humidity, in Berlin compared to its surroundings throughout the 21st century.

The second part explores how crossing spatial scales from 12.5 km to 3 km model grid size affects unprecedented humidity extremes and related variables under future climate conditions for Berlin and its surroundings. Based on the unique HAPPI regional climate model dataset, two unprecedented humidity extremes are identified happening under 1.5 °C and 2 °C global mean warming, respectively SH>0.02 kg/kg and RH<30 %. Employing a double-nesting approach, specifically designed for this study, the two humidity extremes are downscaled to the 12.5 km grid resolution with the regional climate model REMO, and thereafter to the 3 km with the convection-permitting model version of REMO (REMO-NH). The findings indicate that the convection-permitting scale mitigates the SH>0.02 kg/kg moist extreme and intensifies the RH<30 % dry extreme. The multi-variate process analysis shows that the more profound urban drying effect on the convection-permitting resolution is mainly due to better resolving the physical processes related to the land surface scheme and land-atmosphere interactions on the 3 km compared to the 12.5 km grid resolution. The results demonstrate the added value of the convection-permitting resolution to simulate future humidity extremes in the urban-rural context.

The third part of the research investigates the added value of convection-permitting models to simulate humidity related meteorological conditions driving specific climate change impacts, for the Berlin region. Three novel humidity related impact cases are defined for this research: influenza spread and survival; ragweed pollen dispersion; and in-door mold growth. Simulations by the regional climate model REMO are analyzed for the near future (2041–2050) under emission scenario RCP8.5, on the 12.5 km and 3 km grid resolution. The findings show that the change signal reverses on the convection-permitting resolution for the impact cases pollen, and mold (positive and negative). For influenza, the convection-permitting resolution intensifies the decrease of influenza days under climate change. Longer periods of consecutive influenza and mold days are projected

under near-term climate change. The results show the potential of convection-permitting simulations to generate improved information about climate change impacts in urban regions to support decision makers.

Generally, all results show an urban drying effect in Berlin compared to its surroundings for relative and specific humidity under climate change, respectively for the urban-rural contrast throughout the 21st century, for the downscaled future extreme conditions, and for the three humidity related impact cases. Added value for the convection-permitting resolution is found to simulate humidity extremes and the meteorological conditions driving the three impacts cases.

The research makes novel contributions that advance science, through demonstrating the potential of regional climate models, and especially the added value of convection-permitting models, to understand urban-rural humidity contrasts under climate change, supporting the development of knowledge-based climate information for urban regions.

Zusammenfassung

Der Klimawandel hat starke Auswirkungen auf Städte. Gleichzeitig lebt die Weltbevölkerung zunehmend in Städten. Vor diesem Hintergrund besteht ein wachsender Bedarf, städtische Entscheidungsträger mit evidenzbasierten Klimainformationen auszustatten, die auf ihren spezifischen Kontext zugeschnitten sind, um sich an den zukünftigen Klimawandel anzupassen und sich darauf vorzubereiten.

Für die Erstellung von Klimainformationen sind hochauflösende regionale Klimamodelle und ihre Projektionen von zentraler Bedeutung, um ein besseres Verständnis des einzigartigen Stadtklimas und seiner Entwicklung unter dem Einfluss des Klimawandels zu ermöglichen. Es besteht die Notwendigkeit, über die Analyse typischer Variablen wie Temperatur und Niederschlag hinauszugehen, um einen breiteren Bereich möglicher Klimaausfolgen abzudecken. Vor diesem Hintergrund konzentriert sich die in dieser Arbeit vorgestellte Forschung auf die Verbesserung des Verständnisses des regionalen und lokalen Klimawandels in Berlin und seiner Umgebung, mit dem Schwerpunkt auf Luftfeuchtigkeit.

Die vorliegende Doktorarbeit verwendet regionale Klimamodellierungsmethoden und spezielle Datenanalyseverfahren, um das Potenzial regionaler Klimamodelle und den möglichen Mehrwert von konvektionserlaubenden Simulationen zu erforschen und um die Entwicklung hochwertiger Klimainformationen für Städte sowie wissensbasierte Entscheidungen zu unterstützen.

Im ersten Teil der Arbeit wird untersucht, was bereits mit verfügbaren regionalen Klimamodellsimulationen über den zukünftigen Klimawandel in Berlin und Umgebung ermittelt werden kann, insbesondere in Bezug auf Luftfeuchtigkeit und verwandte Variablen. Zehn EURO-CORDEX Modellkombinationen werden für das RCP8.5-Emissionsszenario im Zeitraum 1970-2100 für die Region Berlin analysiert. Die Ergebnisse des EURO-CORDEX Ensembles zeigen ein Stadt-Land-Feuchtedefizit von etwa -6 % relativer Luftfeuchte und eine robuste Zunahme des städtischen Trocknungseffekts von etwa -2 bis -4 % relativer Luftfeuchtigkeit am Ende des 21. Jahrhundert.

Der zweite Teil untersucht, wie sich der Übergang von 12,5 km auf 3 km Modellgittergröße auf außergewöhnliche Feuchtigkeitsextreme und verwandte Variablen unter zukünftigen Klimabedingungen für Berlin und seine Umgebung auswirkt. Basierend auf den regionalen Klimamodellsimulationen des einzigartigen HAPPI-Datensatzes werden zwei Feuchtigkeitsextreme identifiziert, die erst bei einer mittleren Erderwärmung von 1,5 °C bzw. 2 °C auftreten können: jeweils spezifische Feuchte (SH) >0,02 kg/kg und relative Feuchte (RH) <30 %. Unter Verwendung eines speziell für diese Studie entwickelten Double-Nesting-Verfahrens werden die beiden Feuchtigkeitsextreme mit dem regionalen Klimamodell REMO auf 12,5 km Gitterauflösung regional verfeinert und danach mit der konvektionserlaubenden Modellversion von REMO (REMO-NH) auf 3 km Gitterweite lokal weiter verfeinert. Die Ergebnisse zeigen, dass in den konvektionserlaubenden Simulationen die feuchten Extreme (SH > 0,02 kg/kg) abgemildert und das trockene Extreme (RH < 30 %) verstärkt werden. Die multivariate Prozessanalyse zeigt, dass der verstärkte städtische Trocknungseffekt in den hochaufgelösten Simulationen hauptsächlich auf die verbesserte Abbildung von physikalischen Prozessen im Zusammenhang mit dem Landoberflächenmodell und den damit verbundenen Land-Atmosphäre-Wechselwirkungen in den Simulationen mit 3 km Gitterweite im Vergleich zu den 12,5 km Simulationen zurückzuführen ist. Die Ergebnisse zeigen den Mehrwert der konvektionserlaubenden Auflösung für die Simulation zukünftiger Feuchtigkeitsextreme im Stadt-Land-Kontext.

Im dritten Teil der Arbeit wird der Mehrwert konvektionserlaubender Modelle im Hinblick die Bestimmung von feuchtigkeitsbezogene Auswirkungen des Klimawandels in der Region Berlin untersucht. Drei neuartige feuchtigkeitsbezogene Auswirkungen werden speziell für diese Untersuchung definiert: Ausbreitung und Überleben von Influenzaviren; Ambrosia-Pollen-Freisetzung; und Schimmelbildung in Innenräumen. Simulationen des regionalen Klimamodells REMO werden für die nahe Zukunft (2041–2050) für das Emissionsszenario RCP8.5 mit einer Rasterauflösung von 12,5 km und 3 km analysiert. Die Ergebnisse zeigen, dass sich das Änderungssignal für Pollen- und Schimmelausbreitung (positiv und negativ) beim Übergang von 12,5 auf 3 km Auflösung umkehrt. Bei Influenza verstärkt die konvektionserlaubende Auflösung die klimawandelbedingte Abnahme der Influenzatage. In naher Zukunft werden unter Klimawandelbedingungen längere Perioden aufeinanderfolgender Influenza- und Schimmelpilztage erwartet. Die Ergebnisse zeigen das Potenzial konvektionserlaubender Simulationen zur Erstellung verbesserter Informationen über die Auswirkungen des Klimawandels in städtischen Regionen zur Unterstützung von Entscheidungsträgern.

Generell zeigen alle Ergebnisse dieser Arbeit einen klimawandelbedingten städtischen Austrocknungseffekt in Berlin im Vergleich zu seinem Umland sowohl in der relativen- als auch in der spezifischen Luftfeuchte. Dieser ist sichtbar in einem verstärkten RH Stadt-Land-Kontrast am Ende des 21. Jahrhundert, in den herunterskalierten zukünftigen Extrembedingungen und in den drei untersuchten feuchtebezogenen Klimafolgen. Die konvektionserlaubende Auflösung zeigt einen Mehrwert bei der Simulation von Feuchtigkeitsextremen und den meteorologischen Bedingungen für die drei ausgewählten Klimafolgen. Die Ergebnisse dieser Arbeit verdeutlichen das Potenzial regionaler Klimamodelle und insbesondere den Mehrwert von konvektionserlaubenden regionalen Klimamodellen für das Verständnis der Feuchtigkeitsunterschiede zwischen Stadt und Umland unter den Bedingungen des Klimawandels und für die Erstellung wissensbasierter Klimainformationen für städtische Regionen.

Contents

List of papers

Paper 1

Urban Areas and Urban-Rural Contrasts under Climate Change: What Does the EURO-CORDEX Ensemble Tell Us? — Investigating near Surface Humidity in Berlin and Its Surroundings
Gaby S. Langendijk, Diana Rechid, Daniela Jacob

Published: Atmosphere (IF: 3.110), 2019, 10(12), 730.
Doi: https://doi.org/10.3390/atmos10120730
Citations: 23
Cited in IPCC AR6, WGI Report (IPCC, 2021)

Referenced in the German news, following a press release by the German Press Agency (DPA):
- *"Studie: Klimawandel macht Städte heißer und trockener"* (RND, 2021)
- *"Besonders in den Städten wird es immer heißer"* (Welt, 2021)
- *"Mehr Hitze in Städten befürchtet"* (Fränkischer Tag, 2021)

Paper 2

Added value of convection-permitting simulations for understanding future urban humidity extremes: case studies for Berlin and its surroundings
Gaby S. Langendijk, Diana Rechid, Kevin Sieck, Daniela Jacob

Published: Weather and Climate Extremes Journal (IF: 7.761), 2021, 33, p.100367.
Doi: https://doi.org/10.1016/j.wace.2021.100367
Citations: 4

Paper 3

Improved models, improved information? Exploring how climate change impacts pollen, influenza, and mold in Berlin and its surroundings
Gaby S. Langendijk, Diana Rechid, Daniela Jacob

Published: Urban Climate Journal (IF: 6.663), 2022, 43, p.101159.
Doi: https://doi.org/10.1016/j.uclim.2022.101159

Acronyms

AMIP	Atmospheric Model Intercomparison Project
CDC	Climate Data Center
CORDEX	Coordinated Regional Downscaling Experiment
CP	Convection permitting
DWD	German Weather Service
EUCP	European Climate Prediction - project
EURO-CORDEX	European Coordinated Regional Climate Downscaling Experiment
GCM	General Circulation Model / Global Climate Model
GEV-PDF	Generalized Extreme Value Probability Density Function
HAPPI	Half a degree Additional warming, Prognosis and Projected Impacts - project
IPCC	Intergovernmental Panel on Climate Change
MBE	Mean Bias Error
MK-test	Mann-Kendall test
MWW-test	Mann-Whitney-Wilcoxon test (or U-test)
RCM	Regional Climate Model
RCP	Representative Concentration Pathway
REMO	Regional Climate Model (named “REMO”)
REMO-NH	Non-Hydrostatic version of REMO
RG	Research Gap
RH	Relative Humidity
RMSE	Root Mean Square Error
RQ	Research Question
SH	Specific Humidity
SST	Sea Surface Temperature
St. Dev.	Standard Deviation
UDI	Urban Dry Island
UHI	Urban Heat Island
WMO	World Meteorological Organisation

1. Introduction: motivation and research gaps

Human-induced climate change is one of the most pressing challenges humanity faces in the course of the 21st century (IPCC, 2021). Occupying only ~3% of the Earth's land surface, urban areas accommodate more than 50% of the world's population, and up to 70 % is projected to reside in cities by 2050 (UN-HABITAT, 2016). Due to the high population density, their compact character, and the uniqueness of urban climates, cities are specifically vulnerable to climate change impacts such as storm surges, flooding, heat/cold waves, and sea level rise, among others (Rosenzweig et al., 2018).

To adequately face climate change related challenges urban decision makers require tailored, high-quality climate information and services to develop mitigation and adaptation strategies to build the resilient cities of tomorrow (Bai et al., 2018; Baklanov et al., 2018; González et al., 2021; Grimmond et al., 2010; WMO, 2019). Information needs can differ strongly per sector and application, and shall therefore be context specific, as well as be provided on relevant temporal and spatial scales appropriate to the decision-making context. Commonly, urban decision makers are particularly interested in information about future extremes, and their changes under climate change, as well as climate change impacts (Langendijk et al., 2019a; Lauwaet et al., 2017; Lemos et al., 2012).

Climate services offer a pivotal contribution to the development of context specific, evidence-based climate information. Climate services are defined by the European Union (2015) as "*the transformation of climate-related data - together with other relevant information - into customized products such as projections, forecasts, information, trends, economic analysis, assessments, counselling on best practices, development and evaluation of solutions and any other service in relation to climate that may be of use for the society at large".*

From the definition, it becomes apparent that climate services, and therewith the urban decision makers engaged through the services, heavily rely on constructing reliable climate information. At the heart of this information construction process lay climate model projections, and the understanding of climate processes and their changes under climate change (Gutowski et al., 2021; Jacob et al., 2020). In this light, for urban climate services, it is important that climate model simulations are capable to represent urban areas and the related local-to-regional climatological processes (Baklanov et al., 2018; WMO, 2019).

Urban areas have a unique climate, and associated meteorological conditions. Cities can influence physical processes, fluxes, and interactions on the local-to-regional scale, modifying for instance temperature, humidity, wind, and precipitation (Huszar et al., 2014a; Wiesner et al., 2018). Commonly, urban areas tend to be warmer (urban heat island effect, UHI), and less moist (urban dry island effect, UDI) than its surroundings (Hage, 1975; Lauwaet et al., 2015; Lokoshchenko, 2017). The existing urban regional modeling studies are able to represent and project the UHI fairly well for different case-study cities worldwide (Chen et al., 2011a; De Ridder et al., 2015; Huszar et al., 2014a; Lauwaet et al., 2015; Masson, 2006). Other urban-induced meteorological phenomena are less studied especially under projected climate change, despite the potential relevance to urban decision makers and urban dwellers.

One of the less studied atmospheric variables is humidity, particularly in the urban-rural context, despite the fact that humidity drives critical meteorological processes, such as convection and precipitation (Argüeso et al., 2016). Near surface humidity is also directly related to health impacts, such as human heat stress (Coccolo et al., 2016). Prior observational studies identified humidity differences between cities and their surroundings in past time periods around the world, often detecting an urban dry island effect (Fortuniak et al., 2006; Hage, 1975; Jåuregui and Tejeda, 1997a; Kuttler et al., 2007a; Lee, 1991; Lokoshchenko, 2017; Moriwaki et al., 2013; Robaa, 2003; Tapper,

1990; Unger, 1999a; Unkašević et al., 2001). A recent study published by Zhao et al. (2021) investigates mean temperature and mean humidity changes in urban areas across the globe under climate change for the winter and summer period, employing a crude emulator approach based on global climate model ensemble data. The findings of this global study generally show a decrease in relative humidity for cities situated in the mid-latitude, particularly in the summer season and under RCP8.5. There are hardly any studies explicitly investigating humidity changes and related variables for the urban local-to-regional context under climate change conditions.

RESEARCH GAP 1 | **The change of humidity and related variables under climate change in urban regions**

Regional climate models (RCMs) are a useful tool to investigate local-to-regional climate processes and impacts under climate change. RCMs offer transient climate projections for regions, driven by General Circulation Models (GCMs). The future climate projections are using various emission scenarios that represent different possible futures, such as the Representative Concentration Pathways (RCPs) (Moss et al., 2010). The grid size of regional climate models are typically in the range of 50-10 km (Jacob et al., 2020). Grid sizes up to 20-10 km allow for the simulation of larger urban areas and urban-rural interactions under longer climatological timescales. The Coordinated Regional Climate Downscaling Experiment (CORDEX) offers a state-of-the-art global framework for regional climate model simulations worldwide, and brings together regional climate modeling groups (Giorgi and Gutowski, 2015; Gutowski et al., 2016; Jacob et al., 2014). An active branch within the CORDEX framework exists in Europe (EURO-CORDEX) (Jacob et al., 2020, 2014). Standard regional climate model projections commonly employ a simple urban scheme, the so-called bulk approach. Urban areas are represented as a rock-surface, with a higher roughness length, higher albedo, and no water storage capacity. The regional climate models are capable of simulating urban-rural interactions, and multi-variate regional processes under climate change. However, the bulk scheme is unable to capture inter-city differences and fine-scale urban climate processes (Masson et al., 2020).
More sophisticated urban climate models exist that have great complexity and are able to simulate fine scale meteorological processes and fluxes in the city and on the district, or even building level. These models evolved from a subset of micrometeorology, boundary layer, and air quality modeling and are predominantly designed to simulate shorter-term weather and climatological phenomena, ranging between days up to a few years (González et al., 2021). These urban climate models commonly operate on a 10 m – 3 km grid resolution. Mainly due to limited computing power and model configurations, these models are unable to simulate longer climatological timescales using climate change scenarios, and/or do not capture urban-rural differences and interactions while simulating a large set of meteorological variables (Masson et al., 2020).

Although RCMs do not incorporate urban areas in the most sophisticated manner possible, regional climate models are currently the best models available that provide long-term climate change simulations on the local-to-regional scale for different emission scenarios while simultaneously capturing urban-rural interactions and their evolution under a changing climate. In this light, it would be important to enhance our understanding about the skill of RCMs to simulate urban areas and their surroundings, and what information they can provide for urbanized regions, particularly for less commonly investigated variables, such as humidity (Zhao et al., 2021). This knowledge is crucial to inform urban climate service developments, as well as to guide further research and model development, especially towards the development of cutting-edge regional Earth system models with a well formulated urban component (Baklanov et al., 2018; González et al., 2021; Gutowski et al., 2021).

RESEARCH GAP 2

The skill of regional climate models to simulate humidity and related variables for urban regions, and what climate information can be derived resultantly

In order to get a broad understanding about what RCMs can simulate in the urban-rural context under climate change, it is useful to investigate mean humidity changes, humidity extremes, and climate impacts related to humidity. In addition, another pivotal aspect is to understand if the climate change signal is modified under a future climate, and if the signal is different in the city compared to its surroundings. Urban decision makers are often particularly interested in extreme events and their projected changes under climate change (Langendijk et al., 2019a; Lemos et al., 2012). There are no prior studies investigating humidity extremes in the urban-rural context. Concerning application relevant information, commonly modelling studies have been used to simulate the relation between humidity and heat stress in cities (Coccolo et al., 2016; Huszar et al., 2014b; Zhao et al., 2021). However, humidity is also connected to less eminent health related impacts, for instance influenza spread and survival, and pollen dispersion (D'Amato and Cecchi, 2008; Davis et al., 2016; Deyle et al., 2016; Hamaoui-Laguel et al., 2015; Lowen et al., 2007; Shaman and Kohn, 2009). Built structures, and specifically in-door mold growth, are also influenced by changes in humidity (Ojanen et al., 2010; Ritschkoff et al., 2000; Viitanen, 2007). To gain enhanced understanding about these less well-understood humidity related impacts, it would be critical to connect the impacts with regional climate models output data, to be able to investigate their changes under climate change in urban regions.

RESEARCH GAP 3

The relationship between regional climate model output data and application relevant information related to humidity, including climate extremes and impacts

One recent advancement in the regional climate modelling community further brings resolving the urban component to the forefront, the development of the so-called convection-permitting (CP) models (Coppola et al., 2020; Gutowski et al., 2021; Jacob et al., 2020). Convection-permitting models are high-resolution regional climate models operating on grid resolutions less than ~5x5 km^2. The hydrostatic approximation used in regional climate models fails for grid sizes smaller than 10x10 km^2, making the RCM's solution less reliable at those spatial resolutions. Therefore, CP models directly resolve the vertical momentum equation, leading to a better representation of small-scale mesoscale circulations and convection, as well as extreme events. In addition, CP models more accurately resolve smaller scale atmospheric processes related to the land surface and orography fields, leading to improved representation of complex terrain, such as urban areas (Argüeso et al., 2016; Ban et al., 2014; Coppola et al., 2020; Kendon et al., 2021; Prein et al., 2015).

Convection-permitting models show promise to better resolve cities under climate change, and therefore have the potential to provide improved information to decision makers (Gutowski et al., 2021). The improvements between regional climate models on different resolutions is referred to as "added value" (Di Luca et al., 2015). A few studies investigate cities with CP models, and show valid results for predominantly the variables temperature and precipitation (Argüeso et al., 2016, 2014; Trusilova et al., 2016, 2013). There have been no studies explicitly investigating the added value of CP models compared to lower resolution RCMs to simulate and understand humidity related extremes and impacts under climate change for urban areas and its surroundings.

RESEARCH GAP 4 | The added value of CP models compared to lower resolution RCMs to simulate and understand humidity related extremes and impacts under climate change for urban regions

The major share of urban studies focusses on the city or inter-city scale. If the urban-rural context is addressed, primarily the UHI or the effects of cities on precipitation are investigated (e.g. Chen et al., 2011b; De Ridder et al., 2015; Huszar et al., 2014b; Lauwaet et al., 2015; Masson et al., 2020). Advancing the knowledge about urban-rural contrasts is critical to understand the rural interactions with the unique urban climate, and the effect of climate change on the local-to-regional scale, particularly for less investigated variables such as humidity. It would offer the possibility to tease out the urban-induced climate change effects compared to the background climate of the surroundings. Various urban-rural climate change studies focused on temperature and/or precipitation use statistical or statistical-dynamical downscaling techniques to downscale global climate models (GCMs) and/or RCMs (Daniel et al., 2018; Hamdi et al., 2015; Masson et al., 2020). No prior research investigates urban-rural humidity contrasts under climate change using dynamically downscaled regional climate models, following a multi-variate approach. In this context, of particular relevance is the understanding of meteorological processes and their changes under climate change, especially when going towards CP scales (Fischer and Knutti, 2013; Prein et al., 2015). In this light, there is a need to further investigate urban-rural humidity contrasts, especially under climate change and by employing regional climate models.

RESEARCH GAP 5 | The understanding and simulation of urban-rural humidity contrasts under climate change

Addressing the outlined research gaps advances the knowledge on the evolution of humidity under climate change in the urban-rural context. In addition, it would give a better understanding of the capabilities of regional climate models to provide the underlying scientific knowledge to improve the development of urban climate information to support decision makers.

The following chapter (Chapter 2) outlines the research questions, describes the research approach taken to address the research gaps, and highlights the novelty of the approach. Chapter 3 presents the results, by providing the three papers of the dissertation. Chapter 4 discusses the findings across the papers, and elaborates on the main limitations of this research. Chapter 5 provides the main conclusions of the dissertation by answering the research questions, and by highlighting the novelty of the findings. This chapter also elaborates on the implications for climate service development, as well as outlines possible future research directions.

2. Research approach

2.1. Objectives and research questions

The overarching objective of this research is to enhance the understanding about regional-to-local climate change in the urban-rural context, with a focus on humidity, towards improved climate information for urban areas in order to support knowledge-based decision-making. Ultimately, to contribute to increasing the resilience of urban areas to projected climate change impacts.

In consonance with the outlined research gaps, this research centers around the following objectives. The first objective is to better understand the mean humidity changes in the urban-rural context under climate change (research gaps 1, 2, 5). Secondly, future humidity extremes, and their meteorological drivers are further investigated to understand their behavior in the urban-rural context (research gaps 1, 3, 5). Thirdly, this research connects RCM output data to application relevant information, to analyze how climate change affects humidity related impacts, such as for instance the aforementioned influenza spread and survival; ragweed pollen dispersion; and in-door mold growth (research gaps 1, 3, 5). In order to provide the most leading-edge information available, it is of profound interest to understand if convection-permitting models show added value to simulate climate humidity extremes and impacts in the urban-rural context (research gaps 1, 3, 4, 5). As a first demonstration site, Berlin and its surroundings are selected as the case study region for the research (see Chapter 2.2.).

In this light, the following research questions are defined:

1. What can already be understood with available regional climate model simulations about future climate change in Berlin and its surroundings, with a focus on humidity?

2. How does crossing spatial scales from 12.5 km to 3 km grid size affect unprecedented humidity extremes and related variables under future climate conditions for Berlin and its surroundings?

3. What is the added value of convection-permitting climate models to simulate humidity related climate impacts under climate change, for Berlin and its surroundings?

2.2. Case study region

Berlin and its surroundings are selected as the case study area for this research. The Berlin region is particularly suitable to investigate urban-rural contrasts using regional climate model output data, because of the relatively flat regional topography, Berlin's large city size, its location in-land, and the distinct urban-rural landscape heterogeneity. These characteristics are helpful to tease out the urban-induced effects on the local-to-regional scale, especially using regional climate models.

Berlin, the capital of Germany, is a large-scale city with around 3.6 million inhabitants covering approximately 891.1 km² (Amt für Statistik Berlin-Brandenburg, 2020), located in-land, in the mid-latitudes at approximately 52.52° N, 13.4° E. Berlin has a temperate continental climate with cold winters (mean temperatures around 0-1.5 °C) and warm summers (mean temperatures around 17-18.5 °C). The land cover of Berlin's surroundings is roughly 50 % agricultural and grass land, 36 % forest and 14 % build up areas and water bodies (Figure 1b) (Amt für Statistik Berlin-Brandenburg, 2020). The primary investigated domain throughout this research, referred to as the Berlin region, is approximately 140 km x 140 km centered around Berlin (black rectangular, Figure 1b).

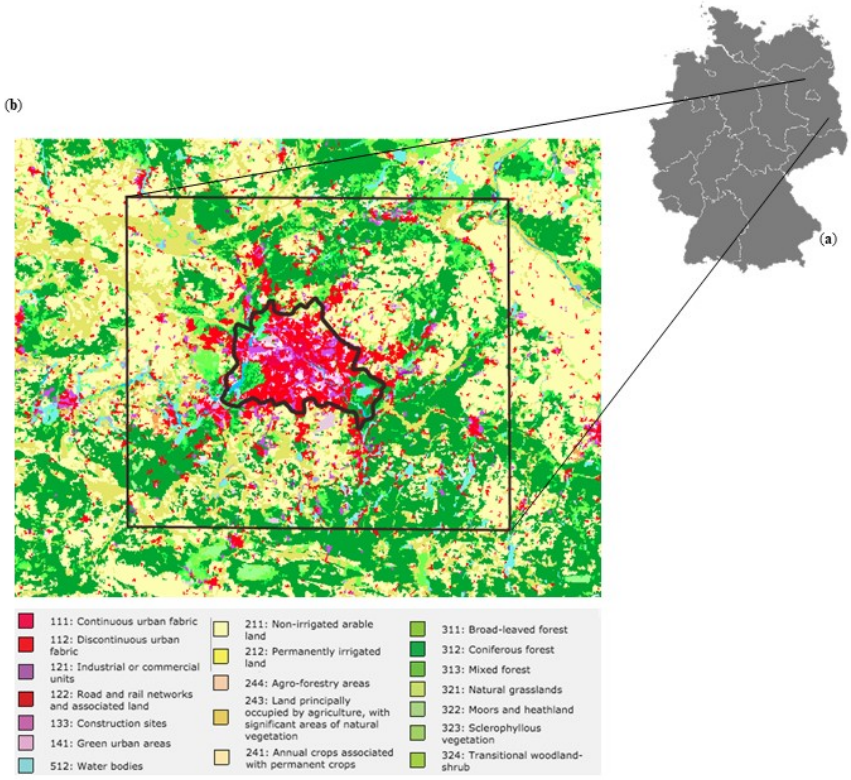

*Figure 1. Research area. (**a**) Germany and (**b**) a land-cover map indicating Berlin's administrative boundaries (black polygon) and research domain including the surroundings (black rectangular). Land cover following CORINE land cover map (EEA, 2000).*

2.3. Humidity

Humidity is the central variable investigated in this research. Various humidity variables have been designed to understand the amount and the change of moisture in the atmosphere. The choice of the humidity variable is critical for the results gained, and should be determined by how humidity is fundamentally related to the process or condition of interest. In addition, for certain studies it could be more informative to use a humidity variable for a specific time or multiple times per day (when available), rather than using a day mean (Davis et al., 2016).

The most commonly used humidity variables are specific humidity and relative humidity. Specific humidity is the amount of water vapor in relation to the total mass of water vapor and air combined, expressed in kilograms of water vapor per kilogram of moist air (kg/kg). Relative humidity is the saturation of the air compared to the maximum water vapor saturated air could contain at a specific temperature, expressed as a percentage (%). Hence, relative humidity depends on both humidity and temperature. Other humidity variables are for instance vapor pressure, mixing ratio, and absolute humidity. These measures have a high inter-correlation with specific humidity, and are at times used interchangeably.

This research focusses on specific humidity and relative humidity, in combination with other meteorological variables, depending on the specific research question and process or condition of interest. Specific and relative humidity are commonly used in the decision-making context (e.g. Lauwaet et al., 2017). In addition, regional climate models provide these two humidity measures as output variables. These aspects make specific and relative humidity particularly suitable for this research.

2.4. Regional climate model REMO

The main model used for this research is the regional climate model REMO. REMO is a three-dimensional, hydrostatic limited-area model of the atmosphere that has been extensively used and tested in climate change studies for Europe (Jacob et al., 2012b; Teichmann et al., 2013). It originates from the 'Europa-Modell' of the German Weather Service (DWD) (Majewski, 1991). The physical parameterizations are largely based on the global climate model ECHAM-4 (Roeckner et al., 1996) and have been further developed over the course of the last decades. Further detailed model specifications can be found in Jacob et al. (2012a) and in Jacob and Podzun (1997).

The land cover scheme within REMO follows a tile approach, based on three basic land surface types; land, water, and sea ice (Semmler, 2002). The turbulent surface fluxes and the surface radiation flux are calculated separately for each tile and are subsequently averaged within the lowest atmospheric level using the respective areas as weights (Rechid and Jacob, 2006; Semmler, 2002). Subgrid fractions are specifying further land cover types, including an urban sub-fraction. These fractions are not assumed to be located in a specific area of a grid box, but cover a percentage of the total grid box area, together summing up to 100 %. For the urban sub-fraction, the REMO model follows the so-called 'bulk'-approach. Sealed urban areas are represented as a rock surface, which is described in the model by a relatively high roughness length, high albedo, and no water storage capacities. Urban areas also contain water, bare soil, and vegetated surfaces.

The hydrostatic approximation used in regional climate models fails for grid sizes smaller than 10x10 km^2, making the RCM's solution less reliable at those spatial resolutions (Prein et al. 2015). Therefore the non-hydrostatic, convection-permitting model version REMO-NH was developed to directly resolve the vertical momentum equation, leading to a better representation of small-scale mesoscale circulations and convection (Goettel, 2009). In addition, REMO-NH more accurately resolves the orography and the surface types, such as urban areas and its characteristics.

2.5. Research design and overview on papers

To answer the research questions, the design of this PhD thesis follows a three-step approach, resulting in three papers, each one addressing one of the three main research questions. The subsequent section connects the three parts of the research by providing a short introduction to each paper, the methods used, and how they address the research questions and research gaps. The structure of the research approach is visually summarized in Figure 2.

Paper 1: Urban Areas and Urban-Rural Contrasts under Climate Change: What Does the EURO-CORDEX Ensemble Tell Us? — Investigating near Surface Humidity in Berlin and Its Surroundings
Gaby S. Langendijk, Diana Rechid, Daniela Jacob

Research question one seeks to understand what can already be understood with available regional climate model simulations about humidity under projected climate change, comparing Berlin to its surroundings. This first step forms the groundwork of the research and is presented in Chapter 3.1. This part of the research has been published in Langendijk et al. (2019b). It contributes to addressing the research gaps 1, 2, and 5, through investigating if regional climate models adequately simulate humidity in the urban-rural context, and how humidity changes under climate change (Figure 2).

Ten regional climate model combinations of the EURO-CORDEX ensemble are analyzed. The EURO-CORDEX multi-model ensemble is selected, because it provides the best state-of-the-art coordinated regional climate model dataset on the 12.5 km (0.11°) grid resolution, with transient climate simulations from 1970 up to 2100 (Jacob et al., 2014). Multi-model ensembles are proven to provide more robust information than using single climate models (Christensen et al., 2007; Pfeifer et al.,

2015). This approach enables us to derive robust information on potential humidity changes in urban areas compared to their surroundings, using transient climate change projections. The EURO-CORDEX model data therefore forms the foundation to investigate humidity under climate change for the Berlin region.

Using the emission scenario RCP8.5, three main aspects are investigated to answer research question 1. Firstly the study explores the climate change trend for relative humidity, specific humidity, and temperature through calculating the 30-year running mean for Berlin and its surroundings. The Mann-Kendall test (MK-test) is employed to understand the robustness of the multi-model ensemble to detect the monotonic trend and direction of change across the model combinations. Secondly, to further investigate the climate change signal, the Mann-Whitney-Wilcoxon test (MWW-test) calculates whether the future distribution (2070–2099) differs significantly from the historic climate (1971–2000). Thirdly, the mean change between the future and historic climate is investigated for the annual cycle, and the annual cycle is analyzed on a decadal basis between 1970–2100.

The outcomes, described in Chapter 3.1. (paper 1), are the first in its kind to show the potential of the EURO-CORDEX ensemble to understand humidity changes in the urban-rural context under climate change, underpinning the development of climate change information for decision makers.

Paper 2: Added value of convection-permitting simulations for understanding future urban humidity extremes: case studies for Berlin and its surroundings

Gaby S. Langendijk, Diana Rechid, Kevin Sieck, Daniela Jacob

The second research question investigates how moving to the convection-permitting scale affects unprecedented humidity extremes under future climate conditions for Berlin and its surroundings. This part of the research is presented in Chapter 3.2. and is published in Langendijk et al. (2021). It contributes to addressing research gaps 1, 3, 4, and 5 (Figure 2), by exploring the added value of convection-permitting models to simulate future humidity extremes in the urban-rural context.

This paper starts with identifying unprecedented humidity extremes happening under future climate change. The identification of future humidity extremes and their potential occurrence requires robust statistics on large datasets that offer many years of possible climate futures. Transient regional climate model projections are limited in this extent, as they commonly provide data up to around 80 years into the future. A unique modelling effort by the "Half a degree Additional warming, Prognosis and Projected Impacts (HAPPI)" project offers a large set of global climate model simulations for possible future decades under 1.5°C and 2.0°C warmer global mean surface temperature than pre-industrial (1861–1880) conditions (Mitchell et al., 2017). A large ensemble of simulations is created by initializing each so-called member with slightly different initial conditions, leading to a large ensemble of possible climates. This ensemble had been downscaled to the 50 km (0.44°) grid resolution by the regional climate model REMO for 100 ensemble members, for three decades (historic, 1.5°C, and 2.0°C), resulting in a total of 3000 years of climate data (Sieck et al., 2021). This amount of climate data allows a robust identification of future extremes, and therefore the downscaled HAPPI dataset is selected for addressing the second research question.

To understand how the future humidity extremes are affected going from 50 km to the convection-permitting scale, the identified extremes are downscaled following a two-step approach, to the 12.5 km (0.11°) with the REMO model, and thereafter to the 3 km (0.0275°) grid resolution with the non-hydrostatic, convection-permitting version of REMO (REMO-NH). A novel double-nesting downscaling set-up is specifically designed for this research step, particularly applicable to the urban-rural context. The new data on humidity extremes acquired through the downscaling, is analyzed following a process-understanding approach investigating 14 meteorological model output variables

on a daily to hourly time scale. The process-understanding approach taken, shows whether the RCM represents the meteorological phenomena driving the humidity extremes adequately, and whether the extreme meteorological conditions change across spatial resolutions. This approach is particularly critical, as unprecedented humidity extremes did not happen in the past climate, and therefore have no counterpart with observations to validate their representation in the model data. To ensure the urban area is analyzed similarly throughout the spatial resolutions, a novel masking approach is developed to extract Berlin from its surroundings across the spatial resolutions.

Up to date, there has been no studies investigating whether or not convection-permitting simulations improve the understanding and simulations of future humidity extremes for cities. As a first exploratory study, the results presented in Chapter 3.2. show the added value of the convection-permitting scale to simulate two unprecedented humidity extremes under climate change for Berlin and its surroundings.

Paper 3: Improved models, improved information?
Exploring how climate change impacts pollen, influenza, and mold in Berlin and its surroundings
Gaby S. Langendijk, Diana Rechid, Daniela Jacob

The final research question is geared towards the application side, and aims at providing insights into how humidity related climate impacts are affected by climate change going to the convection-permitting scale. Chapter 3.3. takes the Berlin region as its testbed and contributes to addressing research gap 1, 2, 3, and 5 (Figure 2). Mainly, this is done through connecting RCM data with humidity related climate change impacts, and by understanding the added value of convection-permitting models in the urban-rural context. This part of the research is published in Langendijk et al. (2022).

The third paper aims to improve the understanding about the added value of convection-permitting models to simulate humidity related meteorological conditions driving climate change impacts. Following an in-depth literature review, three novel impact cases are specifically designed for this research in order to connect regional climate model data with humidity related impacts. The three impact cases: influenza spread and survival; ragweed pollen dispersion; and in-door mold growth. All have direct or in-direct effects on human health, and are therefore specifically of relevance to urban dwellers. The impact cases have not been previously investigated with regional climate model data under climate change in the urban-rural context. The REMO model output data for the 12.5 km (0.11°) and the 3 km (0.0275°) (REMO-NH) grid resolutions are utilized for the historical time period (1996–2005) and a near-term future time period (2041–2050) under the emission scenario RCP8.5 (Moss et al., 2010). The dataset is produced as a part of the European Climate Prediction (EUCP) project (Ban et al., 2021; Lowe et al., 2020). These REMO simulations are selected because they offer a cutting-edge dataset that allows for the cross-comparison between the two spatial grid resolutions under climate change. In addition, the near-term future period (2041–2050) is particularly of relevance for policy timeframes, as urban decision makers tend to be specifically interested in timespans ranging from multi-annual up to the near-term future (Lauwaet et al., 2017). Chapter 3.3. gives insight, for the first time, into the added value of convection-permitting models to simulate humidity related meteorological conditions underpinning the three novel impact cases under future climate conditions for the Berlin region.

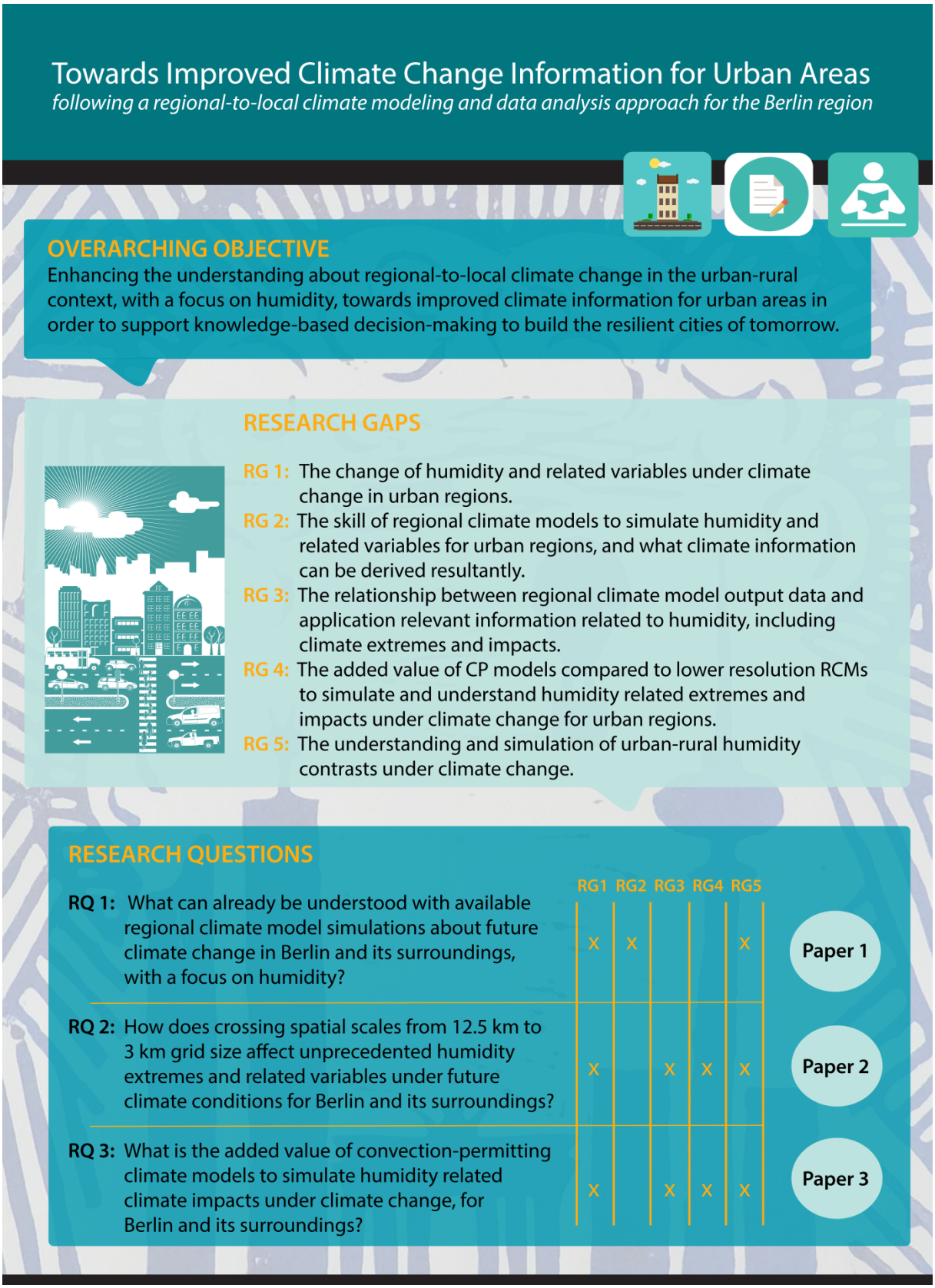

Figure 2. Overview of the research design, including the overarching objective, research gaps (RG), and research questions (RQ).

2.6. Novelty of the research approach

The three papers presented in Chapter 3 offer a knowledge building chain, from gaining a general understanding on mean humidity changes under climate change, to investigating in-depth humidity extremes across spatial resolutions, and up to exploring the added value of convection-permitting simulations to simulate humidity related impacts under future climate conditions – all for the Berlin region. The research questions are framed within the broader climate services context, and are therefore directed towards information development and the needs of decision makers.

The above sections highlight that none of the posed research questions have been answered in prior research. This study is the first to specifically investigate humidity, and related variables in the urban-rural context under climate change with regional climate models. Convection-permitting modelling is an emerging field. There have been hardly any studies on the urban-rural context, and none particularly investigated the added value of CP models to simulate humidity extremes and humidity related impacts under climate change, in order to understand whether CP models could improve climate information for cities. In Chapter 3.2., new future humidity extremes are identified, downscaled, and analyzed. A new double-nesting downscaling set-up was particularly designed to investigate the urban-rural context with regional climate models at various scales. The set-up could serve as a blueprint for similar subsequent studies. Usually "known" extremes are selected and downscaled under future climate conditions. The unique approach taken by this thesis offers an opportunity to identify and analyze "unknown", unprecedented humidity extremes. The multi-variate process-understanding approach taken to analyze the humidity extremes offers a fresh perspective compared to more commonly used approaches that quantify the added value of CP models with statistics. The increased attention by society on urban climate change impacts, enhances the need for high-quality climate information. This study, is the first to investigate whether the CP resolution shows added value to simulate the effect of future climate change on humidity related impact cases: influenza spread and survival; ragweed pollen dispersion; and in-door mold growth. The results presented in this thesis offer new insights into how regional climate models, and particularly convection-permitting models, can provide the underpinning science to construct climate information, in relation to humidity, for the urban-rural context. This is pivotal for the development of urban climate services, to enable informed decision-making.

3. Results

The subsequent chapter presents the three papers in correspondence with the three research questions, and in accordance with the research approach described in Chapter 2.5.

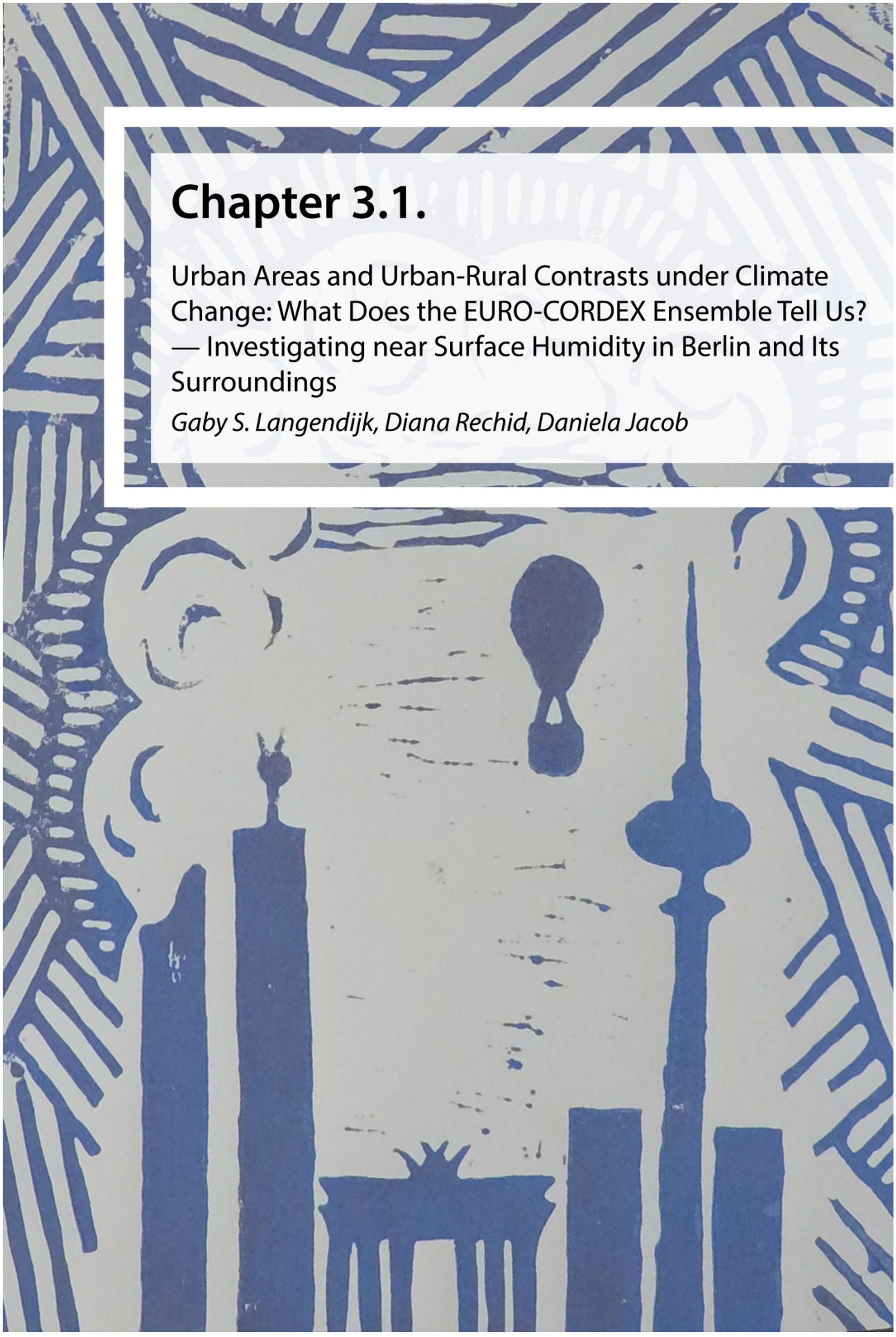

Chapter 3.1.

Urban Areas and Urban-Rural Contrasts under Climate Change: What Does the EURO-CORDEX Ensemble Tell Us? — Investigating near Surface Humidity in Berlin and Its Surroundings

Gaby S. Langendijk, Diana Rechid, Daniela Jacob

Paper 1

atmosphere

MDPI

Article

Urban Areas and Urban–Rural Contrasts under Climate Change: What Does the EURO-CORDEX Ensemble Tell Us?—*Investigating Near Surface Humidity in Berlin and Its Surroundings*

Gaby S. Langendijk[1,2,*], Diana Rechid[1] and Daniela Jacob[1,2]

[1] *Climate Service Center Germany (GERICS), Helmholtz-Zentrum Geesthacht (HZG), Chilehaus, Fischertwiete 1, 20095 Hamburg, Germany; diana.rechid@hzg.de (D.R.); daniela.jacob@hzg.de (D.J.)*

[2] *Faculty of Sustainability, Leuphana University of Lüneburg, Universitätsallee 1, 21335 Lüneburg, Germany*

**Correspondence: gaby.langendijk@hzg.de*

Received: 10 October 2019; **Accepted**: 18 November 2019; Published: 21 November 2019

Abstract: Climate change will impact urban areas. Decision makers need useful climate information to adapt adequately. This research aims to improve understanding of changes in moisture and temperature projected under climate change in Berlin compared to its surroundings. Simulations for the Representative Concentration Pathway (RCP) 8.5 scenario from the European Coordinated Regional Climate Downscaling Experiment (EURO-CORDEX) 0.11° are analyzed, showing a difference in moisture and temperature variables between Berlin and its surroundings. The running mean over 30 years shows a divergence throughout the twenty-first century for relative humidity between Berlin and its surroundings. Under this scenario, Berlin gets drier over time. The Mann-Kendall test quantifies a robust decreasing trend in relative humidity for the multi-model ensemble throughout the twenty-first century. The Mann-Whitney-Wilcoxon test for relative humidity indicates a robust climate change signal in Berlin. It is drier and warmer in Berlin compared to its surroundings for all months with the largest difference existing in summer. Additionally, the change in humidity for the period 2070–2099 compared to 1971–2000 is larger in the summer months. This study presents results to better understand near surface moisture change and related variables under long-term climate change in urban areas compared to their rural surroundings using a regional climate multi-model ensemble.

Keywords: urban climate change; urban–rural interactions; humidity; Berlin; regional climate modeling; EURO-CORDEX

1. Introduction

Climate change poses severe challenges to urban areas and climate change impacts will magnify throughout the century alongside rapid ongoing and projected urbanization [1–3]. To adequately face these climate-change-related challenges, urban decision makers require tailored climate information to develop mitigation and adaptation strategies to build the sustainable cities of tomorrow [4–6].

At the foundation of reliable science-driven climate information lies climate projections by climate models which can be used to understand and adapt to future climatic changes. Currently, most climate data and information produced by urban or climate models are either not scale compliant for cities, offer only a limited set of climatological parameters, or are unable to simulate urban–rural

interactions. Regional climate models are a promising tool to bridge scales between global climate models and local scale urban models, simulating regional scale processes and urban– rural interactions under climate change.

The Coordinated Regional Climate Downscaling Experiment (CORDEX) offers a state-of-the-art global framework for regional climate model (RCM) simulations and brings together around 30 regional climate modeling groups from across the globe [7–9]. Presently, only a limited sub-set of RCMs have developed a more complex representation of urban structures for their models and have conducted explicit studies on urban areas [10–12]. Due to limited available computing power, most of the detailed urban model projections with higher spatial resolutions (100 m^{-3} km grid size) simulate short time ranges, from a few days to a few years, and only focus on a sub-set of climatological variables. Often these sophisticated urban climate models simulate mainly meteorological phenomena based on temperature and/or heat budgets, such as the urban heat island effect (UHI) [11–16]. Existing urban modeling studies are able to represent and project the UHI fairly well for different case-study cities worldwide [11,12,15,17–19]. Several studies have indicated that urban areas have an influence on their surroundings and their local-to-regional climate, particularly for temperature, wind, and precipitation [18,20].

It remains challenging to provide longer time-scale climate projections tailored to urban areas for a more diverse set of climatological phenomena [6]. Particularly, change in moisture, and its dependent variables such as specific humidity, relative humidity, and temperature, are not well understood. Observational studies have identified moisture differences between cities and their surroundings in past time periods around the world [21–30]. Some studies have quantified a drying in the city, the so-called urban dry island (UDI) effect [e.g., 31,32]. However, to our knowledge no studies have explicitly investigated changes in moisture in urban areas relative to their surroundings under climate change conditions using a regional climate multi-model ensemble.

Changes in moisture in urban areas under climate change could impact city sectors such as building structure, health, and biodiversity, resulting in a profound effect on the livability of cities. For instance, relative humidity is of direct importance to human heat stress and health [33–35]. Additionally, moisture levels can influence the sustainability of buildings by, for instance, altering the moist risks or endurance of building material [36,37]. Furthermore, humidity has an impact on vegetation growth, biodiversity, and ecosystem services in urban areas [38].

Despite its importance to living conditions, the impact of climate change on moisture in cities, as well as urban–rural moisture contrasts, remains under explored [39]. Enhanced understanding of these moisture phenomena and urban–rural interactions would improve climate information. This would enable informed adaptation decisions that influence the livability of cities under climate change [4–6]. In this context, the main objective of this research was to investigate changes in moisture and related variables under climate change conditions in the urban–rural context. Berlin and its surroundings were selected as the case study area. According to our knowledge, this study is the first of its kind to investigate whether the EURO-CORDEX multi-model ensemble captures urban–rural contrasts for moisture and related variables such as temperature in Berlin and its surroundings. In addition, the study explores the presence of a UDI and quantifies change in the urban–rural moisture contrast throughout the twenty-first century under climate change conditions. The research outcomes improve understanding of the opportunities and limitations of EURO-CORDEX data´s applicability to urban areas and could inform further research on this topic.

2. Experiments

2.1. Research Area

To investigate humidity under climate change in urbanized areas, we selected Berlin and its surroundings. Berlin, the capital of Germany, is a large-scale city with around 3.6 million inhabitants covering approximately 891.1 km² [40]. The city is located in-land in a relatively flat topography and is surrounded by predominantly forests and agricultural land. The size and geographical location of Berlin makes it a suitable case-study to investigate using regional climate model output data.

The grid boxes of the EURO-CORDEX models are around 11 km × 11 km (0.11°), being together roughly 120 km^2. Approximately seven grid boxes include an urban land-use type for Berlin. Some EURO-CORDEX models follow a fractional approach where the fluxes are calculated based on a mix of land-use types within one grid box. Other RCMs contain a dominant tile approach in which the fluxes are calculated based on the dominant land-use type within one grid box. This results in a different representation of the urban surface in the models. In this research, we considered Berlin per its administrative borders. Berlin was sliced out from the regional climate model output data through a geographically referenced weighted polygon of the administrative city boundaries (black polygon, Figure 1b). Because grid boxes and urban representation differ among the investigated models, this method provided a consistent data selection approach for Berlin across the model output data. The surroundings of Berlin were selected through a rectangular domain from approximately 140 km by 100 km located around the administrative boundaries of the city (black rectangle, Figure 1b). The land cover of the surroundings is roughly 50% agricultural and grass land, 36% forest, and 14% built-up areas and water bodies (Figure 1b) [41].

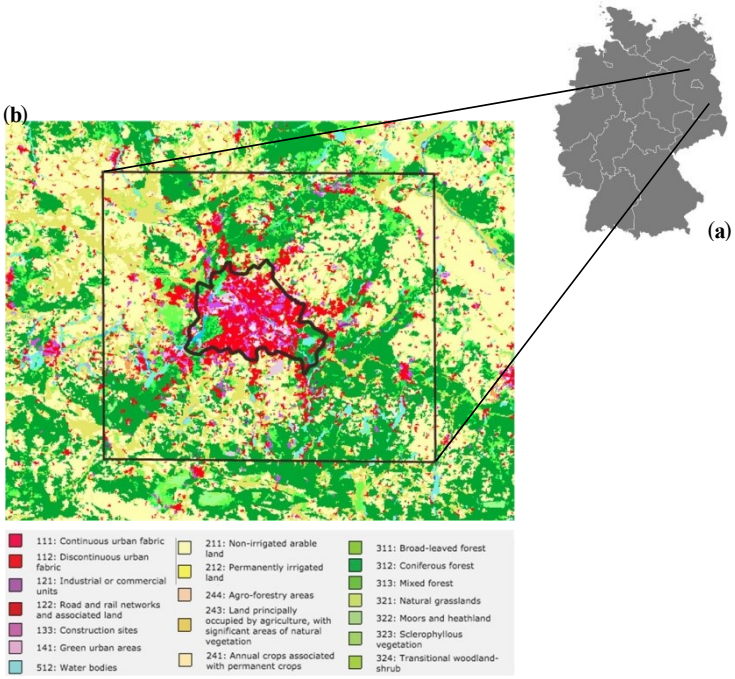

Figure 1. Research area. (**a**) Germany and (**b**) a land-cover map indicating Berlin's administrative boundaries (black polygon) and research domain including its surroundings (black rectangle). Land cover follows the CORINE land cover map [42].

2.2. Data, Variables, and Climate Scenarios

This research investigated regional climate model output data provided by the European CORDEX (EURO-CORDEX) using an approximately 12 km^2 spatial resolution (0.11°) for the period 1970–2099 [7]. The data used for this study was obtained from the Earth System Grid Federation, CORDEX data node [43]. The multi-model ensemble considered for this study consists of ten model combinations, including several global circulation models (GCM), which are presented in Table 1. To understand how parameterization schemes of regional climate models represent urban areas, we conducted a short online survey within the EURO-CORDEX community and studied model documentation [44–52].

Relative humidity (RH) and specific humidity (SH) are the primary focus variables of this research as well as surface temperature at 2 m height (Tas) and minimum and maximum surface temperature at 2 m height (Tasmin and Tasmax, respectively). Relative humidity (RH in%) is generally calculated by the mass of the actual water vapor (Mv in g/m³) at a temperature divided by the mass of water vapor in saturation, depending on the temperature (Mg (T) in g/m³) (Equation (1)).

$$\mathrm{RH} = \frac{Mv}{Mg\ (T)} \times 100\% \quad (1)$$

Table 1. Regional climate models and model combinations and their respective simulated variables which were investigated in this research ('x' means this variable was investigated). Legend: GCM, global circulation model; RCM, regional climate model; RH, relative humidity; SH, specific humidity; Tas, surface temperature at 2 m height; Tasmax, maximum surface temperature at 2 m height; Tasmin, minimum surface temperature at 2 m height.

Driving Data (GCM)	Regional Model (RCM)	Regional Modeling Group	Humidity Variables (RH and SH)	Temperature Variables (Tas, Tasmax, Tasmin)
EC-EARTH	RCA4	SMHI	x	x
EC-EARTH	RACMO22E	KNMI	x	x
EC-EARTH	HIRHAM5	DMI	x	x
CM5A-MR	WRF331F	IPSL	x	x
CM5A-MR	RCA4	SMHI	x	x
HadGEM2	RCA4	SMHI	x	x
HadGEM2	RACMO22E	KNMI	x	x
MPI-ESM-LR	REMO2009	GERICS	x	x
MPI-ESM-LR	RCA4	SMHI	x	x
EC-EARTH	CCLM4-8-17	CLM community	SH only	x

Observations were compared to the model output data to examine if both showed an urban-rural contrast for the variables, as well as to determine whether the magnitudes of these contrasts were similar. In situ measurements of individual meteorological stations in Berlin and its surroundings were obtained from the Climate Data Center (CDC) of the German Weather Service (DWD) [53]. These stations are selected and operated according to guidelines of the World Meteorological Organisation (WMO) as well as quality controlled to ensure homogeneity across the time series and between the different datasets. The particular datasets used for this research are based on hourly measurements and/or contain annual means calculated from the hourly data for each variable and observation station [54–57]. The measurement data from ten

observation stations, of which six are in Berlin and four in the surroundings of Berlin, were compared to the multi-model mean between 1970 and 2017. The annual standard deviation for each model variable was calculated to investigate the climate variability. The period 1970 until 2017 was selected to cover the longest timespan available for the observational data as well as to comply with the historical model run period. The observation stations are spread across Berlin and located in different areas in its surroundings. The exact locations have been presented on a map in the Appendix (Appendix A, Figure A1). Local effects influence measurements from observation stations [58]. Figure A1b shows the direct surroundings of the observation stations through Google Earth images to assist understanding of the local circumstances at each measurement station and to get a sense of its representativeness to the urban or rural context. RCM projections for the high emission, business-as-usual, Representative Concentration Pathway 8.5 (RCP 8.5), as defined by the Intergovernmental Panel on Climate Change (IPCC) [59], were selected for this study. This high-emission scenario has been chosen because it represents the most severe possible future under climate change among the available scenarios. We chose the worst-case scenario because it probably gives the most striking results for the investigated variables between Berlin and its surroundings as well as between the models. The RCP 8.5 scenario could be a stepping stone to investigation of other RCP scenarios.

2.3. Calculations and Statistics

To investigate whether the EURO-CORDEX multi-model ensemble captures urban-rural contrasts for moisture, model output data and the differences between the regional climate models were investigated. Additionally, compliance between the models and the observations was explored. The annual mean of the in situ measurements was compared with the annual multi-model mean for Berlin, as well as for the surroundings, to analyze the differences and agreements between the models and the observations.

The running mean was calculated to explore whether a climate change trend is present in the climate output data for Berlin and its surroundings as well as to understand the differences between trends in urban and rural contexts. The running 30-year climatological mean was calculated from the annual mean for each variable and model combination for Berlin as well as for its surroundings. The multi-model running mean was calculated from the annual running mean of the individual model combinations [60]. The Mann-Kendall test (MK test) explores whether there is a monotonic trend and the direction of change of a time series (increasing/decreasing) [61,62]. Hence, the MK test was performed for each individual model's running mean for all the investigated variables. A robust result of a monotonic trend and direction of change for a variable was considered to have been obtained if more than 66% of the models showed similar, statistically significant (p value < 0.05) outcomes for the test [63].

To further understand the climate change signal, the Mann-Whitney-Wilcoxon test (MWW-test) (or U-test) was applied to all investigated variables. The test investigates whether the future distribution (in this case 2070–2099) differs significantly for a variable compared to the distribution for the historic climate (in this case 1971–2000). A robust result was considered to have been obtained if more than 66% of the models showed similar results, implying a significant climate change signal for a variable [63]. One of the underlying assumptions for conducting a MWW-test is that the data is homogeneous of variances. To ensure this criterion was met the Levene test was conducted [64]. If the test outcome was not significant, meaning there was homogeneity of variances, the MWW-test was undertaken. Model combinations that could not pass the Levene test were left out of the climate change signal analysis for each variable.

Annual cycles of the variables were studied to understand changes per month and changes in annual cycles throughout the century as well as shifts in the seasons for humidity and temperature under climate change. The differences between Berlin and its surroundings were analyzed. Firstly, the annual cycle on a decadal basis between 1970 and 2100 was calculated for the investigated variables through calculating the annual multi-model mean averaged per decade. Secondly, a boxplot was created to understand the mean change when comparing 1971–2000 to 2070–2099, as well as the standard deviation and spread per month of the multi-model ensemble.

2.4. Daily Cycle

To further understand the urban–rural daily temperature contrast, underpinning the results for humidity, the hourly temperature data of the regional climate model REMO (version: MPI-M-ESM-LR_r1i1p1_REMO2009) was investigated [49,50] in addition to the minimum and maximum temperature for all the EURO-CORDEX models.

The mean daily cycle was calculated over the period 1971–2000 for hourly data of the REMO model and compared to the observational mean of the hourly data over the same period for each day. The hourly data was obtained from the CDC of the DWD [65]. Based hereupon, for January, April, July, and October, the daily mean over the month was calculated to understand the daily cycle differences throughout the year. For Berlin as well as its surroundings the mean of the respective observation stations was considered in the analysis. Differences in the diurnal temperature cycle between Berlin and its surroundings were explored for the models and the observations to understand the urban–rural contrasts and whether these had been adequately simulated by the models. The mean daily minimum and maximum temperature for the period 1971–2000 in Berlin and for its surroundings were investigated for each EURO-CORDEX model for January, April, July, and October to understand whether the models showed comparable results to REMO for the daily cycle urban–rural contrast.

3. Results

The results section is divided into two main parts. The first part investigates how the EURO-CORDEX models represent urban areas in their models and whether differences are simulated for humidity and temperature between Berlin and its surroundings. To complement the first part, the model outcomes were compared with observations. The second part focuses on quantifying urban–rural contrasts for humidity and temperature variables under climate change conditions in the twenty-first century in Berlin and its surroundings.

3.1. Models and Observations

The running mean, calculated over 30 years for each EURO-CORDEX model and variable, was investigated to explore the general differences between the models and model combinations as well as the main differences between Berlin and its surroundings (Figure 2). Climate change trend analysis based on the running mean is discussed in the second part of the results section.

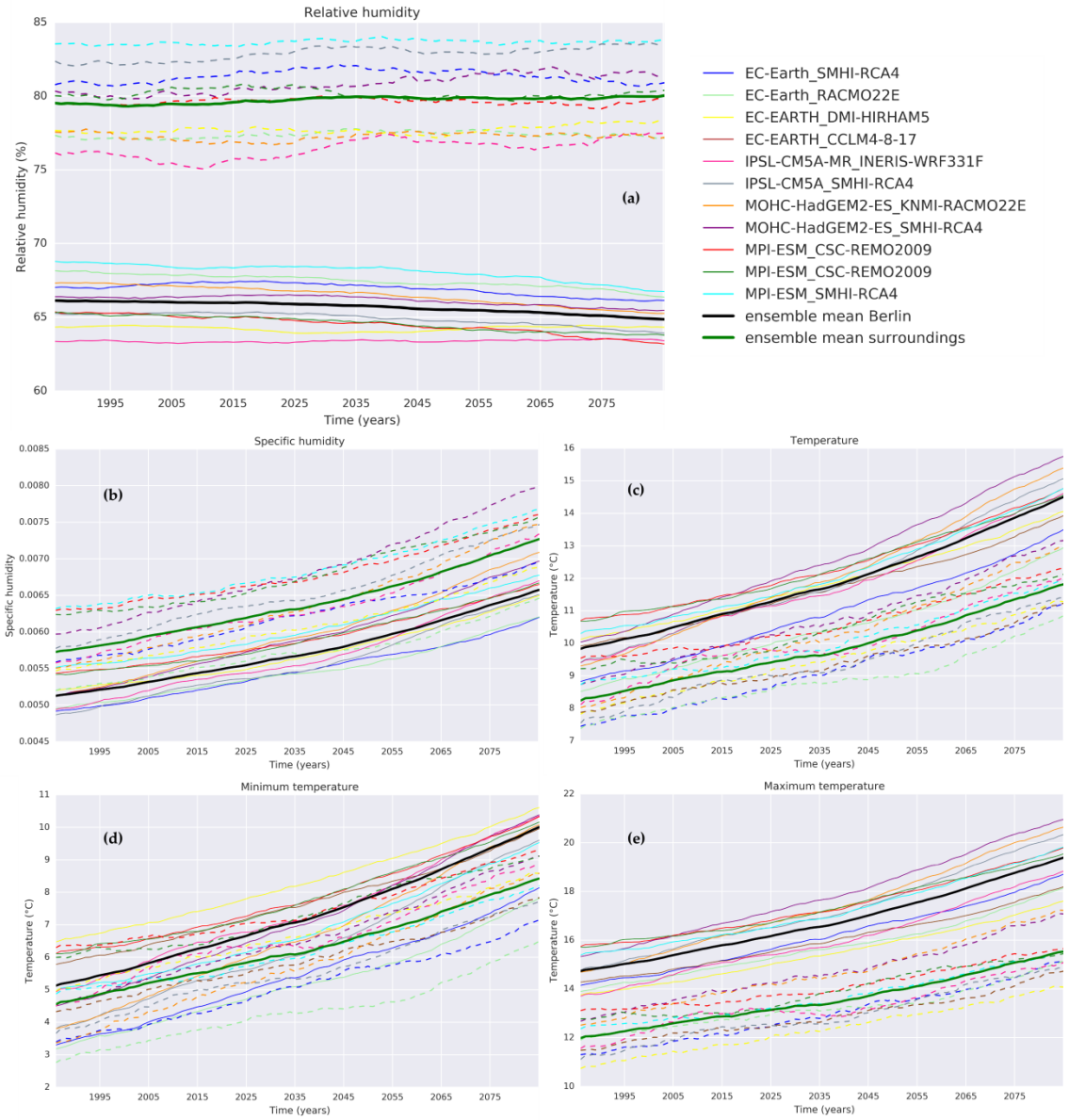

Figure 2. Running 30-year mean for 1970–2099 for individual European Coordinated Regional Climate Downscaling Experiment (EURO-CORDEX) models and the multi-model mean for (**a**) relative humidity, (**b**) specific humidity, (**c**) temperature, (**d**) minimum temperature, and (**e**) maximum temperature for Representative Concentration Pathway (RCP) 8.5, comparing Berlin (solid lines) and its surroundings (dashed lines).

Figure 2 clearly demonstrates that all EURO-CORDEX models simulate distinct differences between Berlin and its surroundings for each variable. More specifically, the relative humidity and specific humidity are lower in Berlin than its surroundings, resulting in a water vapor deficit in Berlin compared to its surroundings (Figure 2a,b). Similarly, the temperatures are higher in Berlin than in its surroundings for all temperature variables considered in this study (Figure 2c–e). The EURO-CORDEX community survey (Appendix A: Table A1) and the studied model documentation indicate that the models represent urban areas through their land surface scheme and parameterizations, commonly by means of the 'bulk' scheme. Following this 'bulk' approach, sealed urban areas are represented as a rock surface, which is described in the models by a relatively high roughness length, high albedo, and no water storage capacities [18,46,49,66]. Model outcomes for Berlin show lower RH and higher temperature values than its surroundings (Figure 2). This general outcome can be explained as follows. In the models, large areas of Berlin

are represented by a rock surface with a high surface runoff rate and a low capacity to store water. Hence, the evaporation rates are low and the atmospheric humidity levels decrease. Additionally, this leads to a low latent heat flux and a high sensible heat flux [10]. This results in higher temperatures and drier conditions simulated for Berlin compared to its surroundings.

The observations also show that Berlin is drier and warmer compared to its surroundings (Figure 3). There is a spread among the observations, particularly for RH, temperature, and minimum temperature. The spread of the rural stations is considerably small compared to the stations in Berlin. The direct surroundings of all the rural observation stations are characterized by agricultural or grass fields (see Appendix A, Figure A1b). This similar land-use type explains the relatively small spread among the observational stations in rural areas. In Berlin, the spread between the stations is larger. The stations are located in different areas of the city, near (former) airports (Tegel and Tempelhof), green spaces (Dahlem), or roads and buildings (Ostkreuz, Marzahn, and Alexanderplatz) (see Appendix A, Figure A1b). The direct surroundings of observational stations have a profound influence on their measurements [58]. The observation station 'Alexanderplatz' is located in the city center of Berlin and is surrounded by compact buildings and an almost fully sealed surface. This station shows the highest temperature values (Figure 3b), which can be explained by the combined influence of its direct surroundings and its central location, which is where the city is at its hottest. The measurement values for RH and temperature of the stations 'Tegel' and 'Tempelhof', which are both near (former) airports, are similar. Trees and green areas can have a cooling effect in the city. 'Dahlem' is slightly cooler and more humid than the other stations because it is located near a green space. The colors of Figure 3 reflect the urban gradient, respectively showing the darkest red colors for the stations located in the inner city and lighter orange-yellow colors for sub-urban observation stations.

Comparing the model outcomes with the observations, similar generic outcomes can be seen to arise for the studied variables. Berlin is drier and warmer compared to its surroundings. Figure 3a shows that the multi-model mean simulates the RH annual mean by a slightly lower amount, i.e., by 3–10%, than the observations indicate for Berlin. The models slightly overestimate, i.e., by 0–4%, the relative humidity for the surroundings. This leads to a total overestimation by the models of the water vapor deficit in Berlin compared to its surroundings of around 3–14%. The model spread is presented in the Appendix (Figure A2). The models are centered around the multi-model mean and do not show a distinct exception for one or a few models. The standard deviation (Appendix, Table A3) for Berlin is lower than 1% for each model and is between 1.5% and 2.5% for the surroundings. To summarize, the models are able to capture the rural–urban relative humidity contrast, with a dry overestimation in Berlin. This modeled water vapor deficit might be an effect of the urban parameterization scheme that results in low evaporation rates due to an overestimation of sealed rock surfaces compared to the actual urban surface with green spaces [10]. This leads to an increased drying effect in the model simulations compared to the observations. The observational station 'Alexanderplatz' in Berlin corresponds most correctly to the multi-model mean for RH (Figure 3a) and to a lesser extent for temperature (Figure 3b), which is in contrast to the other stations further away from the city center. The observation station 'Alexanderplatz',in the city center, is surrounded by compact buildings and an almost fully sealed surface (see Appendix A, Figure A1). This hints that the simple urban 'bulk' scheme in RCMs could represent sealed, central urban areas quite adequately with respect to climatological annual mean values. Nevertheless (sub-) urban areas with vegetated spaces remain more challenging to simulate correctly by regional climate models on the 0.11° spatial scale.

For the mean annual temperature the models simulate temperature change over the past time period in a similar fashion to the observations, simulating namely an approximate increase of

around 1.2–1.5 °C between 1970 and 2017 (Figure 3b–d). The temperature difference between Berlin and its surroundings is overestimated by the models with a ~2 °C difference between the two multi-model means compared to a ~1 °C difference for the observations. This is mainly due to an underestimation of the temperature in the surroundings by the models (Figure 3b).

The standard deviation for the temperature variables calculated over the annual mean for each model is <1 °C in Berlin and between 0.5 °C and 1.5 °C for its surroundings (Appendix, Table A3). The climate variability is low because it was calculated on an annual basis for a relatively small domain. The model spread (Appendix, Figure A2) for the temperature variables is approximately 3 °C in Berlin and ~4 °C for its surroundings. The global climate models driving RCMs largely affect the results for the temperature variables, particularly for CM5A-MR, HADGEM2, and MPI-ESM. Generally, the models capture the urban–rural contrast for temperature in a similar fashion as the observations, with a slight underestimation of the temperature in the surroundings. The models simulate the temperature trend in a comparable manner to the observations. This is expected to persist for future projections. The relative humidity trend is largely dependent on the temperature trend and therefore expected to be projected adequately by the models.

The annual maximum and annual minimum temperature show opposite urban–rural contrasts for Berlin and its surroundings when comparing the multi-model means with the respective observations (Figure 3c,d). The simulated difference in the maximum temperature between Berlin and its surroundings is larger than the simulated difference in the minimum temperature between both areas. By contrast, the observations show a smaller difference between the maximum temperature and the minimum temperature when comparing Berlin and its surroundings. This suggests that the models possibly do not capture the temperature difference correctly for the nighttime between Berlin and its surroundings. According to previous studies, the largest temperature difference between the urban and rural areas, the largest UHI, is expected during the night. In winter, the temperature difference between Berlin and its surroundings is expected to be smaller compared to other seasons [67,68].

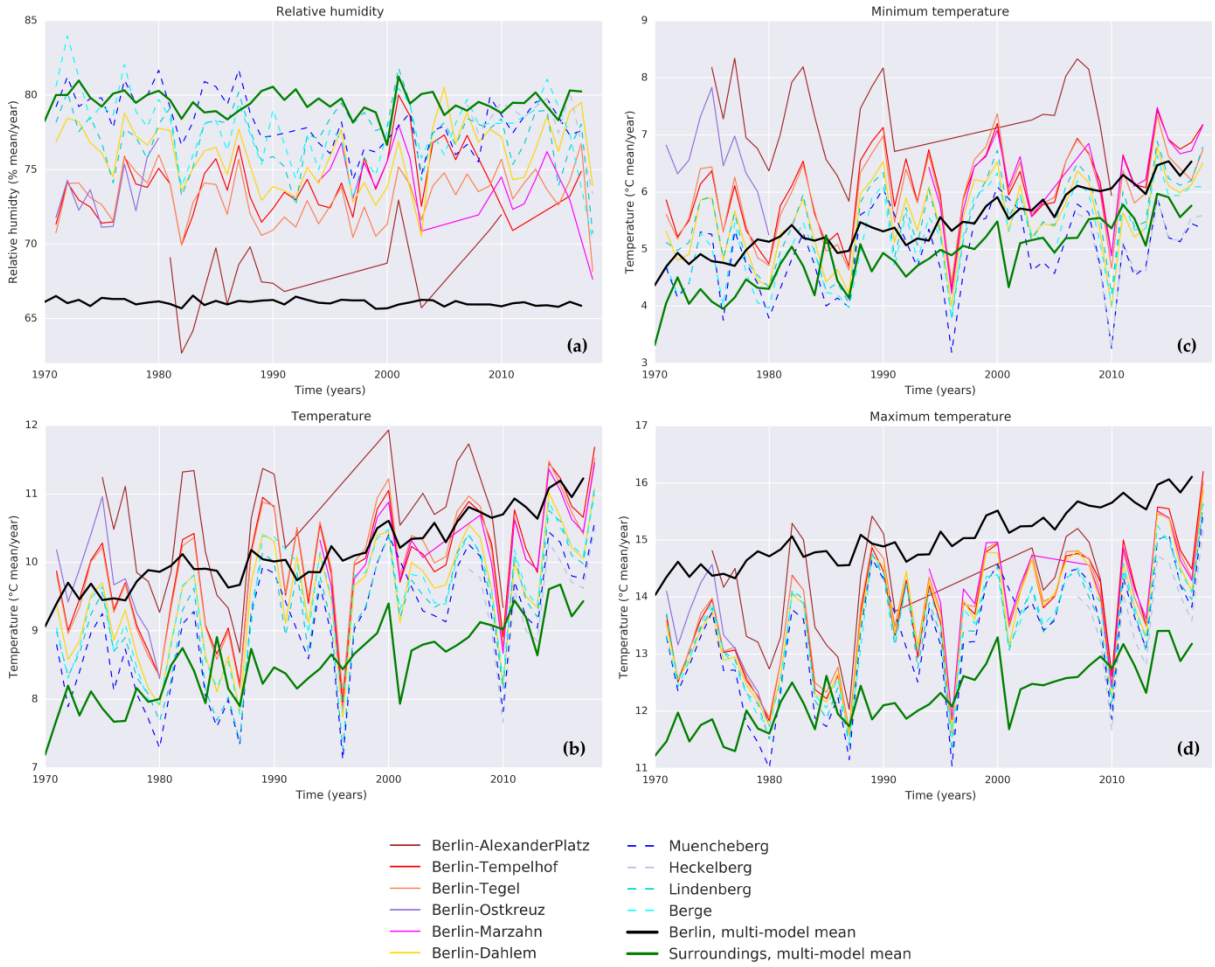

Figure 3. EURO-CORDEX multi-model annual mean compared to observation station data annual mean in Berlin and its surroundings for (**a**) relative humidity, (**b**) temperature, (**c**) minimum temperature, and (**d**) maximum temperature for 1970–2017.

Based on the results presented in Figure 3c,d, there is a need to further understand whether the nighttime and daytime temperature differences between Berlin and its surroundings are adequately simulated by the regional climate models. The EURO-CORDEX community survey (Appendix A, Table A1) indicates that all RCMs represent urban areas in a similar fashion through a 'bulk' parameterization scheme. Hence, each model could be taken as a representative example for the other models. In this case, the REMO model was selected to further investigate the daily cycle because hourly data was directly available. The REMO hourly historic model mean on a daily basis between 1971 and 2000 for January, April, July, and October was compared to the equivalently calculated observational mean averaged over the observational stations in and outside Berlin. The diurnal cycle of the observations shows a daytime temperature maximum and nighttime minimum for both Berlin and its surroundings (Figure 4). Generally, it is during nighttime that the largest difference in temperature between Berlin and its surroundings occurs. For most months the modeled diurnal temperature cycles show a similar curve to the observations. Nonetheless, REMO simulates the largest temperature difference between Berlin and its surroundings during the daytime instead of the nighttime, opposing the observations and leading to an underestimation of the nighttime urban–rural temperature difference (Figure 4).

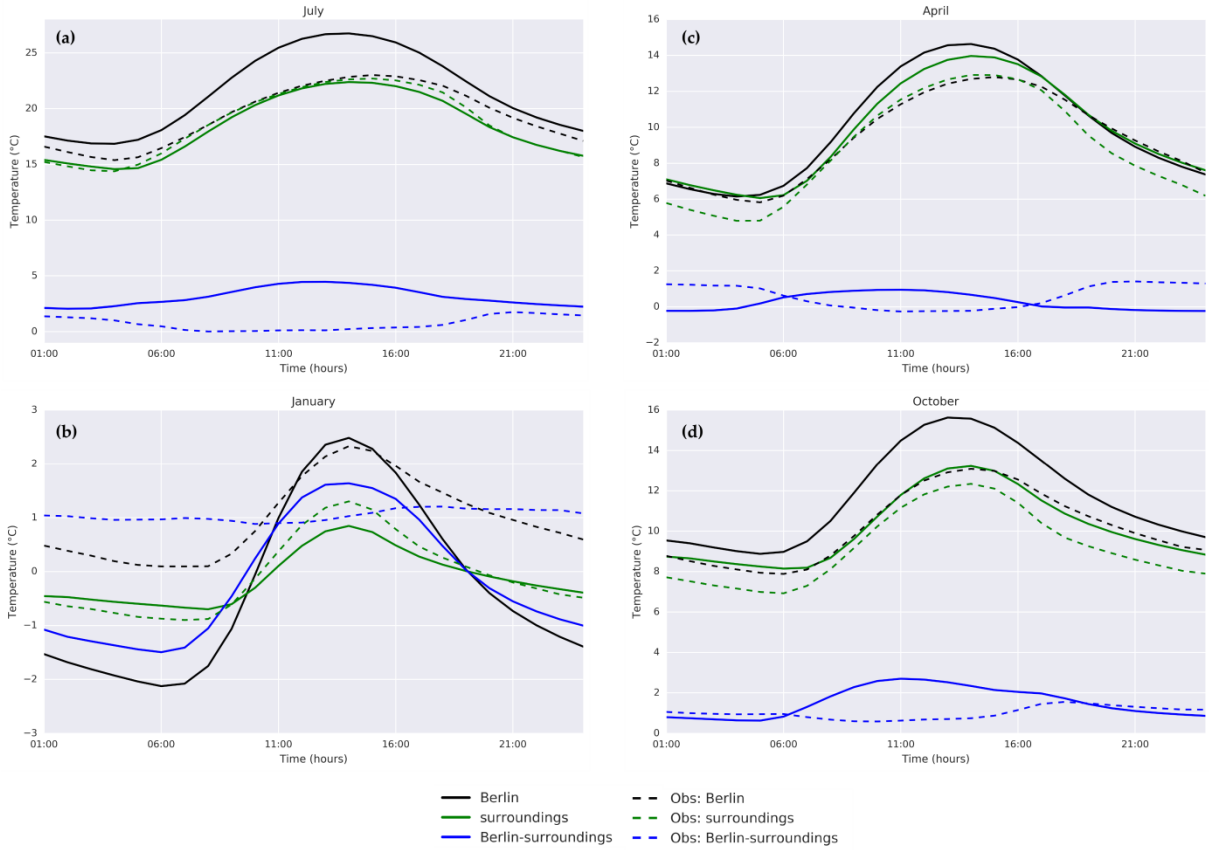

Figure 4. Temperature diurnal cycle. Hourly average between 1971–2000 for the monthly mean of (**a**) July, (**b**) January, (**c**) April, and (**d**) October. The hourly mean of regional climate model REMO (solid lines) is compared to the observational data (dashed lines) for Berlin (black) and its surroundings (green) as well as the hourly mean of the surroundings subtracted from the hourly mean of Berlin (blue).

During January the urban diurnal cycle is exacerbated, with a slightly stronger warming during the day and generally a stronger cooling at night. This is possibly due to long winter nights and short days with limited incoming solar radiation to warm up the urban surface and limited heat storage capacity. In reality, urban areas generally warm up faster than their surroundings and the heat is stored during the day and slowly released at night, leading to a larger temperature difference between a city and its surroundings at nighttime. This is in line with the observational diurnal cycles displayed in Figure 4. Conceivably, as a result of the 'bulk' parameterization scheme, the model is unable to trap the energy adsorbed during the day in the street canyons as heat is only stored in the surface layer with minimal thickness and no heat exchange between city elements is parameterized in the scheme. Additionally, anthropogenic heat is not considered explicitly, further limiting the nocturnal cooling potential of the surface and low atmosphere. Consequently, the model results show a stronger temperature difference between Berlin and its surroundings during daytime, misrepresenting the actual urban–rural largest temperature difference at night measured by the observations.

Similarly to REMO, the other EURO-CORDEX models investigated contain a 'bulk' scheme for urban areas. In this light, REMO can be seen to be representative of the other models and similar results may be expected. To validate the latter, an additional analysis investigates the daily minimum and maximum temperature for each model, comparing Berlin to its surroundings. According to previous studies, the UHI should be larger at night than during the day [67]. The

results of the analysis are presented in Figure 5. Generally, the models do not show the expected outcome. The difference between the minimum temperature in Berlin (urbmin) and the minimum temperature in its surroundings (surrmin) is generally smaller (and in January even reversed) than the difference between the maximum temperature in Berlin (urbmax) compared to the maximum temperature in its surroundings (surrmax). The results for the EURO-CORDEX models are comparable to the results found for REMO. In summary, all EURO-CORDEX models simulate the UHI. However, the models do not simulate the timing of the UHI correctly. The temperature difference between Berlin and its surroundings peaks during the daytime instead of the nighttime.

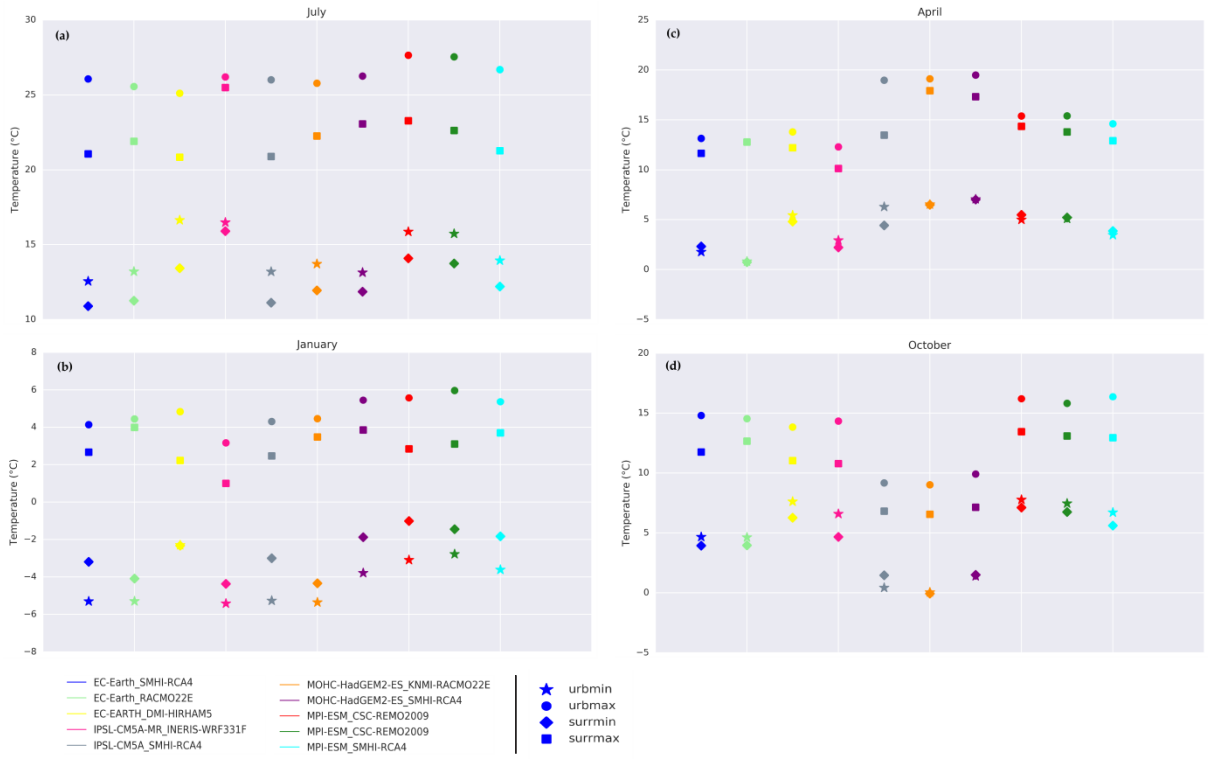

Figure 5. Temperature minimum and maximum for Berlin (urbmin/urbmax) and its surroundings (surrmin/surrmax) for the ten-model combination from the EURO-CORDEX multi-model ensemble. Daily average between 1971–2000 for the monthly mean of (**a**) July, (**b**) January, (**c**) April, and (**d**) October.

3.2. Humidity under Climate Change

As mentioned in the first part of the results section, the models generally indicate a water vapor deficit in Berlin, and it is on the whole warmer in Berlin compared to its surroundings throughout the twenty-first century (Figure 2). With respect to the 30 years running mean, specific humidity and temperatures increase throughout the century, both in Berlin and in its surroundings. For specific humidity, the difference in the multi-model mean between Berlin and its surroundings is constant over time. The temperature difference between Berlin and its surroundings is enlarged during the twenty-first century and is particularly characterized by a stronger warming in Berlin. Relative humidity is directly related to changes in temperature and specific humidity. The temperature increase is larger in Berlin throughout the twenty-first century, causing a decrease in RH in Berlin and a slight RH increase in its surroundings (Figure 2a). Urban areas retain heat better than their rural surroundings. The model results show that this urban heat island effect is likely to be amplified under rising temperatures and climate change conditions. The urban–rural diverging pattern for relative humidity was further analyzed with an MK test. The outcomes of

the MK test show a robust result for Berlin, with 78% of the assessed models agreeing on a significant decreasing monotonic trend in Berlin for relative humidity throughout the century. For the surroundings the model agreement of a significant increasing monotonic trend is only 50% across the models and therefore not robust. For specific humidity, temperature, and minimum and maximum temperature the MK test shows 100% model agreement of a significant increasing trend for Berlin as well as for its surroundings (Appendix A, Table A2).

To enhance understanding of the climate change signal for the studied variables in Berlin and its surroundings, an MWW test was conducted. The MWW test outcome for relative humidity indicates, for the seven models that passed the Levene test, 71% of the models agree that the future distribution (2070–2099) is different from the historical distribution (1971–2000). In other words, the climate change signal in Berlin is robust for relative humidity. Thus, RH would decrease in Berlin under RCP 8.5 climate change conditions in the twenty-first century. For the surroundings, only 25% of the model combinations (eight out of nine passed the Levene test) show a different distribution in the future for relative humidity. Hence, the climate change signal for RH is not robust for the surroundings of Berlin (Appendix A, Table A2). The GCM CM5A-* driven model combinations show a different result for RH than the other model families. The RH decrease in Berlin is not significant for the CM5A-* family and the increase in RH in Berlin's surroundings shows significant results for the MWW test.

To gain insight into the change in the annual cycle under projected climate change in Berlin and its surroundings, the monthly multi-model mean on a decadal basis between 1970 and 2100 was investigated for each variable (Figure 6).

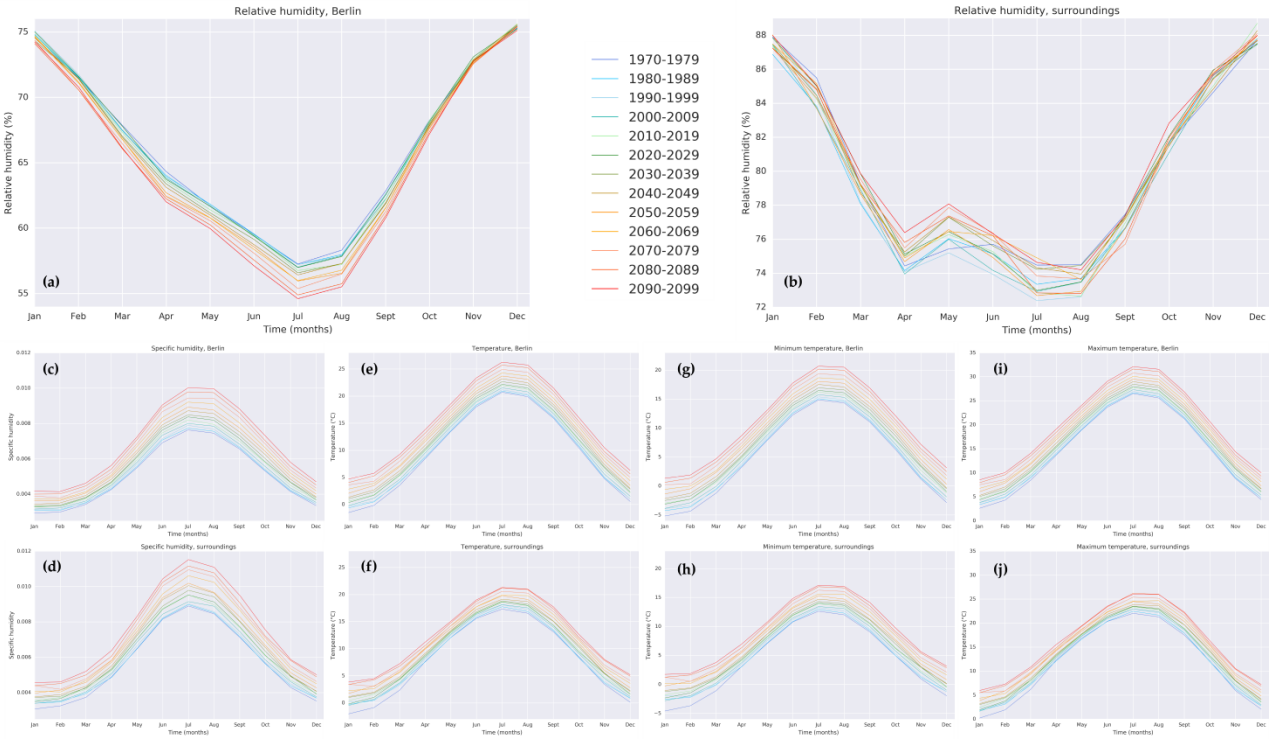

Figure 6. Decadal annual mean cycle for the period 1970–2100 of the EURO-CORDEX multi-model ensemble for RCP 8.5 and for Berlin and its surroundings. The figure shows the outcomes for the different variables: RH (**a**/**b**), SH (**c**/**d**), temperature (**e**/**f**), minimum temperature (**g**/**h**), and maximum temperature (**i**/**j**).

Figure 2 shows that Berlin would get consistently drier (lower RH) than its surroundings throughout the year for each decade, particularly in the summer months (Figure 6a). The strongest RH change would occur in Berlin in the summer months, with an RH decrease of up to 6% in 2090– 2100 compared to 1970–1980 in contrast to hardly any change during the winter months. The up to 6% decrease in relative humidity (RH) in Berlin contrasts with an average RH of about 66% projected by the RCMs (Figure 2a) and an average of about 73% RH measured by suburban stations and 68% RH by the inner-city station (Figure 3a). In addition, the 6% projected decrease in RH is comparable to the model spread of 4–5% (Figure 2a). Climate change has its strongest effect on the RH annual cycle in the summer months. This stronger change pattern in the summer months is also visible for specific humidity throughout the decades and to a lesser extent for temperature, underpinning the RH results. The strong change in the summer months can be explained by the increase in incoming solar radiation in the summer compared to winter, resulting in higher summer temperatures [69,70]. This increase in temperature exacerbates the air moisture deficit in summer, leading to a stronger drying effect in the urban areas in the summer months. An increase in relative humidity in the surroundings of Berlin is visible in May and to a lesser extent in June throughout the twenty-first century. This could be explained by low evaporation, predominantly cloudy skies, and dormant vegetation resulting in increased soil moisture with minimal fluctuations in winter. In spring, around April–May, increased vegetation growth removes moisture from the soil through intensive evapotranspiration, increasing RH in the atmosphere [70,71].

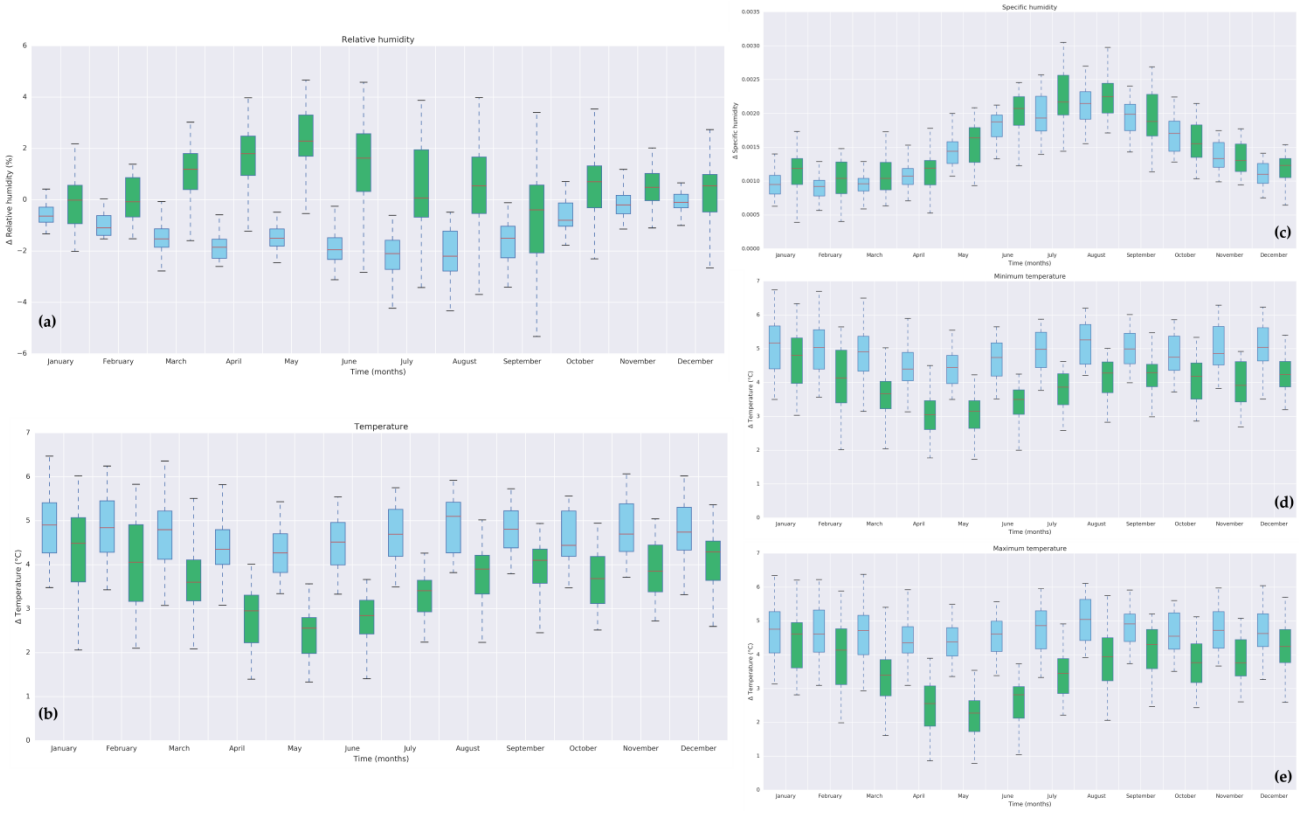

Figure 7. Mean monthly change for each variable under climate change conditions, comparing 1971– 2000 to 2070–2099 for Berlin (grey-blue) and its surroundings (green) for (**a**) RH, (**b**) temperature, (**c**) SH, (**d**) minimum temperature, and (**e**) maximum temperature for RCP 8.5. The multi-model median (red line), quartiles (Q1: 25% and Q3: 75%) and whiskers, including interquartile range (IQR) (1.5 × IQR (IQR = Q3 − Q1)) indicate the model spread.

Figure 7 improves the understanding of the mean monthly change for each variable under climate change conditions, comparing 1971–2000 to 2070–2099. It uses box and whisker plots. In agreement with previous results, Figure 7 shows the strongest RH decrease by the end of the century in the summer months in Berlin of around 2%, in contrast to hardly any change during the winter months. It shows a ~2% increase in relative humidity for the surroundings in spring, which could be a result of the increase in evaporation as mentioned above. The biggest spread among the RCMs occurs in the surroundings and is generally slightly stronger at the end of summer (August– September). This could be due to differences in the available soil moisture in Berlin's surroundings. Because of increased evapotranspiration and decreased precipitation, the soil moisture is expected to be lower in the summer months. During the end of summer and fall the soil moisture recharge phase starts because harvest reduces the biomass and precipitation increases [70,71]. August and September are just on the verge of this phase transition, leading to potentially higher model uncertainties in relative humidity in the surroundings of Berlin.

With respect to temperature, the change between 1971–2000 and 2070–2099 would be around 4– 5 °C in Berlin, with a slightly lower increase in spring (Figure 7). For the surroundings this change would be around 2–3 °C in spring and 3–4.5 °C in the other months. Minimum and maximum temperature would follow a similar monthly change pattern. However, the minimum temperature change would increase slightly more than the maximum temperature, especially in spring and summer, with a difference of around 0.0–0.5 °C for Berlin and around 0.0–0.7 °C for its surroundings.

The model spread is around 2 °C for all temperature variables in Berlin and its surroundings, except for the minimum temperature in the surroundings, which shows a 4–5 °C difference between the models (Figure 2c–e).

In summary, according to the EURO-CORDEX multi-model ensemble data for the RCP 8.5 scenario, Berlin is getting drier and faces a larger temperature increase than its surroundings by the end of the century under climate change conditions, especially in summer.

4. Discussion

All ten EURO-CORDEX model combinations showed a clear difference for humidity and related variables between Berlin and its surroundings. Several previous studies have also demonstrated a temperature difference between an urban area and its surroundings simulated by one or several EURO-CORDEX models [e.g., 10,20,72]. Hence, to our knowledge, this is the first study to take into consideration the EURO-CORDEX multi-model ensemble when analyzing humidity variables for Berlin and its surroundings. Only this approach enables us to derive information on potential future moisture changes in urban areas compared to their surroundings under climate change conditions.

Previous observational studies have investigated moisture differences between a city and its surroundings for past time periods. However, the main focus of many of these studies has been the diurnal cycle and these studies have been based on observational records only. These studies considered a wide range of different methods to analyze moisture, e.g., wet bulb temperature, specific humidity, and water vapor pressure. Throughout the world, in many cities a moisture deficit has been predominantly found (Cairo: 21, Chicago: 22, Christchurch: 23, Edmonton: 24, Lodz: 25, Mexico City: 26, Moscow: 31), but nevertheless urban moisture excess has also been identified primarily in others (Belgrade: 27, Krefeld: 28, London: 29, Szeged: 30). Some cities have shown a daytime urban moisture deficit, mainly because of reduced evapotranspiration and better turbulent mixing in cities and a nocturnal moisture surplus due to continued

evapotranspiration, more anthropogenic moisture sources, and fewer surfaces for condensation. In addition, some cities have shown a moisture deficit in specific months and a surplus in other months. The methods used to measure or derive humidity-related variables vary strongly between the studies. The comparableness is limited among the observational studies as well as to this regional climate model data driven research. Regional climate models are not yet able to represent the complex fine-scale daily humidity cycles described by observational studies. Nevertheless, RCMs are the best tool currently available to understand urban– rural moisture contrasts under climate change during the twenty-first century. As this is one of the first climate model output data studies considering humidity changes under future climate change conditions, further research and comparative studies are needed to gain an improved understanding of commonalities and differences between cities as well as to assess the main generic conclusions.

To our knowledge, this is the first study to derive an increase in the moisture deficit in Berlin compared to its surroundings under climate change conditions throughout the twenty-first century. In line with other studies that have defined the UDI [31,32], it could be concluded that Berlin shows an increasing urban dry island effect under climate change. Additionally, underpinning the findings of the UDI, an increasing UHI was detected in Berlin under climate change conditions throughout the century. An in-depth process understanding study is needed to identify which parameters lead to these results, e.g., evaporation, radiation, and cloudiness, etc. This could further enhance our knowledge of urban–rural interactions under climate change. Additionally, the mean change in the UDI throughout the century could imply a change in extremes, variability, or compound events. These are all interesting topics for further research.

The described UHI for Berlin should be considered with caution. The temperature difference between Berlin and its surroundings for the diurnal cycle, particularly at nighttime, is not represented adequately by the models. Daniel at al. [10] have also found that the nighttime temperature differences between the city and rural areas are underestimated using an RCM with a 'bulk' approach for the city of Paris as well as other urban areas in France. Sophisticated urban schemes would improve the diurnal temperature difference according to Daniel et al. [10]. Further research and incorporation of sophisticated urban schemes in RCMs are required to address the inadequate representation of the UHI by regional climate models. The misrepresentation of the diurnal cycle temperature difference between Berlin and its surroundings implies that no comprehensive conclusions for the daily temperature cycle can be worked out from this research. The models simulate the timing of the temperature difference inadequately on a sub-daily scale. The models capture the mean daily heat budget and urban–rural temperature contrast. The mean climate change trend results could therefore give a plausible indication for the future for temperature and humidity variables. Prior studies have identified a connection between the UHI effect and humidity fluctuations in urban areas [e.g., 21,29,30]. As described previously, the models would be expected to simulate the difference in minimum temperature larger between Berlin and its surroundings, and vice versa for maximum temperature. Based hereupon, the maximum temperature as well as the simulated maximum temperature difference could be overestimated. Higher temperatures lead to an increase in saturated water vapor pressure and therefore decreased relative humidity (following Equation (1)). Due to overestimation of the daytime maximum temperature difference by the models, Berlin might be less dry compared to its surroundings than the models present currently.

Climate models are subject to uncertainties, though it is commonly conceived that multi-model ensemble studies result in a more accurate representation of possible futures than those using one single model, reducing the expected uncertainty of the outcomes of this study [73]. The results of the MWW test show that the driving GCM influences RCM outcomes for urban–rural

contrasts of relative humidity. Further research would be favorable to further improve our understanding of this topic. Taking this into consideration, the results of this research should be treated with caution and only provide an indication of a possible future change of humidity for Berlin compared to its surroundings.

Running the EURO-CORDEX coordinated simulations with sophisticated urban schemes could potentially change and profoundly improve the outcomes of this type of research, in particular with respect to the daily temperature cycle [10]. Furthermore, it would be of high interest to explore whether the climate change signal for relative humidity would change under state-of-the-art convection permitting models to understand whether simulations on higher spatial resolutions would result in an improved representation of climate change impacts in urban areas.

It would also be important to explore the usability of the findings, particularly with respect to relative humidity for different city sectors and to seek an improved understanding of how to tailor information in a useful manner for urban decision makers.

5. Conclusions

Humidity changes under climate change conditions are poorly understood in urban areas. Changes in humidity can alter living conditions for city inhabitants and an increasing need therefore exists to enhance our knowledge. However, many urban models and climate models are currently either not scale compliant for cities and offer only a limited set of climatological parameters, or do not simulate urban–rural interactions. This work aimed to improve understanding of the change in moisture and temperature variables under climate change, ultimately to be able to equip urban decision makers with science-based information to adapt to projected humidity changes. EURO-CORDEX regional climate model simulations (0.11°) were analyzed for RCP 8.5 with a focus on relative and specific humidity, as well as temperature variables, throughout the century for Berlin and its surroundings.

The main results show that Berlin is getting drier and is facing a larger temperature increase than its surroundings towards the end of the century under climate change conditions. This is particularly profound in summer, with a mean decadal RH decrease of up to 6% when comparing 1970–1979 with 2090–2099. Berlin is warming more strongly than its surroundings throughout the entire year, i.e., by ~2° C when comparing 1971–2000 with 2070–2099. This study discloses for the first time that the EURO-CORDEX multi-model ensemble is able to capture a humidity difference between Berlin and its surroundings, as well as quantifies the respective climate change urban–rural trends throughout the century. Additionally, the study also shows limitations of the RCMs in this respect. For the historic climate period (1970–2017), the outcomes are similar between the model simulations and observations, though there is a slight overestimation of the water vapor deficit in Berlin by the models. A comparison between the REMO model and observations for the historic diurnal temperature cycle shows that REMO simulates a larger UHI during daytime. The RCMs are unable to represent the expected dominant nighttime urban heat island effect adequately. This might have profound influence on overall RCM results for urban areas and needs to be addressed in the future. The running mean over 30 years shows a divergence throughout the twenty-first century for relative humidity between Berlin and its surroundings, with Berlin getting drier over time, which was validated by the Mann-Kendall test. The Mann-Whitney-Wilcoxon test for relative humidity indicates a robust climate change signal in Berlin. Berlin is drier and warmer for all months, with the largest difference compared to its surroundings in the summer. Also, the change in humidity in 2070–2099 compared to 1971–2000 is largest in the summer months. In summary, this study shows for the first time an increasing urban dry island under climate change conditions throughout the twenty-first century in Berlin.

Author Contributions: Conceptualization, G.S.L., D.R., and D.J.; data curation, G.S.L.; formal analysis, G.S.L.; investigation, G.S.L.; methodology, G.S.L.; project administration, G.S.L.; resources, G.S.L.; software, G.S.L.; supervision, D.R. and D.J.; validation, G.S.L.; visualization, G.S.L.; writing—original draft, G.S.L.; writing—review and editing, G.S.L., D.R., and D.J.

Funding: This research received no external funding. The research was funded by the Climate Service Center Germany (GERICS), Helmholtz-Zentrum Geesthacht (HZG) as a part of G.S.L's doctorate.

Acknowledgments: We wish to acknowledge the World Climate Research Programme's Working Group on Regional Climate and the Working Group on Coupled Modeling, the former coordinating body of CORDEX and the panel responsible for CMIP5. We also thank the climate modeling groups for producing and making available their model output. The authors acknowledge the contributing climate modeling centers for the EURO-CORDEX simulations and for making them freely available. We also acknowledge the Earth System Grid Federation infrastructure, an international effort led by the US Department of Energy's Program for Climate Model Diagnosis and Intercomparison, the European Network for Earth System Modeling, and other partners in the Global Organization for Earth System Science Portals (GO-ESSP). In addition, we acknowledge the contributions of the EURO-CORDEX regional climate modeling groups to the survey on urban representation in RCMs used for EURO-CORDEX 0.11° simulations. We thank R. Parks for proofreading the manuscript and providing suggestions to improve readability. We wish to acknowledge the reviewers for their valuable feedback that greatly improved the manuscript.

Conflicts of Interest: The authors declare no conflict of interest.

Appendix A

Table A1. EURO-CORDEX community survey outcomes on urban representation in RCMs used for EURO-CORDEX 0.11° simulations.

Name of Institution	Model Versions Used for EURO-CORDEX Simulations on ESGF	Urban Representation	Description and References
Climate Service Center Germany (GERICS)	REMO2009	Bulk	Land-use type urban. Urban is treated as rock surfaces. Roughness length and albedo adjusted. No field capacity, nor vegetation. Fractional approach [49,50].
Swedish Meteorologic al and Hydrological Institute (SMHI)	RCA4	Bulk	Land-use physiography is based on ECOCLIMAP land-surface database [45]. RCA4 includes no further direct reference to urban parameterizations [48].
Royal Netherlands Meteorologic al Institute (KNMI)	RACMO22E	Bulk	RACMO22E is based on CY31r1 Urban fraction based on ECOCLIMAP land-surface database [45]. Dominant tile approach. Roughness lengths and surface interactions adjusted for urban land cover [46].
Danish Meteorologic al Institute (DMI)	HIRHAM5	Bulk	HIRHAM5 [51] includes ECHAM4 [52]. Urban represented through adjusted constant surface parameters.
Institute Pierre Simon Laplache (IPSL)	CM5A-MR- WRF331F	Bulk	The vegetation/soil parameters are adjusted for urban land surface type (e.g., albedo and roughness length) [66] in NOAH-LSM [47]. Urban Canopy model available but not turned on for EURO-CORDEX simulations.
Climate Limit-Area Modeling Community (CLM)	COSMO-CLM	Bulk	Surface land cover type urban. Each sub-grid land cover type is a separate column for energy and water calculations [44]. TERRA-LM is used for EURO-CORDEX simulations.

Table A2. Outcomes of the Mann-Kendall (MK) test, Levene test, and Mann-Whitney-Wilcoxon (MWW) test for relative humidity for Berlin and its surroundings.

		MK Test		Levene Test		MWW Test	
	Model Combination (GCM_RCM)	**Direction**	***p* Value**	***t* Value**	***p* Value**	***t* Value**	***p* Value**
Berlin	EC-EARTH_RCA4	Decreasing	2.58×10^{-06}	0.0003	0.9855	226	0.0002
	EC-EARTH_RACMO22E	Decreasing	3.33×10^{-15}	0.2236	0.6380	156	2.54×10^{-06}
	EC-EARTH_HIRHAM5	No trend	0.8689	0.3136	0.5775	446	0.3161
	CM5A-MR_WRF331F	No trend	0.5196	16.184	0.2082	405	0.1455
	CM5A-MR_RCA4	Decreasing	3.97×10^{-11}	61.218	0.0162	159	3.10×10^{-06}
	HadGEM2_RCA4	Decreasing	5.64×10^{-07}	21.851	0.1446	231	0.0002
	HadGEM2_RACMO22E	Decreasing	0.0000	0.1718	0.6800	40	2.92×10^{-10}
	MPI-ESM-LR_REMO2009(r1)	Decreasing	2.22×10^{-16}	57.208	0.0199	80	8.94×10^{-09}
	MPI-ESM-LR_REMO2009(r2)	Decreasing	4.88×10^{-14}	24.869	0.1201	102	5.14×10^{-08}
Surroundings	EC-EARTH_RCA4	No trend	0.3124	91.139	0.0037	447	0.3211
	EC-EARTH_RACMO22E	No trend	0.7353	29.544	0.0908	474	0.4663
	EC-EARTH_HIRHAM5	Increasing	0.0329	0.4255	0.5167	372	0.0642
	CM5A-MR_WRF331F	Increasing	0.0061	0.6487	0.4238	331	0.0180
	CM5A-MR_RCA4	Increasing	0.0001	0.3001	0.5858	227	0.0002
	HadGEM2_RCA4	Increasing	0.0225	0.0003	0.9870	364	0.0512
	HadGEM2_RACMO22E	No trend	0.7967	0.0299	0.8632	460	0.3891
	MPI-ESM-LR_REMO2009(r1)	No trend	0.4589	0.0414	0.8395	452	0.3467
	MPI-ESM-LR_REMO2009(r2)	No trend	0.8154	0.0099	0.9212	462	0.4000

Table A3. Standard deviation for each model combination and for the investigated variables calculated over the annual mean for the period 1970–2016.

		Variables				
	Model Combination (GCM_RCM)	**RH** (%)	**SH** (-)	**Tas** (°C)	**Tasmax** (°C)	**Tasmin** (°C)
Berlin	EC-EARTH_RCA4	0.80	0.00017	0.60	0.59	0.62
	EC-EARTH_RACMO22E	0.76	0.00017	0.62	0.60	0.64
	EC-EARTH_HIRHAM5	0.46	0.00013	0.48	0.46	0.52
	CM5A-MR_WRF331F	0.55	0.00022	0.85	0.83	0.88
	CM5A-MR_RCA4	0.58	0.00021	0.79	0.80	0.78
	HadGEM2_RCA4	0.61	0.00019	0.71	0.71	0.71
	HadGEM2_RACMO22E	0.71	0.00021	0.78	0.77	0.79
	MPI-ESM-LR_REMO2009(r1)	0.72	0.00014	0.47	0.47	0.49
	MPI-ESM-LR_REMO2009(r2)	0.68	0.00014	0.52	0.54	0.54
Surroundings	EC-EARTH_RCA4	1.83	0.00026	0.75	0.79	0.78
	EC-EARTH_RACMO22E	1.64	0.00024	0.82	0.83	0.80
	EC-EARTH_HIRHAM5	1.51	0.00021	0.79	0.80	0.81
	CM5A-MR_WRF331F	2.14	0.00029	1.34	1.35	1.38
	CM5A-MR_RCA4	1.56	0.00030	1.09	1.20	1.04
	HadGEM2_RCA4	2.39	0.00030	0.99	1.14	0.90
	HadGEM2_RACMO22E	1.98	0.00025	1.06	1.08	1.06
	MPI-ESM-LR_REMO2009(r1)	1.88	0.00026	0.71	0.77	0.72
	MPI-ESM-LR_REMO2009(r2)	2.11	0.00023	0.82	0.87	0.86

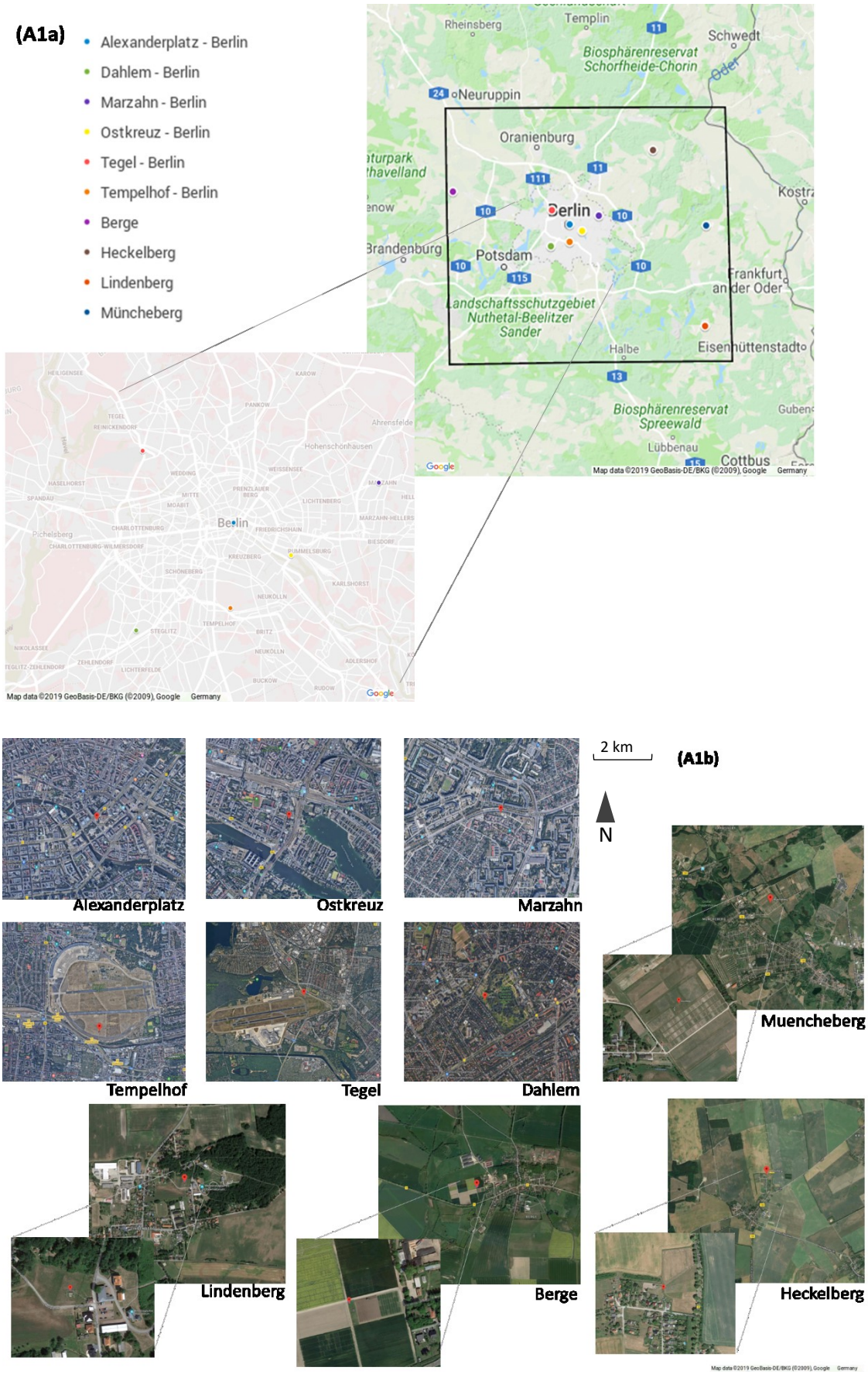

Figure A1. Locations of observational stations (**a**) and their surrounding environments (**b**). Map data from 2019 GeoBasis DE/BKG, Google, Germany.

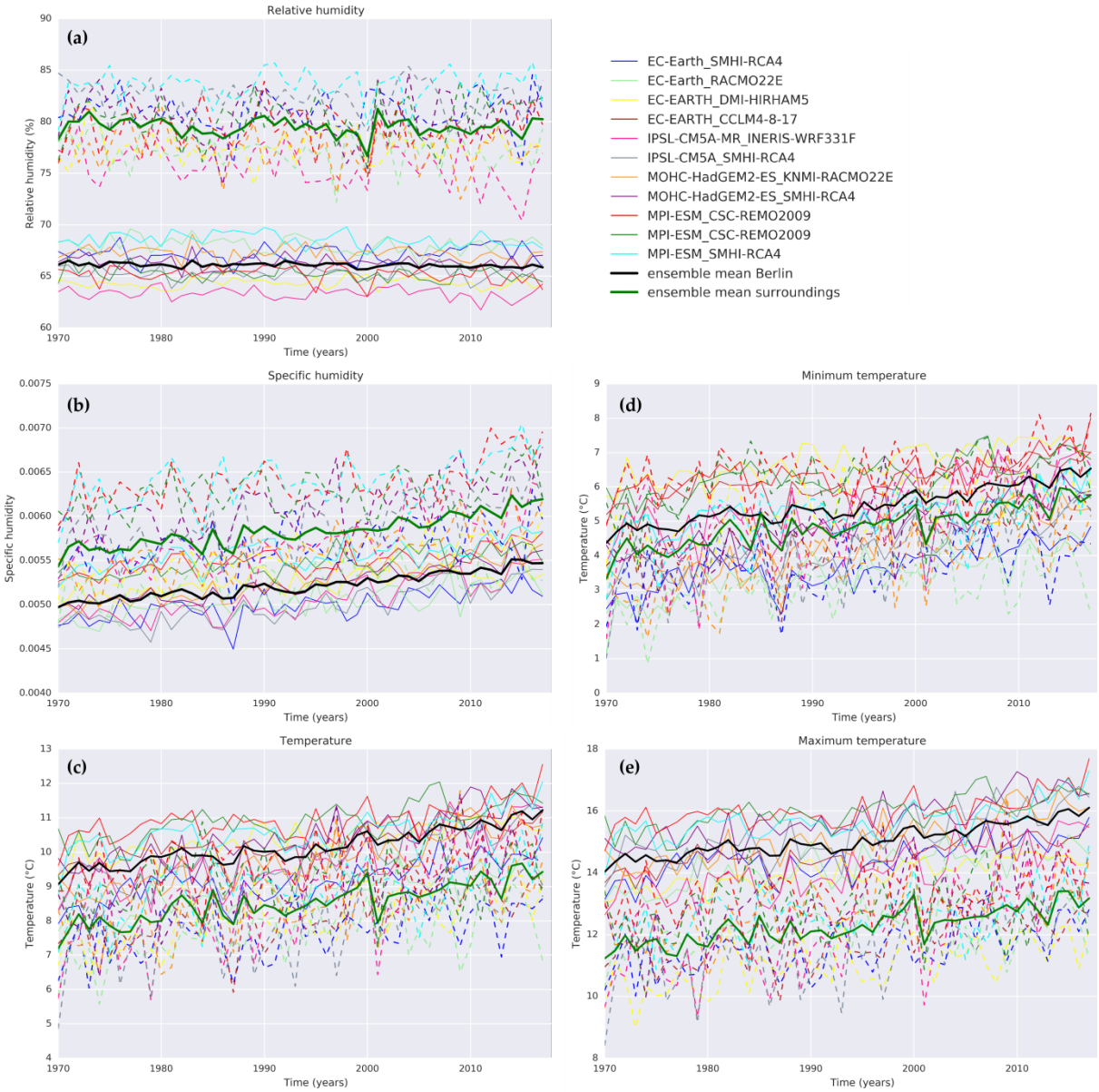

Figure A2. Yearly mean for each model of the EURO-CORDEX multi-model ensemble compared to the multi-model mean for 1970–2017. The variables presented are (**a**) relative humidity, (**b**) specific humidity, (**c**) temperature, (**d**) minimum temperature, and (**e**) maximum temperature.

References

1. UN-HABITAT. *Urbanization and Development: Emerging Futures World Cities Report 2016*. United Nations Human Settlements Programme (UN-Habitat), Nairobi, Kenya. 2016, doi:10.1016/S0264-2751(03)00010-6.
2. ONU. New Urban Agenda. In *Health Visit;* United Nations Habitat III, Geneva, Switzerland; 2017; ISBN 978-92-1-132757-1.
3. Rosenzweig, C.; Solecki, W.; Romero-Lankao, P.; Mehrotra, S.; Dhakal, S.; Bowman, T.; Ibrahim, S.A. Climate Change and Cities: Second Assessment Report of the Urban Climate Change Research Network. In *Climate Change and Cities*; Cambridge University Press, 2018; doi:10.1017/9781316563878.007.
4. Baklanov, A.; Grimmond, C.S.B.; Carlson, D.; Terblanche, D.; Tang, X.; Bouchet, V.; Lee, B.; Langendijk, G.; Kolli, R.K.; Hovsepyan, A. From Urban Meteorology, Climate and Environment Research to Integrated City Services. *Urban Clim.* **2018**, *23*, 330–341, doi:10.1016/j.uclim.2017.05.004.
5. Grimmond, C.S.B.; Roth, M.; Oke, T.R.; Au, Y.C.; Best, M.; Betts, R.; Carmichael, G.; Cleugh, H.; Dabberdt, W.; Emmanuel, R.; et al. Climate and More Sustainable Cities: Climate Information for Improved Planning and Management of Cities (Producers/Capabilities Perspective). *Procedia Environ. Sci.* **2010**, *1*, 247–274, doi:10.1016/j.proenv.2010.09.016.
6. Bai, X.; Dawson, R.J.; Ürge-Vorsatz, D.; Delgado, G.C.; Salisu Barau, A.; Dhakal, S.; Dodman, D.; Leonardsen, L.; Masson-Delmotte, V.; Roberts, D.C.; et al. Six Research Priorities for Cities and Climate Change. *Nature* **2018** , *555*, 23–25, doi:10.1038/d41586-018-02409-z.

7. Jacob, D.; Petersen, J.; Eggert, B.; Alias, A.; Christensen, O.B.; Bouwer, L.M.; Braun, A.; Colette, A.; Déqué, M.; Georgievski, G.; et al. EURO-CORDEX: New High-Resolution Climate Change Projections for European Impact Research. *Reg. Environ. Chang.* **2014**, *14*, 563–578, doi:10.1007/s10113-013-0499-2.
8. Giorgi, F.; Gutowski, W.J. Regional Dynamical Downscaling and the CORDEX Initiative. *Annu. Rev. Environ. Resour.* **2015**, *40*, 467–490, doi:10.1146/annurev-environ-102014-021217.
9. Gutowski, J.W.; Giorgi, F.; Timbal, B.; Frigon, A.; Jacob, D.; Kang, H.S.; Raghavan, K.; Lee, B.; Lennard, C.; Nikulin, G.; et al. WCRP COordinated Regional Downscaling EXperiment (CORDEX): A Diagnostic MIP for CMIP6. *Geosci. Model Dev.* **2016,** *9*, 4087–4095, doi:10.5194/gmd-9-4087-2016.
10. Daniel, M.; Lemonsu, A.; Déqué, M.; Somot, S.; Alias, A.; Masson, V. Benefits of Explicit Urban Parameterization in Regional Climate Modeling to Study Climate and City Interactions. In *Climate Dynamics*; Springer: Berlin, Germany, 2018; pp. 1–20, doi:10.1007/s00382-018-4289-x.
11. Chen, F.; Kusaka, H.; Bornstein, R.; Ching, J.; Grimmond, C.S.B.; Grossman-Clarke, S.; Loridan, T.; Manning, K.W.; Martilli, A.; Miao, S.; et al. The Integrated WRF/Urban Modelling System: Development, Evaluation, and Applications to Urban Environmental Problems. *Int. J. Climatol.* **2011**, *31*, 273–288, doi:10.1002/joc.2158.
12. Trusilova, K.; Schubert, S.; Wouters, H.; Früh, B.; Grossman-Clarke, S.; Demuzere, M.; Becker, P. The Urban Land Use in the COSMO-CLM Model: A Comparison of Three Parameterizations for Berlin. *Meteorol. Z.* **2016**, *25*, 231–244, doi:10.1127/metz/2015/0587.
13. Best, M.J.; Grimmond, C.S.B. Analysis of the Seasonal Cycle Within the First International Urban Land-Surface Model Comparison. *Bound. Layer Meteorol.* **2013**, *146*, 421–446, doi:10.1007/s10546-012-9769-7.
14. Best, M.J.; Grimmond, C.S.B. Investigation of the Impact of Anthropogenic Heat Flux within an Urban Land Surface Model and PILPS-Urban. *Theor. Appl. Climatol.* **2016**, *126*, 51–60, doi:10.1007/s00704-015-1554-3.
15. Masson, V. Urban Surface Modeling and the Meso-Scale Impact of Cities. *Theor. Appl. Climatol.* **2006**, *84*, 35–45, doi:10.1007/s00704-005-0142-3.
16. Karlický, J.; Huszár, P.; Halenka, T.; Belda, M.; Žák, M.; Pišoft, P.; Mikšovský, J. Multi-Model Comparison of Urban Heat Island Modelling Approaches. *Atmos. Chem. Phys.* **2018**, *18*, 10655–10674, doi:10.5194/acp-18-10655-2018.
17. De Ridder, K.; Lauwaet, D.; Maiheu, B. UrbClim—A Fast Urban Boundary Layer Climate Model. *Urban Clim.* **2015**, *12*, 21–48, doi:10.1016/j.uclim.2015.01.001.
18. Huszar, P.; Halenka, T.; Belda, M.; Zak, M.; Sindelarova, K.; Miksovsky, J. Regional Climate Model Assessment of the Urban Land-Surface Forcing over Central Europe. *Atmos. Chem. Phys.* **2014**, *14*, 12393– 12413, doi:10.5194/acp-14-12393-2014.
19. Lauwaet, D.; Hooyberghs, H.; Maiheu, B.; Lefebvre, W.; Driesen, G.; Van Looy, S.; De Ridder, K. Detailed Urban Heat Island Projections for Cities Worldwide: Dynamical Downscaling CMIP5 Global Climate Models. *Climate* **2015**, *3*, 391–415, doi:10.3390/cli3020391.
20. Wiesner, S.; Bechtel, B.; Fischereit, J.; Gruetzun, V.; Hoffmann, P.; Leitl, B.; Rechid, D.; Schlünzen, K.; Thomsen, S. Is It Possible to Distinguish Global and Regional Climate Change from Urban Land Cover Induced Signals? A Mid-Latitude City Example. *Urban Sci.* **2018**, *2*, 12, doi:10.3390/urbansci2010012.
21. Robaa, S.M. Urban-Suburban/Rural Differences over Greater Cairo, Egypt. *Atmosfera* **2003**, *16*, 157–171.
22. Ackerman, B. Climatology of Chicago Area Urban-Rural Differences in Humidity. *J. Clim. Appl. Meteorol.* **2002**, *26*, 427–430, doi:10.1175/1520-0450 (1987).
23. Tapper, N.J. Urban Influences on Boundary Layer Temperature and Humidity: Results from Christchurch, New Zealand. *Atmos. Environ. Part B Urban Atmos.* **1990**, *24*, 19–27, doi:10.1016/0957-1272(90)90005-F.
24. Hage, K.D. Urban-Rural Humidity Differences. *J. Appl. Meteorol.* **1975**, *14*, 1277–1283, doi:10.1175/1520-0450 (1975).
25. Fortuniak, K.; Kłysik, K.; Wibig, J. Urban—Rural Contrasts of Meteorological Parameters in Łódź. *Theor. Appl. Climatol.* **2006**, *84*, 91–101, doi:10.1007/s00704-005-0147-y.
26. Jåuregui, E.; Tejeda, A. Urban-Rural Humidity Contrasts in Mexico City. *Int. J. Climatol.* **1997**, *17*, 187–196, doi:10.1002/(SICI)1097-0088(199702)17:2.
27. Unkašević, M.; Jovanović, O.; Popović, T. Urban-Suburban/Rural Vapour Pressure and Relative Humidity Differences at Fixed Hours over the Area of Belgrade City. *Theor. Appl. Climatol.* **2001**, *68*, 67–73, doi:10.1007/s007040170054.
28. Kuttler, W.; Weber, S.; Schonnefeld, J.; Hesselschwerdt, A. Urban/Rural Atmospheric Water Vapour Pressure Differences and Urban Moisture Excess in Krefeld, Germany. *Int. J. Climatol.* **2007**, *27*, 2005–2015, doi:10.1002/joc.1558.
29. Lee, D.O. Urban–Rural Humidity Differences in London. *Int. J. Climatol.* **1991**, *11*, 577–582, doi:10.1002/joc.3370110509.
30. Unger, J. Urban-Rural Air Humidity Differences in Szeged, Hungary. *Int. J. Climatol.* **1999**, *19*, 1509–1515, doi:10.1002/(SICI)1097-0088(19991115)19:13.
31. Lokoshchenko, M.A. Urban Heat Island and Urban Dry Island in Moscow and Their Centennial Changes. *J. Appl. Meteorol. Climatol.* **2017**, *56*, 2729–2745, doi:10.1175/JAMC-D-16-0383.1.
32. Moriwaki, R.; Watanabe, K.; Morimoto, K. Urban dry island phenomenon and its impact on cloud base level. *J. JSCE* **2013**, *1*, 521–529, doi:10.2208/journalofjsce.1.1_521.

33. Coccolo, S.; Kämpf, J.; Scartezzini, J.L.; Pearlmutter, D. Outdoor Human Comfort and Thermal Stress: A Comprehensive Review on Models and Standards. In *Urban Climate*; Elsevier B.V.: Amsterdam, The Netherlands, 2016; pp. 33–57, doi:10.1016/j.uclim.2016.08.004.
34. Chiabai, A.; Quiroga, S.; Martinez-Juarez, P.; Higgins, S.; Taylor, T. The Nexus between Climate Change, Ecosystem Services and Human Health: Towards a Conceptual Framework. *Sci. Total Environ.* **2018**, *635*, 1191–1204, doi:10.1016/j.scitotenv.2018.03.323.
35. Rohat, G.; Flacke, J.; Dosio, A.; Dao, H.; van Maarseveen, M. Projections of Human Exposure to Dangerous Heat in African Cities Under Multiple Socioeconomic and Climate Scenarios. *Earth's Futur* **2019**, *7*, 528– 546, doi:10.1029/2018EF001020.
36. Abuku, M.; Janssen, H.; Roels, S. Impact of Wind-Driven Rain on Historic Brick Wall Buildings in a Moderately Cold and Humid Climate: Numerical Analyses of Mould Growth Risk, Indoor Climate and Energy Consumption. *Energy Build.* **2009**, *41*, 101–110, doi:10.1016/j.enbuild.2008.07.011.
37. Blocken, B.; Carmeliet, J. A Review of Wind-Driven Rain Research in Building Science. *J. Wind Eng. Ind. Aerodyn.* **2004**, *92*, 1079–1130, doi:10.1016/j.jweia.2004.06.003.
38. Elmqvist, T.; Goodness, J.; Marcotullio, P.J.; Parnell, S.; Sendstad, M.; Wilkinson, C.; Fragkias, M.; Güneralp, B.; McDonald, R.I.; Schewenius, M.; et al. *Urbanization, Biodiversity and Ecosystem Services: Challenges and Opportunities: A Global Assessment*; Springer: Heidelberg, Germany, 2013, doi:10.1007/978-94-007-7088-1.
39. Lahr, E.C.; Dunn, R.R.; Frank, S.D. Getting Ahead of the Curve: Cities as Surrogates for Global Change. *Proc. R. Soc. B Biol. Sci.* **2018**, *285*, 20180643, doi:10.1098/rspb.2018.0643.
40. Amt für Statistik Berlin-Brandenburg. Statistiken Berlin und Brandenburg. Available online: https://www.statistik-berlin-brandenburg.de/statistiken/Inhalt-Statistiken.asp (accessed on 26 July 2019).
41. Statistiken Berlin und Brandenburg Flaechenutzung. Available online: https://www.statistik-berlin-brandenburg.de/BasisZeitreiheGrafik/Bas-Flaechennutzung.asp?Ptyp=300&Sageb=33000&creg=BBB&anzwer=6 (accessed on 10 June 2019).
42. EEA. *The Revised and Supplemented Corine Land Cover Nomenclature*, *EEA Technical Report No. 40*; European Environment Agency, Copehagen, Denmark; 2000.
43. German Climate Computing Centre (DKRZ); Earth System Grid Federation (ESGF); World Climate Research programme (WCRP); Coordinated Regional Climate Downscaling Experiment (CORDEX); G.C.C. Earth System Grid Federation WCRP CORDEX Data Node. Available online: https://esgf-data.dkrz.de/search/cordex-dkrz/ (accessed on 20 November 2018).
44. Rockel, B.; Will, A.; Hense, A. The Regional Climate Model COSMO-CLM (CCLM). *Meteorol. Z.* **2008**, *17*, 347–348, doi:10.1127/0941-2948/2008/0309.
45. Masson, V.; Champeaux, J.L.; Chauvin, F.; Meriguet, C.; Lacaze, R. A Global Database of Land Surface Parameters at 1-Km Resolution in Meteorological and Climate Models. *J. Clim.* **2003**, *16*, 1261–1282, doi:10.1175/1520-0442-16.9.1261.
46. Van Meijgaard, E.; Van Ulft, L.H.; Van De Berg, W.J.; Bosveld, F.C.; Van Den Hurk, B.J.J.M.; Lenderink, G.; Siebesma, A.P. *The KNMI Regional Atmospheric Climate Model RACMO* Version 2.1; Koninklijk Nederlands Meteorologisch Instituut (KNMI), de Bilt, the Netherlands. 2008.
47. Niu, G.Y.; Yang, Z.L.; Mitchell, K.E.; Chen, F.; Ek, M.B.; Barlage, M.; Kumar, A.; Manning, K.; Niyogi, D.; Rosero, E.; et al. The Community Noah Land Surface Model with Multiparameterization Options (Noah-MP): 1. Model Description and Evaluation with Local-Scale Measurements. *J. Geophys. Res. Atmos.* **2011**, *116*, doi:10.1029/2010JD015139.
48. Samuelsson, P.; Jones, C.G.; Willén, U.; Ullerstig, A.; Gollvik, S.; Hansson, U.; Jansson, C.; Kjellström, E.; Nikulin, G.; Wyser, K. The Rossby Centre Regional Climate Model RCA3: Model Description and Performance. *Tellus Ser. A Dyn. Meteorol. Oceanogr.* **2011**, *63*, 4–23, doi:10.1111/j.1600-0870.2010.00478.x.
49. Jacob, D.; Elizalde, A.; Haensler, A.; Hagemann, S.; Kumar, P.; Podzun, R.; Rechid, D.; Remedio, A.R.; Saeed, F.; Sieck, K.; et al. Assessing the Transferability of the Regional Climate Model REMO to Different Coordinated Regional Climate Downscaling Experiment (CORDEX) Regions. *Atmosphere (Basel)* **2012**, *3*, 181–199, doi:10.3390/atmos3010181.
50. Jacob, D.; Podzun, R. Sensitivity Studies with the Regional Climate Model REMO. *Meteorol. Atmos. Phys.* **1997**, *63*, 119–129, doi:10.1007/BF01025368.
51. Christensen, O.B.; Drews, M.; Christensen, J.H.; Dethloff, K.; Ketelsen, K.; Hebestadt, I.; Rinke, A. *The HIRHAM Regional Climate Model Version 5 (Beta)*, *Technical Report 06-17*; Danish Climate Center (DMI), Copenhagen, Denmark. 2007.
52. Roeckner, E.; Arpe, K.; Bengtsson, L.; Christoph, M.; Claussen, M.; Dümenil, L.; Esch, M.; Giorgetta, M.A.; Schlese, U.; Schulzweida, U. *The Atmospheric General Circulation Model Echam-4: Model Description and Simulation of Present-Day Climate*; Max-Planck-Institut für Meteorologie: Hamburg, Germany. 1996.
53. Deutsche Wetter Dienst (DWD). German Weather Service, Climate Data Center (CDC). Available online: https://cdc.dwd.de/portal/ (accessed on 25 January 2019).
54. DWD Climate Data Center (CDC): Annual Mean of Station Observations of Relative Humidity at 2 m above Ground in %, Version V18.3. Available online: https://cdc.dwd.de/portal/ (accessed on 20 May 2019).
55. DWD Climate Data Center (CDC): Annual Mean of Station Observations of Daily Air Temperature Minimum at 2 m above Ground in °C (for TasMin), Version V18.3. Available online: https://cdc.dwd.de/portal/ (accessed on 20 May 2019).

56. DWD Climate Data Center (CDC): Annual Mean of Station Observations of Daily Air Temperature Maximum at 2 m above Ground in °C (for TasMax), Version V18.3. Available online: https://cdc.dwd.de/portal/ (accessed on 20 May 2019).
57. DWD Climate Data Center (CDC): Annual Mean of Station Observations of Air Temperature at 2 m above Ground in °C (for Tas), Version V18.3. Available online: https://cdc.dwd.de/portal/ (accessed on 20 May 2019).
58. Hass, A.L.; Ellis, K.N.; Mason, L.R.; Hathaway, J.M.; Howe, D.A. Heat and Humidity in the City: Neighborhood Heat Index Variability in a Mid-Sized City in the Southeastern United States. *Int. J. Environ. Res. Public Health* **2016**, *13*, 117, doi:10.3390/ijerph13010117.
59. van Vuuren, D.P.; Edmonds, J.; Kainuma, M.; Riahi, K.; Thomson, A.; Hibbard, K.; Hurtt, G.C.; Kram, T.; Krey, V.; Lamarque, J.F.; et al. The Representative Concentration Pathways: An Overview. *Clim. Chang.* **2011**, *102*, 5, doi:10.1007/s10584-011-0148-z.
60. Hennemuth, B.; Bender, S.; Bülow, K.; Dreier, N.; Keup-Thiel, E.; Krüger, O.; Mudersbach, C.; Radermacher, C.; Schoetter, R. Statistical Methods for the Analysis of Simulated and Observed Climate Data Applied in Projects and Institutions Dealing with Climate Change Impact and Adaptation. *CSC Rep.* **2013**, *13*, 1–135.
61. Mann, H.B. Nonparametric Tests Against Trend. *Econometrica* **1945**, *13*, 245–259. doi:10.2307/1907187.
62. Kendall, M.G. Rank Correlation Methods. By Maurice G. Kendall, M.A. [Pp. Vii + 160. London: Charles Griffin and Co. Ltd., 42 Drury Lane, 1948. 18 S]. *J. Inst. Actuar.* **1949**, *75*, 140–141, doi:10.1017/s0020268100013019.
63. Pfeifer, S.; Bülow, K.; Gobiet, A.; Hänsler, A.; Mudelsee, M.; Otto, J.; Rechid, D.; Teichmann, C.; Jacob, D. Robustness of Ensemble Climate Projections Analyzed with Climate Signal Maps: Seasonal and Extreme Precipitation for Germany. *Atmosphere (Basel)* **2015**, *6*, 677–698, doi:10.22444/IBVS.6227_old.
64. Brown, M.B.; Forsythe, A.B. Robust Tests for the Equality of Variances. *J. Am. Stat. Assoc.* **1974**, *69*, 364–367, doi:10.1080/01621459.1974.10482955.
65. DWD Climate Data Center (CDC): Hourly Station Observations of Air Temperature at 2 m above Ground in °C, Version V18.3. Available online: https://cdc.dwd.de/portal/ (accessed on 10 April 2019).
66. Skamarock, W.C.; Klemp, J.B.; Dudhia, J.; Gill, D.O.; Barker, D.M.; Duda, M.G.; Huang, X.-Y.; Wang, W.; Powers, J.G. *A Description of the Advanced Research WRF* Version 3; National Center for Atmospheric Research, Boulder, Colorado, USA. 2008.
67. Li, H.; Zhou, Y.; Li, X.; Meng, L.; Wang, X.; Wu, S.; Sodoudi, S. A New Method to Quantify Surface Urban Heat Island Intensity. *Sci. Total Environ.* **2018**, *624*, 262–272, doi:10.1016/j.scitotenv.2017.11.360.
68. Zhou, B. *On The Assessment Of Surface Urban Heat Island: Size, Urban Form, and Seasonality*; Institutional Repository of the University of Potsdam: Potsdam, Germany, 2017.
69. Li, H.; Meier, F.; Lee, X.; Chakraborty, T.; Liu, J.; Schaap, M.; Sodoudi, S. Interaction between Urban Heat Island and Urban Pollution Island during Summer in Berlin. *Sci. Total Environ.* **2018**, *636*, 818–828, doi:10.1016/j.scitotenv.2018.04.254.
70. Wang, L.; Gao, Z.; Miao, S.; Guo, X.; Sun, T.; Liu, M.; Li, D. Contrasting Characteristics of the Surface Energy Balance between the Urban and Rural Areas of Beijing. *Adv. Atmos. Sci.* **2015**, *32*, 505–514, doi:10.1007/s00376-014-3222-4.
71. Illston, B.G.; Basara, J.B.; Crawford, K.C. Seasonal to Interannual Variations of Soil Moisture Measured in Oklahoma. *Int. J. Climatol.* **2004**, *24*, 1883–1896, doi:10.1002/joc.1077.
72. Jänicke, B.; Meier, F.; Fenner, D.; Fehrenbach, U.; Holtmann, A.; Scherer, D. Urban–Rural Differences in near-Surface Air Temperature as Resolved by the Central Europe Refined Analysis (CER): Sensitivity to Planetary Boundary Layer Schemes and Urban Canopy Models. *Int. J. Climatol.* **2017**, *37*, 2063–2079, doi:10.1002/joc.4835.
73. Christensen, J.H.; Carter, T.R.; Rummukainen, M.; Amanatidis, G. Evaluating the Performance and Utility of Regional Climate Models: The PRUDENCE Project. *Clim. Chang.* **2007**, *81*, 1–6, doi:10.1007/s10584-006-9211-6.

Chapter 3.2.

Added value of convection-permitting simulations for understanding future urban humidity extremes: case studies for Berlin and its surroundings

Gaby S. Langendijk, Diana Rechid, Kevin Sieck, Daniela Jacob

Paper 2

Weather and Climate Extremes 33 (2021) 100367

Contents lists available at ScienceDirect

Weather and Climate Extremes

journal homepage: www.elsevier.com/locate/wace

Added value of convection-permitting simulations for understanding future urban humidity extremes: case studies for Berlin and its surroundings

G.S. Langendijk[a,b]*, D. Rechid[a], K. Sieck[a], D. Jacob[a,b]

[a] *Climate Service Center Germany (GERICS), Helmholtz-Zentrum Hereon, Fischertwiete 1, 20095 Hamburg, Germany*
[b] *Faculty of Sustainability, Leuphana University of Lüneburg, Universitatsallee 1, 21335 Lüneburg, Germany*

ARTICLE INFO

Keywords:
Urban-rural contrasts Humidity
Future climate extremes
Regional climate modelling
Convection permitting

ABSTRACT

Climate extremes affected cities and their populations during the last decades. Future climate projections indicate climate extremes will increasingly impact urban areas during the 21st century. Humidity related fluctuations and extremes directly underpin convective processes, as well as can influence human health conditions. Regional climate models are a powerful tool to understand regional-to-local climate change processes for cities and their surroundings. Convection-permitting regional climate models, operating on very high resolutions, indicate improved simulation of convective extremes, particularly on sub-daily timescales and in regions with complex terrain such as cities. This research aims to understand how crossing spatial resolutions from ~12.5 km to ~3 km grid size affect humidity extremes and related variables under future climate change for urban areas and its surroundings. Taking Berlin and its surroundings as the case study area, the research identifies two categories of unprecedented future extreme atmospheric humidity conditions happening under 1.5 °C and 2.0 °C mean warming based on statistical distributions, respectively near surface specific humidity >0.02 kg/kg and near surface relative humidity <30%. Two example cases for each future extreme condition are dynamically downscaled for a two months period from the 0.44° horizontal resolution following a double-nesting approach: first to the 0.11° (~12.5 km) horizontal resolution with the regional climate model REMO and thereafter to the 0.0275° (~3 km) horizontal resolution with the non-hydrostatic version of REMO. The findings show that crossing spatial resolutions from ~12.5 km to ~3 km grid size affects humidity extremes and related variables under climate change. Generally, a stronger decrease in moisture (up to 0.0007–0.005 kg/kg SH and 10–20% RH) and an increase in temperature (1–2 °C) is found on the 0.0275° compared to the 0.11° horizontal resolution, which is more profound in Berlin than in the surroundings. The convection-permitting scale mitigates the specific humidity moist extreme and intensifies the relative humidity dry extreme in Berlin, posing challenges with respect to health for urban dwellers.

* Corresponding author. Climate Service Center Germany (GERICS), Helmholtz-Zentrum Hereon, Fischertwiete 1, 20095 Hamburg, Germany.
E-mail address: gaby.langendijk@hereon.de (G.S. Langendijk).

https://doi.org/10.1016/j.wace.2021.100367
Received 15 February 2021; Received in revised form 28 May 2021; Accepted 5 August 2021;
Available online 8 August 2021

1. Introduction

Urban populations have become increasingly affected by climate extremes over the course of the last decades (Masson et al., 2020; Mishra et al., 2015; Rosenzweig et al., 2018). Climate projections indicate extreme events will further increase in frequency and intensity in the future under climate change (Alexander, 2016; IPCC et al., 2012; Myhre et al., 2019). Urban areas and its population are prone to the impacts of climate extremes, for instance heatwaves and heavy precipitation (Grimmond et al., 2010; Rosenzweig et al., 2018). Commonly investigated underlying climatic variables, such as temperature and mean precipitation are relatively well understood for urban areas (Argüeso et al., 2016; Wiesner et al., 2018). Other climatic variables such as humidity and particularly its extremes, are less commonly investigated despite their critical importance to urban areas.

Humidity fluctuations and extremes are key to convective meteorological phenomena and related extreme events. It is a direct source of water influencing the intensity and frequency of precipitation events, droughts, as well as heatwaves (Fischer and Knutti, 2013; Hardwick Jones et al., 2010). High humidity levels combined with high temperatures result in greater thermal stress for humans, and can lead to increased mortality rates, especially during heat waves (Coccolo et al., 2016; Raymond et al., 2020). Exposure to heat-humidity extremes is projected to increasingly pose health challenges to the global population in the upcoming decades under 1.5° and 2.0 °C warming (Li et al., 2020). Whereas, low humidity levels can lead to more severe influenza epidemics by providing the right conditions for influenza spread and survival, particularly in fall and winter in temperate climates (Dalziel et al., 2018; Davis et al., 2016; Lowen et al., 2007; Shaman and Kohn, 2009). Much of the observed wintertime increase of mortality in temperate regions is attributed to influenza (Shaman et al., 2010). This shows that humidity levels can impact human health. It is therefore pivotal to understand humidity fluctuations and extremes, particularly under future climate change.

To gain a thorough understanding on humidity extremes and their impacts it is critical to advance the knowledge on the drivers of humidity extremes, at various spatial scales, and particularly in a multivariate context with a focus on process understanding (Bai et al., 2018; Fischer and Knutti, 2013; Sharma et al., 2013; Sillmann et al., 2017). Improved regional-to-local understanding of humidity extremes under climate change for cities supports the development of climate information tailored to the needs of urban decision-makers and stakeholders, to inform adaptation towards increased resilience in urban areas (Aerts and Botzen, 2014; Bai et al., 2018; Baklanov et al., 2018; Langendijk et al., 2019a). Regional climate models (RCMs) are a powerful tool to understand meteorological processes on regional-to-local scales under climate change, as they simulate multivariate dynamical interactions including those of urban areas and their surroundings. RCMs currently simulate a variety of horizontal grid resolutions, from roughly 50 km × 50 km, to 12.5 km × 12.5 km, and further down to 3 km × 3 km grid resolutions (Jacob et al., 2020). The very high horizontal resolution of 3 km × 3 km, the so-called convection-permitting scale, offers promising prospects to improve the simulation of convective systems, clouds, and precipitation, particularly for areas with complex terrain such as cities (Ban et al., 2014; Coppola et al., 2020; Masson et al., 2020; Prein et al., 2015). Previous studies indicate convection-permitting simulations particularly show large benefits on sub-daily timescales and for extreme values, compared to little improvements for mean values averaged over time (Argüeso et al., 2016; Prein et al., 2015). Despite being propitious, until now, no research investigated whether or not finer spatial resolutions improve the understanding and simulation of future humidity extremes for cities.

Two main humidity variables are investigated in this research. Firstly, specific humidity, which is the amount of water vapor in relation to the total mass of water vapor and air combined, expressed in kilograms of water vapor per kilogram of moist air. Secondly, relative humidity, which indicates how

saturated the air is compared to the water vapor fully saturated air could contain at a specific temperature, expressed as a percentage. The following abbreviation are used in this research for referring to specific humidity: SH, and relative humidity: RH.

This study takes Berlin and its surroundings as the case study area. Prior research shows urban areas are generally less moist than its surroundings, often referred to as the urban dry island (UDI) effect (Hage, 1975; Langendijk et al., 2019b; Lokoshchenko, 2017). Langendijk et al. (2019b) indicates that Berlin shows an increase in specific humidity, and a decrease in relative humidity until the end of the century. The latter is stronger in Berlin than in its surroundings. It remains unknown how urban areas, for instance through this "drying" effect, influence the meteorological conditions characterizing humidity extremes.

By the authors' knowledge, there has been no study until now that investigates if increased model resolutions affects the simulation of urban-rural meteorological processes for unprecedented future humidity extremes under climate change. Therefore, with a focus on Berlin, this first study is centered on the following research question: "How does crossing spatial resolutions from ~12.5 km to ~3 km grid size affect unprecedented future humidity extremes and related variables under climate change for Berlin and its surroundings?"

2. Method

The research contains three main methodological parts: 1) the identification of unprecedented future extreme conditions for the Berlin region; 2) new experiment set up for downscaling extremes; 3) analysis of the downscaled model output data.

2.1. Research area

Berlin and its surroundings are selected as the case-study region, because of the relatively flat regional topography, Berlin's large city size, and the distinct urban-rural landscape heterogeneity. These aspects make Berlin and its surroundings suitable to investigate urban-rural contrasts using regional climate model output data.

Berlin, the capital of Germany, is a large-scale city with around 3.6 million inhabitants covering approximately 891.1 km2 (Amt für Statistik Berlin-Brandenburg, 2020), located in-land at approximately 52.52° N, 13.4° E. The land cover of Berlin's surroundings is roughly 50% agricultural and grass land, 36% forest and 14% build up areas and water bodies (Fig. 1b) (Amt für Statistik Berlin-Brandenburg, 2020). The primary investigated domain is approximately 140 km by 140 km centered around Berlin (black rectangular, Fig. 1b).

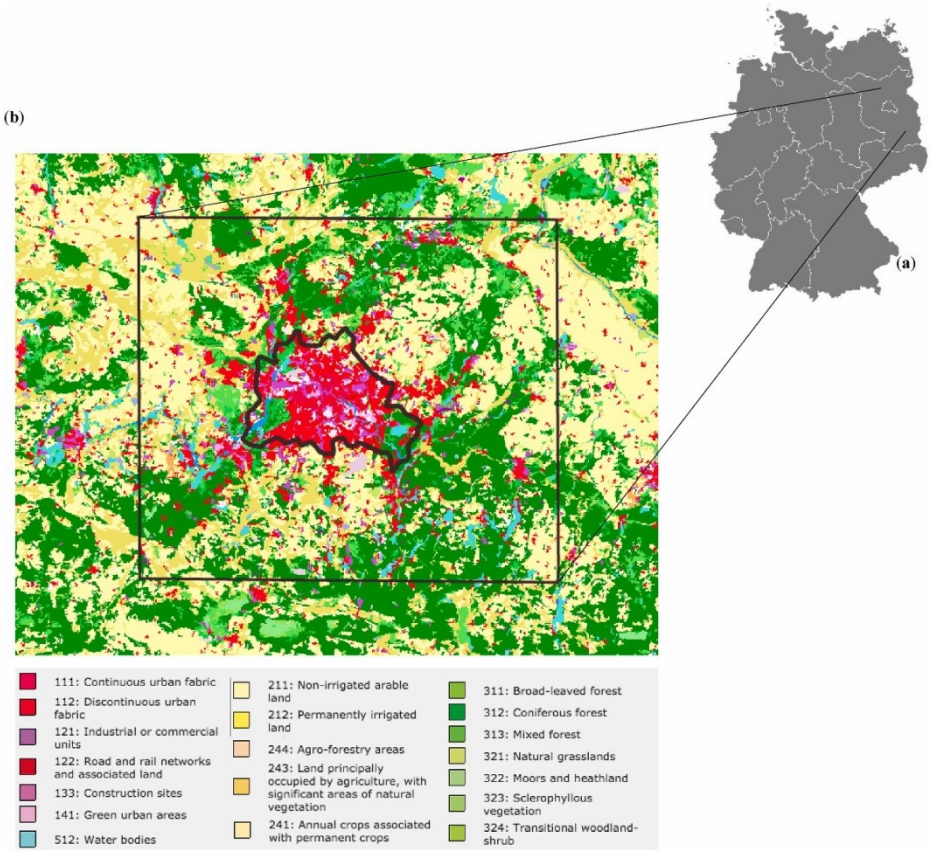

Fig. 1. Research area. (a) Germany and (b) a land-cover map indicating Berlin's administrative boundaries (black polygon) and research domain including the surroundings (black rectangular). Land cover following CORINE land cover map (EEA, 2000; Langendijk et al., 2019b).

2.2. Identifying future extreme conditions

2.2.1. Models and data

The first step of the research identifies future extreme conditions related to atmospheric moisture, occurring under 1.5 °C and 2.0 °C global warming. This research uses the model output data produced by the "Half a degree Additional warming, Prognosis and Projected Impacts" (HAPPI) project (Mitchell et al., 2017; Sieck et al., 2021). This dataset is a unique modelling effort that aims at generating large ensembles of climate model simulations which enable investigations on how the climate, and in particular extreme events, might differ from present day under 1.5 °C and 2.0 °C warmer futures than pre-industrial conditions. The HAPPI global circulation model (GCM) simulations use prescribed sea-surface temperatures (SST) for respective periods, following the Atmospheric Model Intercomparison Project (AMIP) style (Gates, 1992). Three simulation periods are selected: a historical decade (2006–2015) with observed SSTs, and two projected periods with 1.5 °C and 2.0 °C warmer global mean surface temperature than pre-industrial (1861–1880) conditions. For the latter two periods, CMIP5 mean SST anomaly patterns for the respective global warming are added to the observed SST pattern used for the historical decade. Lastly, greenhouse gas forcing is constructed from RCP2.6 and RCP4.5 emission scenarios, respectively. For each period a large ensemble of simulations are performed, each member initialized with slightly different initial conditions, leading to a large ensemble of possible climates. A detailed description of the HAPPI experiment design can be found in Mitchell et al. (2017).

From the larger HAPPI consortium, the ensemble simulations from the GCMs are dynamically downscaled by the regional climate model REMO (Sieck et al., 2021). The REMO 2015-HAPPI version (Jacob et al., 2012a) was applied for the standard European CORDEX domain on a 0.44° (~50 km) horizontal resolution, using the boundary conditions from the HAPPI GCM model ECHAM6 (Stevens et al., 2013) with 100 members per period, resulting in a total of 1000 model output years for each global warming period (3000 years of climate data). The large number of model output years can cover a wide range of possible extremes, leading to more robust statistics and results. The HAPPI model output data is available on a daily resolution. A further description of the downscaling approach can be found in Sieck et al. (2021).

2.2.2. Extreme event distributions

Statistical distributions of the historical, 1.5 °C, and 2.0 °C periods are calculated from the HAPPI data to identify future extreme conditions under 1.5 °C and 2.0 °C global mean warming, particularly related to moisture.

A domain centered around Berlin is selected, consisting of four grid boxes (Annex Fig. A1) that approximately match the primary domain of investigation showed in Fig. 1. The studied variables are: specific humidity (SH), relative humidity (RH), 2m-temperature, 2m-minimum temperature, 2m-maximum temperature and precipitation. Two types of extreme value distributions are calculated in order to define categories of unprecedented future extreme events under and/or above a specific humidity threshold. Firstly, the generalized extreme value probability density function (GEV-PDF) over the 90th and 10th percentile of each variable is computed for each period over the spatially averaged domain (Annex Fig. A1). The GEV-PDF constructs a distribution over the values above the 90th and below the 10th percentile for all years for each variable. For RH and SH the 5th and 95th percentile distributions are also calculated. Secondly, the GEV-PDF is calculated over the block maxima and block minima of each variable for each year for all ensemble members in each period. The block maxima and minima are respectively the largest and smallest values within each simulated year. Based on the tails of the distributions the extreme conditions are selected that only happen under 1.5–2.0 °C mean warming and do not occur during the historical period.

2.3. Downscaling

2.3.1. Models

The identified extreme conditions based on the HAPPI (0.44°) model output data (ECHAM6-REMO2015) are downscaled following a double-nesting approach with a first downscaling step to the 0.11° horizontal resolution (~12.5 × 12.5 km grid box size) by REMO (2015-HAPPI version) and thereafter to the 0.0275° horizontal resolution (~3 × 3 km grid box size) by applying the non-hydrostatic, convection-permitting version of REMO (REMO-NH, 2015-HAPPI version).

The regional climate model REMO is a three-dimensional, hydrostatic limited-area model of the atmosphere that has been extensively used and tested in climate change studies for Europe (Jacob et al., 2012b; Kotlarski et al., 2014). It originates from the 'Europa-Modell' of the German Weather Service (DWD) (Majewski, 1991). The physical parameterizations are largely based on the global climate model ECHAM-4 (Roeckner et al., 1996) and have been further developed over the course of the last decades. Model specifications can be found in Jacob et al. (2012a) and in Jacob and Podzun (1997).

The land cover scheme within REMO follows a tile approach, based on three basic land surface types; land, water, and sea ice. Subgrid fractions are specifying further land cover types, including an urban sub- fraction. These fractions are not assumed to be located in a specific area of a grid box, but cover

a percentage of the total grid box area, together summing up to 100 %. The turbulent surface fluxes and the surface radiation flux are calculated separately for each tile and are subsequently averaged within the lowest atmospheric level using the respective areas as weights (Rechid and Jacob, 2006; Semmler, 2002).

For the urban sub-fraction, the REMO model follows the so-called 'bulk'-approach. Sealed urban areas are represented as a rock surface, which is described in the model by a relatively high roughness length, high albedo, and no water storage capacities (Langendijk et al., 2019b). Langendijk et al. (2019b) indicates that the simple urban bulk-scheme shows the urban-rural contrast for temperature and humidity variables. The simple scheme is less skilled in simulating the timing of the peak of the urban heat island at night.

The hydrostatic approximation used in climate models fails for grid sizes smaller than 10 × 10 km (Prein et al., 2015) making the RCM's solution less reliable at those spatial resolutions. Therefore the non-hydrostatic model version REMO-NH was developed to directly resolve the vertical momentum equation, leading to a better representation of small-scale mesoscale circulations and convection (Goettel, 2009). In addition, REMO-NH more accurately represents the surface and orography fields. The non-hydrostatic formulation significantly improves model simulation output on fine horizontal resolutions, particularly for mountainous regions and urban areas (Argüeso et al., 2016; Ban et al., 2014; Coppola et al., 2020; Prein et al., 2015).

2.3.2. Set-up

A downscaling experiment set-up is developed to downscale the identified extreme conditions from the 0.44° spatial scale to finer spatial and temporal resolutions, particularly tailored to the needs of this research.

The domain sizes are defined for the 0.11° and 0.0275° horizontal resolutions to support the double-nesting approach. Matte et al. (2017) show that the distance needed for the small-scale features (so-called spatial spin-up) to develop is proportional to the jump of resolution (Matte et al., 2016). The boundaries used within our nesting approach (e.g. the boundaries of the nested model and our analysis domain) is respecting the spatial spin-up zone as recommended by Matte et al. (2017). The resulting domains for the double-nesting downscaling are presented in Fig. 2. The domains have a size of respectively 129 × 129 grid boxes centered around Berlin for the 0.11°, as well as for the 0.0275° horizontal resolution. The domains are selected based on the above rationale, whilst balancing computing costs and the strength of the boundary forcing in order for the model to capture the extreme when downscaled.

The appropriate spin-up time is determined to be around 15 days. This is comparable to spin-up times set by similar studies (Leps et al., 2019; Matte et al, 2016, 2017). The spin-up time is tested for REMO (0.11°) and REMO-NH (0.0275°) for one case of each identified extreme. The following model output variables are investigated: SH, RH, 2m-temperature, evaporation, soil wetness, soil temperature, deep soil temperature, surface pressure, vertically integrated SH, and surface sensible heat flux. A stable state is found for most variables within 1–4 days after starting the simulation, and after ~10 days for 2m-temperature, surface pressure, evaporation, soil wetness (not shown). This is in line with studies by Denis et al. (2002) and Jerez et al. (2020). Following similar studies, the total simulation period for downscaling each extreme condition is 2 months for the first downscaling step from 0.44° to 0.11° horizontal resolution, and 1.5 month for the second step from 0.11° to 0.0275° horizontal resolution (Denis et al., 2002; Herceg et al., 2006; Leps et al., 2019; Matte et al, 2016, 2017). The nesting interval frequency for downscaling the HAPPI data to the 0.11° horizontal resolutions is 6-hourly, and 1-hourly for further downscaling from the 0.11° to the 0.0275° horizontal

resolution. The time step for all downscaled simulations is 60 seconds. The downscaled model output data is available on an hourly temporal resolution.

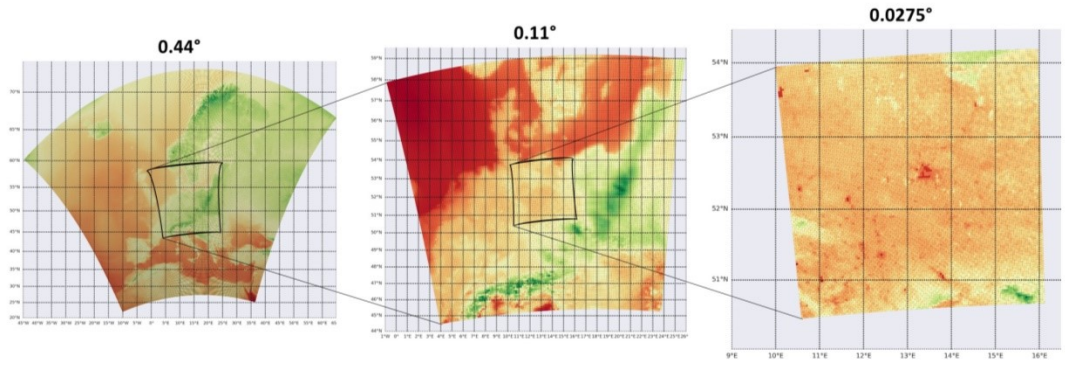

Fig. 2. The domains for the double-nesting approach, the HAPPI (0.44°) standard European domain (left), the 0.11°- domain (middle) and the 0.0275°- domain (right).

2.4. Data analysis

The analysis of the model output data across the spatial resolutions (0.11°, 0.0275°) is focused on Berlin and its direct surroundings (Fig. 1b). In order to compare the results across the horizontal scales, a coherent masking approach is developed to distinguishing Berlin from its surroundings. The urban area is defined by the grid cells containing an urban fraction larger than 0.3 as prescribed by the REMO land surface cover scheme. The grid boxes with an urban fraction >0.3 outside of the administrative boundaries of Berlin are excluded from the city mask (black polygon, Fig. 1b). This approach is followed for both horizontal resolutions. The resulting city masks for 0.11° and 0.0275° horizontal resolutions cover relatively similar areas for Berlin, with the 0.0275° mask capturing the actual city size and boundaries more accurately (Fig. 3). The masks for the surroundings include all grid boxes outside the city mask and within the primary domain of interest of 140 km by 140 km centered around Berlin (black rectangular, Fig. 1b). Table 1 shows the amount of grid boxes for different urban fractions for Berlin on the 0.11° and 0.0275° horizontal resolutions.

The downscaled extreme conditions are studied with a focus on understanding meteorological processes characterizing the extreme conditions. The following 14 model output variables are spatially averaged over the grid boxes representing Berlin (black polygon Fig. 1) and its surroundings (black rectangle Fig. 1) and thereafter analyzed: SH, RH, 2m-temperature, 2m-maximum temperature, 2m-minimum temperature, surface evaporation, relative soil moisture, soil temperature, surface pressure, 10-m wind speed, vertically integrated SH (integrated over the total atmospheric column up to the model top), surface sensible heat flux, sensible latent heat flux, and total precipitation. The analysis particularly focusses on four aspects: 1) differences due to spatial resolution (0.11° vs. 0.0275°); 2) urban-rural contrast (Berlin vs. surroundings); 3) comparison of cases (two examples of each selected extreme condition); 4) cross-comparing selected extreme conditions.

One additional analysis is performed to understand if the models on the different horizontal resolutions (0.11° and 0.0275°) behave similarly to the observations and in order to put the results for the humidity extremes into context. Observations are compared with historical model output data for the months when the selected extremes occur, for the time slice 1996–2005. The hourly in-situ measurements are obtained from the DWD Climate Data Center (DWD, 2019), stemming from ten observation stations, of which six are located in Berlin, and four in the surroundings of Berlin. The

observation stations and their respective locations are presented in the appendix of Langendijk et al. (2019b). DWD does not provide in-situ observations for specific humidity. Therefore, specific humidity is derived from observed mean daily vapor pressure (e) in hPa and air pressure (P) in hPa from observations (DWD, 2021), using the following formula (Stull, 2017):

$$Specific\ humidity = \frac{\varepsilon * e}{P - e * (1 - \varepsilon)} \qquad (1)$$

Where ε = 0.622 g vapor/g dry air is the ratio of gas constants for dry air to that for water vapor.

The model data consists out of EURO-CORDEX REMO2015 transient model simulations on a 0.11° horizontal resolution driven by the MPI-ECHAM6 model, and the REMO-NH (version 2015, driven by REMO 2015) model output data on convection-permitting scales produced as a part of the European Climate Prediction system project (EUCP) for the period 1996–2005 (Lowe et al., 2020). The main variables of interest are investigated, respectively RH, SH and temperature, to understand the general differences between the horizontal resolutions and observations.

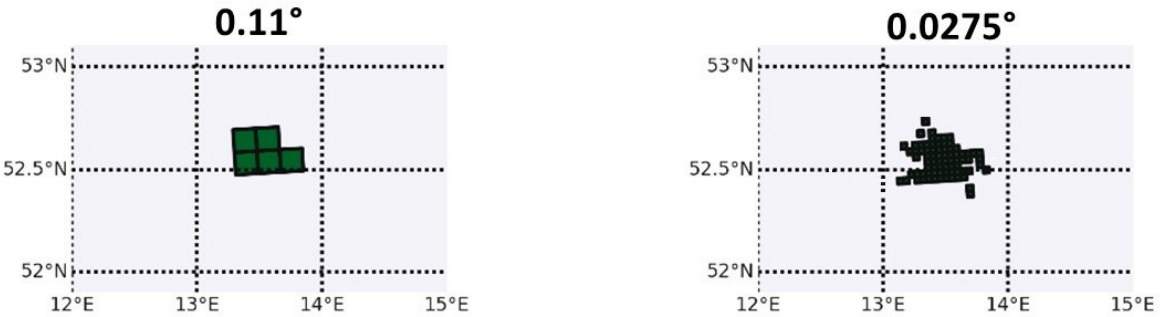

Fig. 3. Masks for Berlin, based on urban fraction > 0.3 for 0.11° (left) and 0.0275° (right) horizontal resolutions.

Table 1
Amount of grid boxes for different urban fractions for Berlin on the 0.11° and 0.0275° horizontal resolutions.

	Amount of grid boxes	
Urban fraction	0.11°	0.0275°
>0.3	5	76
>0.4	3	63
>0.5	3	60
>0.6	2	47
>0.7	2	42
>0.8	0	30
>0.9	0	20
1	0	18

3. Results

The result section is divided into two main parts: 1) identification of unprecedented future extreme conditions and respective meteorological process understanding; 2) analysis of the downscaled extreme conditions across spatial and temporal scales. The discussion of the results is directly carried out while presenting the findings throughout the results section.

3.1. Future extreme conditions

3.1.1. Identification of future extreme conditions

Statistical distributions are calculated based on the HAPPI data (0.44°, ECHAM6-REMO2015) to identify future extreme conditions (see section 2.2.2). Generally, the investigated domain shows a shifted mean with warmer (~1–2 °C) and more humid (SH) conditions under 1.5 °C and 2.0 °C, which is more profound under 2.0 °C (Annex, Fig. A2). The 90th and 95th percentile distributions for relative humidity show a decrease in RH for 1.5 °C and 2.0 °C compared to historical simulations, and an increase in RH for the 5th and 10th percentile distributions. The RH block maxima and minima distributions both show a slight decrease in moisture for 1.5 °C and 2.0 °C warming compared to the historical decade, particularly for the block minima. The percentile distributions for precipitation do not show a clear tendency. The precipitation block maxima shows increased frequency and intensity of rain extremes, particularly under 2.0 °C warming (Annex, Fig. A2).

Generally, there is an increase in the intensity and frequency visible for the tail-extremes under 1.5 °C and 2.0 °C warming compared to the historical decade, for the block maxima distributions for 2m-temperature, 2m-minimum temperature, 2m-maximum temperature, precipitation, SH, and for the block minima distributions for RH. These tail- extremes are more profound under 2.0 °C warming than 1.5 °C warming (Annex, Fig. A2).

This research particularly concerns moisture related variables, respectively SH and RH. Based on the above findings, the block maxima for SH and block minima for RH are therefore further investigated to identify future extreme conditions. Fig. 4 shows the respective distributions for SH (block maxima) and RH (block minima). In the tails of both distributions, roughly above 0.02 kg/kg SH and below 30 % RH, extreme conditions occur that only happen under 1.5 °C and 2.0 °C warming, and not during the historical decade. The thresholds SH>0.02 kg/kg and RH<30 % are therefore selected to further investigate extreme conditions.

The selected thresholds, SH>0.02 kg/kg and RH<30 %, occur 0 days in the historical decade simulated by the HAPPI ensemble members. For SH>0.02 kg/kg, the threshold is surpassed 2 days under 1.5 °C warming, and 10 days under 2.0 °C warming. For RH<30 %, the threshold is surpassed 6 days under 1.5 °C warming, and 5 days under 2.0 °C warming. These extreme condition days occur in different years of the simulated decades and within different ensemble members of the HAPPI dataset. In-situ observations for relative humidity daily means (DWD, 2019) show that, although extreme conditions of around 30–40% exists, no extreme conditions of RH<30 % occurred in Berlin and its surroundings during the respective simulated historical period (2006–2015). The specific humidity values derived from the DWD in-situ observations for 2006–2015 do not show values larger than 0.02 kg/kg. This indicates that the selected extreme conditions, SH>0.02 kg/kg and RH<30 %, are a category of unprecedented future extreme humidity events.

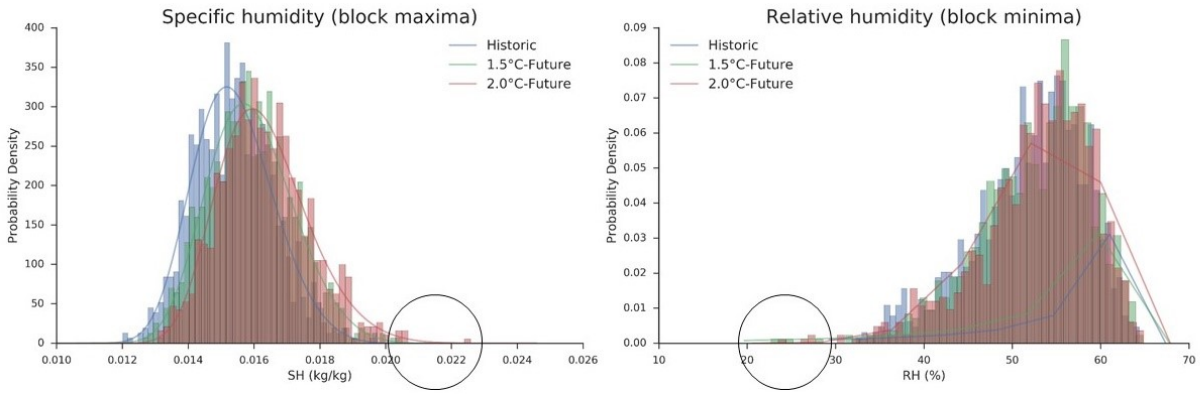

Fig. 4. The block maxima for SH (left) and block minima for RH (right) distributions based on the HAPPI ensemble members for the historical decade (1996–2005), 1.5°C and 2.0°C simulated periods.

3.1.2. Meteorological process understanding of future extreme conditions

The main meteorological characteristics are investigated for the extreme condition days surpassing the SH>0.02 kg/kg and RH<30 % thresholds, in order to understand whether the extreme conditions show similarities and to identify representative extreme conditions for further downscaling. This analysis also verifies if the extreme conditions are an artifact of one ensemble member, or a result of odd, not physically plausible, model behavior.

The findings show that all extreme condition SH>0.02 kg/kg days occur in July and August, and are characterized by very high specific humidity values (SH: 0.020–0.023 kg/kg), mean daily temperature of around 30 °C, and maximum daily values reaching almost 40 °C shortly before and during the peak of the extreme condition. Generally, warm air can hold more moisture than cold air, therefore the high specific humidity levels are expected to occur during these warm summer days. No precipitation occurs during the extreme condition and the incoming shortwave radiation is relatively high (250 W/m2) compared to the mean of the historic decade (100 W/m2) (Table 2). During the weeks before the extreme condition precipitation occurs within regular bounds, providing the soil with sufficient moisture content (soil moisture >0.7). This enables relatively high latent heat fluxes and therefore high evaporation rates shortly before and during the extreme condition (Table 2).

These meteorological conditions are driven by the synoptic weather conditions of a warm front, where temperatures and moisture rise after the warm front replaced the cold air mass. Before the warm front passes precipitation is likely to occur, and after the warm front the skies become clear, and temperatures as well as humidity levels increase. This is the so-called warm sector. The combination of the above meteorological characteristics lead to extreme days with SH>0.02 kg/ kg. A visualization describing the meteorological processes is provided in Fig. 5. In addition, Table 2 shows the mean values of all extreme conditions for each variable, as well as the comparison to the respective overall mean values of the historical decade.

Table 2
Daily mean values calculated over all ensemble members of each extreme condition for 1.5 °C and 2.0 °C future warming, compared to the overall mean of the historical decade (1996–2005).

	SH>0.02 kg/kg		**RH<30 %**	
Variables	*1.5°C*	*2.0°C*	*1.5°C*	*2.0°C*
SH (kg/kg)	0.02015	0.0211	0.0019	0.0017
RH (%)	79	74	27	26.25
2m-temperature (°C)	29.4	30.4	8.5	9
2m-maximum temperature (°C)	36	37	11.3	13
2m-minimum temperature (°C)	23.5	24.5	7	6.5
Soil wetness (m)	0.37	0.38	0.34	0.22
Relative soil moisture (%)	0.86	0.88	0.79	0.51
Surface pressure (Pa)	101700	101400	101060	102000
Shortwave radiation (W/m2)	259	261	44	66
Longwave radiation (W/m2)	425	433	277	271
Sensible heat flux (W/m2)	5	10	− 35	− 38
Latent heat flux (W/m2)	143	65	12	7
Precipitation (kg/m2/s)	0.00001	0.000019	~0	~0
Surface wind speed (m/s)	2.6	2.6	6.7	6.7

All extreme condition RH<30 % days occur in November, and are characterized by very low relative humidity (RH: 23–30 %) and specific humidity (SH: 0.0016–0.0020 kg/kg) values (Table 2). During the autumn months before the extreme condition occurs, the relative soil moisture is lower than usual for most (approx. 80 %) ensemble members (not shown). In the course of the days before the extreme only little precipitation occurs. The mean daily temperature is around 9 °C. The incoming shortwave radiation is lower than the historical average, as well as the relative soil moisture and latent heat flux (Table 2). The meteorological characteristics indicate that this extreme is driven by the synoptic weather condition of a passing cold front. The high wind speeds (~6.7 m/s) are also typical for a fast moving cold front (Fig. 5, Table 2). After the cold front passes the skies clear up, surface pressure increases, and the dry air advection leads to low humidity levels (Spankuch et al., 2011). The combination of the above meteorological characteristics lead to the extreme days with RH<30 %. A visualization describing the meteorological processes is provided in Fig. 5.

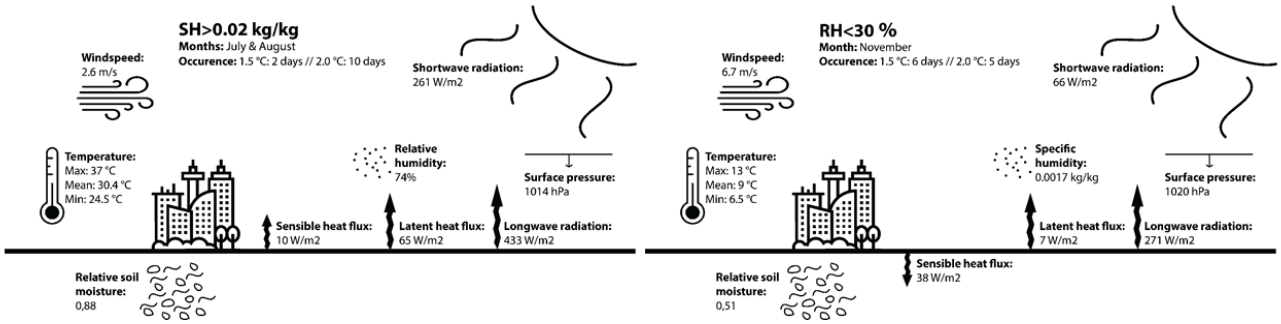

Fig. 5. Schematic visualization of meteorological characteristics of the extreme conditions SH>0.02 kg/kg (left) and RH<30 % (right), mean values for 2.0°C warming (see Table 2).

All the extreme days of each individual extreme condition, SH>0.02 kg/kg and RH<30 %, show similar meteorological characteristics. This similarity among the extreme days implies that the identified extreme conditions (SH>0.02 kg/kg and RH<30 %) are not physically improbable model artifacts.

The extreme condition days are generally slightly extremer under 2.0 °C than under 1.5 °C warming, up to 0.03 kg/kg moister (SH) and 3 % less moist (RH). Particularly for SH>0.02 kg/kg the extreme days occur more frequent under 2.0 °C warming, respectively 10 days compared to 2 days under 1.5 °C warming. Warm air can hold more moisture than cold air, therefore it can be expected that higher global mean global temperatures could lead to more extreme moist days, particularly in summer. In total 4 ensemble members, 2 ensemble members each for both RH<30 % and SH>0.02 kg/kg, show two consecutive days of the extreme condition under 2.0 °C warming. No consecutive extreme days occur under 1.5 °C. This indicates humidity extremes might occur more frequent and could last longer under 2.0 °C warming compared to 1.5 °C warming, and could potentially become even more profound under stronger temperature increase. This is in line with previous studies, such as Alexander (2016) and IPCC et al. (2012). For each threshold (SH>0.02 kg/kg and RH<30 %) two ensemble member extreme condition examples, further referred to as cases, are selected for further downscaling. The cases are picked from the simulated decades with a 2.0 °C warmer future in order to understand the more extreme possible future conditions for Berlin and its surroundings. For both extreme conditions, SH>0.02 kg/kg and RH<30 %, the first example case (Case1) is a single day peak extreme condition and the second example case (Case2) is an extreme condition lasting two consecutive days. The meteorological differences between the example cases of each extreme conditions are relatively similar. Therefore the final example cases for downscaling are arbitrarily selected from the available cases based upon the above criteria. The cases are labelled according to their extreme, respectively for SH>0.02 kg/kg CaseSH1 and CaseSH2, and for RH<30 % CaseRH1 and CaseRH2.

The example cases for each extreme condition can be described as follows. CaseSH1, with a peak value of 0.021 kg/kg SH, occurs in HAPPI ensemble member number 32 on 14 July in year 9 within the simulated decade under 2.0 °C warming. With a peak value of 0.023 kg/kg SH, CaseSH2 is simulated by HAPPI ensemble member number 87 and happens on 7 and 8 August in year 7. For RH<30 % CaseRH1, with a bottom low of 27 % RH, originates from HAPPI ensemble member number 26 and occurs on 10 November of year 2 of the simulated decade under 2.0 °C warming. With its lowest value of 25 % RH, CaseRH2 happens on 1 and 2 November in year 4 within the simulation of HAPPI ensemble member number 6.

3.2. Extremes across scales

3.2.1. Downscaled extreme conditions

Following the described double nesting approach (section 2.2.), Case1 and Case2 of each extreme condition, respectively SH>0.02 kg/kg and RH<30 %, are dynamically downscaled from 0.44° to 0.11°, and thereafter from the 0.11° to the 0.0275° horizontal resolution (Fig. 2).

A 1.5 month time series for all four downscaled cases, CaseSH1, CaseSH2, CaseRH1, and CaseRH2, is presented in Fig. 6 (SH>0.02 kg/ kg, top row; RH<30 %, bottom row). The model output data shows that all four cases occur approximately around the same dates as in the original HAPPI data (0.44°), on the 0.11° as well as on the 0.0275° horizontal resolution. The extreme cases are clearly detectable for Berlin and its surroundings. CaseSH1 and CaseRH1 do not surpass the extreme conditions thresholds anymore, respectively SH>0.02 kg/kg and RH<30 %. Nevertheless an extreme peak is still clearly visible for these downscaled cases, almost reaching the respective extreme conditions thresholds. CaseSH2 and CaseRH2 do surpass the respective extreme conditions thresholds. This can

be explained by the fact that Cases1 only just surpasses the extreme thresholds in the HAPPI data (by 0.001 kg/kg for CaseSH1 and 3 % for CaseRH1), and both Cases2 are two consecutive days in the HAPPI data and therefore result in more profound extreme values when downscaled to finer resolutions. In addition, the selected domain for downscaling has been relatively small with a strong boundary forcing, which enables the extreme condition to persist across model grid resolutions.

CaseSH1 and CaseSH2 of the SH>0.02 kg/kg extreme condition are surpassing the threshold of SH>0.02 kg/kg on additional dates besides the expected extreme event date in the downscaled simulation period, for the 0.11° and thereafter the 0.0275° horizontal resolution (Fig. 6). These extreme conditions are not present in the HAPPI (0.44°) data (not shown). These additional extreme conditions are on 19 July and around 30 July for CaseSH1, particularly surpassing the SH>0.02 kg/kg threshold around 30 July. A less distinct extreme condition can be found for CaseSH2 on 14 August, with a peak SH value of almost 0.2 kg/kg (Fig. 6). CaseRH1 and CaseRH2 of the RH<30 % extreme condition are spread over approximately 3–4 days on the 0.11° and 0.0275° horizontal resolution, compared to 1 day (Case1) and 2 days (Case2) at the 0.44° horizontal resolution.

The additional occurrence of the extremes for SH>0.02 kg/kg and the prolonged duration of the extremes for RH<30 % can be explained as follows. The coarser resolution (0.44°) averages values within a grid box over a relatively large area, as well as averages over the temporal resolution of a day mean. The land-atmosphere interactions and its fluxes get better resolved when the grid resolution increases to the 0.11° and thereafter the 0.0275° horizontal resolution. The finer grid boxes can generate larger and more peak values, resulting in additional extremes. Following similar rationale for the temporal scales, resolving fine temporal resolutions of up to an hour can prolong the duration of the extreme condition. This corresponds with similar findings for low-level aerosol concentration peaks in REMO by Pietikäinen et al. (2012).

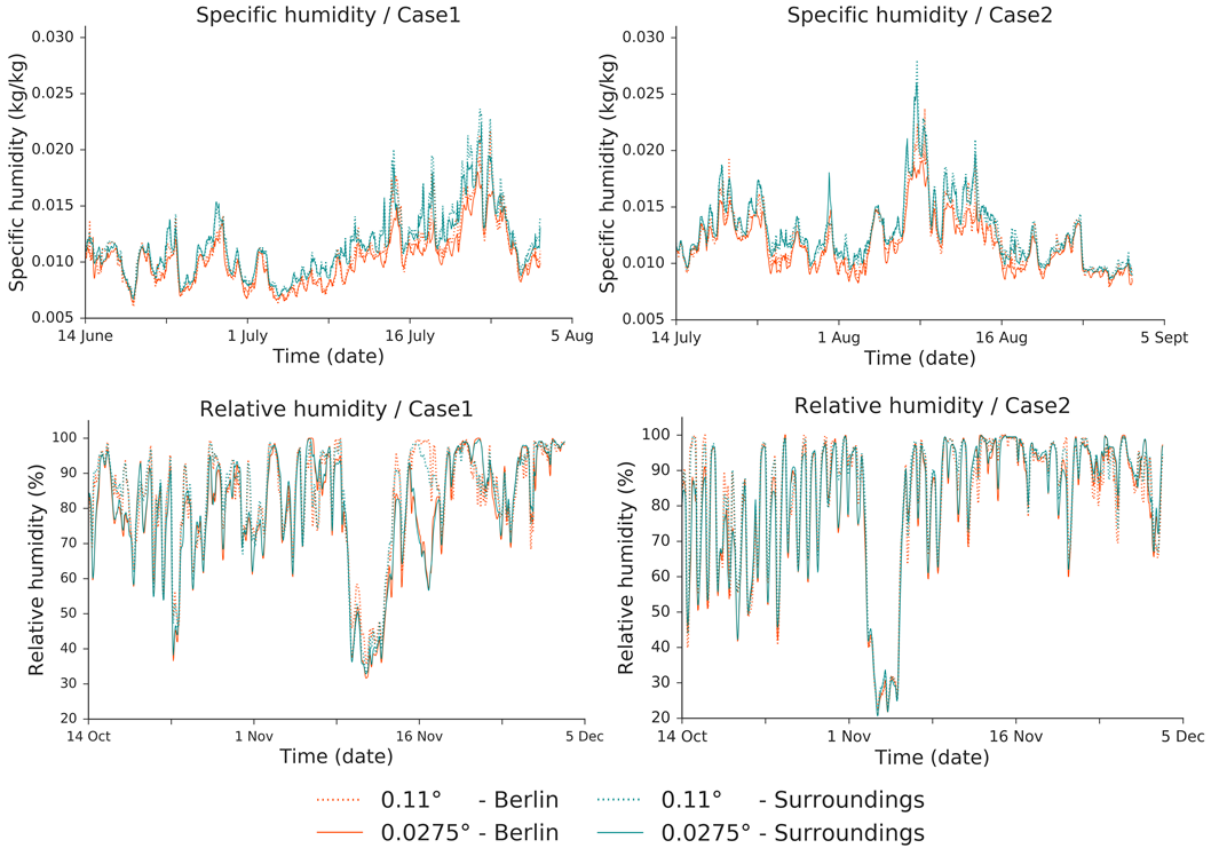

Fig. 6. The 1.5 month time series for Case1 and Case2 of both extreme conditions (SH>0.02 kg/kg, upper row; RH<30 %, bottom row) on 0.11° and 0.0275° horizontal resolutions, for Berlin and its surroundings.

Spatial maps are presented in Fig. 7 showcasing CaseSH1 and CaseRH1 during the peak hour of the extreme condition. The city boundaries and inner city differences are increasingly visible for Berlin on the 0.0275° horizontal resolutions for CaseSH1, showing a clear urban dry island. CaseRH1 shows Berlin moister than its surroundings on the 0.11° and hardly any urban-rural contrast on the 0.0275° horizontal resolution. The reason behind the latter finding is further explained in section 3.2.3.

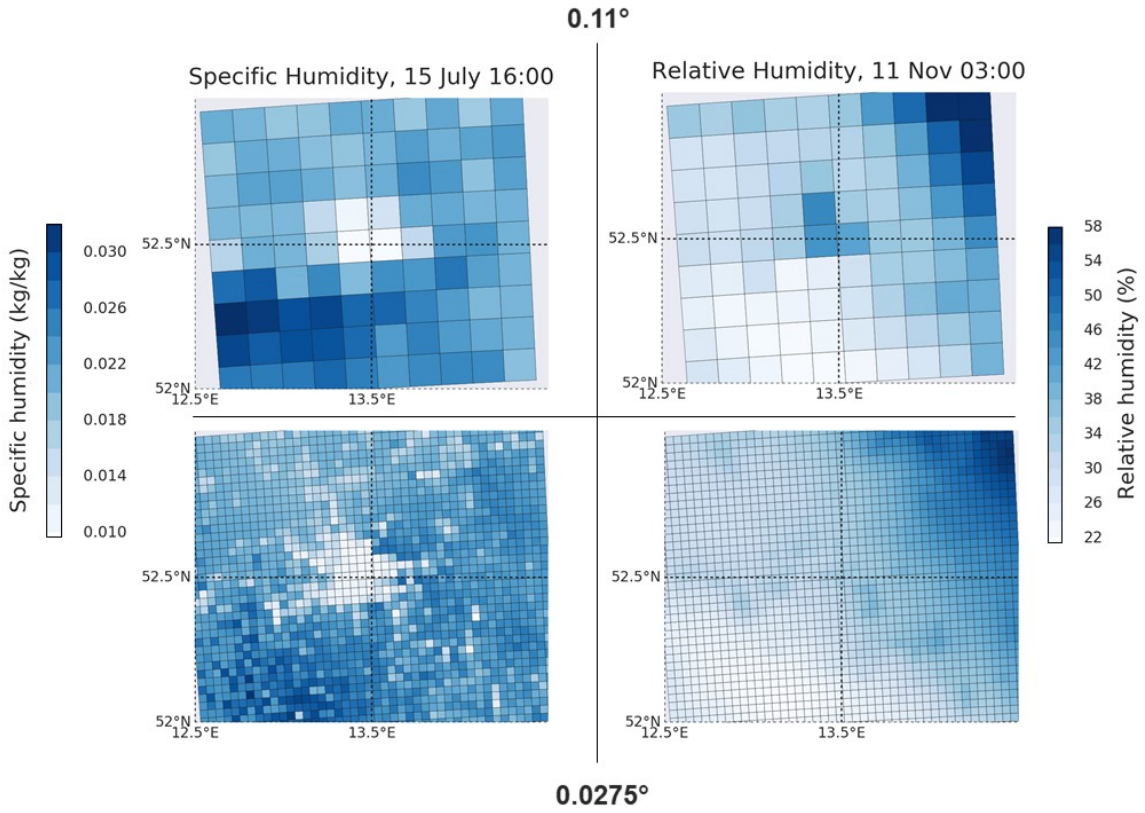

Fig. 7. Spatial maps for Berlin and its surroundings on the 0.11° (top row) and 0.0275° (bottom row) horizontal resolutions for SH for the peak hour of CaseSH1 (left column), and for RH for the peak hour of CaseRH1 (right column).

3.2.2. Context of the extremes

Before further analyzing the downscaled extreme conditions in more detail, the following analysis is presented to provide supporting context to interpret the results. Historical model output data from the EUCP dataset is compared with in-situ observations (DWD, 2021, 2019), for Berlin and its surroundings, on the 0.11° and 0.0275° horizontal resolution.

Fig. 8 shows boxplots for the variables RH, SH, and temperature for the period 1996–2005, averaged over the months in which the extreme conditions occur, respectively July and August (SH>0.02 kg/kg), and October and November (RH<30 %).

The boxplots show that overall the models (0.11° and 0.0275°) are in line with the observations. Relative humidity is lower in Berlin than its surroundings for the observations and model data, by approximately 5 %. Specific humidity is lower in Berlin than its surroundings for the observations, by 0.0001 kg/kg in October–November and 0.0012 kg/kg in July–August. This urban-rural SH contrast is not well captured by the model data in October–November, but is captured in July–August on the 0.0275° horizontal resolution, showing a clear added value on the convection-permitting scale for these months. The temperature is higher by 1–2 °C in Berlin. This urban-rural contrast is largest in summer months, underpinning the SH>0.02 kg/kg extreme condition.

The observations for October and November show a larger urban-rural contrast than the model simulations, for both RH (approx. ~4 percentage points) and temperature (+1–2 °C). Overall, the observations are not clearly closer to the 0.11° or to the 0.0275° horizontal resolution. Concluding, when looking at these mean values no substantial added value is derived from going to finer resolutions except for the specific humidity urban- rural contrast (Fig. 8).

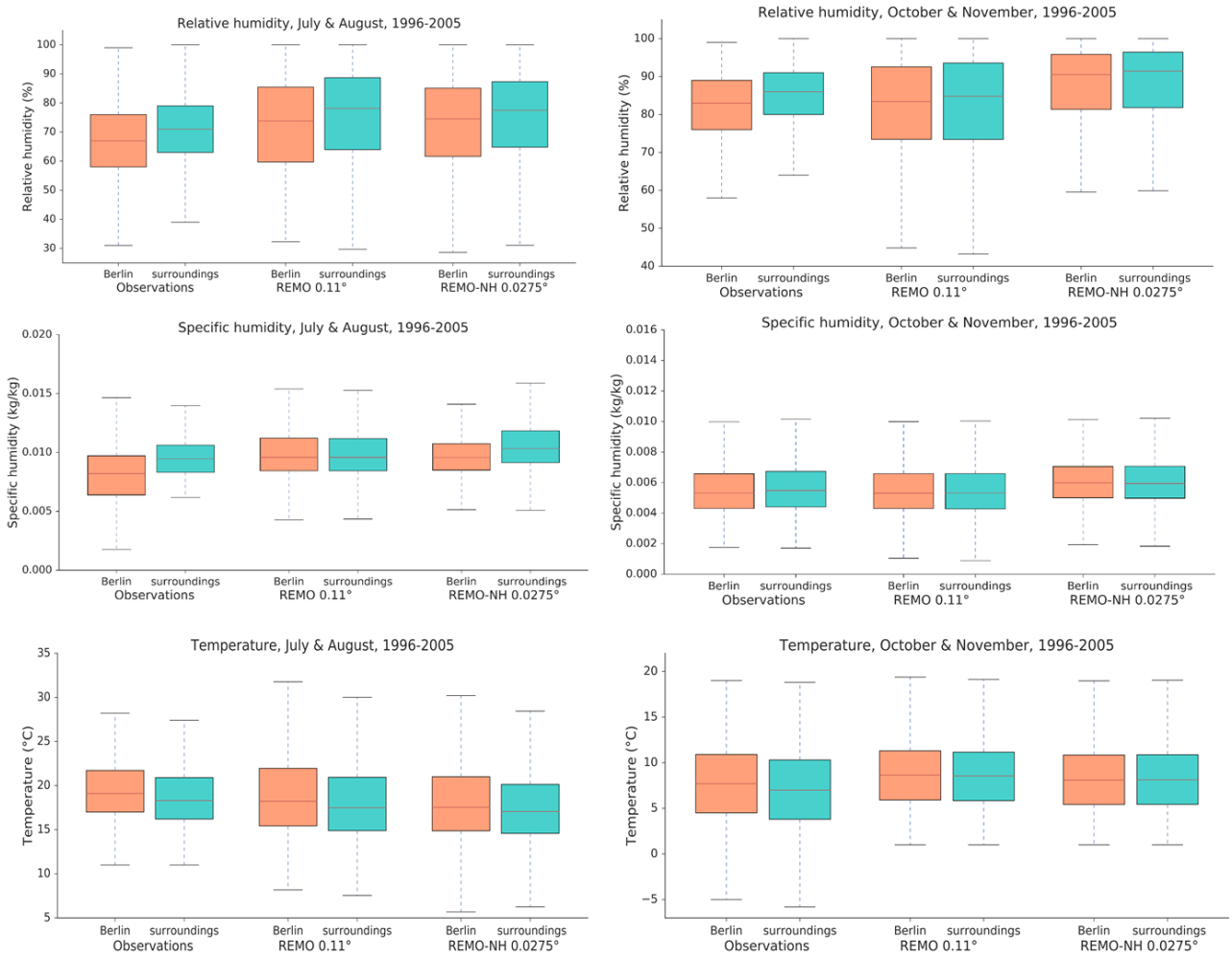

Fig. 8. Boxplots comparing observations with EUCP model output data of REMO (0.11°) and REMO-NH (0.0275°) for the variables RH, SH (no in-situ observations available through DWD), and temperature for the period 1996–2005, for the months in which the extreme conditions occur, respectively July and August (SH>0.02 kg/kg), and October and November (RH<30 %).

3.2.3. Added value of convection-permitting simulations

The downscaled cases, Case1 and Case2, for each extreme condition, SH>0.02 kg/kg and RH<30 %, are further analyzed to understand the differences between the spatial resolutions, for Berlin and its surroundings. Fourteen model output variables are studied for five days around the extreme condition, 2–3 days before as well as 2–3 days after the extreme peak.

The 5-day time series are based on the spatial average calculated over the grid boxes representing Berlin (see black polygon Fig. 1, and Fig. 3) and its surroundings (black rectangle Fig. 1). The analysis focusses on four main aspects: 1) differences between spatial resolutions (0.11° vs. 0.0275°); 2)

urban-rural contrast (Berlin vs. surroundings); 3) comparing the cases (Case1 vs. Case2 of each extreme condition); 4) comparing the extreme conditions (SH>0.02 kg/kg vs. RH<30 %).

To visually guide the analysis, Fig. 9 presents plots for eight selected key variables showing the computed differences between Berlin and its surroundings (difference = Berlin – surroundings), for the 0.11° and the 0.0275° horizontal resolution, for each case (Case1 and Case2), and for each extreme condition SH>0.02 kg/kg (Fig. 9A) and RH<30 % (Fig. 9B). The full time series, for all the fourteen model output variables are presented in the Annex (Fig. A3, Fig. A4, and Table A1).

Overall, the meteorological characteristics of the downscaled cases are in line with the meteorological characteristics and synoptic situation described for each extreme condition on the 0.44° horizontal resolution based on the HAPPI simulations (section 3.1.2, Fig. 5, and Table 2). Among Case1 and Case2 of each of the extreme conditions, SH>0.02 kg/ kg and RH<30 %, similar overall meteorological characteristics are found (Annex Fig. A3 and Fig. A4). This implies that REMO captures the extreme events and its meteorological conditions adequately in the downscaled simulations. However, detailed differences are found investigating the downscaled cases further.

Looking into the SH>0.02 kg/kg extreme condition, the two downscaled cases (CaseSH1 and CaseSH2) show that the urban area mitigates the high specific humidity levels, indicating a clear urban dry island effect, which is enhanced on the convection permitting scale (Fig. 10). On the 0.0275° horizontal resolution the SH decreases up to 0.005 kg/kg and the RH up to 20 % compared to the 0.11° horizontal resolution (Fig. 9A–a,b). Concerning the urban-rural contrast, Berlin is up to 10 % RH and up to 0.008 kg/kg SH less moist than its surroundings (Fig. 9A–a, b). Nevertheless, the city still faces high SH levels up to 0.016 kg/kg (CaseSH1) and 0.020 kg/kg (CaseSH2) on the 0.11° horizontal resolution (Fig. 10). The SH peak values are lower in Berlin for the 0.0275° horizontal resolutions, with SH levels up to 0.013 kg/kg (CaseSH1) and 0.016 kg/kg (CaseSH2) (Fig. 10). It implies extreme moist summer days will be less humid in Berlin than its surroundings under 2.0 °C global warming, particularly on the 0.0275° horizontal resolution.

The results for the RH<30 % extreme condition show, despite a small urban-rural contrast, that the downscaled extreme events will be less moist on the convection permitting scale, particularly in Berlin. On the 0.0275° horizontal resolution the SH decreases up to 0.0007 kg/kg and the RH up to 10 % compared to the 0.11° horizontal resolution (Fig. 9B–a,b). Only a small urban-rural moisture contrast is found, especially on the 0.0275° horizontal resolution. Interestingly, Berlin is moister (RH and SH) than its surroundings for the 0.11° horizontal resolution for both cases during the bottom low of the extreme condition (Fig. 10). This reverses for RH on the 0.0275° horizontal resolution, where Berlin shows lower relative humidity levels than its surroundings, particularly for CaseRH1 (Figs. 7 and 10). The small urban-rural contrast and slight urban drying effect for CaseRH1 on the 0.0275° horizontal resolution corresponds with the Boxplots (Fig. 8), which show a small urban-rural RH contrast in October and November. The findings for the RH<30 % extreme condition indicate an intensification of the dry extreme condition on the convection-permitting scale during the peak of the extreme events, particularly for CaseRH1.

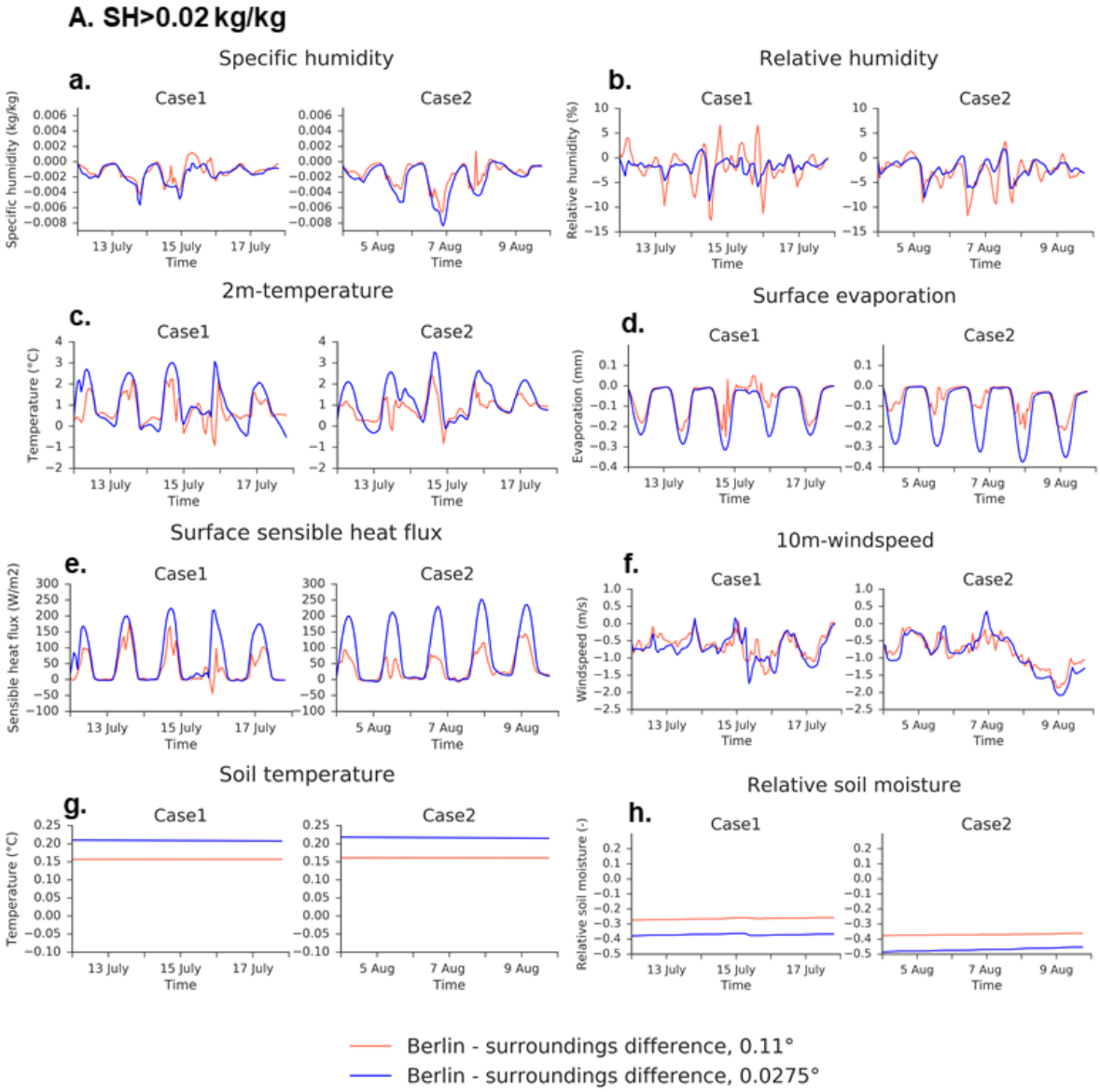

Fig. 9A. Differences plots during the 5 days around the downscaled extreme condition SH>0.02 kg/kg for each case (Case1 and Case2). Differences between Berlin and its surroundings calculated for the 0.11° and the 0.0275° resolution (difference = Berlin-surroundings).

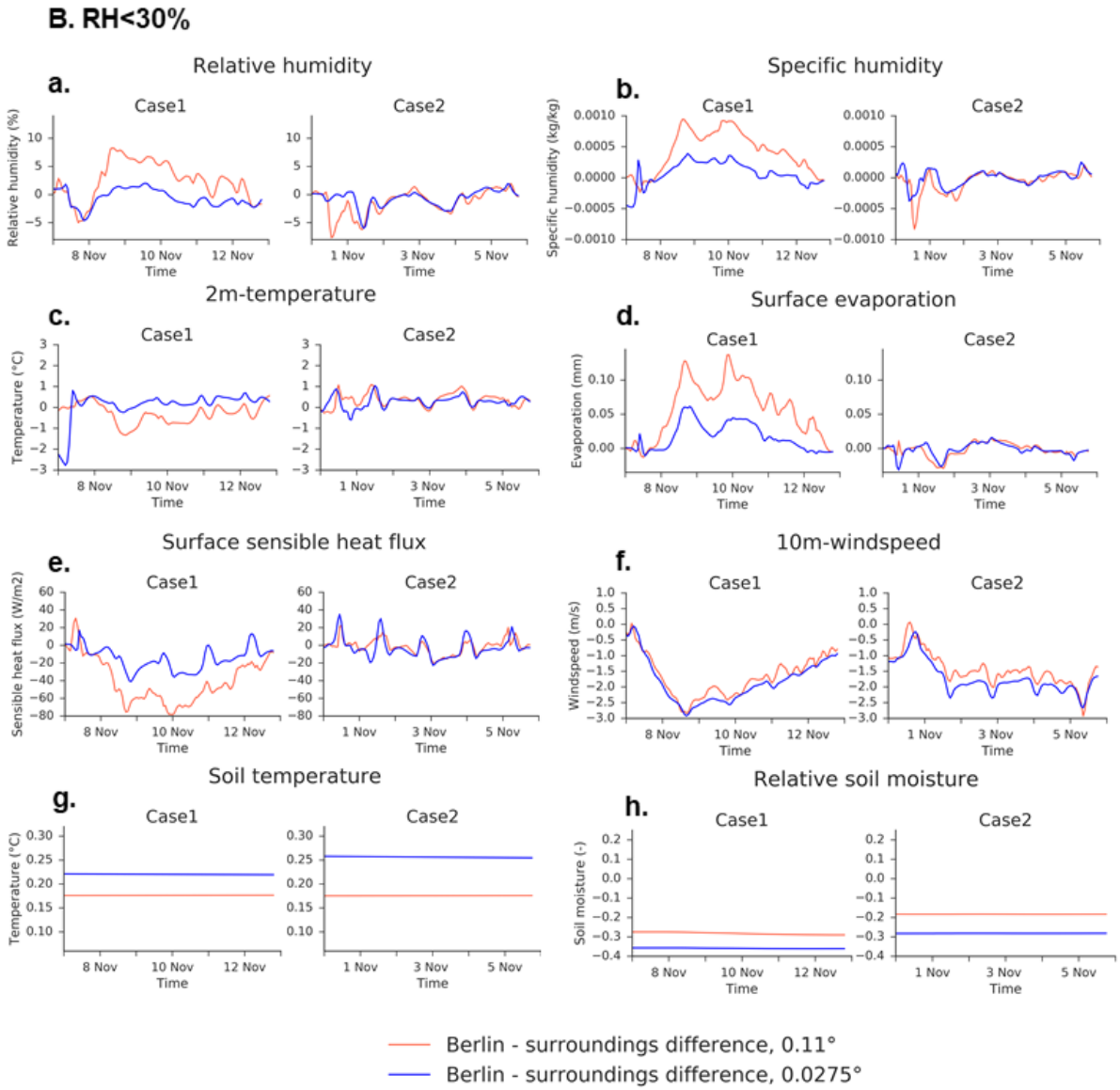

Fig. 9B. Differences plots during the 5 days around the downscaled extreme condition RH<30 % for each case (Case1 and Case2). Differences between Berlin and its surroundings calculated for the 0.11° and the 0.0275° resolution (difference = Berlin-surroundings).

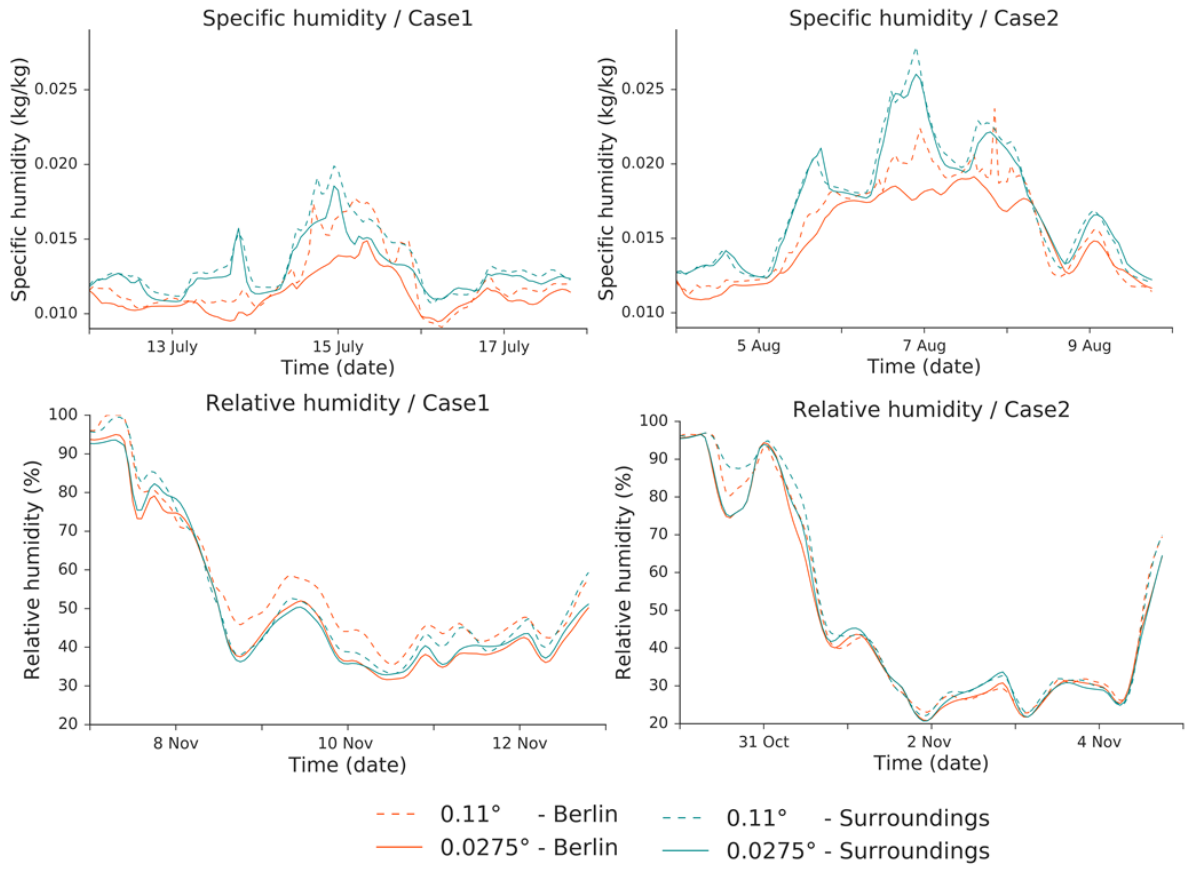

Fig. 10. 5-day time series around the extreme conditions, SH>0.02 kg/kg (top row) and RH<30 % (bottom row), for respectively SH and RH, showing Case1 and Case2, for Berlin and its surroundings, for the spatial resolutions 0.0275° and 0.11°.

Overall, the results for both extreme humidity conditions, SH>0.02 kg/kg and RH<30 %, show that the convection-permitting scale is less moist than the 0.11° horizontal resolution, especially in Berlin compared to its surroundings.

The intensified moisture reduction on the 0.0275° horizontal resolution in Berlin can be explained by the fact that urban areas are represented in the REMO model through a sealed “rock” surface. The urban representation is characterized by a greater heat capacity and reduced water storage, resulting in higher soil temperatures, lower soil moisture, and reduced surface evaporation, explaining the reduced humidity levels and higher temperatures in Berlin compared to its surroundings (Langendijk et al. 2019a). The model results for the respective variables show this urban effect clearly for both extreme conditions (Fig. 9A/B, Annex; Fig. A2, Fig. A3). Higher temperatures of approximately 0.5 °C–4.0 °C are found for both extreme conditions in Berlin compared to its surroundings, which is more profound by ~1.0 °C for the 0.0275° compared to 0.11° horizontal resolution (Fig. 9A/B-c). Furthermore, the soil moisture in Berlin is up to 0.3 lower than its surroundings, and the urban-rural soil moisture contrast is up to 0.1 larger on the 0.0275° than on the 0.11° horizontal resolution (Fig. 9A/B-h). In addition, the soil temperature in Berlin is up to 0.25 °C higher than its surroundings (Fig. 9A/B-g), and the urban-rural soil temperature contrast is approximately 0.05 °C larger on the 0.0275° than 0.11° horizontal resolution. The surface evaporation is up to 0.35 mm less in Berlin than its surroundings, and the urban-rural evaporation contrast is up to 0.2 mm larger on the 0.0275° compared to the 0.11° horizontal resolution (Fig. 9A/B-d).

Clearly, the typical urban characteristic are more pronounced on the 0.0275° than on the 0.11° horizontal resolution. This is mainly due to the larger amount of urban grid boxes on the 0.0275° horizontal resolution (Fig. 3). In addition, these grid boxes contain a larger urban fraction, of around 0.6–1, compared to the 0.11° horizontal resolution, with no grid boxes containing an urban fraction larger than 0.8 (Table 1). Therefore, the urban grid boxes on the convection-permitting scale are better resolved, particularly leading to a stronger reduction in moisture and stronger warming, especially in Berlin compared to its surroundings.

In summary, the presented results in this chapter show the convection-permitting scale resolves Berlin, and its typical urban characteristics, more pronounced than the 0.11° horizontal resolution. For both extreme conditions, SH>0.02 kg/kg and RH<30 %, the 0.0275° horizontal resolution is drier and warmer than the 0.11° horizontal resolution, particularly in Berlin compared to its surroundings. The convection-permitting scale mitigates the SH>0.02 kg/kg moist extreme and intensifies the RH<30 % dry extreme.

4. Discussion

This research shows how crossing spatial resolutions from ~12.5 km to ~3 km grid size affects two humidity extreme conditions, SH>0.02 kg/kg and RH<30 %, occurring under 2 °C global mean temperature change, comparing Berlin to its surroundings. The results section directly discussed the outcomes in detail, therefore this discussion section focuses on key aspects underpinning the study.

The results of this research indicate temporal mean values only show limited differences and improvements going to finer horizontal resolutions, except for the specific humidity urban-rural contrast in July–August which shows added value on the 0.0275° horizontal resolution (Fig. 8). For the extreme conditions, and its drivers, changes in the variables are clearly visible for all the downscaled cases on the finer scales, particularly for Berlin (Fig. 9). This is in line with Ban et al. (2014) and Prein et al. (2015), who indicate convection-permitting simulations show larger benefits in the tail-distributions compared to mean values.

Climate model projections are inherently subject to uncertainty. Regional climate models are dependent on global climate models for their boundary conditions, feeding in the large scale climate conditions. Global climate models may not simulate all key dynamical patterns adequately that influence natural variability and related extremes on the local scale, such as atmospheric blocking, jet stream position, or teleconnections (Sillmann et al., 2017). The HAPPI method, by its design, specifically targets to reduce the uncertainty in climate model responses and internal variability, in order to understand the impact of an additional half degree of warming from 1.5 °C to 2.0 °C (Mitchell et al., 2017). Nevertheless, the identified extreme conditions of this research remain subject to internal variability and related uncertainties. Additionally, dynamical downscaling methods can result in model artifacts. For instance the choice of domain, spin-up, and nesting approach may result in a too strong or too weak boundary forcing, leading to misrepresenting extremes while downscaling to finer resolutions (Bellprat et al., 2019; Matte et al., 2016; Sillmann et al., 2017; von Trentini et al., 2019).

Commonly scientific studies relate their findings to observations to gain understanding about uncertainties and biases to enhance the robustness of the results. Because it is virtually impossible to compare unprecedented future extreme conditions that did not happen in the past with observations, this research took a physical process-understanding approach. The in-depth meteorological characterization of the extreme conditions validated the physical plausibility of the extremes and the underlying drivers. To further enhance the robustness of the presented results it could be desirable to assess in more detail how the spatial differences and urban-rural contrasts

found in this study relate to natural and internal variability, as well as to the uncertainty arising from the downscaled model simulations. In addition, it would be beneficial to understand if slightly less extreme conditions would have similar meteorological characteristics to the downscaled extremes investigated in this research.

The results show the convection-permitting scale resolves Berlin, and its typical urban characteristics, more pronounced than the 0.11° horizontal resolution. The convection permitting scale mitigates the SH>0.02 kg/kg moist extreme and intensifies the RH<30 % dry extreme. This indicates that the convection permitting scale is able to better capture the urban characteristics than the HAPPI data (Annex; Fig. A1), as well as the 0.11° resolution. To ensure we adequately simulate climate change extremes and impacts in cities, it is important to move towards convection-permitting resolutions.

The REMO model represents urban areas through a bulk-scheme. Forgone studies show that including a sophisticated urban parameterization scheme or an urban model can enhance the urban heat island effect, improve the diurnal cycle, and potentially lead to stronger warming and increased drying in urban areas compared to the bulk- approach (Daniel et al., 2019; Karlický et al., 2018; Langendijk et al., 2019b). This implies the reduced moisture and enhanced warming found for Berlin on finer spatial resolutions in this study might get more profound using sophisticated urban schemes. It would be important for further studies to include urban parameterizations in regional climate models to adequately capture the urban effects, particularly on the convection-permitting scale (Daniel et al., 2018; Hertwig et al., 2021). The SH>0.02 kg/kg and RH<30 % unprecedented extreme conditions may have important implications for human health. The moist extreme, SH>0.02 kg/kg, is mitigated in Berlin, particularly on the convection-permitting resolution, resulting in a reduction of moisture in the city. This implies that urban dwellers would be slightly less affected by the moist extreme than people living in the rural areas, potentially leading to a reduced mortality rate. Nevertheless, it is important to note that this unprecedented extreme moist condition happening under 2.0 °C warming would imply an overall increase in favorable conditions for heat stress compared to the historical period. The RH<30 % extreme provides favorable conditions for the spread and survival of influenza. The convection-permitting resolution shows that Berlin is drier than its surroundings, potentially leading to increased influenza in the city with negative effects on the health of urban dwellers.

This research focuses solely on two humidity extreme conditions in Berlin and its surroundings. It would be important to understand the changes and benefits on the convection-permitting resolution for different types of extremes and for other cities. Further studies on climate extremes in urban areas, with additional regional climate models that potentially include sophisticated urban schemes, could be beneficial to compare the results of this study.

5. Summary and conclusions

This research investigates how crossing spatial resolutions from ~12.5 km to ~3 km grid size affects humidity extremes and related variables under 2 °C global mean temperature change for Berlin and its surroundings. Two meteorologically plausible unprecedented categories of future extreme humidity conditions are identified for Berlin and its surroundings based on statistical distributions of the HAPPI data, respectively SH>0.02 kg/kg and RH<30 %. Two example cases of each extreme condition are downscaled following a double-nesting approach, from the 0.44° to the 0.11° horizontal resolution by REMO and thereafter from the 0.11° to the 0.0275° horizontal resolution with REMO- NH. The differences between the spatial resolutions and the urban- rural contrast are analyzed for Berlin and its surroundings, following a meteorological process-understanding approach.

The main results show that the convection-permitting scale resolves Berlin, and its typical urban characteristics, more pronounced than the 0.11° horizontal resolution. The 0.0275° horizontal resolution is less moist than the 0.11° horizontal resolution for the downscaled cases of both extreme conditions, for SH>0.02 kg/kg (0.005 kg/kg SH and 20 % RH) and for RH<30 % (0.0007 kg/kg SH and 10 % RH). Higher temperatures of approximately 1.0 °C–2.0 °C are found for both extreme conditions for the 0.0275° simulations compared to 0.11° horizontal resolution. The differences between the 0.11° to the 0.0275° horizontal resolution are generally more profound in Berlin compared to its surroundings, especially indicating warmer temperatures and a stronger decrease in moisture (RH and SH) on the 0.0275° horizontal resolution in the city. This urban drying effect and the associated urban-rural contrast is larger for the SH>0.02 kg/kg extreme condition compared to the RH<30 % extreme condition, particularly on the convection- permitting scale. The convection-permitting scale mitigates the SH>0.02 kg/kg moist extreme and intensifies the RH<30 % dry extreme.

The enhanced reduction in moisture is predominantly due to the increase of urban grid boxes with larger urban fractions on the 0.0275° horizontal resolution compared to the 0.11° horizontal resolution. On the 0.0275° horizontal resolution the underpinning variables show higher 2-m temperatures, higher soil temperatures, lower soil moisture, reduced surface evaporation, and lower wind speeds, especially in Berlin. This implies the sealed urban surface is resolved more profoundly on the 0.0275° horizontal resolution. It demonstrates the improved capability of the convection-permitting simulations to capture the typical urban drying effect in Berlin for the two extreme conditions.

The results for the SH>0.02 kg/kg extreme condition imply that extreme moist summer days will be less humid in Berlin than its surroundings under 2.0 °C global warming, particularly when simulated on the convection-permitting scale. This humidity reduction could partly mitigate human heat stress in the city during the extreme event compared to its surroundings, potentially reducing the mortality rate. The RH<30 % extreme condition, with its low relative humidity values, could possibly favor the spread and survival of influenza particularly in Berlin, leading to negative health effects. Follow-up studies would be needed to further investigate the relationships between the extremes and various sectors, and applications. This could inform the development of climate information and services for urban areas, as well as the modelling needs and directions for RCM developments in the context of cities.

Declaration of competing interest

The authors declare that they have no known competing financial interests or personal relationships that could have appeared to influence the work reported in this paper.

Acknowledgements

We thank the "Half a degree Additional warming, Prognosis and Projected Impacts (HAPPI)" project (https://www.happimip.org/) for making the data available which enabled this research. We would like to express great gratitude to the GERICS staff members working on REMO development for their support while conducting the REMO simulations, and particularly thank them for their help to fix technical model errors; Lars Buntemeyer, Thomas Frisius, Joni-Pekka Pietikäinen, and Thomas Remke. We are grateful for the helpful suggestions by our colleague Joni-Pekka Pietikäinen to improve the first draft of the manuscript. We would like to thank the staff members at the German Climate Computing Center (DKRZ) for their technical expertise and support. The research was kindly funded by the Climate Service Center Germany (GERICS), Helmholtz-Zentrum Hereon, Germany.

Appendix A. Supplementary data

Supplementary data related to this article can be found at https://doi.org/10.1016/j.wace.2021.100367

Author contributions

Conceptualization; G.S.L., D.R., K.S., D.J. Data curation; G.S.L. Formal analysis; G.S.L. Investigation; G.S.L. Methodology; G.S.L. Supervision; D.R., K.S., D.J. Validation; G.S.L. Visualization; G.S.L. Writing – original draft; G.S.L. Writing - review & editing; G.S.L., D.R., K. S., D.J.

References

Aerts, J., Botzen, W., 2014. Adaptation: cities' response to climate risks. Nat. Clim. Change 4, 759–760. https://doi.org/10.1038/nclimate2343.

Alexander, L.V., 2016. Global observed long-term changes in temperature and precipitation extremes: a review of progress and limitations in IPCC assessments and beyond. Weather Clim. Extrem. 11, 4–16. https://doi.org/10.1016/j.wace.2015.10.007.

Amt für Statistik Berlin-Brandenburg, 2020. Statistiken Berlin und Brandenburg [WWW Document]. Statistiken. URL. https://www.statistik-berlin-brandenburg.de/statistiken/Inhalt-Statistiken.asp. accessed 7.26.19.

Argüeso, D., Di Luca, A., Evans, J.P., 2016. Precipitation over urban areas in the western Maritime Continent using a convection-permitting model. Clim. Dynam. 47, 1143–1159. https://doi.org/10.1007/s00382-015-2893-6.

Bai, X., Dawson, R.J., Ürge-Vorsatz, D., Delgado, G.C., Salisu Barau, A., Dhakal, S., Dodman, D., Leonardsen, L., Masson-Delmotte, V., Roberts, D.C., Schultz, S., 2018. Six research priorities for cities and climate change. Nature 23–25. https://doi.org/10.1038/d41586-018-02409-z.

Baklanov, A., Grimmond, C.S.B., Carlson, D., Terblanche, D., Tang, X., Bouchet, V., Lee, B., Langendijk, G., Kolli, R.K., Hovsepyan, A., 2018. From urban meteorology, climate and environment research to integrated city services. Urban Clim 23, 330–341. https://doi.org/10.1016/j.uclim.2017.05.004.

Ban, N., Schmidli, J., Schar, C., 2014. Evaluation of the convection-resolving regional climate modeling approach in decade-long simulations. J. Geophys. Res. 119, 7889–7907. https://doi.org/10.1002/2014JD021478.

Bellprat, O., Guemas, V., Doblas-reyes, F., Donat, M.G., 2019. Event attribution. Nat. Commun. 10, 29–31. https://doi.org/10.1038/s41467-019-09729-2.

Coccolo, S., Kampf, J., Scartezzini, J.L., Pearlmutter, D., 2016. Outdoor Human Comfort and Thermal Stress: A Comprehensive Review on Models and Standards. Urban Clim. https://doi.org/10.1016/j.uclim.2016.08.004.

Coppola, E., Sobolowski, S., Pichelli, E., Raffaele, F., Ahrens, B., Anders, I., Ban, N., Bastin, S., Belda, M., Belusic, D., Caldas-Alvarez, A., Cardoso, R.M., Davolio, S., Dobler, A., Fernandez, J., Fita, L., Fumiere, Q., Giorgi, F., Goergen, K., Güttler, I., Halenka, T., Heinzeller, D., Hodnebrog, Jacob, D., Kartsios, S., Katragkou, E., Kendon, E., Khodayar, S., Kunstmann, H., Knist, S., Lavín-Gullon, A., Lind, P., Lorenz, T., Maraun, D., Marelle, L., van Meijgaard, E., Milovac, J., Myhre, G., Panitz, H.J., Piazza, M., Raffa, M., Raub, T., Rockel, B., Schar, C., Sieck, K., Soares, P. M.M., Somot, S., Srnec, L., Stocchi, P., Tolle, M.H., Truhetz, H., Vautard, R., de Vries, H., Warrach-Sagi, K., 2020. A first-of-its-kind multi-model convection permitting ensemble for investigating convective phenomena over Europe and the Mediterranean. Clim. Dynam. 55, 3–34. https://doi.org/10.1007/s00382-018-4521-8.

Dalziel, B.D., Kissler, S., Gog, J.R., Viboud, C., Bjørnstad, O.N., Metcalf, C.J.E., Grenfell, B.T., 2018. Urbanization and humidity shape the intensity of influenza epidemics in U.S. cities. Science (80- 362, 75–79. https://doi.org/10.1126/science.aat6030.

Daniel, M., Lemonsu, A., D´eque, M., Somot, S., Alias, A., Masson, V., 2019. Benefits of ´ explicit urban parameterization in regional climate modeling to study climate and city interactions. Clim. Dynam. 5, 2745–2764. https://doi.org/10.1007/s00382-018-4289-x.

Daniel, M., Lemonsu, A., Deque, M., Somot, S., Alias, A., Masson, V., 2018. Benefits of explicit urban parameterization in regional climate modeling to study climate and city interactions. Clim. Dynam. 1–20. https://doi.org/10.1007/s00382-018-4289-x.

Davis, R.E., McGregor, G.R., Enfield, K.B., 2016. Humidity: a review and primer on atmospheric moisture and human health. Environ. Res. 144, 106–116. https://doi.org/10.1016/j.envres.2015.10.014

Denis, B., Laprise, R., Caya, D., Cote, J., 2002. Downscaling ability of one-way nested regional climate models: the Big-Brother Experiment. Clim. Dynam. 18, 627–646. https://doi.org/10.1007/s00382-001-0201-0.

Dwd, D., 2021. German weather service, climate data center (CDC) [WWW Document]. URL. https://cdc.dwd.de/portal/. accessed 5.8.21.

Dwd, D.W.D., 2019. German weather service, climate data center (CDC) [WWW Document]. URL. https://cdc.dwd.de/portal/. accessed 1.25.19.

EEA, 2000. The revised and supplemented Corine land cover nomenclature. EEA Tech. Rep 40.

Fischer, E.M., Knutti, R., 2013. Robust projections of combined humidity and temperature extremes. Nat. Clim. Change 3, 126–130. https://doi.org/10.1038/nclimate1682.

Gates, W.L., 1992. AMIP: the atmospheric model Intercomparison project. Bull. Am. Meteorol. Soc. 73, 1962–1970. https://doi.org/10.1175/1520-0477(1992)

Goettel, H., 2009. Einfluss der nichthydrostatischen Modellierung und der Niederschlagsverdriftung auf die Ergebnisse regionaler Klimamodellierung. Reports Earth Syst. Sci. 125.

Grimmond, C.S.B., Roth, M., Oke, T.R., Au, Y.C., Best, M., Betts, R., Carmichael, G., Cleugh, H., Dabberdt, W., Emmanuel, R., Freitas, E., Fortuniak, K., Hanna, S.,

Klein, P., Kalkstein, L.S., Liu, C.H., Nickson, A., Pearlmutter, D., Sailor, D., Voogt, J., 2010. Climate and more sustainable cities: climate information for improved planning and management of cities (Producers/Capabilities Perspective). In: Procedia Environmental Sciences. https://doi.org/10.1016/j.proenv.2010.09.016.

Hage, K.D., 1975. Urban-rural humidity differences. J. Appl. Meteorol. 7, 1277–1283. https://doi.org/10.1175/1520-0450(1975)014.

Hardwick Jones, R., Westra, S., Sharma, A., 2010. Observed relationships between extreme sub-daily precipitation, surface temperature, and relative humidity. Geophys. Res. Lett. 37 https://doi.org/10.1029/2010GL045081.

Herceg, D., Sobel, A.H., Liqiang, S., Zebiak, S.E., 2006. The Big Brother Experiment and seasonal predictability in the NCEP regional spectral model. Clim. Dynam. 27, 69–82. https://doi.org/10.1007/s00382-006-0130-z.

Hertwig, D., Ng, M., Grimmond, S., Vidale, P.L., McGuire, P.C., 2021. High-resolution global climate simulations: representation of cities. Int. J. Climatol. 5, 3266–3285. https://doi.org/10.1002/joc.7018.

IPCC, 2012. In: Field, C.B., Barros, V., Stock, T.F., Qin, D., Dokken, D.J., Ebi, K.L., Mastrandrea, M.D., Mach, K.J., Plattner, G.-K., Allen, S.K., Tignor, M., Midgley, P.M. (Eds.), Managing the Risks of Extreme Events and Disasters to Advance Climate Change Adaptation: Special Report of the Intergovernmental Panel on Climate Change. A Spec. Rep. Work. Groups I II Intergov. Panel Clim. Chang., vol. 9781107025, pp. 1–582. https://doi.org/10.1017/CBO9781139177245.

Jacob, D., Elizalde, A., Haensler, A., Hagemann, S., Kumar, P., Podzun, R., Rechid, D., Remedio, A.R., Saeed, F., Sieck, K., Teichmann, C., Wilhelm, C., 2012a. Assessing the transferability of the regional climate model REMO to different coordinated regional climate downscaling experiment (CORDEX) regions. Atmosphere 3, 181–199. https://doi.org/10.3390/atmos3010181.

Jacob, D., Haensler, A., Saeed, F., Elizalde, A., Hagemann, S., Kumar, P., Podzun, R., Rechid, D., Remedio, A.R., Sieck, K., Teichmann, C., Wilhelm, C., 2012b. Assessing the transferability of the regional climate model REMO to different coordinated regional climate downscaling experiment (CORDEX) regions. Atmosphere 3 (1), 181–199. https://doi.org/10.3390/atmos3010181.

Jacob, D., Podzun, R., 1997. Sensitivity studies with the regional climate model REMO. Meteorol. Atmos. Phys. 63 (1), 119–129. https://doi.org/10.1007/BF01025368.

Jacob, D., Teichmann, C., Sobolowski, S., Katragkou, E., Anders, I., Belda, M., Benestad, R., Boberg, F., Buonomo, E., Cardoso, R.M., Casanueva, A., Christensen, O. B., Christensen, J.H., Coppola, E., De Cruz, L., Davin, E.L., Dobler, A., Domínguez, M., Fealy, R., Fernandez, J., Gaertner, M.A., García-Díez, M., Giorgi, F., Gobiet, A., Goergen, K., Gomez-Navarro, J.J., Aleman, J.J.G., Gutierrez, C., Gutierrez, J.M., Güttler, I., Haensler, A., Halenka, T., Jerez, S., Jimenez-Guerrero, P., Jones, R.G., Keuler, K., Kjellstrom, E., Knist, S., Kotlarski, S., Maraun, D., van Meijgaard, E., Mercogliano, P., Montavez, J.P., Navarra, A., Nikulin, G., de Noblet-Ducoudre, N., Panitz, H.J., Pfeifer, S., Piazza, M., Pichelli, E., Pietikainen, J.P., Prein, A.F., Preuschmann, S., Rechid, D., Rockel, B., Romera, R., Sanchez, E., Sieck, K., Soares, P.M.M., Somot, S., Srnec, L., Sørland, S.L., Termonia, P., Truhetz, H., Vautard, R., Warrach-

Sagi, K., Wulfmeyer, V., 2020. Regional climate downscaling over Europe: perspectives from the EURO-CORDEX community. Reg. Environ. Change 20. https://doi.org/10.1007/s10113-020-01606-9.

Jerez, S., Lopez-Romero, J.M., Turco, M., Lorente-Plazas, R., Gomez-Navarro, J.J., Jimenez-Guerrero, P., Montavez, J.P., 2020. On the spin-up period in WRF simulations over Europe: trade-offs between length and seasonality. J. Adv. Model. Earth Syst. 12, 1–18. https://doi.org/10.1029/2019MS001945.

Karlický, J., Huszar, P., Halenka, T., Belda, M., Zak, M., Pisoft, P., Miksovský, J., 2018. Multi-model comparison of urban heat island modelling approaches. Atmos. Chem. Phys. 18, 10655–10674. https://doi.org/10.5194/acp-18-10655-2018.

Kotlarski, S., Keuler, K., Christensen, O.B., Colette, A., Deque, M., Gobiet, A., Goergen, K., Jacob, D., Lüthi, D., Van Meijgaard, E., Nikulin, G., Schar, C., Teichmann, C., Vautard, R., Warrach-Sagi, K., Wulfmeyer, V., 2014. Regional climate modeling on European scales: a joint standard evaluation of the EURO- CORDEX RCM ensemble. Geosci. Model Dev. (GMD) 7, 1297–1333. https://doi.org/10.5194/gmd-7-1297-2014.

Langendijk, G.S., Aubry-Wake, C., Osman, M., Gulizia, C., Attig-Bahar, F., Behrens, E., Bertoncini, A., Hart, N., Indasi, V.S., Innocenti, S., van der Linden, E.C., Mamnun, N., Rasouli, K., Reed, K.A., Ridder, N., Rivera, J., Ruscica, R., Ukazu, B.U., Walawender, J.P., Walker, D.P., Woodhams, B.J., Yilmaz, Y.A., 2019a. Three ways forward to improve regional information for extreme events: an early career perspective. Front. Environ. Sci. 7 https://doi.org/10.3389/fenvs.2019.00006.

Langendijk, G.S., Rechid, D., Jacob, D., 2019b. Urban areas and urban-rural contrasts under climate change: what does the EURO-CORDEX ensemble tell us?-Investigating near surface humidity in berlin and its surroundings. Atmosphere 10. https://doi.org/10.3390/ATMOS10120730.

Leps, N., Brauch, J., Ahrens, B., 2019. Sensitivity of limited area atmospheric simulations to lateral boundary conditions in idealized experiments. J. Adv. Model. Earth Syst. 11, 2694–2707. https://doi.org/10.1029/2019MS001625.

Li, D., Yuan, J., Kopp, R.E., 2020. Escalating global exposure to compound heat-humidity extremes with warming. Environ. Res. Lett. 6 (064003) https://doi.org/10.1088/1748-9326/ab7d04.

Lokoshchenko, M.A., 2017. Urban heat island and urban dry island in Moscow and their centennial changes. J. Appl. Meteorol. Climatol. 10, 2729–2745. https://doi.org/10.1175/JAMC-D-16-0383.1.

Lowe, J.A., McSweeney, C., Hewitt, C., 2020. An overview of the EUCP project-towards improved European Climate Predictions and Projections. EGU Gen. Assem. Conf. Abstr. 19475.

Lowen, A.C., Mubareka, S., Steel, J., Palese, P., 2007. Influenza virus transmission is dependent on relative humidity and temperature. PLoS Pathog. 3, 1470–1476. https://doi.org/10.1371/journal.ppat.0030151.

Majewski, D., 1991. The europa-modell of the deutscher wetterdienst. ECMWF Semin. Numer. methods Atmos. Model. 2, 147–191.

Masson, V., Lemonsu, A., Hidalgo, J., Voogt, J., 2020. Urban climates and climate change. Annu. Rev. Environ. Resour. 45, 411–444. https://doi.org/10.1146/annurev-environ-012320-083623.

Matte, D., Laprise, R., Theriault, J.M., 2016. Comparison between high-resolution ´ climate simulations using single- and double-nesting approaches within the Big- Brother experimental protocol. Clim. Dynam. 47, 3613–3626. https://doi.org/10.1007/s00382-016-3031-9.

Matte, D., Laprise, R., Theriault, J.M., Lucas-Picher, P., 2017. Spatial spin-up of fine scales in a regional climate model simulation driven by low-resolution boundary conditions. Clim. Dynam. 49, 563–574. https://doi.org/10.1007/s00382-016-3358-2.

Mishra, V., Ganguly, A.R., Nijssen, B., Lettenmaier, D.P., 2015. Changes in observed climate extremes in global urban areas. Environ. Res. Lett. 10, 024005 https://doi.org/10.1088/1748-9326/10/2/024005.

Mitchell, D., AchutaRao, K., Allen, M., Bethke, I., Beyerle, U., Ciavarella, A., Forster, P. M., Fuglestvedt, J., Gillett, N., Haustein, K., Ingram, W., Iversen, T., Kharin, V., Klingaman, N., Massey, N., Fischer, E., Schleussner, C.-F., Scinocca, J., Seland, Ø., Shiogama, H., Shuckburgh, E., Sparrow, S., Stone, D., Uhe, P., Wallom, D., Wehner, M., Zaaboul, R., 2017. Half a degree additional warming, prognosis and projected impacts (HAPPI): background and experimental design. Geosci. Model Dev. (GMD) 10, 571–583. https://doi.org/10.5194/gmd-10-571-2017.

Myhre, G., Alterskjær, K., Stjern, C.W., Hodnebrog, Marelle, L., Samset, B.H., Sillmann, J., Schaller, N., Fischer, E., Schulz, M., Stohl, A., 2019. Frequency of extreme precipitation increases extensively with event rareness under global warming. Sci. Rep. 9 (1), 1–10. https://doi.org/10.1038/s41598-019-52277-4.

Pietikainen, J.P., O'Donnell, D., Teichmann, C., Karstens, U., Pfeifer, S., Kazil, J., Podzun, R., Fiedler, S., Kokkola, H., Birmili, W., O'Dowd, C., Baltensperger, U., Weingartner, E., Gehrig, R., Spindler, G., Kulmala, M., Feichter, J., Jacob, D., Laaksonen, A., 2012. The regional aerosol-climate model REMO-HAM. Geosci. Model Dev. (GMD) 5, 1323–1339. https://doi.org/10.5194/gmd-5-1323-2012.

Prein, A.F., Langhans, W., Fosser, G., Ferrone, A., Ban, N., Goergen, K., Keller, M., Tolle, M., Gutjahr, O., Feser, F., Brisson, E., Kollet, S., Schmidli, J., Van Lipzig, N.P. M., Leung, R., 2015. A review on regional convection-permitting climate modeling: demonstrations, prospects, and challenges. Rev. Geophys. 53, 323–361. https://doi.org/10.1002/2014RG000475.

Raymond, C., Matthews, T., Horton, R.M., 2020. The emergence of heat and humidity too severe for human tolerance. Sci. Adv. 6 https://doi.org/10.1126/sciadv.aaw1838.

Rechid, D., Jacob, D., 2006. Influence of monthly varying vegetation on the simulated climate in Europe. Meteorol. Z. 15, 99–116. https://doi.org/10.1127/0941-2948/2006/0091.

Roeckner, E., Arpe, K., Bengtsson, L., Christoph, M., Claussen, M., Dümenil, L., Esch, M., Giorgetta, M., Schlese, U., Schulzweida, U., 1996. The atmospheric general circulation model ECHAM-4: model description and simulation of present-day climate. MPI Rep 218, 171.

Rosenzweig, C., Solecki, W., Romero-Lankao, P., Mehrotra, S., Dhakal, S., Bowman, T., Ibrahim, S.A., 2018. Climate change and cities: second assessment report of the urban climate change research network. In: Climate Change and Cities. https://doi.org/10.1017/9781316563878.007.

Semmler, T., 2002. Der Wasser- und Energiehaushalt der arktischen Atmosphare. Examensarbeit - Max-Planck-Institut fur Meteorol, pp. 101–106.

Shaman, J., Kohn, M., 2009. Absolute humidity modulates influenza survival, transmission, and seasonality. Proc. Natl. Acad. Sci. Unit. States Am. 106, 3243–3248. https://doi.org/10.1073/PNAS.0806852106.

Shaman, J., Pitzer, V.E., Viboud, C., Grenfell, B.T., Lipsitch, M., 2010. Absolute humidity and the seasonal onset of influenza in the continental United States. PLoS Biol. 8 https://doi.org/10.1371/journal.pbio.1000316.

Sharma, A.S., Baker, D.N., Bhattacharyya, A., Bunde, A., Dimri, V.P., Gupta, H.K., Gupta, V.K., Lovejoy, S., Main, I.G., Schertzer, D., Von Storch, H., Watkins, N.W., 2013. Complexity and extreme events in geosciences: an overview. Extrem. Events Nat. Hazards Complex. Perspect 1–16. https://doi.org/10.1029/2012GM001233

Sieck, K., Nam, C., Bouwer, L.M., Rechid, D., Jacob, D., 2021. Weather Extremes over Europe under Regional Climate Ensemble Simulations, pp. 457–468.

Sillmann, J., Thorarinsdottir, T., Keenlyside, N., Schaller, N., Alexander, L.V., Hegerl, G., Seneviratne, S.I., Vautard, R., Zhang, X., Zwiers, F.W., 2017. Understanding, modeling and predicting weather and climate extremes: challenges and opportunities. Weather Clim. Extrem. 18, 65–74. https://doi.org/10.1016/j.wace.2017.10.003.

Spankuch, D., Güldner, J., Steinhagen, H., Bender, M., 2011. Analysis of a dryline-like feature in northern Germany detected by ground-based microwave profiling. Meteorol. Z. 20, 409–421. https://doi.org/10.1127/0941-2948/2011/0222.

Stevens, B., Giorgetta, M., Esch, M., Mauritsen, T., Crueger, T., Rast, S., Salzmann, M., Schmidt, H., Bader, J., Block, K., Brokopf, R., Fast, I., Kinne, S., Kornblueh, L., Lohmann, U., Pincus, R., Reichler, T., Roeckner, E., 2013. Atmospheric component of the MPI-M earth system model: ECHAM6. J. Adv. Model. Earth Syst. 5, 146–172. https://doi.org/10.1002/jame.20015.

Stull, R., 2017. Practical Meteorology: an Algebra-Based Survey of Atmospheric Science. Univ. of British Columbia.

von Trentini, F., Leduc, M., Ludwig, R., 2019. Assessing natural variability in RCM signals: comparison of a multi model EURO-CORDEX ensemble with a 50-member single model large ensemble. Clim. Dynam. 53, 1963–1979. https://doi.org/10.1007/s00382-019-04755-8.

Wiesner, S., Bechtel, B., Fischereit, J., Gruetzun, V., Hoffmann, P., Leitl, B., Rechid, D., Schlünzen, K., Thomsen, S., 2018. Is it possible to distinguish global and regional climate change from urban land cover induced signals? A mid-latitude city example. Urban Sci 2, 12. https://doi.org/10.3390/urbansci2010012.

ANNEX

Figure A1. Selected domain (four grid boxes) for identifying the extremes based on the HAPPI (0.44°) data, centered around Berlin. Example variable shown is temperature.

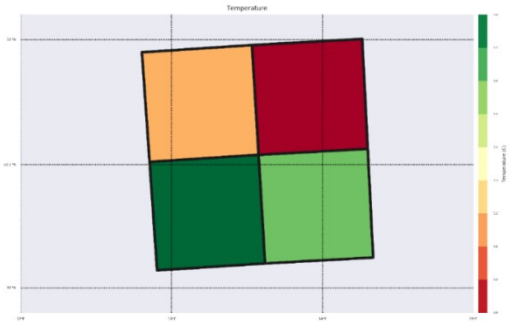

Figure A2. The block maxima and block minima distributions, and 90th and 10th percentile distributions (for RH & SH also 5th and 95th percentiles) based on the HAPPI ensemble members, for RH, SH, 2-m temperature, 2-m maximum temperature, 2-m minimum temperature, and precipitation, for the historic decade (1996 – 2005), 1.5°C and 2.0°C simulated periods.

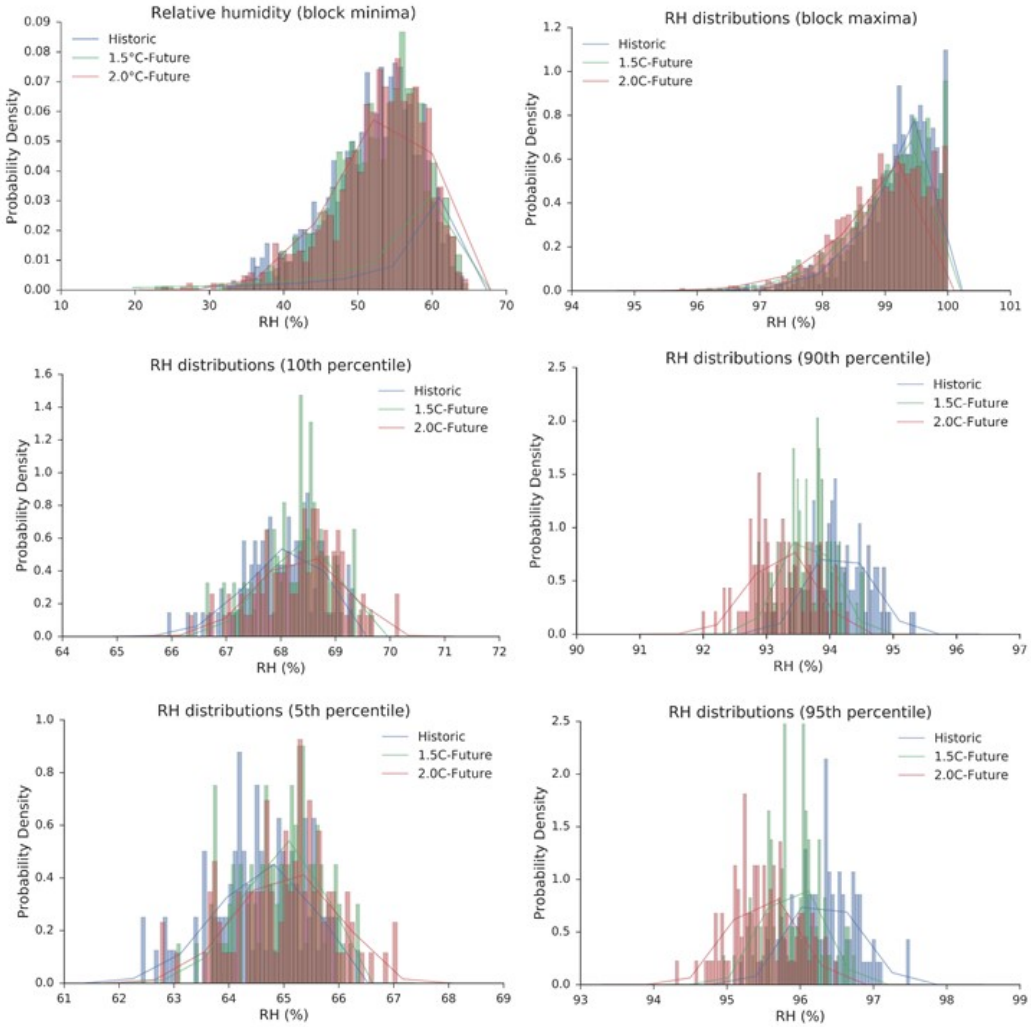

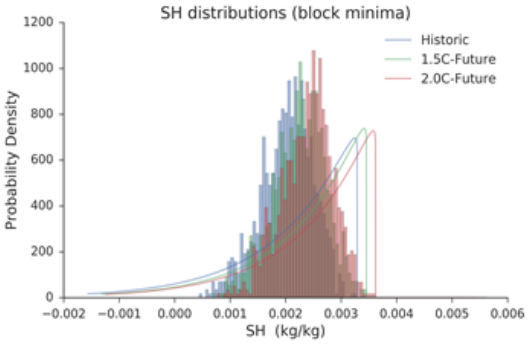
SH distributions (block minima)
Historic
1.5C-Future
2.0C-Future
Probability Density
SH (kg/kg)

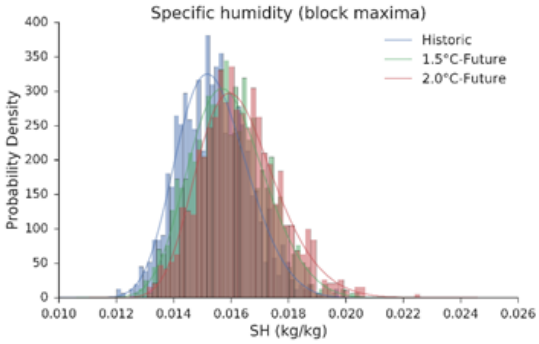
Specific humidity (block maxima)
Historic
1.5°C-Future
2.0°C-Future
Probability Density
SH (kg/kg)

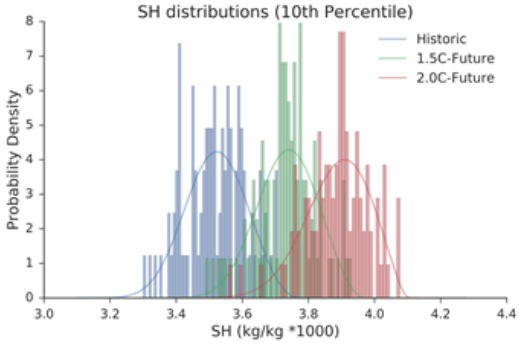
SH distributions (10th Percentile)
Historic
1.5C-Future
2.0C-Future
Probability Density
SH (kg/kg *1000)

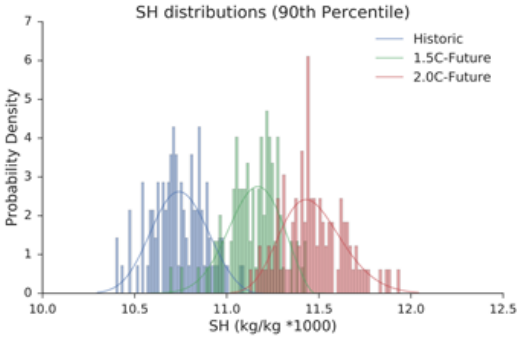
SH distributions (90th Percentile)
Historic
1.5C-Future
2.0C-Future
Probability Density
SH (kg/kg *1000)

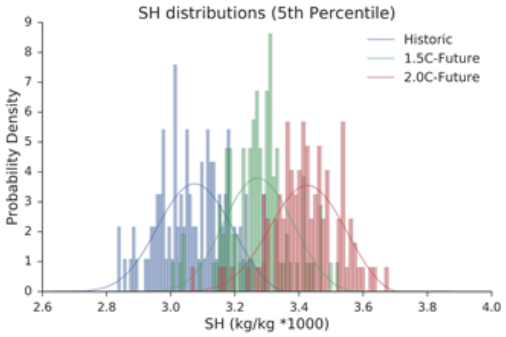
SH distributions (5th Percentile)
Historic
1.5C-Future
2.0C-Future
Probability Density
SH (kg/kg *1000)

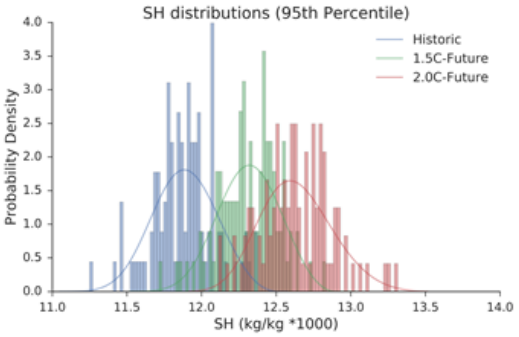
SH distributions (95th Percentile)
Historic
1.5C-Future
2.0C-Future
Probability Density
SH (kg/kg *1000)

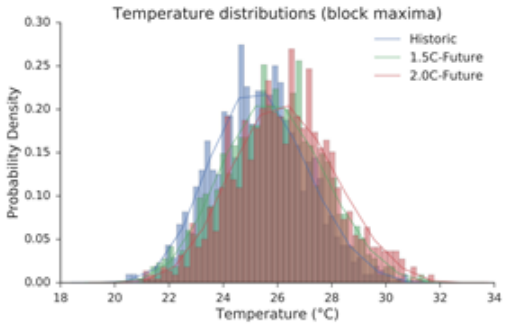
Temperature distributions (block maxima)
Historic
1.5C-Future
2.0C-Future
Probability Density
Temperature (°C)

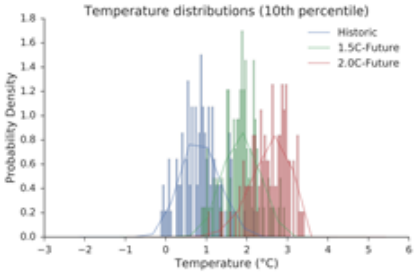
Temperature distributions (10th percentile)
Historic
1.5C-Future
2.0C-Future
Probability Density
Temperature (°C)

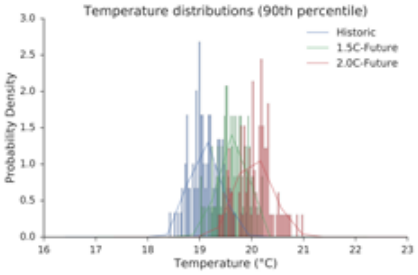
Temperature distributions (90th percentile)
Historic
1.5C-Future
2.0C-Future
Probability Density
Temperature (°C)

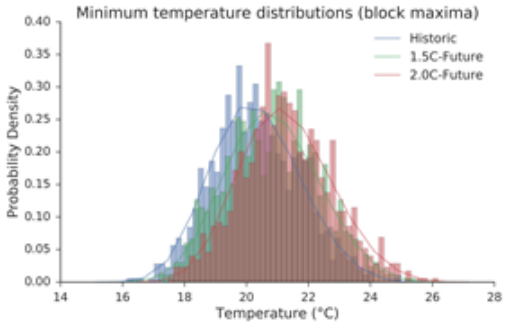
Minimum temperature distributions (block maxima)
Historic
1.5C-Future
2.0C-Future
Probability Density
Temperature (°C)

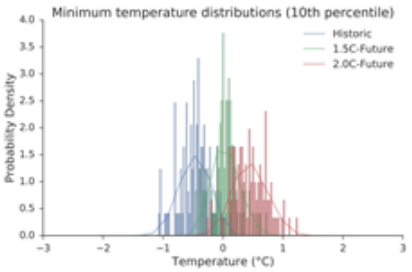
Minimum temperature distributions (10th percentile)
Historic
1.5C-Future
2.0C-Future
Probability Density
Temperature (°C)

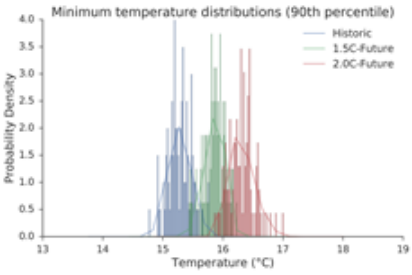
Minimum temperature distributions (90th percentile)
Historic
1.5C-Future
2.0C-Future
Probability Density
Temperature (°C)

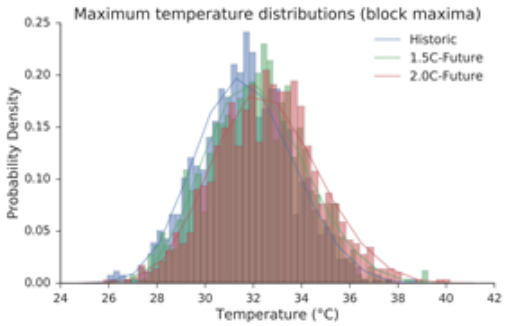
Maximum temperature distributions (block maxima)
Historic
1.5C-Future
2.0C-Future
Probability Density
Temperature (°C)

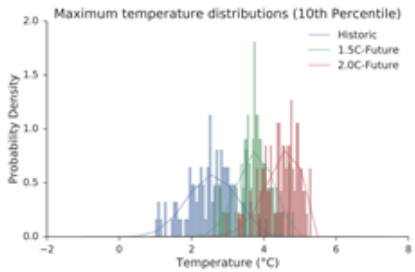
Maximum temperature distributions (10th Percentile)
Historic
1.5C-Future
2.0C-Future
Probability Density
Temperature (°C)

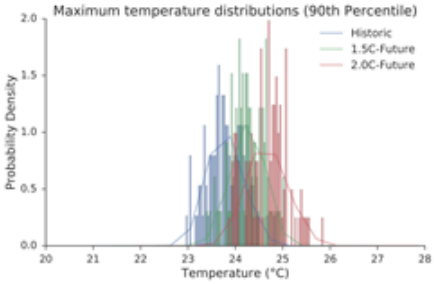
Maximum temperature distributions (90th Percentile)
Historic
1.5C-Future
2.0C-Future
Probability Density
Temperature (°C)

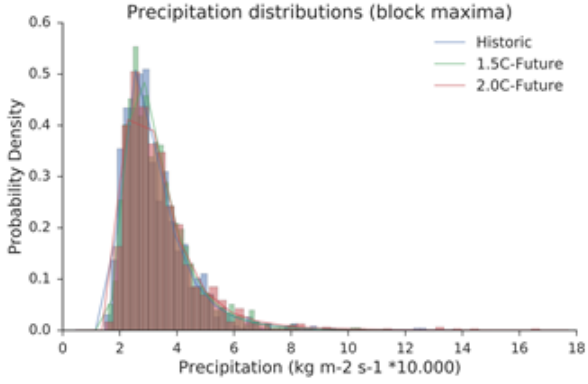
Precipitation distributions (block maxima)
Historic
1.5C-Future
2.0C-Future
Probability Density
Precipitation (kg m-2 s-1 *10.000)

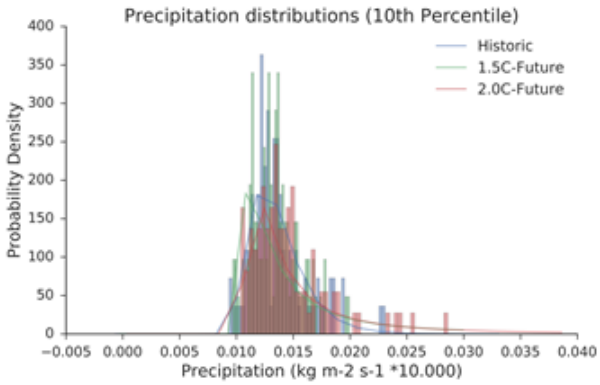
Precipitation distributions (10th Percentile)
Historic
1.5C-Future
2.0C-Future
Probability Density
Precipitation (kg m-2 s-1 *10.000)

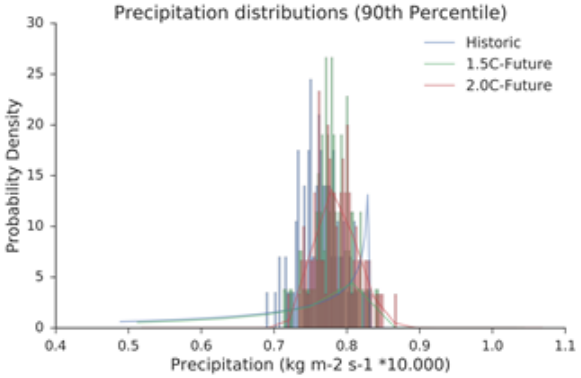
Precipitation distributions (90th Percentile)
Historic
1.5C-Future
2.0C-Future
Probability Density
Precipitation (kg m-2 s-1 *10.000)

Figure A3. SH>0.02 kg/kg extreme condition, 5-days time series around the extreme conditions.

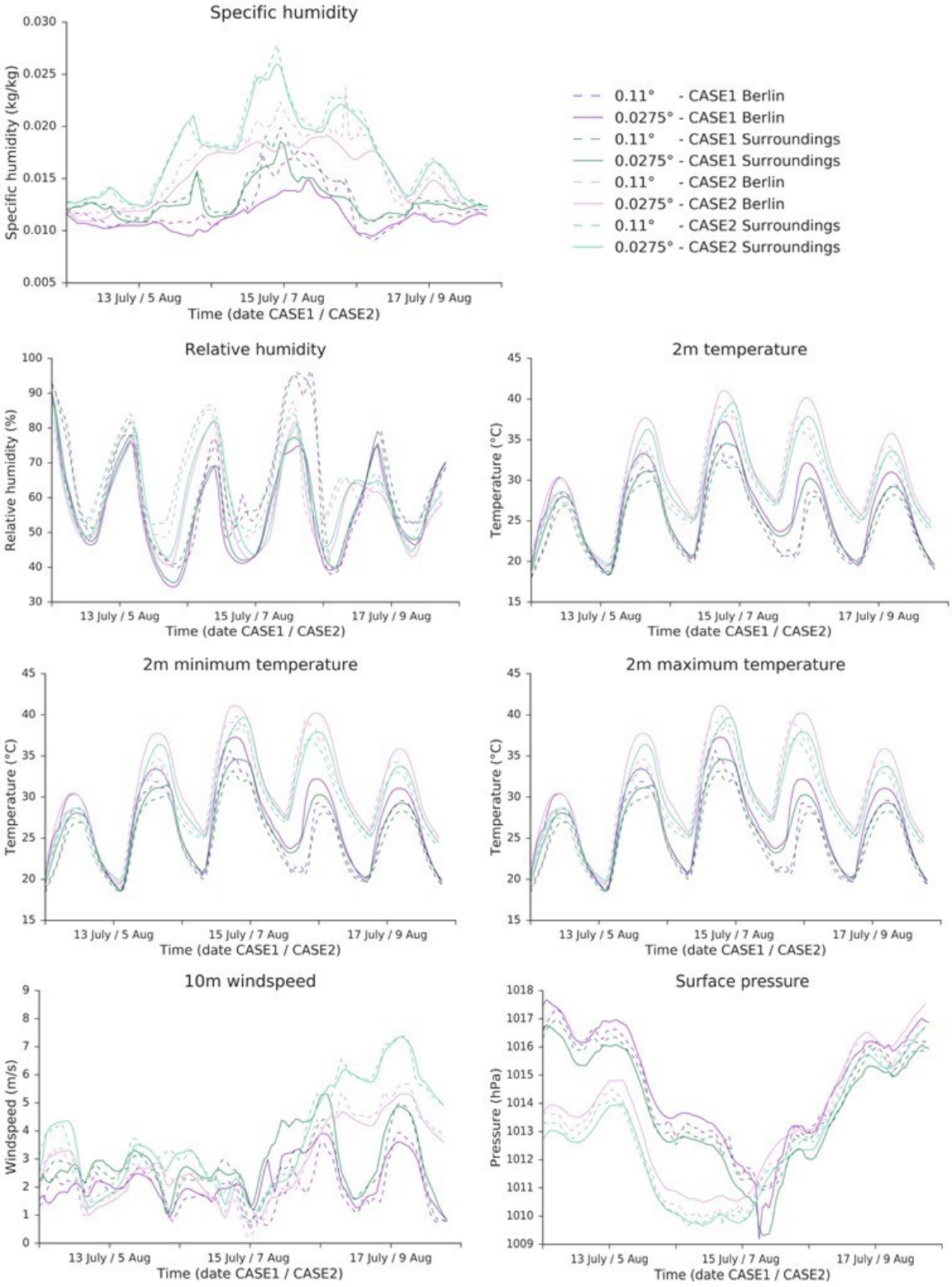

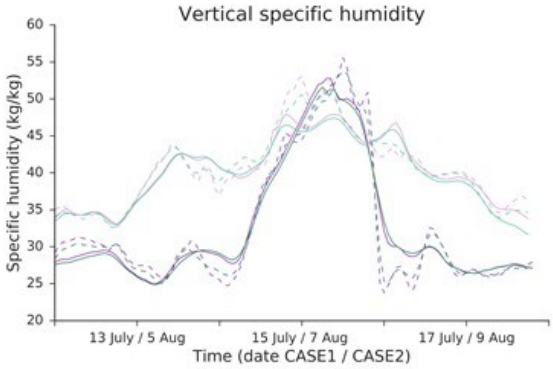
Vertical specific humidity
Specific humidity (kg/kg)
60
55
50
45
40
35
30
25
20
13 July / 5 Aug
15 July / 7 Aug
17 July / 9 Aug
Time (date CASE1 / CASE2)

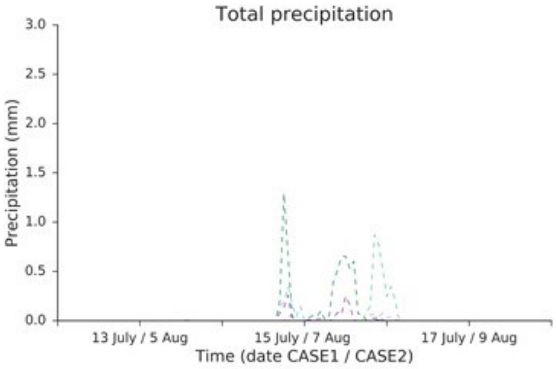
Total precipitation
Precipitation (mm)
3.0
2.5
2.0
1.5
1.0
0.5
0.0
13 July / 5 Aug
15 July / 7 Aug
17 July / 9 Aug
Time (date CASE1 / CASE2)

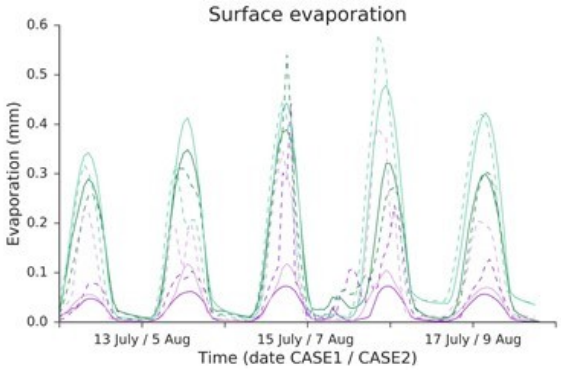
Surface evaporation
Evaporation (mm)
0.6
0.5
0.4
0.3
0.2
0.1
0.0
13 July / 5 Aug
15 July / 7 Aug
17 July / 9 Aug
Time (date CASE1 / CASE2)

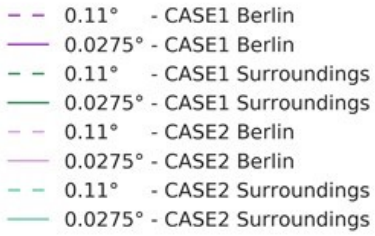
0.11° - CASE1 Berlin
0.0275° - CASE1 Berlin
0.11° - CASE1 Surroundings
0.0275° - CASE1 Surroundings
0.11° - CASE2 Berlin
0.0275° - CASE2 Berlin
0.11° - CASE2 Surroundings
0.0275° - CASE2 Surroundings

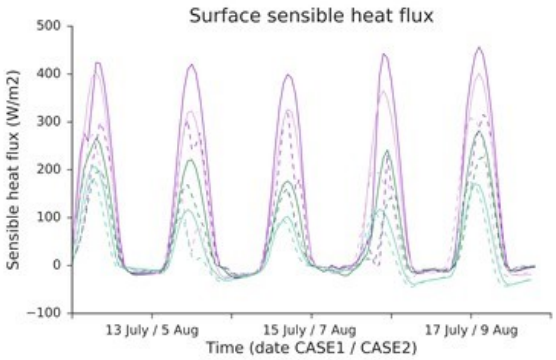
Surface sensible heat flux
Sensible heat flux (W/m2)
500
400
300
200
100
0
−100
13 July / 5 Aug
15 July / 7 Aug
17 July / 9 Aug
Time (date CASE1 / CASE2)

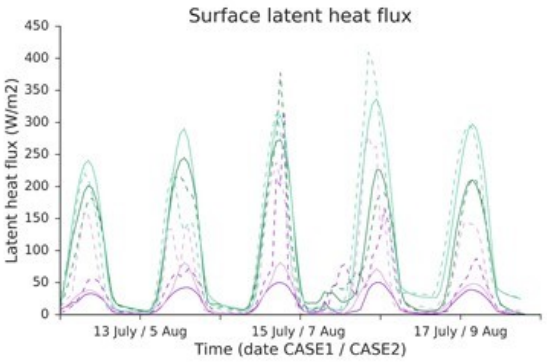
Surface latent heat flux
Latent heat flux (W/m2)
450
400
350
300
250
200
150
100
50
0
13 July / 5 Aug
15 July / 7 Aug
17 July / 9 Aug
Time (date CASE1 / CASE2)

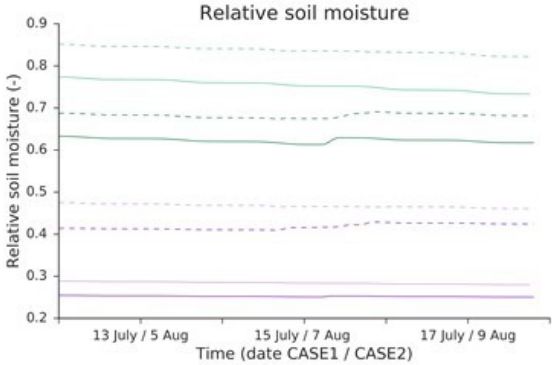
Relative soil moisture
Relative soil moisture (-)
0.9
0.8
0.7
0.6
0.5
0.4
0.3
0.2
13 July / 5 Aug
15 July / 7 Aug
17 July / 9 Aug
Time (date CASE1 / CASE2)

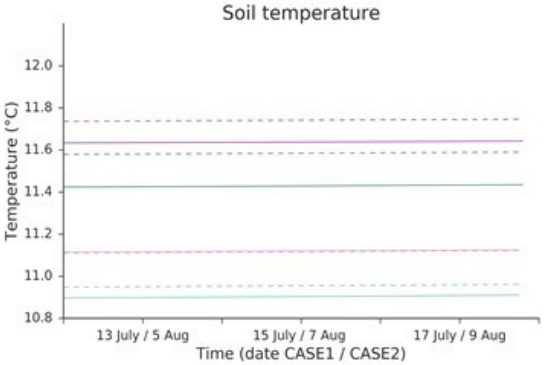
Soil temperature
Temperature (°C)
12.0
11.8
11.6
11.4
11.2
11.0
10.8
13 July / 5 Aug
15 July / 7 Aug
17 July / 9 Aug
Time (date CASE1 / CASE2)

Figure A4. RH<30 % extreme condition, 5-days time series around the extreme conditions.

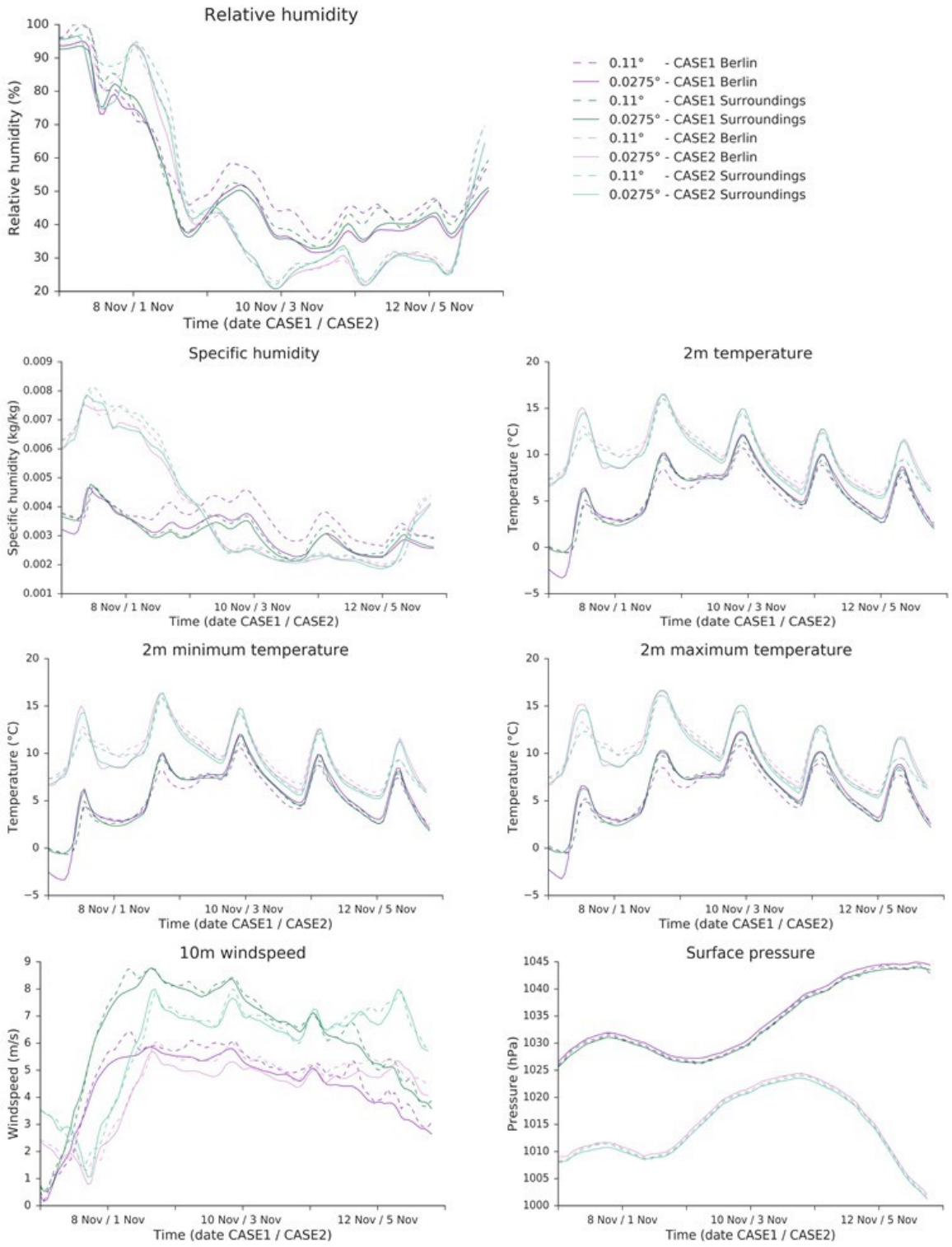

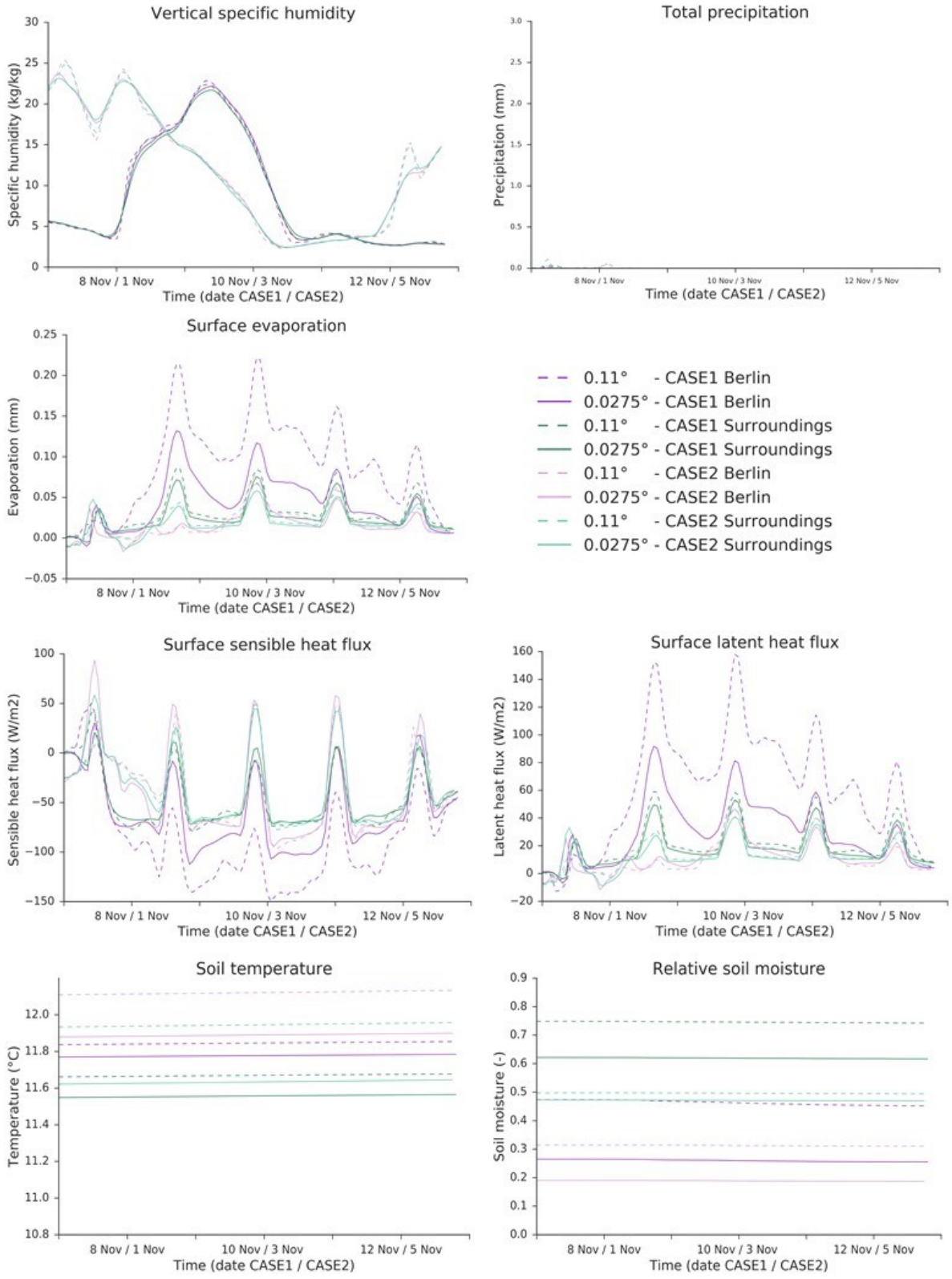
Vertical specific humidity
Specific humidity (kg/kg)
Time (date CASE1 / CASE2)
Total precipitation
Precipitation (mm)
Surface evaporation
Evaporation (mm)
0.11° - CASE1 Berlin
0.0275° - CASE1 Berlin
0.11° - CASE1 Surroundings
0.0275° - CASE1 Surroundings
0.11° - CASE2 Berlin
0.0275° - CASE2 Berlin
0.11° - CASE2 Surroundings
0.0275° - CASE2 Surroundings
Surface sensible heat flux
Sensible heat flux (W/m2)
Surface latent heat flux
Latent heat flux (W/m2)
Soil temperature
Temperature (°C)
Relative soil moisture
Soil moisture (-)
8 Nov / 1 Nov
10 Nov / 3 Nov
12 Nov / 5 Nov

Table A1. Summary of key results, based on four main aspects: difference between spatial resolutions (0.11° vs. 0.0275°); urban-rural contrast (Berlin vs. surroundings); comparing the cases (Case1 vs. Case2 of each extreme condition); comparing the extreme conditions (SH>0.02 kg/kg *vs. RH<30 %).*

	Spatial differences *(going from 0.11° to 0.0275°)*		**Urban-rural contrast** *(Berlin compared to surroundings)*	
Variable	**SH>0.02**	**RH<30**	**SH>0.02**	**RH<30**
Relative humidity (RH) (%)	decrease up to 20%	decrease up to 10% (particularly CaseRH1)	decrease up to 10%	varying between decrease and increase, for 0.0275° and CaseRH2. CaseRH1: Berlin ~5% moister than surroundings for 0.11°.
Specific humidity (SH) (kg/kg)	decrease up to 0.005 kg/kg	decrease up to 0.0007 kg/kg (particularly CaseRH1)	decrease up to 0.008 kg/kg	varying between decrease and increase, for 0.0275° and CaseRH2. CaseRH1: Berlin up to 0.0008 kg/kg moister than surroundings for 0.11°.
2-m temperature (°C)	increase by 1-2°C (especially during day time)	increase by ~1°C (especially during day time)	increase up to 2°C (increase for 0.0275° up to 0.03°C larger than for 0.11°)	increase up to 1°C CaseRH1: decrease up to 1.2°C for 0.11°
2-m minimum temperature (°C)	increase by 1-2°C (especially during day time)	increase by ~1°C (especially during day time)	increase up to 2°C (increase for 0.0275° up to 0.03°C larger than for 0.11°)	increase up to 1°C CaseRH1: decrease up to 1.2°C for 0.11°
2-m maximum temperature (°C)	increase by 1-2°C (especially during day time)	increase by ~1°C (especially during day time)	increase up to 2°C (increase for 0.0275° up to 0.03°C larger than for 0.11°)	increase up to 1°C CaseRH1: decrease up to 1.2°C for 0.11°
10-m windspeed (m/s)	increase up to 1 m/s	decrease up to 0.8 m/s	decrease up to 1.5 m/s	decrease up to 3 m/s
Surface pressure (hPa)	increase up to 1 hPa	increase up to 1 hPa	increase up to 1hPa (increase for 0.0275° up to 0.5 hPa larger than for 0.11°)	increase up to 1hPa (increase for 0.0275° up to 0.5 hPa larger than for 0.11°)
Vertically integrated SH (kg/kg)	decrease, particularly during extreme event peak	Minimal spatial differences	increase up to 1 kg/kg	Limited urban-rural contrast, increase up to 1 kg/kg
Relative soil moisture (-)	decrease up to 0.2	decrease up to 0.2	decrease up to 0.5 (decrease for 0.0275° up to 0.1 larger than 0.11°)	decrease up to 0.35 (decrease for 0.0275° up to 0.1 larger than 0.11°)
Surface evaporation (mm)	decrease up to 0.2 mm	minimal urban-rural contrast CaseRH1: decrease up to 0.1 mm in Berlin	decrease up to 0.3 mm. (decrease for 0.0275° up to 0.2 mm larger than for 0.11°)	CaseRH1: increase up to 0.1 mm. Urban-rural contrast smaller for 0.0275° than 0.11°. CaseRH2: minimal urban-rural contrast.
Surface latent heat flux (W/m2)	increase up to 200 W/m2	minimal urban-rural contrast CaseRH1: increase up to 100 W/m2	decrease up to 250 W/m2. (decrease for 0.0275° up to ~150W/m2 larger than for 0.11°)	CaseRH1: increase up to 100 W/m2. For 0.0275° urban-rural contrast is up to ~80W/m2 smaller than 0.11°. CaseRH2: minimal urban-rural contrast.
Surface sensible heat flux (W/m2)	increase up to 100 W/m2	minimal urban-rural contrast CaseRH1: increase up to 100 W/m2 in Berlin	increase up to 200 W/m2. (increase for 0.0275° up to ~150W/m2 larger than for 0.11°)	minimal urban-rural contrast. (CaseRH1: decrease up to 80 W/m2 for 0.11°)
Total precipitation (mm)	0.11° light precipitation events, 0.0275° hardly any precipitation	light precipitation for 0.11° before extreme condition. 0.0275° no precipitation	no clear urban-rural contrast	no clear urban-rural contrast
Soil temperature (°C)	decrease up to 0.2°C	decrease up to 0.2°C	increase up to 0.2°C. (increase for 0.0275° up to 0.05°C larger than for 0.11°)	increase up to 0.25°C. (increase for 0.0275° up to 0.07°C larger than 0.11°)

Chapter 3.3.

Improved models, improved information? Exploring how climate change impacts pollen, influenza, and mold in Berlin and its surroundings

Gaby S. Langendijk, Diana Rechid, Daniela Jacob

Paper 3

Urban Climate 43 (2022) 101159

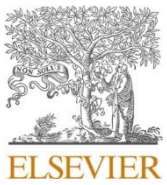

Contents lists available at ScienceDirect

Urban Climate

journal homepage: www.elsevier.com/locate/uclim

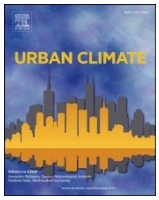

Improved models, improved information? Exploring how climate change impacts pollen, influenza, and mold in Berlin and its surroundings

Gaby S. Langendijk[a,b,*], Diana Rechid[a], Daniela Jacob[a,b]

[a] Climate Service Center Germany (GERICS), Helmholtz-Zentrum Hereon, Fischertwiete 1, 20095 Hamburg, Germany

[b] Faculty of Sustainability, Leuphana University of Lüneburg, Universitätsallee 1, 21335 Lüneburg, Germany

ARTICLEINFO

Keywords:
Climate change impact
Convection-permittingmodel
Added value
Regional climate model
Pollen
Mold
Influenza
Humidity
Berlin

ABSTRACT

Urban decision makers rely on evidence-based climate information tailored to their needs to adequately adapt and prepare for future climate change impacts. Regional climate models, with grid sizes between 10–50 km, are a useful outset to understand potential future climate change impacts in urban regions. Recently developed convection-permitting climate models have grid sizes smaller than 5 km, and better resolve atmospheric processes related to the land surface like convection, and complex terrain such as cities. This study investigates how the convection- permitting model REMO simulates changes in climate conditions in the urban-rural context, compared to its conventional hydrostatic version. We analyze three impact cases: influenza spread and survival; ragweed pollen dispersion; and indoor mold growth. Simulations are analyzed for the near future (2041–2050) under emission scenario RCP8.5. Taking the Berlin region as a testbed, we show that the change signal (positive or negative impact) reverses for the 3 km compared to the 12.5 km grid resolution for the impact cases pollen, and mold, indicating added value. For influenza, the convection-permitting resolution intensifies the decrease of influenza days under climate change. The results show the potential of convection-permitting simulations to generate improved information about climate change impacts for urban regions to support decision making.

* Corresponding author at: Climate Service Center Germany (GERICS), Helmholtz-Zentrum Hereon, Fischertwiete 1, 20095 Hamburg, Germany.
E-mail address: gaby.langendijk@hereon.de (G.S. Langendijk).

https://doi.org/10.1016/j.uclim.2022.101159
Received 21 September 2021; Received in revised form 17 February 2022; Accepted 20 March 2022
Available online 31 March 2022

1. Introduction

High-quality, science-based climate information for cities and its surroundings is crucial for urban decision makers and dwellers in order to prepare for and adapt to climate change (Baklanov et al., 2018; Rosenzweig et al., 2018). This information shall be tailored to the needs of urban decision makers, suitable for their specific application and context (Bai et al., 2018; Baklanov et al., 2018). Urban areas have distinct climatological characteristics that differ from its surroundings, e.g. the urban heat and dry island effect (e.g. Langendijk et al., 2019; Lokoshchenko, 2017; Masson et al., 2020). Therefore, climate change may manifest differently in cities than its direct surroundings. Environmental factors, and more specifically meteorological conditions, are key drivers for climate change impacts in urban areas (Masson et al., 2020; Rosenzweig et al., 2018).

Models are a useful outset to understand changes in meteorological conditions in cities as a result of climate change. Regional climate models simulate the Earth's key physical climate processes and their interactions. They divide the Earth's surface and overlying atmosphere into a giant grid. The model calculates meteorological variables, such as temperature, humidity and precipitation, for each grid cell. The horizontal grid size, or "grid resolution", of regional climate models are typically in the range of 50–10 km, with around 20–30 vertical layers (Jacob et al., 2020). Grid sizes up to 20–10 km allow for the simulation of larger urban areas under longer climatological timescales, using simple urban schemes. The models are commonly unable to capture intra-city differences and fine-scale urban climate processes (Langendijk et al., 2019).

The newly developed, so-called, convection-permitting (CP) climate models are high-resolution regional models of the Earth's climate that have a horizontal grid size of less than 5 km, and around 40–50 vertical layers. CP models better resolve the land surface and convective processes, leading to improved representation of small-scale processes in the atmosphere and complex terrain, such as cities (Argüeso et al., 2016; Ban et al., 2021, 2014; Coppola et al., 2020; Kendon et al., 2021; Prein et al., 2015). This can result in clear improvements, so-called added value, to simulate climate change impacts, which subsequently allows for better-informed decision making (Di Luca et al., 2015). There has only been limited research on the added value of CP models to simulate and understand climate change impacts in urban areas compared to its surroundings. Therefore, this research explores the potential of convection- permitting models to improve the simulation of climate change impacts in urban areas and its surroundings. The study compares regional climate model output on the 12.5 km grid resolution and the 3 km convection-permitting resolution, using Berlin and its surroundings as testbed.

1.1. Impact cases

To investigate the effect of the convection-permitting scale on climate conditions related to climate change impacts, three so-called impact cases are defined: influenza spread and survival, ragweed pollen dispersion, and indoor mold growth. These impact cases are selected because they all have direct or in-direct effects on human health, and they have been hardly investigated by previous studies, especially not under future climate change and in the urban-rural context. The three impact cases are defined by meteorological conditions, foremost underpinned by the variables humidity and temperature. The change in meteorological conditions for each impact case under climate change is studied. The following section introduces the impact cases and defines the meteorological con- ditions that favor the cases based on existing literature. This study particularly considers humidity and temperature. Humidity is expressed as specific humidity (SH), which is the amount of water vapor in relation to the total mass of water vapor and air combined, expressed in kilograms of water vapor per kilogram of moist air (kg/kg). In addition, it considers relative humidity

(RH), the saturation of the air compared to the water vapor the fully saturated air could contain at a specific temperature, expressed as a percentage (%).

1.1.1 Influenza survival and transmission

The infectious disease influenza, commonly known as "flu", is one of the most deadly of all airborne and upper-respiratory in- fections (Fuhrmann, 2010). Much of the observed wintertime increase of mortality in temperate regions is attributed to seasonal influenza (Shaman et al., 2010). On average, 22,000 deaths and over 3 million hospitalizations in USA are attributed to influenza each year (Fuhrmann, 2010). In 2017/18 around 25.100 people died in Germany during the most deadly influenza wave in 30 years (RKI, 2019). A previous study investigating the historic time period 1970–2016 showed long-term climate variations influenced the influenza-like illness incidence rates in the Netherlands, through changes in absolute humidity and temperature (Caini et al., 2018). Although of profound interest, the potential impacts of future climate change on influenza epidemics is poorly understood, and no studies have directly investigated this interplay (Chong et al., 2020; Goodwins et al., 2019).

The connection between humidity and influenza is likely multifactorial, including impacts on virus stability and viability, host susceptibility, and human behavior (Davis et al., 2016). However, many studies show low humidity, often occurring in combination with low temperatures, is the predominant factor defining the transmission and survival of the influenza virus (Davis et al., 2016; Lowen et al., 2007; Lowen and Steel, 2014; Marr et al., 2019; Park et al., 2020; Peci et al., 2019; Shaman et al., 2011). Model pre- dictions suggest that approximately half of the average seasonal differences in US influenza mortality can be explained by seasonal differences in absolute humidity alone (Barreca and Shimshack, 2012). Soebiyanto et al. (2015) show a clear inverse relationship between specific humidity and influenza exists in Europe, and particularly in Berlin. Two hypotheses are proposed by Shaman and Kohn (2009) to explain the humidity-influenza relationship: (i) virus-laden droplet nuclei are more efficiently produced at lower humidity because of increased evaporation of expelled droplet particles, therefore more virus remains longer in the atmosphere; (ii) influenza virus survival increases as humidity decreases, such that the airborne virus remains viable longer at lower humidity levels (Shaman and Kohn, 2009).

Literature indicates a controversy of the appropriate humidity variable selection to study the humidity and influenza relationship. Many studies showed a relationship between low RH and influenza virus transmission and/or survival (Lowen et al., 2007; Lowen and Steel, 2014; Marr et al., 2019; Noti et al., 2013; Park et al., 2020). Though other studies show that SH or absolute humidity (AH) would be preferable over RH to investigate the humidity-influenza relationship, as SH/AH would constrain the transmission and survival of influenza more significantly than RH (Barreca and Shimshack, 2012; Chong et al., 2020; Peci et al., 2019; Shaman et al., 2011; Shaman and Kohn, 2009). Considering this discussion, specific humidity is selected to define the influenza threshold for this research.

A non-linear relationship between influenza transmission and survival exists that is most sensitive to low humidity values, leading to increases in the spread of influenza among humans (Barreca and Shimshack, 2012; Beest et al., 2013; Shaman et al., 2011, 2010). Specific humidity levels below approximately 6 g of water vapor per kilogram of air (0.006 kg/kg) are associated with increases in influenza mortality (Barreca and Shimshack, 2012). This is also in line with studies by Shaman et al., (2011, 2010 especially Fig. 1). Cold temperatures around ~5°C optimize the influenza conditions (Lowen and Steel, 2014; Park et al., 2020). The Robert Koch Institute (RKI, 2020) points out that influenza is mainly occurring in winter months in Brandenburg and Berlin.

This is confirmed by Soebiyanto et al. (2015) who indicate influenza is mainly prevalent in December – March in Berlin.

The selected meteorological threshold to investigate the influenza impact case is therefore, SH < 0.006 kg/kg, jointly with low temperatures from 2°C up to 6°C, for the period December – March (Table 1).

Table 1
Defined humidity thresholds and meteorological conditions per impact case: influenza spread and survival; ragweed pollen dispersion; and in-door mold growth.

	Influenza	Pollen	Mold
Meteorological variables	SH<0.006 kg/kg & 2 – 6°C	RH<60%	RH>80% & 10°C – 40°C
Months	December – March	July – October	entire year
Time/days	-	5am until 2pm	2 – 10 consecutive days

1.1.2. Ragweed pollen dispersion

Ragweed (Ambrosia artemisiifolia L.) is an invasive annual weed, native from North America, and currently one of the main allergenic species in Europe (Cunze et al., 2013; Ghiani et al., 2016). Ragweed is expected to particularly expand its range due to climate change in Northern Europe (Cunze et al., 2013; Storkey et al., 2014). In this regard, Hamaoui-Laguel et al. (2015) estimate that by 2050 airborne ragweed pollen concentrations will be about four times higher than they are now in Europe. Climate change could increase the length and severity of the pollen season and, as a consequence, the related pollen allergy (D'Amato and Cecchi, 2008; Ziska et al., 2003).

Due to regional urbanization-induced temperature and higher CO2 levels in cities ragweed grows faster, flowers earlier, and produces significantly greater ragweed pollen in urban than rural areas (Bergmann et al., 2012; Ziska et al., 2003). Epidemiological studies have demonstrated that urbanization, high levels of vehicle emissions and western lifestyles are correlated to an increase in the frequency of pollen-induced respiratory allergy, prevalent in people who live in urban areas compared to rural areas (D'Amato and Cecchi, 2008). Reinhardt et al. (2003) estimated the consequential costs for the treatment of patients allergic to ragweed to lie between €19 and €50 million per year for Germany under current climate conditions. In Berlin and its surroundings, extensive ragweed pop- ulations are reported and ragweed pollen are measured (Buters et al., 2015; Kannabei et al., 2013; Zink et al., 2012). Around 15 – 18% of Berlin's population suffers from a pollen allergy, resulting in approXimately 500,000 – 615,000 affected people just in this city (Bergmann et al., 2012).

Different meteorological and human factors influence pollen growth, length of the season, or transport through the atmosphere (e.g. Sofiev et al., 2013). There is specific evidence that low relative humidity, often occurring with higher temperatures, favors the release of pollen locally, directly enhancing pollen dispersion rates, while high humidity is associated with lower airborne pollen concentrations (Bianchi et al., 1959; D'Amato and Cecchi, 2008; Silverberg et al., 2015; Sofiev et al., 2013; Zink et al., 2012). Zink et al. (2012) found that the majority of the pollen in Germany originated in local areas. The ragweed pollen release period from a single flower lasts only up to 6 h (Prank et al., 2013). The pollen release can be strongly reduced, or even halted, by high relative humidity associated with rain, which can cover wider areas than the rain event itself (Sofiev et al., 2013).

Ragweed pollen emissions are considered a threshold process, dominated by low relative humidity, with a threshold of around <60% RH (Bianchi et al., 1959; Menut et al., 2014; Sofiev et al., 2013; Zink et al., 2012). The main ragweed flowering season is from August to September in Europe, however flowers can be found from July to October in the Berlin region (Kannabei et al., 2013; Liu et al., 2016; Prank et al., 2013). The end of flowering has been found to be correlated spatially and temporally with the onset of the first frost (Kannabei et al., 2013; Storkey et al., 2014). Local ragweed pollen emission mainly takes place during the morning hours: it starts shortly after sunrise and continues until early afternoon (Bianchi et al., 1959; Dingle et al., 1959; Laaidi and Laaidi, 1999; Zink et al., 2012).

The selected humidity threshold for the pollen impact case is RH < 60%, from 5 am until 2 pm, during July – October (Table 1).

1.1.3. Indoor mold growth

Indoor mold is a fungal growth that develops on building materials, expedited by particular outdoor temperatures, and humidity conditions (Sedlbauer, 2001). In Germany mold is one of the main causes of damage to buildings. The "Third Report on Building Damages" by the Federal Government of Germany estimated the costs resulting from mold fungi damages to amount more than 200 million Euro per year (Bundesministerium für Raumordnung, 1995). In addition, extensive mold growth in buildings can negatively affect human health, by causing and enhancing respiratory complications and related diseases such as asthma (Davis et al., 2016). Studies show that historic buildings are particularly prone to mold growth and damage (Curtis, 2010; Hao et al., 2020; Huijbregts et al., 2012). In Berlin every fourth house is built in the 1920s/30s, and around 50% of the building are older than 1960 (SSW, 2018).

A literature review by Hao et al. (2020) indicates that moisture risks are more likely to occur in buildings due to changes in the external climate and subsequent changes in the indoor climate. Leissner et al. (2015) particularly project higher mold risks in Northern parts of Germany by the mid as well as by the end of the century, based on derived mold index from regional climate model projections. A study by Huijbregts et al. (2012) found mold growth will increase due to climate change for two historic museum buildings in the Netherlands and Belgium, particularly driven by rising relative humidity levels.

The growth and spreading of mold fungi mainly depends on the climatic boundary conditions at the surfaces of construction parts and inside buildings. The decisive parameters are relative humidity, temperature and the corresponding substrate (Huijbregts et al., 2012; Johansson et al., 2012; Leissner et al., 2015; Lourenço et al., 2006; Ojanen et al., 2010; Pietrzyk, 2015; Sedlbauer, 2001; Viitanen and Ojanen, 2007; Viitanen et al., 2010). Despite the complexity of indoor climate, a direct correlation between internal and external conditions has been found and verified (Hao et al., 2020), including a strong correlation between indoor and outdoor absolute hu- midity (Nguyen et al., 2014). Outside relative humidity, in combination with temperature, is of critical importance to indoor mold growth.

Many studies identify conditions around >80% relative humidity and temperatures of 10°C – 40°C to be favorable for mold growth (Johansson et al., 2012; Leissner et al., 2015; Ojanen et al., 2010; Sedlbauer, 2001; Viitanen et al., 2010). Sedlbauer (2001 (especially Figure 9)) shows 2 – 16 consecutive days of favorable mold growth conditions enhance mold expansion.

The selected meteorological condition for the mold impact case is RH >80% and 10°C – 40°C, during the entire year. 2 –10 consecutive days of favorable mold growth conditions are also considered.

2. Methods

2.1. Study area

Berlin and its surroundings is selected as the case-study region. The capital of Germany, Berlin, is a large-scale city with around 3.6 million inhabitants covering approximately 891.1 km2 (Amt für Statistik Berlin-Brandenburg, 2020), located in-land at approximately 52.52°N, 13.4°E. The land cover of Berlin's surroundings is roughly 50% agricultural and grass land, 36% forest and 14% build up areas and water bodies (Fig. 1b) (Amt für Statistik Berlin-Brandenburg, 2020). Berlin and its surroundings are particularly suitable to investigate urban-rural contrasts using regional climate model output data, because of the relatively flat regional topography, Berlin's large city size, and the distinct urban-rural landscape heterogeneity. The primary investigated domain is approximately 140 km by 140 km centered around Berlin (black rectangular, Fig. 1b).

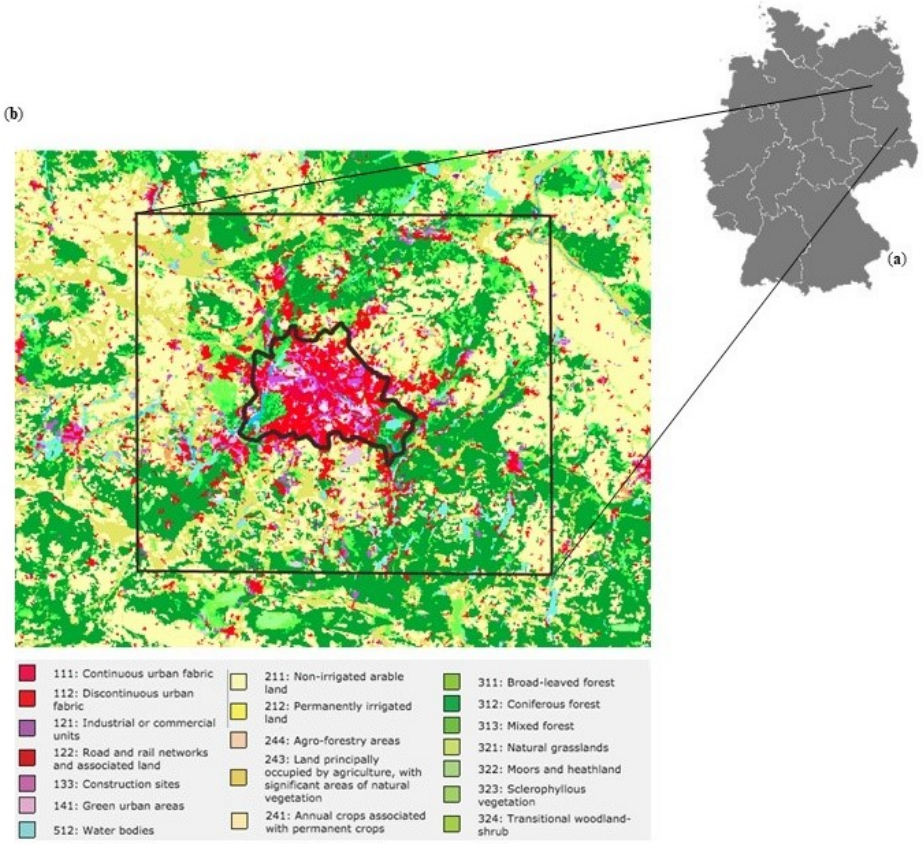

Fig. 1. Research area. (**a**) Germany and (**b**) a land-cover map indicating Berlin's administrative boundaries (black polygon) and research domain including the surroundings (black rectangular). Land cover following CORINE land cover map (EEA, 2000; Langendijk et al., 2019).

2.2. Models, data, and analyses

To evaluate the performance of the regional climate model used to investigate the Berlin region, observations are compared with model output data driven by the ERA-Interim reanalysis dataset on 12.5 km (0.11°) and 3 km (0.0275°) spatial resolution, by respectively the regional climate model REMO, and its non-hydrostatic convection-permitting version (REMO-NH) (Ban et al., 2021; Lowe et al., 2020). REMO is a three dimensional, hydrostatic limited-area model (Jacob et al., 2012; Kotlarski et al., 2014), originating from the 'Europa-Modell' of the German Weather Service (DWD) (Majewski, 1991). The physical parameterizations are largely based on the global climate model ECHAM-4 (Roeckner et al., 1996) and have been further developed over the course of the last decades. Model specifications can be found in Jacob et al. (2012) and in Jacob and Podzun (1997). The non-hydrostatic convection-permitting model version, REMO-NH, directly resolves the vertical momentum equation, leading to a better representation of small-scale mesoscale circulations and convection (Goettel, 2009; Langendijk et al., 2021).

For the model evaluation, relative humidity, specific humidity and 2-m temperature are investigated at a daily time-step, averaged over each year during the ERA-interim driven period 2000–2009. The REMO output data used for this study was produced as part of the European Climate Prediction (EUCP) project (Ban et al., 2021; Lowe et al., 2020). In-situ station observations are obtained from the DWD data store (DWD, 2021), for five stations in Berlin and five in the surroundings. The locations of the observational stations are presented in the appendices, Fig. A1. The DWD does not provide in-situ observations for specific humidity. Therefore specific humidity is derived from observed mean daily vapor pressure (e) in hPa and air pressure (P) in hPa from DWD in-situ station observations (DWD, 2021), using the following formula (Stull, 2017):

$$Specific\ humidity = \frac{\varepsilon * e}{P - e * (1 - \varepsilon)} \quad (1)$$

Where ε = 0.622 g vapor/g dry air is the ratio of gas constants for dry air to that for water vapor.

The land cover scheme of REMO follows a tile approach, based on three basic land surface types; land, water, and sea ice. Subgrid fractions are specifying further land cover types, including an urban sub-fraction. These fractions are not assumed to be located in a specific area of a grid box, but cover a percentage of the total grid box area, together summing up to 100% (Rechid and Jacob, 2006; Semmler, 2002). The urban fraction per grid box for the Berlin region is presented in Fig. 2. For the urban sub-fraction, the REMO model follows the so-called 'bulk' approach. Sealed urban areas are represented as a rock surface, which is described in the model by a relatively high roughness length, high albedo, and no water storage capacities (Langendijk et al., 2019). Langendijk et al. (2019) indicate that the simple urban bulk-scheme shows the urban rural contrast for temperature and humidity variables under climate change. The simple scheme is less skilled in simulating the timing of the peak of the urban heat island at night.

A consistent masking approach is developed (following Langendijk et al., 2021) to define the urban area in the 12.5 km and 3 km model output data to allow for coherent analysis across grid resolutions. The urban area contains all the grid cells with an urban fraction larger than 0.3 as prescribed by the REMO land surface cover scheme within the administrative boundaries of Berlin (Black polygon, Fig. 1b). The masks for the surroundings include all grid boxes outside the city mask and within the primary domain of interest of approximately 140 km by 140 km centered around

Berlin (black rectangular, Fig. 1b). This approach is followed for both horizontal resolutions. The resulting city masks for the 12.5 km and 3 km grid resolutions cover relatively similar areas for Berlin, with the 3 km mask capturing the actual city extent and boundaries more accurately (Appendices: Fig. A3).

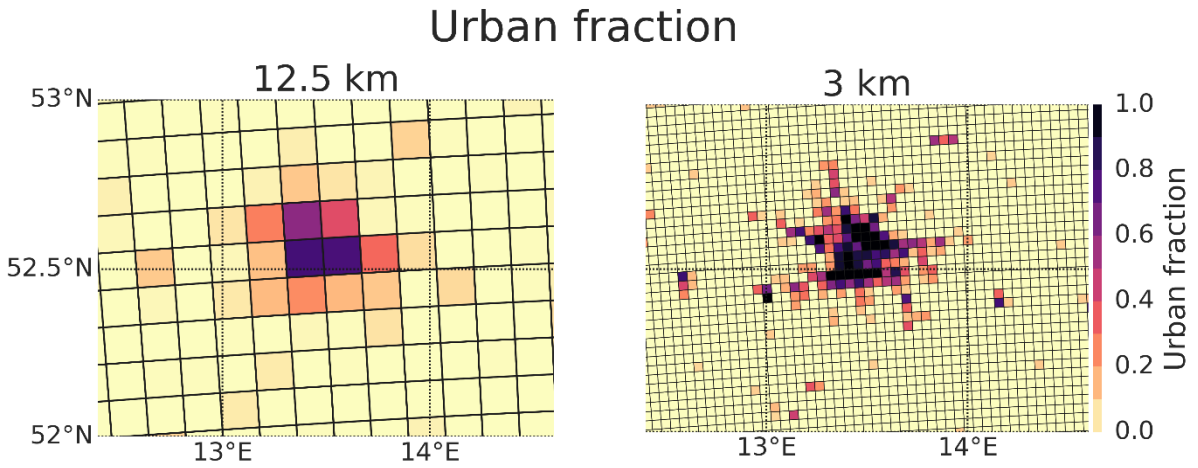

Fig. 2. The urban fraction per grid box of the REMO land surface scheme, for the 12.5 km and 3 km grid resolutions.

To give insight into the model performance compared to observations, the following statistical measures are calculated for the averaged annual mean for the ERA-interim driven period (2000–2009) for Berlin and its surroundings, as well as for the averaged monthly data, respectively called the annual cycle, for the ERA-interim driven period (2000– 2009) for Berlin:

- Root mean square error (RMSE): absolute measure of the overall error in the estimates relative to the observed values, expressed in the same units and scale as the data itself. It can take any positive value with zero indicating a perfect lack of error.
- Mean bias error (MBE): measures the extent to which the estimated value deviates from the observed value. It can take any value, with negative values indicating systematic under-estimation and positive values, over-estimation, and zero indicating a perfect lack of bias.
- Pearson correlation coefficient: varies between 1 and 1 with 0 implying no correlation. Correlations of 1 or 1 imply an exact linear relationship.
- Standard Deviation (St. Dev.): a measure of the amount of variation or dispersion of a set of values. A low standard deviation in- dicates that the values tend to be close to the mean of the set, while a high standard deviation indicates that the values are spread out over a wider range.

In order to conduct the calculations, the model output data is spatially averaged over the grid boxes representing Berlin (black polygon Fig. 1, Appendices: Fig. A3) and its surroundings (black rectangle Fig. 1). The observations are averaged over the different stations, respectively for Berlin and its surroundings (Appendices: Fig. A2). The median, and range of the station measurements are relatively similar, except for Berlin-Alexanderplatz (Appendices: Fig. A2). This station data is slightly warmer and less moist (RH) compared to other stations in Berlin. Probably because the station is located in the city center surrounded by a sealed surface (Appendices: Fig. A1).

The analysis of the impact cases, influenza, pollen, and mold, aims to understand the added value on the 3 km grid resolution, compared to the 12.5 km grid resolution, to simulate climate change impacts in the Berlin region. The REMO model output data for the 12.5 km and the 3 km (REMO-NH)

grid resolutions are utilized for the historical time period (1996–2005) and a near-term future time period (2041–2050) under the emission scenario RCP8.5 (Moss et al., 2010), forced by the global climate model MPI-ESM-LR (Stevens et al., 2013). The REMO output data was produced as part of the European Climate Prediction (EUCP) project (Ban et al., 2021; Lowe et al., 2020).

Using the above-mentioned REMO model data, the specified meteorological conditions for each impact case are investigated (Table 1). Firstly, the change in the occurrence of the days that fulfill the respective conditions is calculated. The number of days on which the impact case occurs within each decade is then divided by ten years, resulting in the mean projected change of days/year (d/yr) for each respective time period (historical and future). Secondly, consecutive periods of days under or above the thresholds are calculated for each impact case, following the same rational. The change in d/yr between the future decade and the historical decade is referred to as "change signal" in this research. To calculate a robust climate change signal, averaging over a time period of 20–30 years in the future as well as over a 20–30 years historical time period would be required (Hawkins et al., 2020; IPCC, 2013). Due to limited computing power convection-permitting simulations are currently only available for decades. Therefore, this study shows the "change signal", which provides an indication of the climate change signal as it carries the fingerprint of climate change. The following comparisons are examined throughout the analysis: the 12.5 km grid resolution vs. the 3 km grid resolution; the historical time period (1996–2005) vs. the near-term future time period (2041–2050); and Berlin vs. its surroundings. The near-term future period (2041–2050) is particularly relevant for policy timeframes, as (urban) decision makers tend to be specifically interested in timespans ranging from multi-annual up to the near-term future (Lauwaet et al., 2017).

3. Results

3.1. Model performance across grid resolutions

The outcomes of the model evaluation show that the REMO model, on both the 12.5 km and 3 km grid resolution performs reasonably in line with the observations for Berlin and its surroundings, based on the statistical tests (Table 2, Appendices: Table A1). For the annual mean values averaged over the period 2000–2009, the 12.5 km grid resolution is frequently outperforming the 3 km convection-permitting resolution, particularly for specific and relative humidity. For temperature, the surroundings show an improvement for the RMSE and MBE on the 3 km resolution compared to the 12.5 km resolution. Worth noting, the RH urban-rural contrast shows a slight improvement for the RMSE and the Pearson correlation coefficient (Appendices: Table A1).

The statistical values for the annual cycle show more improvements than the annual mean values for the 3 km grid resolution, in Berlin. The REMO model outputs for relative humidity shows better correspondence with observations on the 3 km resolution than the 12.5 km resolution for the months August, October, and November (RMSE and MBE), but the model is performing worse during the period from January to April (Table 2). This implies potential improved capability of REMO-NH to simulate the pollen impact case, as the relative humidity threshold occurs in July – October. The 3 km resolution shows improvements for specific humidity in Berlin during the summer months June – August, and in November (RMSE and MBE) (Table 2). The Pearson correlation coefficient is higher for 8 out of 12 months for the 3 km resolution compared to the 12.5 km resolution. This improvement, particularly for the months December – March, increases the confidence that the 3 km resolution may improve the simulations for the influenza impact case. For temperature, the 3 km resolution shows improvements in Berlin for almost all months, except March, April and May (RMSE, and/or MBE, and/or Pearson) (Table 2). This may lead to improved simulation of the impact cases that co-depend on temperature, respectively influenza and mold.

Table 2

Statistical outcomes for the annual cycle, RMSE, MBE and Pearson correlation coefficient for relative humidity, specific humidity, and temperature, comparing monthly mean observations with the 12.5 km and 3 km grid resolution, for Berlin, for the ERA-interim period (2000–2009). The green marking shows where the 3 km outperforms the 12.5 km grid resolution, compared to observations.

Relative Humidity	**Jan.**	**Feb.**	**March**	**April**	**May**	**June**	**July**	**Aug.**	**Sept.**	**Oct.**	**Nov.**	**Dec.**
12.5 km												
RMSE (%):	7.53	8.57	6.56	6.20	4.29	3.73	4.84	3.66	3.29	5.09	4.60	5.87
MBE (%):	-7.14	-8.12	-6.04	-4.32	-2.62	-2.22	-2.62	-1.47	0.69	4.23	2.92	-4.32
Pearson corr.:	0.43	0.45	0.83	0.47	0.47	0.36	-0.12	0.34	0.44	0.31	0.48	0.05
3 km												
RMSE (%):	10.73	13.45	15.44	17.40	8.96	4.46	4.39	3.01	3.34	4.33	3.62	8.87
MBE (%):	-10.43	-13.24	-15.10	-17.07	-7.79	-3.14	-2.87	-0.48	1.39	2.73	-2.18	-8.16
Pearson corr.:	0.13	0.33	0.69	0.66	0.09	0.33	0.08	0.33	0.52	0.16	0.51	0.02
Specific Humidity												
12.5 km												
RMSE (kg/kg):	0.0003	0.0003	0.0006	0.0008	0.0008	0.0011	0.0013	0.0010	0.0008	0.0003	0.00032	0.0003
MBE (kg/kg):	-0.0002	-0.0003	-0.0005	-0.0007	-0.0007	-0.00095	-0.0012	-0.00094	-0.0007	-0.0001	-0.00020	-0.0001
Pearson corr.:	0.74	0.81	0.61	0.93	0.85	0.51	0.66	0.78	0.85	0.91	0.72	0.83
3 km												
RMSE (kg/kg):	0.0005	0.0005	0.0008	0.0012	0.0011	0.0010	0.0010	0.0012	0.0007	0.0004	0.00027	0.0005
MBE (kg/kg):	-0.0004	-0.0005	-0.0007	-0.0011	-0.0010	-0.00087	-0.0009	-0.00089	-0.0006	-0.0002	-0.00016	-0.0004
Pearson corr.:	0.79	0.84	0.61	0.93	0.86	0.61	0.61	-0.36	0.86	0.90	0.77	0.89
2-m Temperature												
12.5 km												
RMSE (°C):	1.05	0.94	1.11	0.71	0.95	1.20	1.07	0.93	1.11	0.87	0.96	1.08
MBE (°C):	0.63	0.79	0.43	-0.17	-0.47	-0.91	-0.86	-0.68	-0.92	-0.49	0.63	0.73
Pearson corr.:	0.68	0.85	0.87	0.96	0.77	0.57	0.76	0.89	0.90	0.89	0.86	0.88
3 km												
RMSE (°C):	0.77	0.93	1.49	1.63	1.14	0.96	0.69	0.66	1.12	0.81	0.88	0.61
MBE (°C):	0.20	0.80	1.11	1.46	0.47	-0.44	-0.21	-0.44	-0.82	-0.21	0.66	0.40
Pearson corr.:	0.77	0.87	0.85	0.96	0.69	0.69	0.73	0.91	0.85	0.89	0.89	0.96

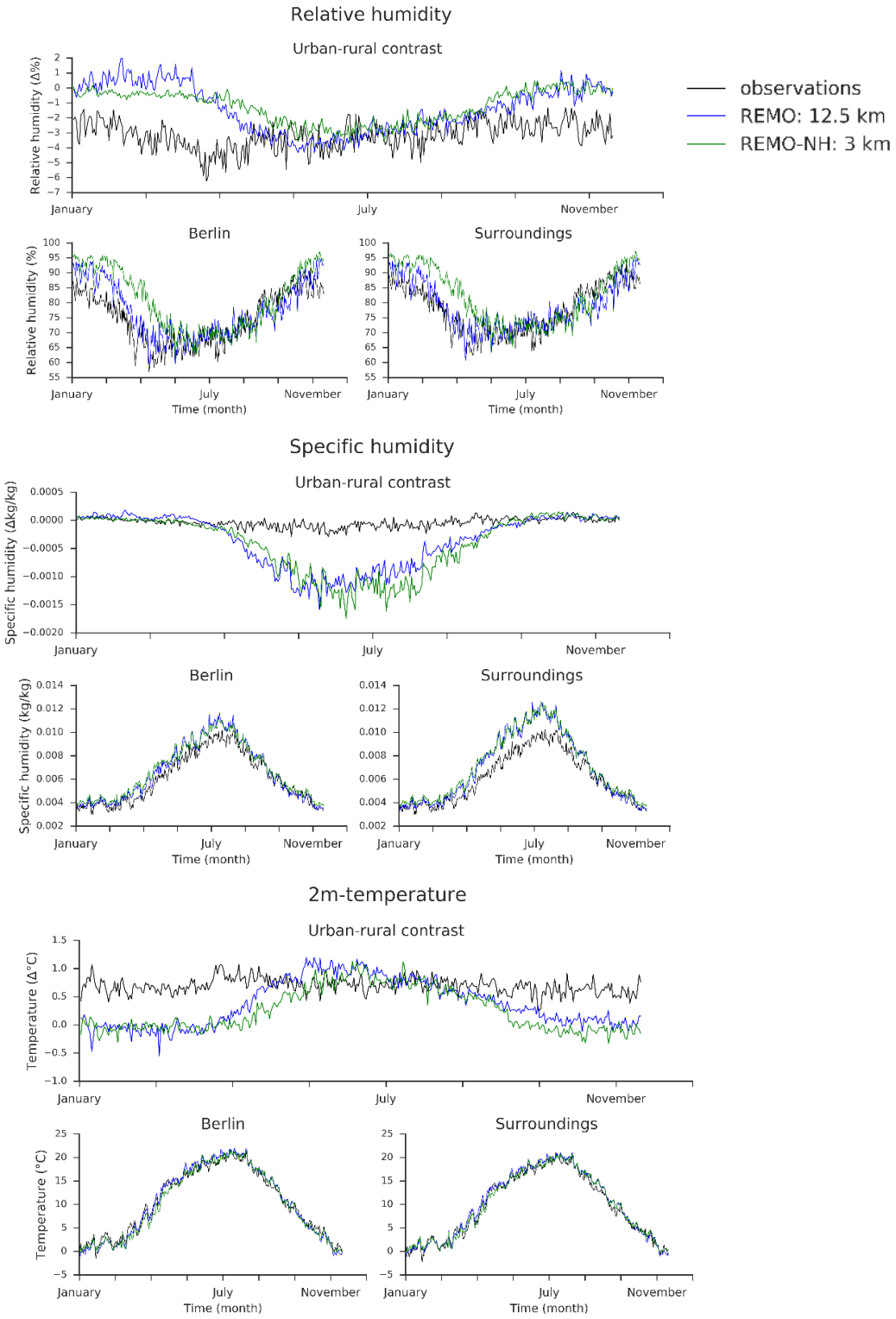

Fig. 3. Annual cycle for daily observations (black), 12.5 km grid resolution (blue) and 3 km grid resolution (green), for relative humidity, specific humidity and 2-m temperature, 10-year mean for the ERA-interim period (2000– 2009). The urban-rural difference is calculated by subtracting the results for the surroundings from those for Berlin. (For interpretation of the references to colour in this figure legend, the reader is referred to the web version of this article.)

These results are underpinned by Fig. 3, showing the time series of the mean annual cycle, averaged over 2000–2009, for Berlin and its surroundings. For relative humidity the REMO model results are in line with the observations for the summer months up to October. The model simulations overestimate relative humidity values for winter and spring, in Berlin and its surroundings. The relative humidity urban-rural contrast shows a similar pattern, and is underestimated in the winter. The 3 km resolution shows an improvement compared to the 12.5 km grid resolution, mainly in January to March. For specific humidity, the models overestimate SH in summer, which is larger for the surroundings than Berlin. This leads to an overestimation of the specific humidity urban-rural contrast in summer months. The REMO model results are largely in line with observations for temperature, for Berlin and its surroundings. The temperature urban-rural contrast, is underestimated in winter months. This can explain the underestimation of the RH urban-rural contrast in the same months, because temperature and RH are closely related. The temperature urban-rural contrast underestimation in winter is most probably caused by the absence of anthropogenic heat in the REMO model, and the limited capacity of the bulk scheme to retain warmth (Jin et al., 2021).

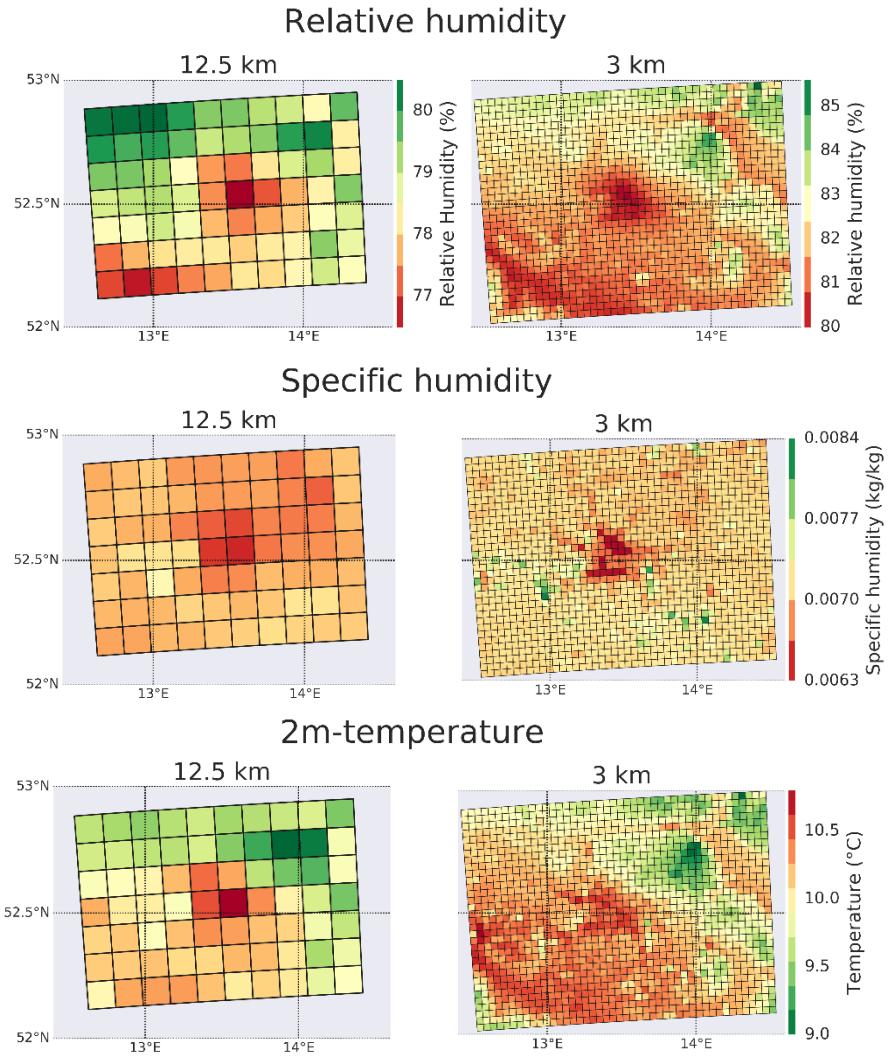

Fig. 4. Spatial maps for the Berlin region on the 12.5 km (left) and 3 km (right) grid resolution, showing the 10-year mean (2000–2009) for relative humidity, specific humidity and 2 m-temperature. Note: relative humidity has a different colour bar for 12.5 km and 3 km grid resolution.

A clear urban-rural difference between Berlin and its surroundings is detectable on the spatial maps presenting the mean for the period 2000–2009, in Fig. 4. Berlin is less humid (SH: ~0.0011 kg/kg, RH: ~2%) and warmer (~0.5°C) than its surroundings for both spatial resolutions. The 3 km grid resolution is overall more moist (RH and SH) in the Berlin region. There is more detail visible on the 3 km than the 12 km spatial resolution. For instance, the city boundaries of Berlin and the suburbs (urban-rural transition) become visible on the 3 km resolution, as well as a decrease in temperature and an increase in humidity can be detected around the river Spree (Fig. 4). This enhanced level of detail on the 3 km resolution can be mainly explained by the increase of the amount of grid boxes with urban fractions and better resolving the land surface on the 3 km grid resolution (Fig. 2).

In summary, the model evaluation shows that the REMO model, on the 12.5 km and 3 km grid resolution, is performing reasonably in line with the observations. Statistical improvements are found on the 3 km resolution for specific months for the different variables, potentially indicating that the 3 km resolution may better simulate the variables that underpin the meteorological conditions for the impact cases. Enhanced spatial detail is clearly detectable on the 3 km compared to the 12.5 km grid resolution.

3.2. Climate change related impacts across grid resolutions: Influenza, pollen, mold

The impact cases, influenza, pollen, and mold, aim to demonstrate the difference and potentially the added value on the 3 km grid resolution, compared to the 12.5 km grid resolution, to simulate climate change impacts in the Berlin region. The following results reveal how the defined meteorological conditions change for each impact case under near-term climate change for Berlin and its surroundings.

3.2.1. Less influenza days per year, but longer periods of consecutive influenza days

The REMO model outcomes show that the influenza days, happening from December to March with a day mean of SH < 0.006 kg/kg and temperatures between 2– 6°C, will decrease under the considered future climate conditions, comparing the near-term period 2041–2050 with the historical period 1996–2005 (Fig. 5). However, the duration of periods with consecutive influenza days are projected to become longer in the considered future decade (Fig. 6).

A stronger change signal is found for the 3 km resolution, with a decrease of 2 influenza d/yr compared to around 1 influenza d/ yr for the 12.5 km resolution for the future period, for both Berlin and its surroundings (Fig. 5, Appendices: Table A3). The decrease in influenza days in the near-term future period could be explained by overall warmer temperatures under climate change, resulting in a smaller amount of cold days in the winter (e.g. Brasseur et al., 2017). The warmer temperatures could lead to higher humidity levels, as warm air can hold more moisture. This is also in line with Langendijk et al. (2019), who indicate specific humidity increases under future climate change (RCP8.5) throughout the 21st century in the Berlin region. The stronger decrease of influenza days on the 3 km resolution may be a result of the convection-permitting scale, which tends to have slightly higher specific humidity levels than the 12.5 km resolution, particularly in the winter months, as shown in Fig. 3 and Fig. 4.

Uninterrupted periods of consecutive influenza days occur in the historical period with an average duration between 2– 8 consecutive days (Fig. 6, interquartile range), with a median of 4 days for all time slices and resolutions, and extreme periods up to 50 consecutive influenza days (Fig. 6). Fig. 6 indicates that the duration of the periods with consecutive influenza days will increase under

near-term future climate change, especially for the 3 km resolution, by ~2 – 3 consecutive days (expansion of upper quartile (Q3) of boxplot). This is shown in Fig. 6 by the interquartile range change from 2 – 8 to 2 – 10 consecutive influenza days for Berlin under near-term climate change.

The model evaluation indicates that the REMO model on the 3 km resolution better simulates specific humidity (Pearson correlation coefficient) and temperature (RMSE, and/or MBE, and/or Pearson) during the months December – March. Despite a relatively small difference between the 3 km and 12.5 km resolution, it is expected that the convection-permitting scale may bring about more reliable results for the influenza impact case.

The urban-rural contrast is minimal for influenza, with a 0 – 0.3 d/yr difference between Berlin and its surroundings (Fig. 5, Appendices: Table A3). This is in line with observations and model outcomes for the winter months for specific humidity (Fig. 3).

3.2.2. More pollen days on the convection-permitting scale, and in Berlin, under future climate conditions

There is an increase in pollen days, characterized by a day mean of RH < 60% in July – October, simulated under future climate conditions on the 3 km resolution, especially in Berlin compared to its surroundings (Fig. 5). Notably, the 12.5 km resolution indicates a decrease of 4 d/yr in Berlin and 1 d/yr for its surroundings in the future period 2041–2050, in contrast to an increase of 0.2 d/yr in Berlin and 2 d/yr in the surroundings for the 3 km resolution. There is a sign change for the change signal going from the 12.5 km to the convection-permitting resolution. Following previous literature, an increase in pollen days under climate change is expected, especially in Berlin, because it would become hotter and less moist in the city, especially in the summer months (Argüeso et al., 2014; Langendijk et al., 2019; Lin et al., 2020; Lokoshchenko, 2017; Zhao et al., 2021). Taking this into consideration, the convention permitting resolution behaves closer to the expectations. This is probably the case because REMO-NH better resolves the urban surface, and therefore better simulates the drier and warmer urban conditions and the urban dry island effect in the summer, compared to the 12.5 km resolution (Table 1). This is in line with the statistical improvements found for the 3 km grid resolution for the RH urban-rural difference (Fig. 3, Appendices: Table A1). Therefore, an added value for the convection-permitting scale is detected to simulate the pollen impact case.

There is a large urban-rural contrast, with more pollen days in Berlin, for both the 12.5 km and 3 km grid resolutions, ranging from 5–6 d/yr in the historical period and 3 d/yr in the future period. The urban-rural difference for relative humidity is also clearly visible on the spatial maps (Fig. 4), and is more detailed for the 3 km resolution. This overall result is expected, as Berlin is generally less moist than its surroundings, resulting in more pollen days in the city (Langendijk et al., 2019; Zhao et al., 2021). The decrease of the urban- rural contrast in the future period compared to the historical period can be explained by the relative increase of pollen days in the surroundings, for the 3 km grid resolution. For the 12.5 km grid resolution the pollen days show a stronger relative decrease in Berlin, compared to the surroundings.

The periods of consecutive pollen days range from 2 – 3 days, with extremes up to 7 days. No major difference is found for the consecutive pollen days under future climate conditions, nor for the different resolutions in this respect.

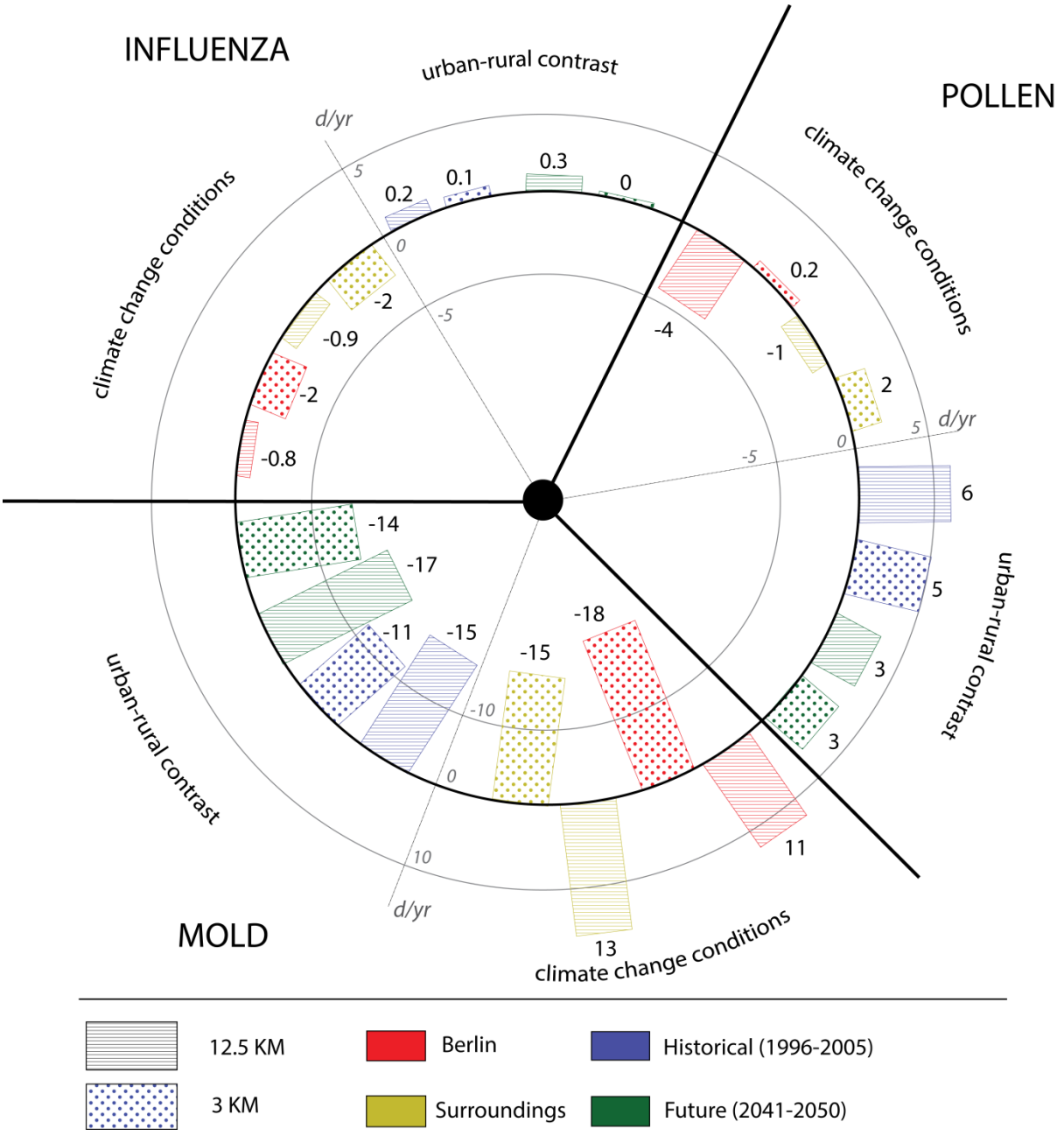

Fig. 5. Mean change in days per year (d/yr) for each impact case: influenza; pollen; and mold. Showing the grid resolutions (3 km and 12.5 km), under near-term future climate conditions vs. historic climate conditions (= future (2041–2050) - historical (1996–2005) and urban-rural contrast (= Berlin - surroundings) (see Appendices: Table A3).

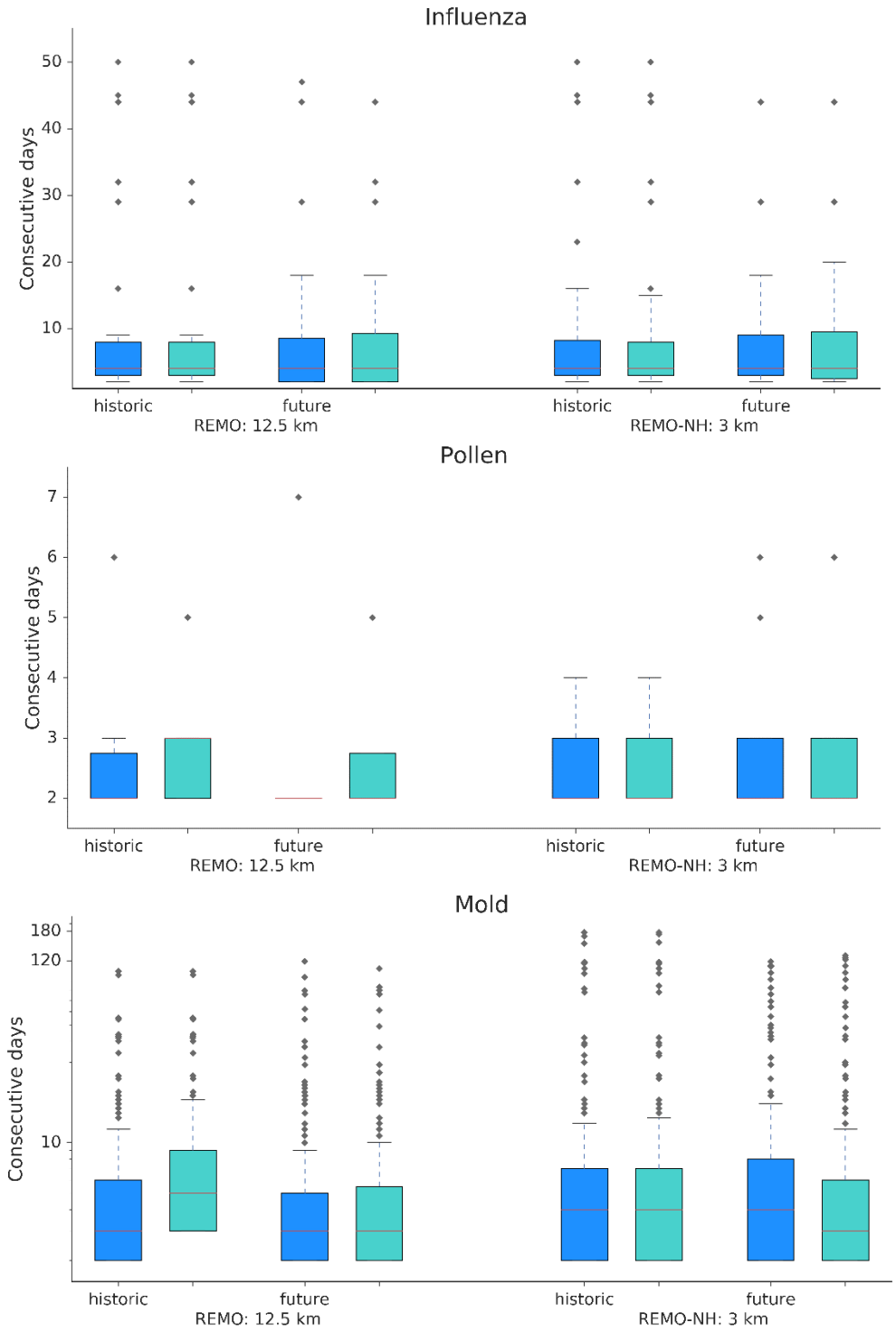

Fig. 6. Boxplots showing the consecutive days for each impact case: influenza; pollen; and mold. For Berlin (blue) and its surroundings (green), for the grid resolutions (12.5 km (left) and 3 km (right)), for historical (1996– 2005) and near-term future (2041– 2050) period. Boxplots: the model median (red line), quartiles (Q1: 25% and Q3: 75%), and whiskers (1.5 * IQR (IQR = Q3 - Q1)) indicate the model spread. (For interpretation of the references to colour in this figure legend, the reader is referred to the web version of this article.)

3.2.3. Less mold days on the convection-permitting resolution, but longer consecutive periods, under future climate conditions

Mold days, defined by a day mean of RH >80% and temperatures between 10 – 40°C, will become less under near-term climate conditions on the 3 km resolution for the Berlin region (Fig. 5). Nevertheless, the periods of consecutive mold days become longer for the future period 2041 – 2050, especially on the convection-permitting resolution (Fig. 6).

Worth noting is the sign change of the change signal going from the 12.5 km to the 3 km grid resolution (Fig. 5). An increase of 11 (Berlin) – 13 (surroundings) mold d/yr is found for the 12.5 km resolution for the future time period, in contrast to the 3 km resolution, which shows a decrease of 18 (Berlin) – 15 (surroundings) mold d/yr under near-term climate change conditions (Fig. 5, Appendices: Table A3). Following previous literature, mold days are expected to decrease under climate change, especially in Berlin in the summer. It will become warmer, and relative humidity decreases particularly in the urban area, as there is little moisture available in the city to be added to the atmosphere (Argüeso et al., 2014; Langendijk et al., 2019; Lokoshchenko, 2017; Zhao et al., 2021). This leads to the conclusion, that the convection-permitting scale (REMO-NH) better resolves the urban surface, leading to warmer temperatures and reduced relative humidity, especially in Berlin, resulting in less mold days under near-term climate conditions. A clear added value on the convection-permitting scale is identified for simulating mold days in an urban-rural context, similar to the pollen impact case.

Longer periods of consecutive mold days are projected for the 3 km and 12.5 km resolution under future climate conditions. The period of consecutive mold days generally ranges between 2 – 8 days, with extremes up to 170 consecutive days (Fig. 6). The median shifts from 3 to 4 consecutive days for the 3 km resolution. This is a critical change, as prior research shows that indoor mold growth strongly increases after four consecutive mold days (Sedlbauer, 2001). In addition, the upper quartile (Q2) increases for the future, especially on the convection-permitting resolution, making longer consecutive mold periods more likely.

Berlin has 15 mold d/yr less than its surroundings on the 12.5 km resolution, and 11 d/yr on the 3 km grid resolution, for the historical period. An even larger urban-rural contrast is found for the future period with Berlin showing less mold days than its sur- roundings by 17 d/yr on the 12.5 km and 14 d/yr on the 3 km resolution (Fig. 5). This urban-rural difference is also clearly visible on the spatial maps (Fig. 4), and is more detailed on the 3 km resolution. Berlin is expected to be less moist than its surroundings and therefore experiencing less mold days. This gets larger under climate change, as the city get drier (RH) and warmer, and its surroundings might have more capacity to add additional moisture to the atmosphere when warming (Langendijk et al., 2019; Zhao et al., 2021).

In summary, the 3 km grid resolution, the convection-permitting scale, improves the simulations for the impact cases in the Berlin region, compared to the 12.5 km grid resolution. This influences the results for influenza, leading to a more profound decrease of influenza days under future climate conditions. A sign change of the change signal is identified for the 3 km compared to the 12.5 km grid resolution for the impact cases pollen, and mold, showing an increase in pollen days and a decrease in mold days under near-term climate conditions. There is an added value detected on the convection-permitting resolution to simulate the climate change impact cases.

4. Discussion and conclusions

The outcomes of this research confirm that the convection-permitting resolution better resolves regional-to-local scales, for complex terrains such as urban areas (Argüeso et al., 2016; Coppola et al., 2020; Kendon et al., 2021; Prein et al., 2015). Improved urban detail is found (Fig. 4), as well as a stronger change signal for influenza, and a sign change of the change signal for the pollen and mold impact case, moving from the 12.5 km to the 3 km grid resolution. The model evaluation and the pollen case indicate that particular added value is found in the summer months, which is in line with other literature that show improvements particularly in this season (Ban et al., 2014; Kendon et al., 2021; Prein et al., 2015). This may be particularly true for Berlin, as the simple urban scheme may better capture the heat retention and related urban moist reduction in the summer months (Fig. 3, Table 2), compared to the winter months. The urban scheme does not include anthropogenic heat, which may be one of the key reasons that the model underestimates the temperature and urban moist reduction in the winter (Jin et al., 2021).

The results show little improvement for the annual mean values for the 3 km grid resolution. This is in contrast to the added value found on a monthly basis for the annual cycle. The REMO-NH model at 3 km resolution shows improved statistical outcomes for specific months for temperature, and to a less extent for relative and specific humidity, as well as for the meteorological conditions of the impact cases, and the RH urban-rural contrast. This is in line with e.g. Argüeso et al. (2016) and Prein et al. (2015), who show that the convection-permitting scale mainly shows added value on shorter timescales, rather than for annual means (Ban et al., 2014; Kendon et al., 2021).

This study relies on one model and one decade under near term future climate conditions using the RCP8.5 scenario. The outcomes are model depended and only reflect one possible future, for one future decade. Therefore, similar studies with different models and under different climate change scenarios are needed, in order to compare and validate the results of this study (Coppola et al., 2020; Fosser et al., 2020). In conjunction, only the near-term period is investigated for climate change impacts. The changes for the impact cases may look different for the far future, e.g. up to 2100. Additionally, comparing historic periods with future periods with a minimal duration of 20–30 years would be needed to distill a robust climate change signal and/or the climate change effect on the impact cases. To adequately assess the impact cases under longer term climate change, transient high-resolution climate change simulations would be preferred.

Despite the added value found for the 3 km grid resolution in this study, it is crucial to further reflect if the change signal is more trustworthy on the convection-permitting scale, and which change signals can be reliably captured by coarser-resolution models (Fosser et al., 2020; Kendon et al., 2021). Although, this research implies that for the pollen and mold impact case the 3 km resolution is showing a more reliable sign of the change signal, robustness shall be further assessed using other models and approaches, as well as longer time periods up to 20 to 30 years (Hawkins et al., 2020; IPCC, 2013). The change in the sign may trigger a difference in the response by decision makers from inaction to action. Here, the challenge arises how to best communicate the divergent results stemming from the 12.5 km and 3 km grid resolution, especially to urban planners and decision makers (Kendon et al., 2021).

In addition, the results on the 3 km show clear improvements, but also highlight that the effect of the urban parametrization is no longer negligible at this grid resolution (Argüeso et al., 2016; Trusilova et al., 2013). Sophisticated urban models have greater complexity and are able to simulate fine scale meteorological processes and fluxes in the city and on the district, or even building level. Sophisticated urban schemes could improve the simulation of the urban local-to-regional interactions, e.g. the overestimation of relative humidity in the winter, and the overestimation of the

SH urban-rural contrast in summer (Daniel et al., 2019). It would be important to consider incorporating anthropogenic heat in the winter. This study calculates averaged values over Berlin, to understand mean changes for the city compared to its surrounding. Nevertheless, local conditions may affect the impact cases significantly, which needs to be investigated with more sophisticated urban models.

4.1. Implications for the impact cases

The results of this research show a stronger decrease of influenza days on the convection-permitting scale under near-term future climate conditions (2041– 2050), but consecutive periods become longer particularly on the 3 km grid resolution. The longer influenza periods might enhance spreading and the survival of the virus and could increase the related infections and therefore hospitalizations, in line with e.g. Chong et al. (2020). Generally, projected warmer and moister winters under climate change could potentially lead to a decrease in influenza. Though, other research shows that a warmer winter might spark an enhanced influenza pandemic with early onset the subsequent year when it is colder and/or less moist (Towers et al., 2013). Further research is needed to investigate seasonal cycles, extremes, and match them with further relevant factors to understand the interactions with climate change (Chong et al., 2020; Goodwins et al., 2019).

Higher amounts of pollen days are simulated on the 3 km grid resolution, especially in Berlin, under near-term future climate conditions. The increase of pollen days on the convection-permitting resolution coincides with the estimation by Hamaoui-Laguel et al. (2015) that by 2050 airborne ragweed pollen concentrations will be about four times higher than they are now in Europe. In addition, climate change could increase the length and severity of the pollen season and, as a consequence, the associated pollen allergy (D'Amato and Cecchi, 2008; Ziska et al., 2003). Ragweed is expected to expand its range due to climate change in Europe, particularly in the Northern parts of the continent (Cunze et al., 2013; Storkey et al., 2014). In this context, the sign change of the change signal on the convection-permitting scale is therefore of particular relevance, as the increase in pollen days coincides with other climate change effects on ragweed pollen prevalence. Urban planners and decision makers shall take people suffering from pollen allergy into account when planting in public spaces (Bergmann et al., 2012). To prevent the further spread of ragweed, the plants shall be systematically registered and destroyed (Buters et al., 2015; Pflanzenschutzamt Berlin, 2021).

A decrease in the amount of mold days/year for the near-term period are expected on the 3 km grid resolution, but the consecutive periods might get longer. This finding is in line with Bertolin and Camuffo (2014), who show a decrease for a relatively similar indicator "Time of wetness" (RH > 85%, and temperatures >0°C), under RCP4.5 in the Berlin region. Despite this overall decrease, the longer periods of consecutive mold days, may imply more indoor mold growth. Particularly the shift in the median from 3 to 4 consecutive days in the future, may enhance indoor mold growth, as this is a critical threshold for mold growth shown by studies from Sedlbauer (2001) and Viitanen and Ojanen (2007). Climate change may lead to warmer winters and prolonged mild temperatures between fall and spring. This could provide improved mold growth conditions and lengthen the optimal mold growth period. Other studies also found possible increases in indoor mold growth under climate change (Huijbregts et al., 2012; Leissner et al., 2015). These studies focus on specific, vulnerably buildings, using sophisticated building models and by constructing a mold index on various variables. Further coupling the climate projections used in this research to building models at specific locations might change the results. More detailed models and follow up studies would be helpful to understand the climate change effects for specific buildings, streets, or a neighborhood.

The impact cases are designed around humidity thresholds, and their simulated changes under near-term future climate conditions. Other factors have not been directly taken into account that could influence the outcomes of the impact cases, and the potential effects on human health.

For instance, for influenza, it would be important to further simulate and understand the role of changes in human behavior, the susceptibility to the virus of city dwellers, the indoor temperature and humidity, as well as to better understand how the effect would be different in other climate regimes (e.g. tropics) (Davis et al., 2016; Deyle et al., 2016). Dalziel et al. (2018) investigated 603 cities in the United States of America (USA) to understand the connection between urbanization and influenza. Influenza epidemics in smaller cities are shorter and strongly linked to humidity fluctuations. Whereas in larger cities non-climate factors have a more profound influence and a milder response to climate factors is found. Outdoor, as well as indoor, air pollution are associated with higher influenza incidence, and increased severity of the health risks related to the virus, particularly in winter months with low temperatures (Meng et al., 2021; Murtas and Russo, 2019; Song et al., 2021; Su et al., 2019; Toczylowski et al., 2021; Wang et al., 2016). Studies show a positive association between higher influenza risks and people who suffer from asthma as well as other respiratory allergies, obesity, or are recipient of a treatment for a chronic disease (Guerrisi et al., 2019; Hirota et al., 1992; Jain and Chaves, 2011; Karki et al., 2018; Yang et al., 2013). Prior studies show lifestyle choices, such as smoking enhance influenza risks (Choi et al., 2014; Guerrisi et al., 2019; Wong et al., 2013). In contrast, regular exercise and healthy diets counter health risks associated with influenza (Hirota et al., 1992; Wong et al., 2013). Certain studies indicate that women are more prone to influenza risks (Guerrisi et al., 2019; WHO, 2010). Particularly, the severity of the disease is worse among pregnant women (WHO, 2010). In this context, it is important to take into account that the rate of exposure to influenza could be higher for women than men, because they more often are caregivers and/or work in health-care occupations (WHO, 2010).

For the pollen impact case, it would be crucial to understand the quantity of ragweed plants in the city and how many allergic people live in the city (D'Amato and Cecchi, 2008). Urban environments provide beneficial growing conditions for ragweed mainly due to higher temperatures and CO2 emissions (Cvetkovski et al., 2018; Deutschewitz et al., 2003). Simultaneously, the high levels of air pollution in cities worsen pollen allergies of its inhabitants (Leru et al., 2021; Sedghy et al., 2018), with ozone being the most inflammatory pollutant (Kay et al., 2020). On another note, Voros et al. (2018) show that parents with the genetic tendency to develop allergic diseases (atopy) have children that develop pollen allergies more frequently (Voros et al., 2018). Also, smokers are more likely to suffer from allergy symptoms (Leru et al., 2021). Kusunoki et al. (2017) investigated 520 children at an age of 10, and found that the sensitization rate to ragweed was significantly decreased with increases in fruit intake. This hinds at diet choices might even influence the severity of ragweed pollen allergies.

For the mold impact case, the substrate and the indoor climate are pivotal to further understand the mold growth in the building (Ojanen et al., 2010; Ritschkoff et al., 2000; Sedlbauer, 2001; Viitanen and Ojanen, 2007). Indoor mold growth has been associated in many studies with an increased risk and amplification of asthma and respiratory illness (Hurraß et al., 2017; Mendell and Kumagai, 2017; Seguel et al., 2017; Sinclair et al., 2018). There is some evidence mold exposure leads to lower lung function, dermatitis, and non-respiratory symptoms (e.g. eye symptoms, headache, fatigue) (Norb¨ack, 2020). Particularly, moldy work and home environments are known to raise the exposure rate, and respectively the related health risks (Dales et al., 1991; Hurraß et al., 2017). In Germany, mold damage is found in every 10th home (Wiesmüller et al., 2016). Studies for the United States of America indicate higher asthma prevalence and related morbidity for Black and Latinx communities than for White Americans, directly associated with the higher levels of mold contamination in their

homes (Grant et al., 2022; Sinclair et al., 2018). This indicates that racial/ethnic/social inequities may enhance the health risks in connection with indoor mold growth (Grant et al., 2022).

Interdisciplinary research shall be undertaken to better understand the interaction between the changing climate and other critical non-climatic factors that influence the health related aspects of each impact case.

4.2. Concluding remarks

Concluding, the convection-permitting scale, improves the simulations for the impact cases, influenza, pollen, and mold in the Berlin region, compared to the 12.5 km grid resolution. This is one of the first studies that explores these impact cases under future climate conditions in the urban-rural context, with convection-permitting models. Influenza shows a more profound decrease of influenza days on the convection-permitting scale under future climate conditions, but longer consecutive periods especially on the 3 km grid resolution. A difference in the sign of the change signal is identified for the 3 km compared to the 12.5 km grid resolution for the impact cases pollen, and mold. The convection-permitting resolution performs more in line with observations, and available literature on urban processes, showing an increase in pollen days and a decrease in mold days under near-term climate conditions. The pollen days are more prevalent in Berlin. Mold periods are projected to increase in its duration under near-term climate conditions, showing a stronger increase on the 3 km grid resolution. The convection-permitting resolution affects, and generally improves the outcomes for the impact cases, and shows an added value, indicating the potential of convection-permitting simulations to generate improved information about climate change impacts for urban areas and its surroundings. This is of importance for the development of climate services for urban areas, as the improved information could enable urban planners and decision makers to more adequately prepare for and adapt to future climate change impacts.

CRediT authorship contribution statement

Gaby S. Langendijk: Conceptualization, Data curation, Formal analysis, Investigation, Methodology, Validation, Visualization, Writing – original draft, Writing – review & editing. **Diana Rechid:** Conceptualization, Supervision, Writing – review & editing. **Daniela Jacob**: Conceptualization, Supervision, Writing – review & editing.

Declaration of Competing Interest

The authors declare that they have no known competing financial interests or personal relationships that could have appeared to influence the work reported in this paper.

Acknowledgements

We wish to thank the European Climate Prediction (EUCP) project (EU H2020 project Grant agreement: 776613) for making the data available enabling this research, and particularly dr. Thomas Frisius for providing the data. The research was kindly funded by the Climate Service Center Germany (GERICS), Helmholtz-Zentrum Hereon, Germany. We kindly thank our colleague dr. Laurens Bouwer for providing constructive feedback on the first version of the manuscript.

Appendices

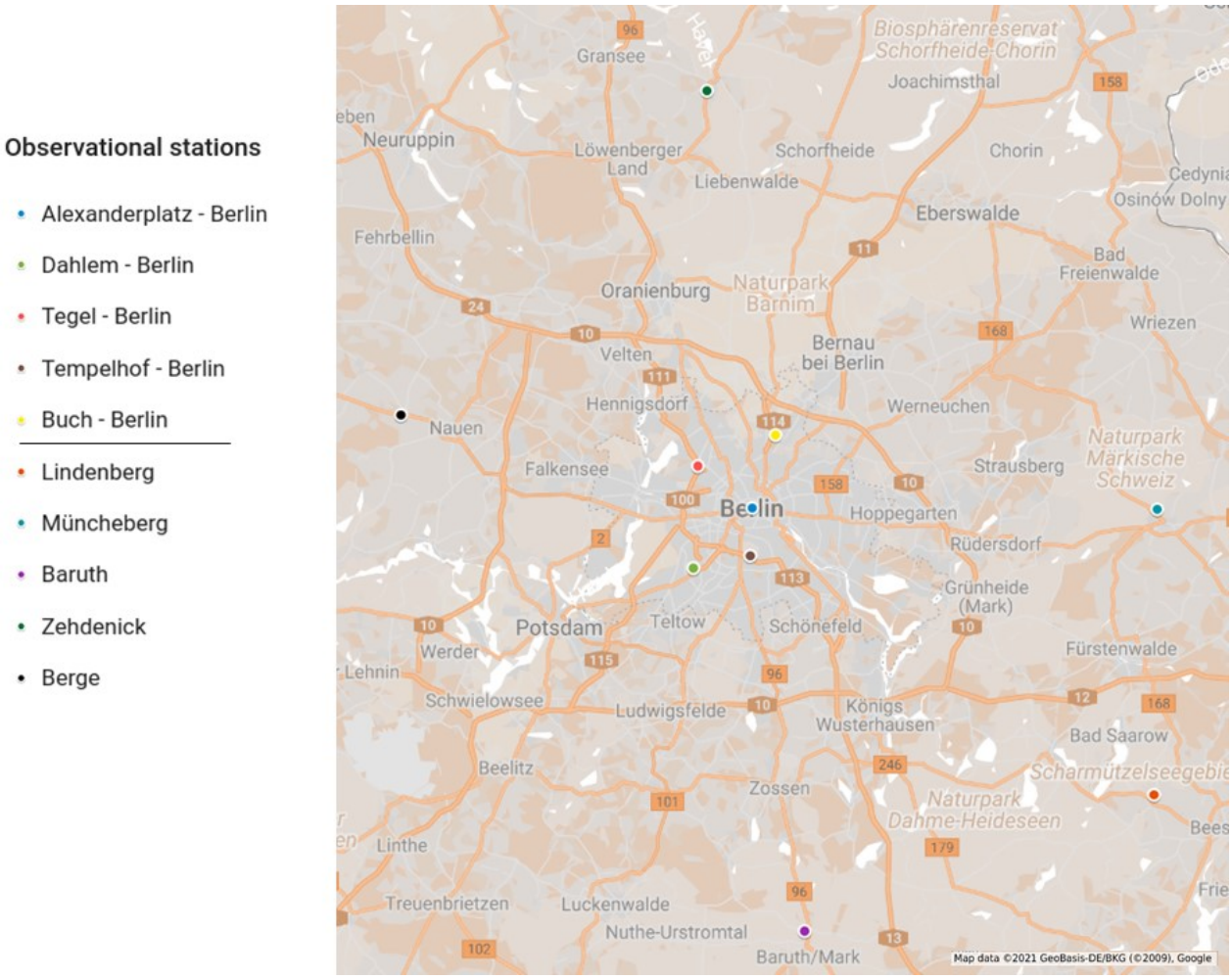

Fig. A1. Locations of the observational stations in Berlin and its surroundings.

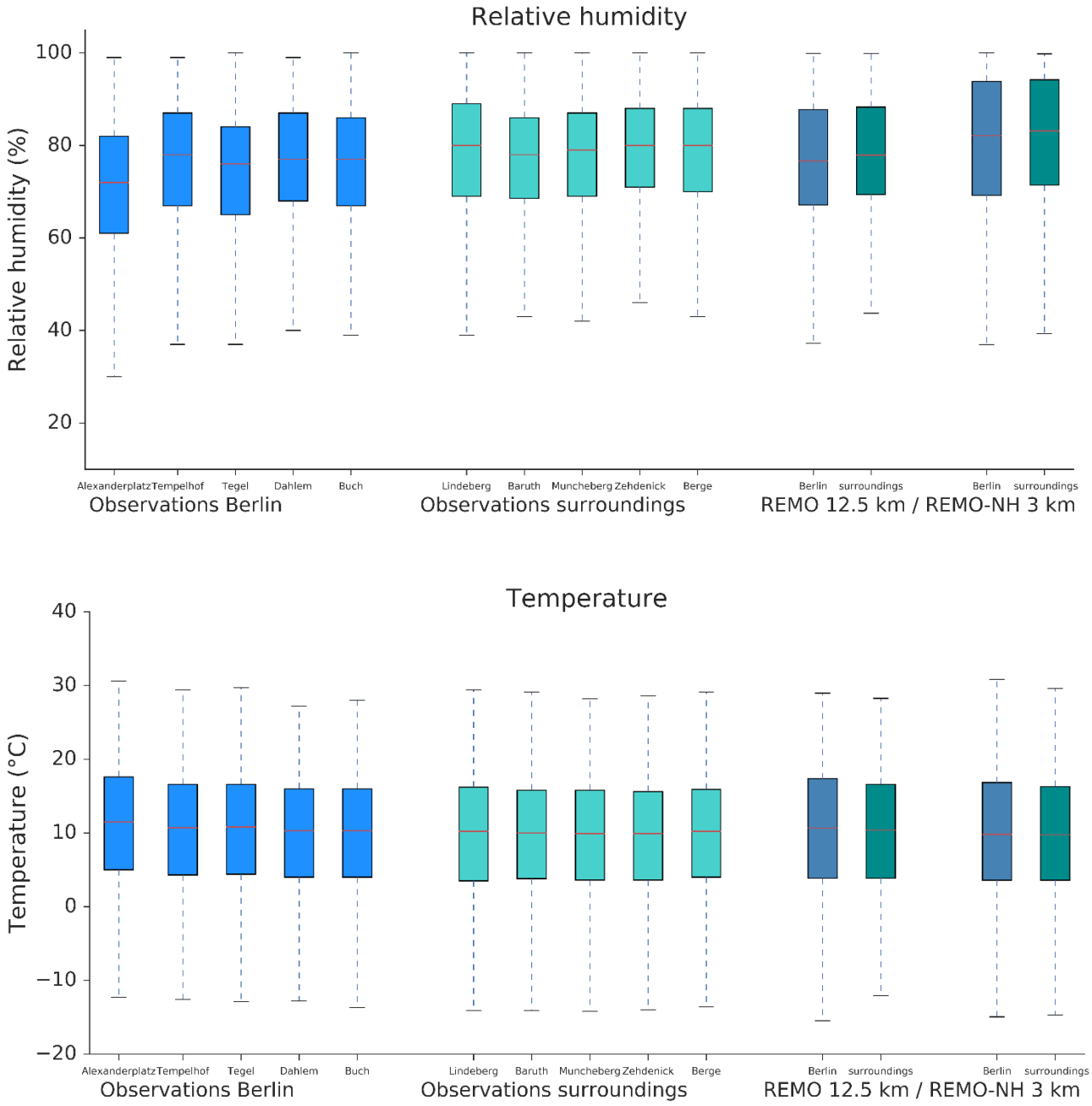

Fig. A2. Boxplots show the averaged day mean of observational station data for relative humidity and 2-m temperature, for the period 2000 – 2009 , for Berlin and its surroundings. REMO model data averaged for the same period 2000 – 2009 is presented on right side of figure, respectively for REMO 12.5 km and REMO-NH 3 km grid resolutions.

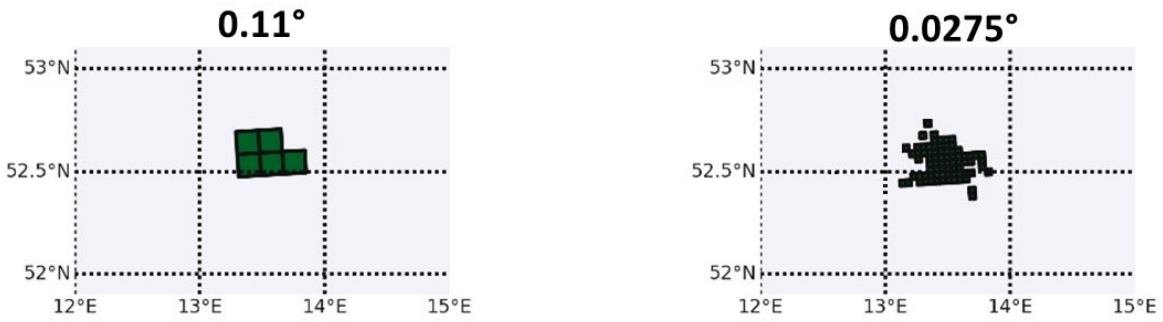

Fig. A3. Masks for Berlin, based on urban fraction >0.3, for 12.5 km (0.11°, left) and 3 km (0.0275°, right) grid resolutions.

Table A1

RMSE, MBE and Pearson correlation coefficient for relative humidity, specific humidity, and temperature, day mean 2000 – 2009, for Berlin comparing observations with the 12.5 km and 3 km grid resolution. Calculated the mean over the 10 years per day.

	Berlin 12.5 km	***Berlin 3 km***	***Surroundings 12.5 km***	***Surroundings 3 km***	***Urb-rur contrast 12.5 km***	***Urb-rur contrast 3 km***	***Obs Berlin vs Obs Surr***
Relative Humidity							
RMSE (%):	5.57	9.50	4.49	7.73	2.43	2.29	3.29
MBE (%):	-2.58	-6.34	-0.81	-4.43	-1.77	-1.91	-3.16
Pearson corr.:	0.85	0.73	0.85	0.74	0.22	0.24	0.996
Specific Humidity							
RMSE (kg/kg):	0.00074	0.00078	0.00121	0.00128	0.00053	0.00060	0.00009
MBE (kg/kg):	-0.00052	-0.00065	-0.00085	-0.00102	0.00033	0.00038	-0.00004
Pearson corr.:	0.984	0.983	0.9803	0.9796	0.653	0.635	0.999
2-m Temperature							
RMSE (°C):	1.01	1.02	0.93	0.88	0.51	0.57	0.71
MBE (°C):	-0.11	0.25	-0.43	-0.19	0.32	0.44	0.69
Pearson corr.:	0.99	0.99	0.99	0.99	0.20	0.21	0.9998

Table A2
Standard deviation for day mean over 2000–2009 for specific humidity, relative humidity (also hourly mean 2000–2009) for observations, 12.5 km and 3 km grid resolutions, for Berlin and its surroundings.

	Obs Berlin	*Berlin 12.5 km*	*Berlin 3 km*	*Obs Surroundings*	*Surroundings 12.5 km*	*Surroundings 3 km*
Relative humidity (%)	8.56	9.15	10.21	8.03	7.86	9.25
Specific humidity (kg/kg)	0.00213	0.00246	0.00227	0.00216	0.00286	0.00275

Table A3
Change in days per year for the grid resolutions (3 km and 12.5 km), for climate change (future – historical) and urban-rural contrast (Berlin – surroundings).

		Climate change ***(future - historical)***			**Urb-rur contrast** ***(Berlin - surr)***	
		12.5 km	**3 km**		**historical**	**future**
Influenza	*Berlin*	-1	-2	*12.5 km*	+0.2	+0.3
	Surroundings	-1	-2	*3 km*	+0.1	0
Pollen	*Berlin*	-4	+0.2	*12.5 km*	+6	+3
	Surroundings	-1	+2	*3 km*	+5	+3
Mold	*Berlin*	+11	-18	*12.5 km*	-15	-17
	Surroundings	+13	-15	*3 km*	-11	-14

References

Amt für Statistik Berlin-Brandenburg, 2020. Statistiken Berlin und Brandenburg [WWW Document]. Statistiken. URL. https://www.statistik-berlin-brandenburg.de/ statistiken/Inhalt-Statistiken.asp (accessed 7.26.19).

Argüeso, D., Evans, J.P., Fita, L., Bormann, K.J., 2014. Temperature response to future urbanization and climate change. Clim. Dyn. https://doi.org/10.1007/s00382- 013-1789-6.

Argüeso, D., Di Luca, A., Evans, J.P., 2016. Precipitation over urban areas in the western maritime continent using a convection-permitting model. Clim. Dyn. 47, 1143–1159. https://doi.org/10.1007/s00382-015-2893-6.

Bai, X., Dawson, R.J., Ürge-Vorsatz, D., Delgado, G.C., Salisu Barau, A., Dhakal, S., Dodman, D., Leonardsen, L., Masson-Delmotte, V., Roberts, D.C., Schultz, S., 2018. Six research priorities for cities and climate change. Nature. https://doi.org/10.1038/d41586-018-02409-z.

Baklanov, A., Grimmond, C.S.B., Carlson, D., Terblanche, D., Tang, X., Bouchet, V., Lee, B., Langendijk, G., Kolli, R.K., Hovsepyan, A., 2018. From urban meteorology, climate and environment research to integrated city services. Urban Clim. 23 https://doi.org/10.1016/j.uclim.2017.05.004.

Ban, N., Schmidli, J., Scha¨r, C., 2014. Evaluation of the convection-resolving regional climate modeling approach in decade-long simulations. J. Geophys. Res. 119, 7889–7907. https://doi.org/10.1002/2014JD021478.

Ban, N., Caillaud, C., Coppola, E., Pichelli, E., Sobolowski, S., Adinolfi, M., Ahrens, B., Alias, A., Anders, I., Bastin, S., Belu˘si´c, D., Berthou, S., Brisson, E., Cardoso, R. M., Chan, S.C., Christensen, O.B., Fern´andez, J., Fita, L., Frisius, T., Ga˘sparac, G., Giorgi, F., Goergen, K., Haugen, J.E., Hodnebrog, Ø., Kartsios, S., Katragkou, E., Kendon, E.J., Keuler, K., Lavin-Gullon, A., Lenderink, G., Leutwyler, D., Lorenz, T., Maraun, D., Mercogliano, P., Milovac, J., Panitz, H.J., Raffa, M., Remedio, A. R., Sch¨ar, C., Soares, P.M.M., Srnec, L., Steensen, B.M., Stocchi, P., To¨lle, M.H., Truhetz, H., Vergara-Temprado, J., de Vries, H., Warrach-Sagi, K., Wulfmeyer, V., Zander, M.J., 2021. The first multi-model ensemble of regional climate simulations at kilometer-scale resolution, part I: evaluation of precipitation. Clim. Dyn. https://doi.org/10.1007/s00382-021-05708-w.

Barreca, A.I., Shimshack, J.P., 2012. Absolute humidity, temperature, and influenza mortality: 30 years of county-level evidence from the United States. Am. J. Epidemiol. https://doi.org/10.1093/aje/kws259.

Beest, D.E.T., Van Boven, M., Hooiveld, M., Van Den Dool, C., Wallinga, J., 2013. Driving factors of influenza transmission in the Netherlands. Am. J. Epidemiol. 178, 1469–1477. https://doi.org/10.1093/aje/kwt132.

Bergmann, K.-C., Zuberbier, T., Augustin, J., Mücke, H.-G., Straff, W., 2012. Klimawandel und Pollenallergie: Sta¨dte und Kommunen sollten bei der Bepflanzung des o¨ffentlichen Raums Rücksicht auf Pollenallergiker nehmenClimate change and pollen allergy: In the plantation of public spaces, cities and municipalities should take into a. Allergo J. 21, 103–108. https://doi.org/10.1007/s15007-012-0045-4.

Bertolin, C., Camuffo, D., 2014. Climate change impact on movable and immovable cultural heritage throughout Europe. Climate for Culture, Deliverable 5.

Bianchi, D.E., Schwemmin, D.J., Wagner, W.H., 1959. Pollen release in the common ragweed (Ambrosia artemisiifolia). Bot. Gaz. https://doi.org/10.1086/336030.

Brasseur, G.P., Jacob, D., Schuck-Zo¨ller, S., 2017. Klimawandel in Deutschland: Entwicklung, Folgen, Risiken und Perspektiven. Chemie in Unserer Zeit.

Bundesministerium für Raumordnung, B. und S., 1995. Dritter_Bericht_ueber_Schaeden_an_Gebaeuden1995_.pdf.

Buters, J., Alberternst, B., Nawrath, S., Wimmer, M., Traidl-Hoffmann, C., Starfinger, U., Behrendt, H., Schmidt-Weber, C., Bergmann, K.-C., 2015. Ambrosia artemisiifolia (ragweed) in Germany – current presence, allergological relevance and containment procedures. Allergo J. Int. 24, 108–120. https://doi.org/ 10.1007/s40629-015-0060-6.

Caini, S., Spreeuwenberg, P., Donker, G., Korevaar, J., Paget, J., 2018. Climatic factors and long-term trends of influenza-like illness rates in the Netherlands, 1970–2016. Environ. Res. https://doi.org/10.1016/j.envres.2018.07.035.

Choi, S.M., Jeong, Y.-J., Park, J.S., Kang, H.J., Lee, Y.J., Park, S.S., Lim, H.-J., Chung, H.S., Lee, C.-H., 2014. The impact of lifestyle behaviors on the acquisition of pandemic (H1N1) influenza infection: a case-control study. Yonsei Med. J. 55, 422–427.

Chong, K.C., Lee, T.C., Bialasiewicz, S., Chen, J., Smith, D.W., Choy, W.S.C., Krajden, M., Jalal, H., Jennings, L., Alexander, B., Lee, H.K., Fraaij, P., Levy, A., Yeung, A. C.M., Tozer, S., Lau, S.Y.F., Jia, K.M., Tang, J.W.T., Hui, D.S.C., Chan, P.K.S., 2020. Association between meteorological variations and activities of influenza a and B across different climate zones: a multi-region modelling analysis across the globe. J. Inf. Secur. 80, 84–98. https://doi.org/10.1016/j.jinf.2019.09.013.

Coppola, E., Sobolowski, S., Pichelli, E., Raffaele, F., Ahrens, B., Anders, I., Ban, N., Bastin, S., Belda, M., Belusic, D., Caldas-Alvarez, A., Cardoso, R.M., Davolio, S., Dobler, A., Fernandez, J., Fita, L., Fumiere, Q., Giorgi, F., Goergen, K., Güttler, I., Halenka, T., Heinzeller, D., Hodnebrog, Jacob, D., Kartsios, S., Katragkou, E., Kendon, E., Khodayar, S., Kunstmann, H., Knist, S., Lavín-Gullo´n, A., Lind, P., Lorenz, T., Maraun, D., Marelle, L., van Meijgaard, E., Milovac, J., Myhre, G., Panitz, H.J., Piazza, M., Raffa, M., Raub, T., Rockel, B., Scha¨r, C., Sieck, K., Soares, P.M.M., Somot, S., Srnec, L., Stocchi, P., To¨lle, M.H., Truhetz, H., Vautard, R., de Vries, H., Warrach-Sagi, K., 2020. A first-of-its-kind multi-model convection permitting ensemble for investigating convective phenomena over Europe and the Mediterranean. Clim. Dyn. https://doi.org/10.1007/s00382-018-4521-8.

Cunze, S., Leiblein, M.C., Tackenberg, O., 2013. Range expansion of Ambrosia artemisiifolia in Europe is promoted by climate change. ISRN Ecol. 2013, 1–9. https://doi.org/10.1155/2013/610126.

Curtis, R., 2010. Climate change and traditional buildings: the approach taken by historic Scotland. J. Archit. Conserv. https://doi.org/10.1080/13556207.2010.10785073.

Cvetkovski, B., Kritikos, V., Yan, K., Bosnic-Anticevich, S., 2018. Tell me about your hay fever: a qualitative investigation of allergic rhinitis management from the perspective of the patient. NPJ Prim. Care Respir. Med. 28, 1–7.

Dales, R.E., Zwanenburg, H., Burnett, R., Franklin, C.A., 1991. Respiratory health effects of home dampness and molds among Canadian children. Am. J. Epidemiol.134, 196–203. https://doi.org/10.1093/oXfordjournals.aje.a116072.

Dalziel, B.D., Kissler, S., Gog, J.R., Viboud, C., Bjørnstad, O.N., Metcalf, C.J.E., Grenfell, B.T., 2018. Urbanization and humidity shape the intensity of influenza epidemics in U.S. cities. Science (80-.). 362, 75–79. https://doi.org/10.1126/science.aat6030.

D'Amato, G., Cecchi, L., 2008. Effects of climate change on environmental factors in respiratory allergic diseases. Clin. EXp. Allergy. https://doi.org/10.1111/j.1365- 2222.2008.03033.X.

Daniel, M., Lemonsu, A., D´equ´e, M., Somot, S., Alias, A., Masson, V., 2019. Benefits of explicit urban parameterization in regional climate modeling to study climate and city interactions. Clim. Dyn. 52 (5), 2745–2764. https://doi.org/10.1007/s00382-018-4289-X.

Davis, R.E., McGregor, G.R., Enfield, K.B., 2016. Humidity: a review and primer on atmospheric moisture and human health. Environ. Res. 144, 106–116. https://doi.org/10.1016/j.envres.2015.10.014.

Deutschewitz, K., Lausch, A., Kühn, I., Klotz, S., 2003. Native and alien plant species richness in relation to spatial heterogeneity on a regional scale in Germany. Glob.Ecol. Biogeogr. 12, 299–311.

Deyle, E.R., Maher, M.C., Hernandez, R.D., Basu, S., Sugihara, G., 2016. Global environmental drivers of influenza. Proc. Natl. Acad. Sci. U. S. A. https://doi.org/ 10.1073/pnas.1607747113.

Di Luca, A., de Elía, R., Laprise, R., 2015. Challenges in the quest for added value of regional climate dynamical downscaling. Curr. Clim. Chang. Rep. https://doi.org/ 10.1007/s40641-015-0003-9.

Dingle, A.N., Gill, G.C., Wagner, W.H., Hewson, E.W., 1959. The emission, dispersion, and deposition of ragweed pollen. Adv. Geophys. https://doi.org/10.1016/ S0065-2687(08)60123-5.

DWD, D., 2021. German Weather Service, Climate Data Center (CDC) [WWW Document]. URL. https://cdc.dwd.de/portal/ (accessed 5.8.21). EEA, 2000. The Revised and Supplemented Corine Land Cover Nomenclature. EEA Tech. Rep. No 40.

Fosser, G., Kendon, E.J., Stephenson, D., Tucker, S., 2020. Convection-permitting models offer promise of more certain extreme rainfall projections. Geophys. Res.Lett. https://doi.org/10.1029/2020GL088151.

Fuhrmann, C., 2010. The effects of weather and climate on the seasonality of influenza: what we know and what we need to know. Geogr. Compass 4, 718–730. https://doi.org/10.1111/j.1749-8198.2010.00343.X.

Ghiani, A., Ciappetta, S., Gentili, R., Asero, R., Citterio, S., 2016. Is ragweed pollen allergenicity governed by environmental conditions during plant growth and flowering? Sci. Rep. 6 https://doi.org/10.1038/srep30438.

Goettel, H., 2009. Einfluss der nichthydrostatischen Modellierung und der Niederschlagsverdriftung auf die Ergebnisse regionaler Klimamodellierung. Rep. Earth Syst.Sci. 125.

Goodwins, L., Menzies, B., Osborne, N., Muscatello, D., 2019. Human seasonal influenza and climate change: a systematic review of the methods used to examine the relationship between meteorological variables and influenza. Environ. Epidemiol. 3, 137. https://doi.org/10.1097/01.EE9.0000607256.48033.53, 2019 Annu. Conf. Int. Soc. Environ. Epidemiol. August 25–28 2019, Utrecht, Netherlands.

Grant, T., Croce, E., Matsui, E.C., 2022. Asthma and the social determinants of health. Ann. Allergy Asthma Immunol. 128, 5–11.

Guerrisi, C., Ecollan, M., Souty, C., Rossignol, L., Turbelin, C., Debin, M., Goronflot, T., Boelle, P.-Y., Hanslik, T., Colizza, V., 2019. Factors associated with influenza- like-illness: a crowdsourced cohort study from 2012/13 to 2017/18. BMC Public Health 19, 1–9.

Hamaoui-Laguel, L., Vautard, R., Liu, L., Solmon, F., Viovy, N., Khvorostyanov, D., Essl, F., Chuine, I., Colette, A., Semenov, M.A., Schaffhauser, A., Storkey, J., Thibaudon, M., Epstein, M.M., 2015. Effects of climate change and seed dispersal on airborne ragweed pollen loads in Europe. Nat. Clim. Chang. https://doi.org/ 10.1038/nclimate2652.

Hao, L., Herrera-Avellanosa, D., Del Pero, C., Troi, A., 2020. What are the implications of climate change for retrofitted historic buildings? A literature review. Sustain. https://doi.org/10.3390/su12187557.

Hawkins, E., Frame, D., Harrington, L., Joshi, M., King, A., Rojas, M., Sutton, R., 2020. Observed emergence of the climate change signal: from the familiar to the unknown. Geophys. Res. Lett. https://doi.org/10.1029/2019GL086259.

Hirota, Y., Tekeshita, S., Ide, S., Kataoka, K., Ohkubo, A., Fukuyoshi, S., Takahashi, K., Hirohata, T., Kaji, M., 1992. Various factors associated with the manifestation of influenza-like illness. Int. J. Epidemiol. 21, 574–582.

Huijbregts, Z., Kramer, R.P., Martens, M.H.J., van Schijndel, A.W.M., Schellen, H.L., 2012. A proposed method to assess the damage risk of future climate change to museum objects in historic buildings. Build. Environ. https://doi.org/10.1016/j.buildenv.2012.01.008.

Hurraß, J., Heinzow, B., Aurbach, U., Bergmann, K.-C., Bufe, A., Buzina, W., Cornely, O.A., Engelhart, S., Fischer, G., Gabrio, T., Heinz, W., Herr, C.E.W., Kleine- Tebbe, J., Klimek, L., Ko¨berle, M., Lichtnecker, H., Lob-Corzilius, T., Merget, R., Mülleneisen, N., Nowak, D., Rabe, U., Raulf, M., Seidl, H.P., Steiß, J.-O., Szewszyk, R., Thomas, P., Valtanen, K., Wiesmüller, G.A., 2017. Medical diagnostics for indoor mold exposure. Int. J. Hyg. Environ. Health 220, 305–328. https:// doi.org/10.1016/j.ijheh.2016.11.012.

IPCC, 2013. Intergovernmental Panel on Climate Change Working Group I. Climate Change 2013: The Physical Science Basis. Long-term Climate Change: Projections, Commitments and Irreversibility. Cambridge Univ. Press, New York.

Jacob, D., Podzun, R., 1997. Sensitivity studies with the regional climate model REMO. Meteorog. Atmos. Phys. https://doi.org/10.1007/BF01025368.

Jacob, D., Haensler, A., Saeed, F., Elizalde, A., Hagemann, S., Kumar, P., Podzun, R., Rechid, D., Remedio, A.R., Sieck, K., Teichmann, C., Wilhelm, C., 2012. Assessing the transferability of the regional climate model REMO to different coordinated regional climate downscaling experiment (CORDEX) regions. Atmosphere (Basel). https://doi.org/10.3390/atmos3010181.

Jacob, D., Teichmann, C., Sobolowski, S., Katragkou, E., Anders, I., Belda, M., Benestad, R., Boberg, F., Buonomo, E., Cardoso, R.M., Casanueva, A., Christensen, O.B., Christensen, J.H., Coppola, E., De Cruz, L., Davin, E.L., Dobler, A., Domínguez, M., Fealy, R., Fernandez, J., Gaertner, M.A., García-Díez, M., Giorgi, F., Gobiet, A., Goergen, K., Go´mez-Navarro, J.J., Alem´an, J.J.G., Guti´errez, C., Guti´errez, J.M., Güttler, I., Haensler, A., Halenka, T., Jerez, S., Jim´enez-Guerrero, P., Jones, R.G., Keuler, K., Kjellstro¨m, E., Knist, S., Kotlarski, S., Maraun, D., van Meijgaard, E., Mercogliano, P., Monta´vez, J.P., Navarra, A., Nikulin, G., de Noblet-Ducoudr´e, N., Panitz, H.J., Pfeifer, S., Piazza, M., Pichelli, E., Pietika¨inen, J.P., Prein, A.F., Preuschmann, S., Rechid, D., Rockel, B., Romera, R., Sa´nchez, E., Sieck, K., Soares, P.

M.M., Somot, S., Srnec, L., Sørland, S.L., Termonia, P., Truhetz, H., Vautard, R., Warrach-Sagi, K., Wulfmeyer, V., 2020. Regional climate downscaling over Europe: perspectives from the EURO-CORDEX community. Reg. Environ. Chang. 20 https://doi.org/10.1007/s10113-020-01606-9.

Jain, S., Chaves, S.S., 2011. Obesity and influenza. Clin. Infect. Dis. 53 (5), 422–424.

Jin, L., Schubert, S., Fenner, D., Meier, F., Schneider, C., 2021. Integration of a building energy model in an urban climate model and its application. Boundary-Layer Meteorol. https://doi.org/10.1007/s10546-020-00569-y.

Johansson, P., Ekstrand-Tobin, A., Svensson, T., Bok, G., 2012. Laboratory study to determine the critical moisture level for mould growth on building materials. Int.Biodeterior. Biodegrad. https://doi.org/10.1016/j.ibiod.2012.05.014.

Kannabei, S., Dümmel, T., Hohlstein, G., Cobau-Lange, S., Basta, D., Bohnen, M., Kühsel, D., 2013. Berliner Aktionsprogramm gegen Ambrosia 2013. Berliner Aktionsprogr. gegen Ambrosia, FU-Berlin, p. 8.

Karki, S., Muscatello, D.J., Banks, E., MacIntyre, C.R., McIntyre, P., Liu, B., 2018. Association between body mass index and laboratory-confirmed influenza in middle aged and older adults: a prospective cohort study. Int. J. Obes. 42, 1480–1488.

Kay, D., Kelly, J., Schaeffer, T., Tuong, T., Leru, P., Addison, W.A., Neamtu, R., 2020. Pollen Allergies in Romania.

Kendon, E.J., Prein, A.F., Senior, C.A., Stirling, A., 2021. Challenges and outlook for convection-permitting climate modelling. Philos. Trans. R. Soc. A Math. Phys.Eng. Sci. https://doi.org/10.1098/rsta.2019.0547.

Kotlarski, S., Keuler, K., Christensen, O.B., Colette, A., D´equ´e, M., Gobiet, A., Goergen, K., Jacob, D., Lüthi, D., Van Meijgaard, E., Nikulin, G., Sch¨ar, C., Teichmann, C., Vautard, R., Warrach-Sagi, K., Wulfmeyer, V., 2014. Regional climate modeling on European scales: a joint standard evaluation of the EURO- CORDEX RCM ensemble. Geosci. Model Dev. 7, 1297–1333. https://doi.org/10.5194/gmd-7-1297-2014.

Kusunoki, T., Takeuchi, J., Morimoto, T., Sakuma, M., Yasumi, T., Nishikomori, R., Higashi, A., Heike, T., 2017. Fruit intake reduces the onset of respiratory allergic symptoms in schoolchildren. Pediatr. Allergy Immunol. 28, 793–800.

Laaidi, K., Laaidi, M., 1999. Airborne pollen of Ambrosia in Burgundy (France) 1996-1997. Aerobiologia (Bologna). https://doi.org/10.1023/A:1007547919559.

Langendijk, G.S., Rechid, D., Jacob, D., 2019. Urban areas and urban-rural contrasts under climate change: what does the EURO-CORDEX ensemble tell us?-investigating near surface humidity in berlin and its surroundings. Atmosphere (Basel). 10 https://doi.org/10.3390/ATMOS10120730.

Langendijk, G.S., Rechid, D., Sieck, K., Jacob, D., 2021. Added value of convection-permitting simulations for understanding future urban humidity extremes: case studies for Berlin and its surroundings. Weather Clim. EXtrem. 33 https://doi.org/10.1016/j.wace.2021.100367.

Lauwaet, D., Hooyberghs, H., Lefebre, F., De Ridder, K., Willems, P., 2017. Climate-fit-City_D5.1: Urban Primary Data Need Analysis.

Leissner, J., Kilian, R., Kotova, L., Jacob, D., Mikolajewicz, U., Brostro¨m, T., Ashley-Smith, J., Schellen, H.L., Martens, M., Van Schijndel, J., Antretter, F., Winkler, M., Bertolin, C., Camuffo, D., Simeunovic,

G., Vyhlídal, T., 2015. Climate for culture: assessing the impact of climate change on the future indoor climate in historic buildings using simulations. Herit. Sci. 3, 1–15. https://doi.org/10.1186/s40494-015-0067-9.

Leru, P.M., Kay, D., Kelly, J., Tuong, T., Schaeffer, T., Addison, B., Neamtu, R., 2021. Atopy and lifestyle survey of allergic patients from urban environment in Romania: preliminary data from an interactive qualifying project. Cureus 13.

Lin, L., Chan, T.O., Ge, E., Wang, X., Zhao, Y., Yang, Y., Ning, G., Zeng, Z., Luo, M., 2020. Effects of urban land expansion on decreasing atmospheric moisture in Guangdong, South China. Urban Clim. https://doi.org/10.1016/j.uclim.2020.100626.

Liu, L., Solmon, F., Vautard, R., Hamaoui-Laguel, L., Zsolt Torma, C., Giorgi, F., 2016. Ragweed pollen production and dispersion modelling within a regional climate system, calibration and application over Europe. Biogeosciences. https://doi.org/10.5194/bg-13-2769-2016.

Lokoshchenko, M.A., 2017. Urban heat island and urban dry island in Moscow and their centennial changes. J. Appl. Meteorol. Climatol. https://doi.org/10.1175/ JAMC-D-16-0383.1.

Lourenço, P.B., Luso, E., Almeida, M.G., 2006. Defects and moisture problems in buildings from historical city centres: a case study in Portugal. Build. Environ. https://doi.org/10.1016/j.buildenv.2005.01.001.

Lowe, J.A., McSweeney, C., Hewitt, C., 2020. An Overview of the EUCP Project-towards Improved European Climate Predictions and Projections. EGU Gen. Assem.Conf. Abstr, p. 19475.

Lowen, A.C., Steel, J., 2014. Roles of humidity and temperature in shaping influenza seasonality. J. Virol. 88, 7692–7695. https://doi.org/10.1128/jvi.03544-13. Lowen, A.C., Mubareka, S., Steel, J., Palese, P., 2007. Influenza virus transmission is dependent on relative humidity and temperature. PLoS Pathog. 3, 1470–1476. https://doi.org/10.1371/journal.ppat.0030151.

Majewski, D., 1991. The Europa-Modell of the Deutscher Wetterdienst. ECMWF Semin. Numer. methods Atmos. Model.

Marr, L.C., Tang, J.W., Van Mullekom, J., Lakdawala, S.S., 2019. Mechanistic insights into the effect of humidity on airborne influenza virus survival, transmission and incidence. J. R. Soc. Interface 16. https://doi.org/10.1098/rsif.2018.0298.

Masson, V., Lemonsu, A., Hidalgo, J., Voogt, J., 2020. Urban climates and climate change. Annu. Rev. Environ. Resour. 45, 411–444. https://doi.org/10.1146/ annurev-environ-012320-083623.

Mendell, M.J., Kumagai, K., 2017. Observation-based metrics for residential dampness and mold with dose–response relationships to health: a review. Indoor Air 27, 506–517.

Meng, Y., Lu, Y., Xiang, H., Liu, S., 2021. Short-term effects of ambient air pollution on the incidence of influenza in Wuhan, China: a time-series analysis. Environ.Res. 192, 110327.

Menut, L., Vautard, R., Colette, A., Khvorostyanov, D., Potier, A., Hamaoui-Laguel, L., Viovy, N., Thibaudon, M., 2014. A new model of ragweed pollen release based on the analysis of meteorological conditions. Atmos. Chem. Phys. Discuss. https://doi.org/10.5194/acpd-14-10891-2014.

Moss, R.H., Edmonds, J.A., Hibbard, K.A., Manning, M.R., Rose, S.K., Van Vuuren, D.P., Carter, T.R., Emori, S., Kainuma, M., Kram, T., Meehl, G.A., Mitchell, J.F.B., Nakicenovic, N., Riahi, K., Smith, S.J.,

Stouffer, R.J., Thomson, A.M., Weyant, J.P., Wilbanks, T.J., 2010. The next generation of scenarios for climate change research and assessment. Nature. https://doi.org/10.1038/nature08823.

Murtas, R., Russo, A.G., 2019. Effects of pollution, low temperature and influenza syndrome on the excess mortality risk in winter 2016–2017. BMC Public Health 19, 1–9.

Nguyen, J.L., Schwartz, J., Dockery, D.W., 2014. The relationship between indoor and outdoor temperature, apparent temperature, relative humidity, and absolute humidity. Indoor Air. https://doi.org/10.1111/ina.12052.

Norba¨ck, D., 2020. Dampness, indoor mould and health. In: Indoor Environmental Quality and Health Risk toward Healthier Environment for all. Springer, pp. 199–216.

Noti, J.D., Blachere, F.M., McMillen, C.M., Lindsley, W.G., Kashon, M.L., Slaughter, D.R., Beezhold, D.H., 2013. High humidity leads to loss of infectious influenza virus from simulated coughs. PLoS One 8, 2–9. https://doi.org/10.1371/journal.pone.0057485.

Ojanen, T., Viitanen, Hannu, La¨hdesma¨ki, K., Vinha, J., Peuhkuri, R., Salminen, K., 2010. Mold Growth Modeling of Building Structures Using Sensitivity Classes of Materials Tuomo. Acta Acust. united with Acust.

Park, J.E., Son, W.S., Ryu, Y., Choi, S.B., Kwon, O., Ahn, I., 2020. Effects of temperature, humidity, and diurnal temperature range on influenza incidence in a temperate region. Influenza Other Respir. Viruses 14, 11–18. https://doi.org/10.1111/irv.12682.

Peci, A., Winter, A.L., Li, Y., Gnaneshan, S., Liu, J., Mubareka, S., Gubbay, J.B., 2019. Effects of absolute humidity, relative humidity, temperature, and wind speed on influenza activity in Toronto, Ontario, Canada. Appl. Environ. Microbiol. 85, 1–13. https://doi.org/10.1128/AEM.02426-18.

Pflanzenschutzamt Berlin, 2021, https://www.berlin.de/pflanzenschutzamt/stadtgruen/ambrosia-bekaempfung/, (accessed: 21.05.2021).

Pietrzyk, K., 2015. A systemic approach to moisture problems in buildings for mould safety modelling. Build. Environ. https://doi.org/10.1016/j.buildenv.2014.12.013.

Prank, M., Chapman, D.S., Bullock, J.M., Belmonte, J., Berger, U., Dahl, A., J¨ager, S., Kovtunenko, I., Magyar, D., Niemela¨, S., Rantio-Lehtim¨aki, A., Rodinkova, V., Sauliene, I., Severova, E., Sikoparija, B., Sofiev, M., 2013. An operational model for forecasting ragweed pollen release and dispersion in Europe. Agric. For. Meteorol. 182–183, 43–53. https://doi.org/10.1016/J.AGRFORMET.2013.08.003.

Prein, A.F., Langhans, W., Fosser, G., Ferrone, A., Ban, N., Goergen, K., Keller, M., To¨lle, M., Gutjahr, O., Feser, F., Brisson, E., Kollet, S., Schmidli, J., Van Lipzig, N.P. M., Leung, R., 2015. A review on regional convection-permitting climate modeling: demonstrations, prospects, and challenges. Rev. Geophys. 53, 323–361. https://doi.org/10.1002/2014RG000475.

Rechid, D., Jacob, D., 2006. Influence of monthly varying vegetation on the simulated climate in Europe. Meteorol. Z. 15, 99–116. https://doi.org/10.1127/0941- 2948/2006/0091.

Reinhardt, F., Herle, M., Bastiansen, F., Streit, B., 2003. O¨ konomische Folgen der Ausbreitung von Neobiota, pp. 1–248.

Ritschkoff, A.C., Viitanen, H., Koskela, K., 2000. The response of building materials to the mould exposure at different humidity and temperature conditions. In: Healthy Buildings 2000, pp. 317–322.

RKI, 2019. Pommes für die Grippeschutzimpfung? Neuer Influenza-Saisonbericht erschienenPommes für die Grippeschutzimpfung? Neuer Influenza-Saisonbericht erschienen [WWW Document]. URL. https://www.rki.de/DE/Content/Service/Presse/Pressemitteilungen/2019/10_2019.html (accessed 2.18.21).

RKI, 2020. Brandenburg und Berlin - Saison 2020/2021, Arbeitsgemeinschaft Influenza [WWW Document]. URL. https://influenza.rki.de/Diagrams.aspX? agiRegion 3 (accessed 2.18.21).

Roeckner, E., Arpe, K., Bengtsson, L., Christoph, M., Claussen, M., Dümenil, L., Esch, M., Giorgetta, M., Schlese, U., Schulzweida, U., 1996. The atmospheric general circulation model ECHAM-4: model description and simulation of present-day climate. MPI Rep. 218, 171.

Rosenzweig, C., Solecki, W., Romero-Lankao, P., Mehrotra, S., Dhakal, S., Bowman, T., Ibrahim, S.A., 2018. Climate Change and Cities: Second Assessment Report of the Urban Climate Change Research Network, in: Climate Change and Cities. https://doi.org/10.1017/9781316563878.007.

Sedghy, F., Varasteh, A.-R., Sankian, M., Moghadam, M., 2018. Interaction between air pollutants and pollen grains: the role on the rising trend in allergy. Reports Biochem. Mol. Biol. 6, 219.

Sedlbauer, K., 2001. Prediction of Mould Fungus Formation on the Surface of/and inside Building Components. Seguel, J.M., Merrill, R., Seguel, D., Campagna, A.C., 2017. Indoor air quality. Am. J. Lifestyle Med. 11, 284–295.

Semmler, T., 2002. Der Wasser- und Energiehaushalt der arktischen Atmospha¨re. EXamensarbeit - Max-Planck-Institut fur Meteorol. 101–106.

Shaman, J., Kohn, M., 2009. Absolute humidity modulates influenza survival, transmission, and seasonality. Proc. Natl. Acad. Sci. 106, 3243–3248. https://doi.org/10.1073/PNAS.0806852106.

Shaman, J., Pitzer, V.E., Viboud, C., Grenfell, B.T., Lipsitch, M., 2010. Absolute humidity and the seasonal onset of influenza in the continental United States. PLoS Biol. 8 https://doi.org/10.1371/journal.pbio.1000316.

Shaman, J., Goldstein, E., Lipsitch, M., 2011. Absolute humidity and pandemic versus epidemic influenza. Am. J. Epidemiol. 173, 127–135. https://doi.org/10.1093/ aje/kwq347.

Silverberg, J.I., Braunstein, M., Lee-Wong, M., 2015. Association between climate factors, pollen counts, and childhood hay fever prevalence in the United States.

J. Allergy Clin. Immunol. https://doi.org/10.1016/j.jaci.2014.08.003.

Sinclair, R., Russell, C., Kray, G., Vesper, S., 2018. Asthma risk associated with indoor mold contamination in hispanic communities in Eastern Coachella Valley, California. J. Environ. Public Health 2018.

Soebiyanto, R.P., Gross, D., Jorgensen, P., Buda, S., Bromberg, M., Kaufman, Z., Prosenc, K., Socan, M., Alonso, T.V., Widdowson, M.A., Kiang, R.K., Shaman, J., 2015. Associations between meteorological parameters and influenza activity in Berlin (Germany), Ljubljana (Slovenia), Castile and Leo´n (Spain) and Israeli districts. PLoS One 10, 1–21. https://doi.org/10.1371/journal.pone.0134701.

Sofiev, M., Siljamo, P., Ranta, H., Linkosalo, T., Jaeger, S., Rasmussen, A., Rantio-Lehtimaki, A., Severova, E., Kukkonen, J., 2013. A numerical model of birch pollen emission and dispersion in the atmosphere. Description of the emission module. Int. J. Biometeorol. 57, 45–58. https://doi.org/10.1007/s00484-012-0532-z.

Song, Y., Zhang, Y., Wang, T., Qian, S., Wang, S., 2021. Spatio-temporal differentiation in the incidence of influenza and its relationship with air pollution in China from 2004 to 2017. Chin. Geogr. Sci. 31, 815–828.

SSW, 2018. Senatsverwaltung für Stadtentwicklung und Wohnen: Gebaudealter der Wohnbebauung (Ausgabe 2018).

Stevens, B., Giorgetta, M., Esch, M., Mauritsen, T., Crueger, T., Rast, S., Salzmann, M., Schmidt, H., Bader, J., Block, K., Brokopf, R., Fast, I., Kinne, S., Kornblueh, L., Lohmann, U., Pincus, R., Reichler, T., Roeckner, E., 2013. Atmospheric component of the MPI-M earth system model: ECHAM6. J. Adv. Model. Earth Syst. 5, 146–172. https://doi.org/10.1002/jame.20015.

Storkey, J., Stratonovitch, P., Chapman, D.S., Vidotto, F., Semenov, M.A., 2014. A process-based approach to predicting the effect of climate change on the distribution of an invasive allergenic plant in Europe. PLoS One 9. https://doi.org/10.1371/journal.pone.0088156.

Stull, R., 2017. Practical Meteorology: An Algebra-Based Survey of Atmospheric Science. Univ. of British Columbia.

Su, W., Wu, X., Geng, X., Zhao, X., Liu, Q., Liu, T., 2019. The short-term effects of air pollutants on influenza-like illness in Jinan, China. BMC Public Health 19, 1–12.

Toczylowski, K., Wietlicka-Piszcz, M., Grabowska, M., Sulik, A., 2021. Cumulative effects of particulate matter pollution and meteorological variables on the risk of influenza-like illness. Viruses 13, 556.

Towers, S., Chowell, G., Hameed, R., Jastrebski, M., Khan, M., Meeks, J., Mubayi, A., Harris, G., 2013. Climate change and influenza: the likelihood of early and severe influenza seasons following warmer than average winters. PLoS currents 5.

Trusilova, K., Früh, B., Brienen, S., Walter, A., Masson, V., Pigeon, G., Becker, P., 2013. Implementation of an urban parameterization scheme into the regional climate model COSMO-CLM. J. Appl. Meteorol. Climatol. 52 (10), 2296–2311. https://doi.org/10.1175/JAMC-D-12-0209.1.

Viitanen, H., Ojanen, T., 2007. Improved model to predict mold growth in building materials. Thermal Performance of the EXterior Envelopes of Whole Buildings X–Proceedings CD 2–7.

Viitanen, H., Toratti, T., Makkonen, L., Peuhkuri, R., Ojanen, T., Ruokolainen, L., Raisanen, J., 2010. Towards modelling of decay risk of wooden materials. Eur. J. Wood Wood Prod. https://doi.org/10.1007/s00107-010-0450-X.

Voros, K., Bobvos, J., Varro´, J.M., Mainasi, T., Rudnai, P., Paldy, A., 2018. Impacts of long-term ragweed pollen load and other potential risk factors on ragweed pollen allergy among schoolchildren in Hungary. Ann. Agric. Environ. Med. 25.

Wang, B., Liu, Y., Li, Zhenjiang, Li, Zhiwen, 2016. Association of indoor air pollution from coal combustion with influenza-like illness in housewives. Environ. Pollut.216, 646–652.

WHO, W.H.O, 2010. Sex, gender and influenza. World Health Organisation, Geneva.

Wiesmüller, G.A., Heinzow, B., Aurbach, U., Bergmann, K.-C., Bufe, A., Buzina, W., Cornely, O.A., Engelhart, S., Fischer, G., Gabrio, T., 2016. AWMF-Schimmelpilz- Leitlinie “Medizinisch klinische Diagnostik bei Schimmelpilzexposition in Innenr¨aumen” AWMF-Register-Nr. 161/001-Endfassung.

Wong, C.M., Yang, L., Chan, K.P., Chan, W.M., Song, L., Lai, H.K., Thach, T.Q., Ho, L.M., Chan, K.H., Lam, T.H., 2013. Cigarette smoking as a risk factor for influenza- associated mortality: evidence from an elderly cohort. Influenza Other Respir. Viruses 7, 531–539.

Yang, L., Chan, K.P., Lee, R.S., Chan, W.M., Lai, H.K., Thach, T.Q., Chan, K.H., Lam, T.H., Peiris, J.S.M., Wong, C.M., 2013. Obesity and influenza associated mortality: evidence from an elderly cohort in Hong Kong. Prev. Med. (Baltim). 56, 118–123.

Zhao, L., Oleson, K., Bou-Zeid, E., Krayenhoff, E.S., Bray, A., Zhu, Q., Zheng, Z., Chen, C., Oppenheimer, M., 2021. Global multi-model projections of local urban climates. Nat. Clim. Chang. https://doi.org/10.1038/s41558-020-00958-8.

Zink, K., Vogel, H., Vogel, B., Magyar, D., Kottmeier, C., 2012. Modeling the dispersion of Ambrosia artemisiifolia L. pollen with the model system COSMO-ART. Int. J. Biometeorol. 669–680.

Ziska, L.H., Gebhard, D.E., Frenz, D.A., Faulkner, S., Singer, B.D., Straka, J.G., 2003. Cities as harbingers of climate change: common ragweed, urbanization, and public health. J. Allergy Clin. Immunol. 111, 290–295. https://doi.org/10.1067/mai.2003.53.

4. Overall discussion

The three papers presented in Chapter 3, all show an urban drying effect in Berlin compared to its surroundings for relative and specific humidity, respectively for the mean values throughout the 21st century (Chapter 3.1.), for the downscaled future extreme conditions (Chapter 3.2.), and for the analysis of the humidity related impact cases (Chapter 3.3.). Prior observational studies investigating humidity differences between a city and its surroundings in past time periods, also found a humidity deficit in urban areas, generally affirming the findings of this study [Cairo (Robaa, 2003); Chicago (Ackerman, 2002); Christchurch (Tapper, 1990); Edmonton (Hage, 1975); Lodz (Fortuniak et al., 2006); Mexico-City (Jåuregui and Tejeda, 1997b); Moscow (Lokoshchenko, 2017)]. Nevertheless, also urban moisture excess was identified in other cities [Belgrade: (Unkašević et al., 2001); Krefeld: (Kuttler et al., 2007b); London: (Lee, 1991); Szeged: (Unger, 1999b)]. The methods to measure, or derive the humidity related variables vary strongly between these observational studies, making it challenging to compare among the studies, as well as directly relate them to the regional climate model data driven research presented in this thesis.

Zhao et al. (2021) present a global study about urban areas under climate change, based on a crude emulator approach downscaling GCM data to calculate the mean difference between the end (2091–2100) and beginning (2006–2015) of the century, in order to highlight urban change signals for two seasons June–August (JJA) and December–February (DJF). The study finds a decrease in urban relative humidity in the Berlin area by the end of the century under RCP4.5 and RCP8.5, in line with the results presented in this study in Chapter 3.1. Worth noting is the relative humidity decrease of 4–8 % RH found by Zhao et al. (2021) in JJA for the RCP8.5 scenario in the Berlin region by the end of the 21st century. This result is comparable to the 6 % relative humidity decrease found in the summer season at the end of the 21st century for Berlin under RCP8.5 in Chapter 3.1., providing more confidence to the presented results.

Previous theoretical and modelling studies without urban representation, project that relative humidity will remain approximately constant at the global scale under climate change (Fischer and Knutti, 2013; Willett et al., 2007). This thesis (particularly Chapter 3.1.), in line with Zhao et al. (2021), clearly identifies an urban induced drying effect for relative humidity in Berlin which enlarges throughout the century, deviating from the projected stable global mean relative humidity described by for instance Willett et al. (2007). This urban-induced humidity effect highlights the critical importance of understanding and simulating the unique urban climate under climate change on the local-to-regional scale.

Global temperatures are projected to continue to rise throughout the 21th century, causing a further increase of specific humidity, as warmer temperatures can hold more moisture (Fischer and Knutti, 2013; Willett et al., 2007). This is in line with the findings presented in Chapter 3.1., which show an increase in specific humidity for Berlin as well as for its surroundings throughout the 21st century. Zhao et al. (2021) also find an increase in urban specific humidity by the end of the century under both RCP4.5 and RCP8.5, particularly for JJA. This specific humidity increase is also the expected driving mechanism behind the decrease in influenza days under climate change for the near term future period, as discussed in Chapter 3.3.

The results presented in Chapter 3.2. and Chapter 3.3. show the added value of the convection-permitting resolution to simulate humidity extremes and humidity related impact cases in the Berlin region. The moist extreme (SH>0.02 kg/kg) (Chapter 3.2.) and the pollen case (Chapter 3.3.), both show added value on the convection-permitting scale compared to the 12.5 km grid resolution. Both occur in the summer season. The results for the model evaluation presented in Chapter 3.3. (paper 3: section 3.1.) also indicate particular added value for the summer months, mainly for relative humidity and temperature. This is in accordance with prior research showing the added

value of convection-permitting simulations is predominantly found for the summer period, for temperature and precipitation (Ban et al., 2021; Prein et al., 2013; Vanden Broucke et al., 2019).

For Chapter 3.2., the downscaled convection-permitting model simulations provide a more detailed picture of the physical processes underpinning the future humidity extremes in the urban-rural context. This is in line with Di Luca et al. (2015), Kendon et al. (2021), Prein et al. (2015), and Gutowski et al. (2021), who point out the potential added value for process understanding on the convection-permitting resolution.

Other studies show promise for convection-permitting models to provide urban climate data on the local-to-regional scale, supporting the findings of this research. For instance, Trusilova et al. (2013) show that the magnitude of the urban heat island in Berlin is better represented at the convection-permitting resolution compared to the coarse horizontal scale (~10 km). Hirsch et al. (2021) demonstrate that the convection-permitting simulations (4km – 800m) can resolve the interaction between local sea breezes and the urban environment that are not currently resolved in coarser resolution models for Sydney, Australia. Wouters et al. (2017) show, using CP urban climate model projections in Belgium for 35 years, that the heat stress increase toward the mid-21st century is twice as large in cities compared to their surrounding rural areas. Despite the fact that there is no prior research showing the added value for humidity in the urban-rural context, the above mentioned studies give general assurance that the results on the convection-permitting resolution presented in this thesis can be treated with stronger confidence.

Chapter 3.1. shows a robust climate change signal for relative and specific humidity, as well as temperature for the Berlin region, based on the EURO-CORDEX ensemble data on the 12.5 km resolution. The results presented in Chapter 3.2. and Chapter 3.3. provide an indication of the climate change signal, as the RCM simulations carry the finger print of climate change. However, the climate change signal cannot be derived in a robust manner for these parts of the thesis. The model simulation periods used here are respectively 1.5 month (Chapter 3.2.) and 10 years (Chapter 3.3.) due to limited computing power and data availability. The former are especially constraining factors for the convection-permitting simulations. Periods of 20–30 years for a historical time period, as well as for a future period are required to be able to robustly assess the climate change signal, on the convection-permitting resolution (Hawkins et al., 2020; IPCC, 2013).

This thesis solely focusses on the Berlin region as a first testbed to analyze humidity under climate change in the urban-rural context. It would be important to understand the transferability of the results to other cities. Potentially similar results may be expected for cities located in a similar climate zone, respectively a moderate continental climate. Nevertheless, the land use in the surroundings can have profound influence on the urban-rural humidity contrast, even if the climate zone is similar. Zhao et al. (2021) show that urban warming and humidity changes are not uniform across regions in the world. Cities in arid regions, or in tropical climate zones can behave considerably different to those in a moderate continental climate. Particularly coastal cities are projected to have indiscernible or no decrease in relative humidity, because of the larger water availability that allows the increase in urban humidity levels to keep up with its rural counterpart (Zhao et al., 2021).

4.1. Limitations

Three main limitations of the presented research are identified.

Firstly, the convection-permitting simulations are conducted with one regional climate model, downscaling two types of future humidity extremes (Chapter 3.2.), and investigating three humidity related impact cases (Chapter 3.3.). The use of a single model approach does not allow for quantifying potential model uncertainties in a robust fashion. Nevertheless, the added value of the convection-permitting resolution has been demonstrated by several other studies (Chapter 4), and the thorough process analysis described in this research, do provide overall confidence in the presented results. The newly developed experiment setup for downscaling extremes under future climate conditions in urban regions can serve as a blueprint for dedicated coordinated downscaling experiments with an ensemble of RCMs, in order to further investigate and quantify the robustness of the results. In addition, the three parts of the thesis only use one urban region, and one emission scenario. Using different regional climate models, urban regions, emissions scenarios, extremes, and impact cases, might lead to other results from the ones found by this thesis. Therefore, the presented findings, especially those in paper 2 and 3, shall be considered a first explorative indication of the potential added value of the convection-permitting resolution to simulate future humidity extremes and impact cases, and their projected changes, under climate change conditions.

Secondly, throughout this research urban areas are represented by the regional climate models through a so-called “bulk scheme”. This simplistic representation can simulate regional-to-local scale climate processes and urban-rural interactions, and can distill an urban-induced signal, as shown by the results of this research. Nevertheless, the bulk scheme fails to capture intra-city details and fine urban-scale processes. The research results indicate that the bulk scheme is most reliable during summer months (Chapter 3.1., 3.2., and 3.3.), but is unable to represent the timing of the peak of the urban heat island correctly at night (Chapter 3.1.). Other studies indicate that improvements of the results could arise by implementing a more sophisticated urban model, especially for the timing and magnitude of the UHI and for the winter period (Daniel et al., 2018; Trusilova et al., 2016; Vanden Broucke et al., 2019). An additional limitation of the approach to represent urban areas used in this study, is that it does not account for future urbanization, urban development, and land use changes in the surroundings, which could influence the results, as shown by e.g. Argüeso et al. (2014).

The third limitation of this research is the lack of a thorough assessment of the usefulness of the new findings for urban decision makers. The posed research questions in this thesis (Chapter 2.1.), and particularly the impact cases defined in paper 3, are based on literature reviews on user needs and humidity related impacts. However, direct engagement with stakeholders is needed to properly understand whether the presented results are useful, and how they could be further tailored to their needs, and how they can be put into context to fit their specific decision-making situation. A translation of the research findings is desirable to distill the useful information, ideally following a co-production approach with relevant urban decision makers (Jack et al., 2021; Langendijk et al., 2019a; Soares et al., 2018; Vincent et al., 2018).

5. Conclusions and outlook

5.1. Answers to research questions

The research presented in this thesis is centered around enhancing the understanding about regional-to-local climate change in the Berlin region, with a focus on humidity, towards improved climate information for urban areas in order to support knowledge-based decision making. Ultimately, this research aims to contribute to increasing the resilience in urban areas to projected climate change impacts. More specifically, following a regional climate modelling and data analysis approach, the research aims to understand the potential of regional climate models, and the possible added value of convection-permitting simulations, to support the provision of knowledge-based climate information for urban regions, particularly with respect to humidity.

The five outlined research gaps in the introduction chapter (Chapter 1) are addressed by the three main research questions (Chapter 2.2.), that underpin the three papers presented as the central part of this thesis (Chapter 3). The following paragraphs highlight the major outcomes of this research and outline how they answer the posed research questions and address the research gaps. The main findings are summarized in Figure 3.

RQ 1: What can already be understood with available regional climate model simulations about future climate change in Berlin and its surroundings, with a focus on humidity?

The first research question is centered around what can already be understood with available regional climate model simulations about humidity under future climate change in the Berlin region. All ten EURO-CORDEX model combinations show an urban-rural contrast for relative and specific humidity, as well as for temperature. Even with the bulk scheme, the regional climate models are able to tease out the urban induced signal, with Berlin being less humid and warmer than its surroundings.

The regional climate model ensemble projects that relative humidity decreases in Berlin compared to its surroundings by up to 6 % RH in summer, enlarging the RH urban-rural contrast throughout the 21st century by 2–4 % under the RCP8.5 emission scenario. The MK-test indicates these results are robust, with 78 % of the model combinations agreeing on a decreasing monotonic trend for relative humidity in Berlin throughout the 21st century. The specific humidity levels increase for the entire Berlin region, resulting in a consistent urban-rural SH contrast throughout the 21st century. Temperature increases are stronger in Berlin than its surroundings under climate change, explaining the relative humidity decrease for Berlin throughout the 21st century. The climate change signal for relative humidity is robust in Berlin, with 71 % of the model combinations agreeing that the future distribution (2070–2099) is different from the historical (1971–2000) distribution following a MWW-test. The largest relative humidity change is found during summer months in Berlin towards the end of the 21st century. One main limitation of the regional climate models is their inability to capture the peak of the urban heat island at nighttime.

The results presented in Chapter 3.1. show for the first time that the EURO-CORDEX regional climate model ensemble can provide robust results for urban-rural humidity contrasts, and their mean changes under future climate change conditions. In this light, the findings provide enhanced understanding about humidity under climate change in the urban-rural context, simulated by regional climate models, addressing research gaps 1, 2, and 5 (Figure 3).

RQ 2: How does crossing spatial scales from 12.5 km to 3 km grid size affect unprecedented humidity extremes and related variables under future climate conditions for Berlin and its surroundings?

Research question two investigates the added value on the convection-permitting scale to simulate unprecedented humidity extremes under future climate conditions for the Berlin region, following a multi-variate process understanding approach. Using the unique HAPPI dataset two extreme humidity conditions, SH>0.02 kg/kg and RH<30 %, are identified that happen under 2.0°C global mean warming. A double-nesting downscaling approach is particularly designed for this study tailored to the urban-rural context, in order to downscale two examples cases of each extreme condition to the 12.5 km (0.11°) and 3 km (0.0275°) grid resolution with the regional climate model REMO.

For both downscaled future humidity extremes, the convection-permitting resolution shows an enhanced urban drying effect. Higher temperatures, and lower evaporation rates, due to the impervious surface characteristics of urban areas, predominantly drive the urban drying effect. The convection-permitting resolution mitigates the SH>0.02 kg/kg moist extreme and intensifies the RH<30 % dry extreme. The summer moist extreme SH>0.02 kg/kg shows a particularly profound urban drying, indicating that the extreme moist days will be less humid in Berlin than its surroundings under 2.0°C global mean warming, especially on the 3 km grid resolution. The multi-variate process understanding analysis shows that the more profound urban drying effect on the convection-permitting resolution is mainly due to better resolving the land surface scheme and the related land-atmosphere interactions. There are more urban grid boxes containing larger urban fractions on the 3 km compared to the 12.5 km grid resolution. In addition, the convection-permitting resolution shows enhanced spatial details while simulating Berlin, its boundaries, and the urban-rural transition.

The research presented in Chapter 3.2. shows an enhanced urban drying effect on the convection-permitting resolution for the downscaled future humidity extremes (SH>0.02 kg/kg and RH<30 %) for Berlin compared to its surroundings. The research contributes to gaining increased understanding on humidity extremes, and their differences simulated by regional climate models across spatial resolutions in the urban-rural context, therefore directly contributing to research gaps 1, 3, 4, and 5 (Figure 3).

RQ 3: What is the added value of convection-permitting climate models to simulate humidity related climate impacts under climate change, for Berlin and its surroundings?

The third research question aims to gain understanding about the added value of convection-permitting climate models to simulate humidity related climate impacts under climate change conditions for the Berlin region. Based on a comprehensive literature analysis three humidity related impact cases are defined: influenza survival and spread, ragweed pollen dispersion, and in-door mold growth. The meteorological conditions driving the impact cases are investigated under near-term climate change (2041–2050) for the 12.5 km and 3 km grid resolution simulated by the regional climate model REMO.

The results show that the convection-permitting resolution improves the simulations for the impact cases and for the monthly mean values in the Berlin region, compared to the 12.5 km grid resolution. The change signal reverses for the 3 km compared to the 12.5 km grid resolution for the impact cases pollen, and mold. Respectively, the convection-permitting resolution shows an increase in pollen days and a decrease in mold days under near-term climate change, in contrast to a decrease in pollen days and an increase in mold days for the 12.5 km resolution. Although less mold days can be expected, longer consecutive periods are projected under future climate conditions. For influenza, the convection-permitting resolution intensifies the decrease of influenza days, nevertheless longer periods of consecutive influenza days are found under near-term climate change. The convection-

permitting resolution performs better in agreement with observations, and the convection-permitting model results for the impact cases are in line with available literature. The results for the impact cases, as well as for the model evaluation with observations, indicates added value on the convection-permitting resolution for the impact cases and monthly mean values, in the Berlin region under near-term climate change conditions, compared to the 12.5 km grid resolution.
The result presented in Chapter 3.3., establish a relationship between regional climate data and humidity related impact cases in the urban-rural context, and show the added value of convection-permitting simulations for the impact cases: influenza; pollen; and mold. Therefore, the outcomes of the research are directly contributing to addressing the research gaps 1, 3, 4, and 5 (Figure 3).

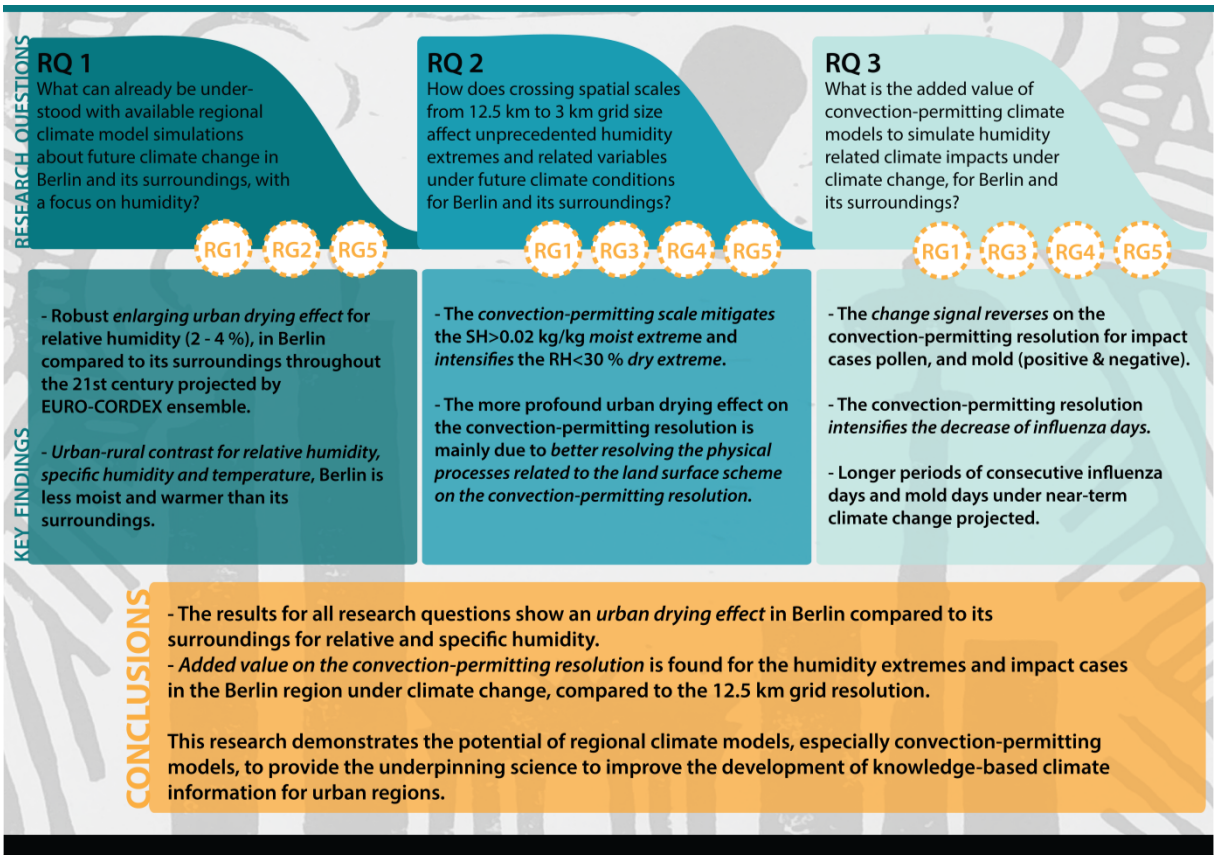

Figure 3. Summary of the key findings, for each research question (RQ), and selected major conclusions of the thesis. "RG" refers to the research gaps, as outlined in Chapter 1.

5.2. Novelty of findings

This research presents novel insights underpinning the development of climate information for urban regions, particularly with respect to humidity under climate change (Chapter 3, and Chapter 5.1.). This study is the first to show an urban-rural humidity contrast based on the EURO-CORDEX RCM ensemble, and a robust enlarging urban drying effect for relative humidity in Berlin compared to its surroundings throughout the 21st century. Convection-permitting modelling is an emerging field. There have been hardly any studies showing the added value of convection-permitting models for urban areas, especially not for humidity extremes and impacts under climate change conditions. This study takes a novel approach by identifying and downscaling two unprecedented humidity extremes, and creating a relationship between regional climate models and three innovative impact cases related to humidity under climate change conditions. It is the premier, explorative study, that shows added value for simulating humidity extremes and impact cases on the convection-permitting resolution for the Berlin region, directly contributing to the leading-edge research field on convection-permitting models. The research demonstrates that regional climate models offer a useful tool to understand urban-rural humidity contrasts under climate change. It clearly shows the potential of regional climate models, especially convection-permitting models, to provide the underpinning science to improve the development of knowledge-based climate information for urban regions.

5.3. Implications for climate services

The research presented in this thesis is framed within the climate services context. It is therefore important to reflect on how the findings are relevant to the development of climate services, particularly for urban areas. The following section provides perspectives on the implications of this research for climate services. This section is not founded on direct research results, but merely presents reflections in line with the findings presented in this thesis and literature in the field.

This research shows that projected local urban drying and warming deviates from the regional background simulated by regional climate models, showing an urban drying effect for relative and specific humidity. In this light, it becomes apparent that it is preferable to extract the urban specific data points from the regional climate model simulations over taking a mean value for a larger region around the city of interest. Climate services for cities shall therefore ensure to derive the urban scale information from regional climate model data for climate change assessments and services. In addition, this research identifies added value for convection-permitting simulations to simulate urban areas, indicating the potential for improving climate information for cities. Climate services shall further employ and develop convection-permitting models for urban areas, to ensure urban decision makers will be provided with the state-of-the-art climate information (Gutowski et al., 2021).

The findings of this study show the importance of humidity in the urban-rural context under climate change. Humidity is connected to critical climate impacts that could influence the livability of cities. Humidity variables are less commonly used in the urban climate services context, compared to temperature and precipitation. Currently, humidity is predominantly considered in connection to heat stress (e.g. Coccolo et al., 2016; Hass et al., 2016; Li et al., 2020). This research shows that humidity is affecting influenza, pollen, and mold. It would therefore be of importance for climate services to increasingly consider humidity variables for their information products for the relevant sectors and applications, in order to adequately inform urban decision makers.
Currently, a broad variety of ways exist to simulate the urban climate, e.g. through micro-scale urban models, statistical-dynamical downscaling, GCM-emulators, and increasingly also regional climate models with urban schemes of various complexity (Hertwig et al., 2021; Masson et al., 2020; Zhao et

al., 2021). The diverse range of approaches need careful consideration to develop urban climate services based on the best available knowledge. To make accurately use of the different approaches, and the results, it is pivotal to understand which type of model is appropriate for which application and/or context. Potentially the different approaches and models could lead to diverging results. A key challenge is how to synthesize the multiple data sources and construct robust climate information, and thereafter how to communicate the information from the different approaches in a coherent way to urban decision makers (Barsugli et al., 2013; Kendon et al., 2021).

Furthermore, it is crucial to acknowledge the complexity of urban systems. A solution for one problem, could bring about difficulties for another sector or application. There is a strong need for a coherent approach on urban services, integrating climate, weather, air quality, hydrology, social systems, and beyond, toward city services that tackle inter-related urban issues in a systematic manner (Baklanov et al., 2018; WMO, 2019).

5.4. Future research directions

The findings presented in this thesis contribute to addressing the research gaps outlined in Chapter 1 and answer the research questions (Chapter 5.1.). Nonetheless, open issues remain that could benefit from further research. This section outlines a few main future research directions.

Investigating more cities, with various models, looking at different impacts, and extremes, is needed to further understand humidity changes under climate change in the urban-rural context, especially on the convection-permitting resolution. It would be critical to understand whether the results found in this study would be similar in other cities, particularly in different climate zones. To make the results more robust, it would be helpful to conduct similar studies with different models and methodological approaches, ideally through coordinated model ensemble experiments (Masson et al., 2020). Transient, ideally multi-model, convection-permitting simulations would be required to robustly assess the climate change signal, with a minimum simulation time of 20–30 years for a historical and a future time period (Hawkins et al., 2020; IPCC, 2013). This could provide insights into the differences between the climate change signals on the various spatial resolutions, in the urban-rural context.

Humidity remains an under investigated variable compared to temperature and precipitation, especially in the urban-rural context. Further research needs to be conducted to enhance our understanding on the urban-induced effect on humidity, and humidity changes under climate change. Taking a multi-variate and process understanding approach is important to gain detailed knowledge about the meteorological conditions, in order to fully understand urban effects on the local-to-regional scale (Fischer and Knutti, 2013). In addition, more studies are required that investigate how humidity changes affect climate related impacts, in line with the presented extremes and the three impact cases in this thesis.

This research shows how important the urban representation in regional climate models becomes when moving to convection-permitting resolutions (Trusilova et al., 2013). It is no longer possible to neglect urban areas at this high-resolution, as the urban areas are increasingly taking up grid boxes, have their own unique climate, and influence the regional climate around them. Simultaneously, ever more people live in cities, increasing the need for urban specific climate information to ensure the continuous livability of cities (Baklanov et al., 2018). In this context, regional climate models shall develop appropriate parameterization schemes to adequately represent urban areas, while retaining a balance between complexity and computing costs. This could also contribute to the on-going developments of cutting-edge regional Earth system models (González et al., 2021; Gutowski et al., 2021). Particularly, incorporating anthropogenic heat into the model, representing the warmth

coming from e.g. cars and heating systems, could improve the results, especially during winter months. In addition, storing incoming heat from solar radiation during the day and releasing the warmth at night could enable improved simulations of the timing and magnitude of the UHI effect (Daniel et al., 2019; Vanden Broucke et al., 2019). Climate adaptation, such as introducing green/blue spaces, and city development are rapidly evolving topics, that may lead to changes in the urban structure and city size (Argüeso et al., 2014). Further research is needed to develop high-resolution land-use-change and urbanization scenarios, as an input for regional climate models, to account for city development and urbanization.

From a climate services perspective, a thorough assessment of the usefulness of the presented findings for urban decision makers would be required, ideally following an interactive approach engaging relevant stakeholders. In addition, further research is needed to understand the suitability of the range of approaches to model and investigate cities for specific applications, sectors, and decision-making contexts. This would allow adequate development of knowledge-based climate information for urban decision makers.

5.5. Closing remark

This research demonstrates that regional climate models offer a useful tool to understand urban-rural humidity contrasts under climate change, by presenting results for mean humidity changes, unprecedented humidity extremes, and humidity related impact cases. It shows the potential of regional climate models, and especially the added value of convection-permitting models, to provide the underpinning science to improve the development of knowledge-based climate information for urban regions. Ultimately, this research makes novel contributions that advance the science, in order to support the development of evidence-based climate information to decision makers, to build the resilient cities of tomorrow in order to ensure the continuous livability of urban areas.

References

Ackerman, B., 2002. Climatology of Chicago Area Urban-Rural Differences in Humidity. J. Clim. Appl. Meteorol. https://doi.org/10.1175/1520-0450(1987)026<0427:cocaur>2.0.co;2

Amt für Statistik Berlin-Brandenburg, 2020. Statistiken Berlin und Brandenburg [WWW Document]. Statistiken. URL https://www.statistik-berlin-brandenburg.de/statistiken/Inhalt-Statistiken.asp (accessed 7.26.19).

Argüeso, D., Di Luca, A., Evans, J.P., 2016. Precipitation over urban areas in the western Maritime Continent using a convection-permitting model. Clim. Dyn. 47, 1143–1159. https://doi.org/10.1007/s00382-015-2893-6

Argüeso, D., Evans, J.P., Fita, L., Bormann, K.J., 2014. Temperature response to future urbanization and climate change. Clim. Dyn. https://doi.org/10.1007/s00382-013-1789-6

Bai, X., Dawson, R.J., Ürge-Vorsatz, D., Delgado, G.C., Salisu Barau, A., Dhakal, S., Dodman, D., Leonardsen, L., Masson-Delmotte, V., Roberts, D.C., Schultz, S., 2018. Six research priorities for cities and climate change. Nature. https://doi.org/10.1038/d41586-018-02409-z

Baklanov, A., Grimmond, C.S.B., Carlson, D., Terblanche, D., Tang, X., Bouchet, V., Lee, B., Langendijk, G., Kolli, R.K., Hovsepyan, A., 2018. From urban meteorology, climate and environment research to integrated city services. Urban Clim. 23. https://doi.org/10.1016/j.uclim.2017.05.004

Ban, N., Caillaud, C., Coppola, E., Pichelli, E., Sobolowski, S., Adinolfi, M., Ahrens, B., Alias, A., Anders, I., Bastin, S., Belušić, D., Berthou, S., Brisson, E., Cardoso, R.M., Chan, S.C., Christensen, O.B., Fernández, J., Fita, L., Frisius, T., Gašparac, G., Giorgi, F., Goergen, K., Haugen, J.E., Hodnebrog, Ø., Kartsios, S., Katragkou, E., Kendon, E.J., Keuler, K., Lavin-Gullon, A., Lenderink, G., Leutwyler, D., Lorenz, T., Maraun, D., Mercogliano, P., Milovac, J., Panitz, H.J., Raffa, M., Remedio, A.R., Schär, C., Soares, P.M.M., Srnec, L., Steensen, B.M., Stocchi, P., Tölle, M.H., Truhetz, H., Vergara-Temprado, J., de Vries, H., Warrach-Sagi, K., Wulfmeyer, V., Zander, M.J., 2021. The first multi-model ensemble of regional climate simulations at kilometer-scale resolution, part I: evaluation of precipitation. Clim. Dyn. https://doi.org/10.1007/s00382-021-05708-w

Ban, N., Schmidli, J., Schär, C., 2014. Evaluation of the convection-resolving regional climate modeling approach in decade-long simulations. J. Geophys. Res. 119, 7889–7907. https://doi.org/10.1002/2014JD021478

Barsugli, J.J., Guentchev, G., Horton, R.M., Wood, A., Mearns, L.O., Liang, X.Z., Winkler, J.A., Dixon, K., Hayhoe, K., Rood, R.B., Goddard, L., Ray, A., Buja, L., Ammann, C., 2013. The practitioner's dilemma: How to assess the credibility of downscaled climate projections. Eos (Washington. DC). https://doi.org/10.1002/2013EO460005

Chen, F., Kusaka, H., Bornstein, R., Ching, J., Grimmond, C.S.B., Grossman-Clarke, S., Loridan, T., Manning, K.W., Martilli, A., Miao, S., Sailor, D., Salamanca, F.P., Taha, H., Tewari, M., Wang, X., Wyszogrodzki, A.A., Zhang, C., 2011a. The integrated WRF/urban modelling system: development, evaluation, and applications to urban environmental problems. Int. J. Climatol. 31, 273–288. https://doi.org/10.1002/joc.2158

Chen, F., Kusaka, H., Bornstein, R., Ching, J., Grimmond, C.S.B., Grossman-Clarke, S., Loridan, T., Manning, K.W., Martilli, A., Miao, S., Sailor, D., Salamanca, F.P., Taha, H., Tewari, M., Wang, X., Wyszogrodzki, A.A., Zhang, C., 2011b. The integrated WRF/urban modelling system: Development, evaluation, and applications to urban environmental problems. Int. J. Climatol. https://doi.org/10.1002/joc.2158

Christensen, J.H., Carter, T.R., Rummukainen, M., Amanatidis, G., 2007. Evaluating the performance and utility of regional climate models: The PRUDENCE project. Clim. Change.

https://doi.org/10.1007/s10584-006-9211-6

Coccolo, S., Kämpf, J., Scartezzini, J.L., Pearlmutter, D., 2016. Outdoor human comfort and thermal stress: A comprehensive review on models and standards. Urban Clim. https://doi.org/10.1016/j.uclim.2016.08.004

Coppola, E., Sobolowski, S., Pichelli, E., Raffaele, F., Ahrens, B., Anders, I., Ban, N., Bastin, S., Belda, M., Belusic, D., Caldas-Alvarez, A., Cardoso, R.M., Davolio, S., Dobler, A., Fernandez, J., Fita, L., Fumiere, Q., Giorgi, F., Goergen, K., Güttler, I., Halenka, T., Heinzeller, D., Hodnebrog, Jacob, D., Kartsios, S., Katragkou, E., Kendon, E., Khodayar, S., Kunstmann, H., Knist, S., Lavín-Gullón, A., Lind, P., Lorenz, T., Maraun, D., Marelle, L., van Meijgaard, E., Milovac, J., Myhre, G., Panitz, H.J., Piazza, M., Raffa, M., Raub, T., Rockel, B., Schär, C., Sieck, K., Soares, P.M.M., Somot, S., Srnec, L., Stocchi, P., Tölle, M.H., Truhetz, H., Vautard, R., de Vries, H., Warrach-Sagi, K., 2020. A first-of-its-kind multi-model convection permitting ensemble for investigating convective phenomena over Europe and the Mediterranean, Climate Dynamics. https://doi.org/10.1007/s00382-018-4521-8

D'Amato, G., Cecchi, L., 2008. Effects of climate change on environmental factors in respiratory allergic diseases. Clin. Exp. Allergy. https://doi.org/10.1111/j.1365-2222.2008.03033.x

Daniel, M., Lemonsu, A., Déqué, M., Somot, S., Alias, A., Masson, V., 2019. Benefits of explicit urban parameterization in regional climate modeling to study climate and city interactions. Clim. Dyn. https://doi.org/10.1007/s00382-018-4289-x

Daniel, M., Lemonsu, A., Déqué, M., Somot, S., Alias, A., Masson, V., 2018. Benefits of explicit urban parameterization in regional climate modeling to study climate and city interactions. Clim. Dyn. 1–20. https://doi.org/10.1007/s00382-018-4289-x

Davis, R.E., McGregor, G.R., Enfield, K.B., 2016. Humidity: A review and primer on atmospheric moisture and human health. Environ. Res. 144, 106–116. https://doi.org/10.1016/j.envres.2015.10.014

De Ridder, K., Lauwaet, D., Maiheu, B., 2015. UrbClim - A fast urban boundary layer climate model. Urban Clim. https://doi.org/10.1016/j.uclim.2015.01.001

Deyle, E.R., Maher, M.C., Hernandez, R.D., Basu, S., Sugihara, G., 2016. Global environmental drivers of influenza. Proc. Natl. Acad. Sci. U. S. A. https://doi.org/10.1073/pnas.1607747113

Di Luca, A., de Elía, R., Laprise, R., 2015. Challenges in the Quest for Added Value of Regional Climate Dynamical Downscaling. Curr. Clim. Chang. Reports. https://doi.org/10.1007/s40641-015-0003-9

EEA, 2000. The revised and supplemented Corine land cover nomenclature. EEA Tech. Rep. No 40.

Fischer, E.M., Knutti, R., 2013. Robust projections of combined humidity and temperature extremes. Nat. Clim. Chang. 3, 126–130. https://doi.org/10.1038/nclimate1682

Fortuniak, K., Kłysik, K., Wibig, J., 2006. Urban - Rural contrasts of meteorological parameters in Łódź. Theor. Appl. Climatol. https://doi.org/10.1007/s00704-005-0147-y

Fränkischer Tag, 2021. Mehr Hitze in Städten befürchtet. 09.01.2021, tageszeitung Fränkischer Tag 22.

Giorgi, F., Gutowski, W.J., 2015. Regional Dynamical Downscaling and the CORDEX Initiative. Annu. Rev. Environ. Resour. https://doi.org/10.1146/annurev-environ-102014-021217

Goettel, H., 2009. Einfluss der nichthydrostatischen Modellierung und der Niederschlagsverdriftung auf die Ergebnisse regionaler Klimamodellierung. Reports Earth Syst. Sci. 125.

González, J.E., Ramamurthy, P., Bornstein, R.D., Chen, F., Bou-Zeid, E.R., Ghandehari, M., Luvall, J., Mitra, C., Niyogi, D., 2021. Urban climate and resiliency: A synthesis report of state of the art and future research directions. Urban Clim. 38. https://doi.org/10.1016/j.uclim.2021.100858

Grimmond, C.S.B., Roth, M., Oke, T.R., Au, Y.C., Best, M., Betts, R., Carmichael, G., Cleugh, H., Dabberdt, W., Emmanuel, R., Freitas, E., Fortuniak, K., Hanna, S., Klein, P., Kalkstein, L.S., Liu, C.H., Nickson, A., Pearlmutter, D., Sailor, D., Voogt, J., 2010. Climate and more sustainable cities: Climate information for improved planning and management of cities (Producers/Capabilities Perspective), in: Procedia Environmental Sciences. https://doi.org/10.1016/j.proenv.2010.09.016

Gutowski, J.W., Giorgi, F., Timbal, B., Frigon, A., Jacob, D., Kang, H.S., Raghavan, K., Lee, B., Lennard, C., Nikulin, G., O'Rourke, E., Rixen, M., Solman, S., Stephenson, T., Tangang, F., 2016. WCRP COordinated Regional Downscaling EXperiment (CORDEX): A diagnostic MIP for CMIP6. Geosci. Model Dev. https://doi.org/10.5194/gmd-9-4087-2016

Gutowski, W.J., Ullrich, P.A., Hall, A., Leung, L.R., O'Brien, T.A., Patricola, C.M., Arritt, R.W., Bukovsky, M.S., Calvin, K. V., Feng, Z., Jones, A.D., Kooperman, G.J., Monier, E., Pritchard, M.S., Pryor, S.C., Qian, Y., Rhoades, A.M., Roberts, A.F., Sakaguchi, K., Urban, N., Zarzycki, C., 2021. The ongoing need for high-resolution regional climate models: Process understanding and stakeholder information. Bull. Am. Meteorol. Soc. https://doi.org/10.1175/BAMS-D-19-0113.1

Hage, K.D., 1975. Urban-Rural Humidity Differences. J. Appl. Meteorol. https://doi.org/10.1175/1520-0450(1975)014<1277:urhd>2.0.co;2

Hamaoui-Laguel, L., Vautard, R., Liu, L., Solmon, F., Viovy, N., Khvorostyanov, D., Essl, F., Chuine, I., Colette, A., Semenov, M.A., Schaffhauser, A., Storkey, J., Thibaudon, M., Epstein, M.M., 2015. Effects of climate change and seed dispersal on airborne ragweed pollen loads in Europe. Nat. Clim. Chang. https://doi.org/10.1038/nclimate2652

Hamdi, R., Giot, O., De Troch, R., Deckmyn, A., Termonia, P., 2015. Future climate of Brussels and Paris for the 2050s under the A1B scenario. Urban Clim. https://doi.org/10.1016/j.uclim.2015.03.003

Hass, A.L., Ellis, K.N., Mason, L.R., Hathaway, J.M., Howe, D.A., 2016. Heat and humidity in the city: Neighborhood heat index variability in a mid-sized city in the Southeastern United States. Int. J. Environ. Res. Public Health. https://doi.org/10.3390/ijerph13010117

Hawkins, E., Frame, D., Harrington, L., Joshi, M., King, A., Rojas, M., Sutton, R., 2020. Observed Emergence of the Climate Change Signal: From the Familiar to the Unknown. Geophys. Res. Lett. https://doi.org/10.1029/2019GL086259

Hertwig, D., Ng, M., Grimmond, S., Vidale, P.L., McGuire, P.C., 2021. High-resolution global climate simulations: Representation of cities. Int. J. Climatol. https://doi.org/10.1002/joc.7018

Hirsch, A.L., Evans, J.P., Thomas, C., Conroy, B., Hart, M.A., Lipson, M., Ertler, W., 2021. Resolving the influence of local flows on urban heat amplification during heatwaves. Environ. Res. Lett. https://doi.org/10.1088/1748-9326/ac0377

Huszar, P., Halenka, T., Belda, M., Zak, M., Sindelarova, K., Miksovsky, J., 2014a. Regional climate model assessment of the urban land-surface forcing over central Europe. Atmos. Chem. Phys. https://doi.org/10.5194/acp-14-12393-2014

Huszar, P., Halenka, T., Belda, M., Zak, M., Sindelarova, K., Miksovsky, J., 2014b. Regional climate model assessment of the urban land-surface forcing over central Europe. Atmos. Chem. Phys. 14, 12393–12413. https://doi.org/10.5194/acp-14-12393-2014

IPCC, 2021. Climate Change 2021: The Physical Science Basis. Contribution of Working Group I to the Sixth Assessment Report of the Intergovernmental Panel on Climate Change [Masson-Delmotte, V., P. Zhai, A. Pirani, S. L. Connors, C. Péan, S. Berger, N. Caud, Y. Chen,.

IPCC, 2013. Intergovernmental Panel on Climate Change Working Group I. Climate Change 2013: The Physical Science Basis. Long-term Climate Change: Projections, Commitments and Irreversibility. Cambridge Univ. Press. New York.

Jack, C.D., Marsham, J., Rowell, D.P., Jones, R.G., 2021. Climate Information: Towards Transparent Distillation, in: Climate Risk in Africa. https://doi.org/10.1007/978-3-030-61160-6_2

Jacob, D., Elizalde, A., Haensler, A., Hagemann, S., Kumar, P., Podzun, R., Rechid, D., Remedio, A.R., Saeed, F., Sieck, K., Teichmann, C., Wilhelm, C., 2012a. Assessing the transferability of the regional climate model REMO to different coordinated regional climate downscaling experiment (CORDEX) regions. Atmosphere (Basel). 3, 181–199. https://doi.org/10.3390/atmos3010181

Jacob, D., Haensler, A., Saeed, F., Elizalde, A., Hagemann, S., Kumar, P., Podzun, R., Rechid, D., Remedio, A.R., Sieck, K., Teichmann, C., Wilhelm, C., 2012b. Assessing the transferability of the regional climate model REMO to different coordinated regional climate downscaling experiment (CORDEX) regions. Atmosphere (Basel). https://doi.org/10.3390/atmos3010181

Jacob, D., Petersen, J., Eggert, B., Alias, A., Christensen, O.B., Bouwer, L.M., Braun, A., Colette, A., Déqué, M., Georgievski, G., Georgopoulou, E., Gobiet, A., Menut, L., Nikulin, G., Haensler, A., Hempelmann, N., Jones, C., Keuler, K., Kovats, S., Kröner, N., Kotlarski, S., Kriegsmann, A., Martin, E., van Meijgaard, E., Moseley, C., Pfeifer, S., Preuschmann, S., Radermacher, C., Radtke, K., Rechid, D., Rounsevell, M., Samuelsson, P., Somot, S., Soussana, J.F., Teichmann, C., Valentini, R., Vautard, R., Weber, B., Yiou, P., 2014. EURO-CORDEX: New high-resolution climate change projections for European impact research. Reg. Environ. Chang. https://doi.org/10.1007/s10113-013-0499-2

Jacob, D., Podzun, R., 1997. Sensitivity studies with the regional climate model REMO. Meteorol. Atmos. Phys. https://doi.org/10.1007/BF01025368

Jacob, D., Teichmann, C., Sobolowski, S., Katragkou, E., Anders, I., Belda, M., Benestad, R., Boberg, F., Buonomo, E., Cardoso, R.M., Casanueva, A., Christensen, O.B., Christensen, J.H., Coppola, E., De Cruz, L., Davin, E.L., Dobler, A., Domínguez, M., Fealy, R., Fernandez, J., Gaertner, M.A., García-Díez, M., Giorgi, F., Gobiet, A., Goergen, K., Gómez-Navarro, J.J., Alemán, J.J.G., Gutiérrez, C., Gutiérrez, J.M., Güttler, I., Haensler, A., Halenka, T., Jerez, S., Jiménez-Guerrero, P., Jones, R.G., Keuler, K., Kjellström, E., Knist, S., Kotlarski, S., Maraun, D., van Meijgaard, E., Mercogliano, P., Montávez, J.P., Navarra, A., Nikulin, G., de Noblet-Ducoudré, N., Panitz, H.J., Pfeifer, S., Piazza, M., Pichelli, E., Pietikäinen, J.P., Prein, A.F., Preuschmann, S., Rechid, D., Rockel, B., Romera, R., Sánchez, E., Sieck, K., Soares, P.M.M., Somot, S., Srnec, L., Sørland, S.L., Termonia, P., Truhetz, H., Vautard, R., Warrach-Sagi, K., Wulfmeyer, V., 2020. Regional climate downscaling over Europe: perspectives from the EURO-CORDEX community. Reg. Environ. Chang. 20. https://doi.org/10.1007/s10113-020-01606-9

Jåuregui, E., Tejeda, A., 1997a. Urban-rural humidity contrasts in Mexico city. Int. J. Climatol. https://doi.org/10.1002/(SICI)1097-0088(199702)17:2<187::AID-JOC114>3.0.CO;2-P

Jåuregui, E., Tejeda, A., 1997b. Urban-rural humidity contrasts in Mexico city. Int. J. Climatol. 17, 187–196. https://doi.org/10.1002/(SICI)1097-0088(199702)17:2<187::AID-JOC114>3.0.CO;2-P

Kendon, E.J., Prein, A.F., Senior, C.A., Stirling, A., 2021. Challenges and outlook for convection-permitting climate modelling. Philos. Trans. R. Soc. A Math. Phys. Eng. Sci. https://doi.org/10.1098/rsta.2019.0547

Kuttler, W., Weber, S., Schonnefeld, J., Hesselschwerdt, A., 2007a. Urban/rural atmospheric water vapour pressure differences and urban moisture excess in Krefeld, Germany, in: International Journal of Climatology. https://doi.org/10.1002/joc.1558

Kuttler, W., Weber, S., Schonnefeld, J., Hesselschwerdt, A., 2007b. Urban/rural atmospheric water vapour pressure differences and urban moisture excess in Krefeld, Germany, in: International Journal of Climatology. pp. 2005–2015. https://doi.org/10.1002/joc.1558

Langendijk, G.S., Aubry-Wake, C., Osman, M., Gulizia, C., Attig-Bahar, F., Behrens, E., Bertoncini, A., Hart, N., Indasi, V.S., Innocenti, S., van der Linden, E.C., Mamnun, N., Rasouli, K., Reed, K.A., Ridder, N., Rivera, J., Ruscica, R., Ukazu, B.U., Walawender, J.P., Walker, D.P., Woodhams, B.J., Yilmaz, Y.A., 2019a. Three ways forward to improve regional information for extreme events: An early career perspective. Front. Environ. Sci. 7. https://doi.org/10.3389/fenvs.2019.00006

Langendijk, G.S., Rechid, D., Jacob, D., 2019b. Urban areas and urban-rural contrasts under climate change: What does the EURO-CORDEX ensemble tell us?-Investigating near surface humidity in berlin and its surroundings. Atmosphere (Basel). 10. https://doi.org/10.3390/ATMOS10120730

Langendijk, G.S., Rechid, D., Sieck, K., Jacob, D., 2021. Added value of convection-permitting simulations for understanding future urban humidity extremes: case studies for Berlin and its surroundings. Weather Clim. Extrem. 33. https://doi.org/https://doi.org/10.1016/j.wace.2021.100367

Langendijk, G. S., Rechid, D., Jacob, D., 2022. Improved models, improved information? Exploring how climate change impacts pollen, influenza, and mold in Berlin and its surroundings. Urban Climate, 43, 101159. https://doi.org/10.1016/j.uclim.2022.101159

Lauwaet, D., Hooyberghs, H., Lefebre, F., De Ridder, K., Willems, P., 2017. Climate-fit-City_D5.1: Urban Primary Data Need Analysis.

Lauwaet, D., Hooyberghs, H., Maiheu, B., Lefebvre, W., Driesen, G., Van Looy, S., De Ridder, K., 2015. Detailed Urban Heat Island Projections for Cities Worldwide: Dynamical Downscaling CMIP5 Global Climate Models. Climate 3, 391–415. https://doi.org/10.3390/cli3020391

Lee, D.O., 1991. Urban—rural humidity differences in London. Int. J. Climatol. 11, 577–582. https://doi.org/10.1002/joc.3370110509

Lemos, M.C., Kirchhoff, C.J., Ramprasad, V., 2012. Narrowing the climate information usability gap. Nat. Clim. Chang. https://doi.org/10.1038/nclimate1614

Li, D., Yuan, J., Kopp, R.E., 2020. Escalating global exposure to compound heat-humidity extremes with warming. Environ. Res. Lett. https://doi.org/10.1088/1748-9326/ab7d04

Lokoshchenko, M.A., 2017. Urban heat island and urban dry island in Moscow and their centennial changes. J. Appl. Meteorol. Climatol. https://doi.org/10.1175/JAMC-D-16-0383.1

Lowe, J.A., McSweeney, C., Hewitt, C., 2020. An overview of the EUCP project-towards improved European Climate Predictions and Projections. EGU Gen. Assem. Conf. Abstr. 19475.

Lowen, A.C., Mubareka, S., Steel, J., Palese, P., 2007. Influenza virus transmission is dependent on relative humidity and temperature. PLoS Pathog. 3, 1470–1476. https://doi.org/10.1371/journal.ppat.0030151

Majewski, D., 1991. The Europa-Modell of the Deutscher Wetterdienst. ECMWF Semin. Numer. methods Atmos. Model.

Masson, V., 2006. Urban surface modeling and the meso-scale impact of cities. Theor. Appl. Climatol. https://doi.org/10.1007/s00704-005-0142-3

Masson, V., Lemonsu, A., Hidalgo, J., Voogt, J., 2020. Urban climates and climate change. Annu. Rev. Environ. Resour. 45, 411–444. https://doi.org/10.1146/annurev-environ-012320-083623

Mitchell, D., AchutaRao, K., Allen, M., Bethke, I., Beyerle, U., Ciavarella, A., Forster, P.M., Fuglestvedt, J., Gillett, N., Haustein, K., Ingram, W., Iversen, T., Kharin, V., Klingaman, N., Massey, N., Fischer, E., Schleussner, C.-F., Scinocca, J., Seland, Ø., Shiogama, H., Shuckburgh, E., Sparrow, S., Stone, D., Uhe, P., Wallom, D., Wehner, M., Zaaboul, R., 2017. Half a degree additional warming, prognosis and projected impacts (HAPPI): background and experimental design. Geosci. Model Dev. 10, 571–583. https://doi.org/10.5194/gmd-10-571-2017

Moriwaki, R., Watanabe, K., Morimoto, K., 2013. Urban dry island phenomenon and its impact on cloud base level. J. JSCE. https://doi.org/10.2208/journalofjsce.1.1_521

Moss, R.H., Edmonds, J.A., Hibbard, K.A., Manning, M.R., Rose, S.K., Van Vuuren, D.P., Carter, T.R., Emori, S., Kainuma, M., Kram, T., Meehl, G.A., Mitchell, J.F.B., Nakicenovic, N., Riahi, K., Smith, S.J., Stouffer, R.J., Thomson, A.M., Weyant, J.P., Wilbanks, T.J., 2010. The next generation of scenarios for climate change research and assessment. Nature. https://doi.org/10.1038/nature08823

Ojanen, T., Hannu Viitanen, Lähdesmäki, K., Vinha, J., Peuhkuri, R., Salminen, K., 2010. Mold Growth Modeling of Building Structures Using Sensitivity Classes of Materials Tuomo. Acta Acust. united with Acust.

Pfeifer, S., Bülow, K., Gobiet, A., Hänsler, A., Mudelsee, M., Otto, J., Rechid, D., Teichmann, C., Jacob, D., 2015. Robustness of ensemble climate projections analyzed with climate signal maps: Seasonal and extreme precipitation for Germany. Atmosphere (Basel). 6, 677–698. https://doi.org/10.22444/IBVS.6227_old

Prein, A.F., Gobiet, A., Suklitsch, M., Truhetz, H., Awan, N.K., Keuler, K., Georgievski, G., 2013. Added value of convection permitting seasonal simulations. Clim. Dyn. https://doi.org/10.1007/s00382-013-1744-6

Prein, A.F., Langhans, W., Fosser, G., Ferrone, A., Ban, N., Goergen, K., Keller, M., Tölle, M., Gutjahr, O., Feser, F., Brisson, E., Kollet, S., Schmidli, J., Van Lipzig, N.P.M., Leung, R., 2015. A review on regional convection-permitting climate modeling: Demonstrations, prospects, and challenges. Rev. Geophys. 53, 323–361. https://doi.org/10.1002/2014RG000475

Rechid, D., Jacob, D., 2006. Influence of monthly varying vegetation on the simulated climate in Europe. Meteorol. Zeitschrift 15, 99–116. https://doi.org/10.1127/0941-2948/2006/0091

Ritschkoff, A.-C., Viitanen, H., Koskela, K., 2000. The response of building materials to the mould exposure at different humidity and temperature conditions. Heal. Build. 2000 Proc. Vol. 1, Expo. Hum. responses Build. Investig. 317–322.

RND, 2021. Studie: Klimawandel macht Städte heißer und trockener. 06.01.2021, by Redaktionsnetzw. Deutschl. - Online https//www.rnd.de/wissen/studie-klimawandel-macht-stadte-heisser-und-trockener-CKLNCL4IVJCBXEWZ4JJ5LA2FXI.html.

Robaa, S.M., 2003. Urban-suburban/rural differences over Greater Cairo, Egypt. Atmosfera.

Roeckner, E., Arpe, K., Bengtsson, L., Christoph, M., Claussen, M., Dümenil, L., Esch, M., Giorgetta, M., Schlese, U., Schulzweida, U., 1996. The atmospheric general circulation model ECHAM-4: Model description and simulation of present-day climate. MPI Rep. 218, 171.

Rosenzweig, C., Solecki, W., Romero-Lankao, P., Mehrotra, S., Dhakal, S., Bowman, T., Ibrahim, S.A., 2018. Climate Change and Cities: Second Assessment Report of the Urban Climate Change Research Network, in: Climate Change and Cities. https://doi.org/10.1017/9781316563878.007

Semmler, T., 2002. Der Wasser- und Energiehaushalt der arktischen Atmosphäre. Examensarbeit - Max-Planck-Institut fur Meteorol. 101–106.

Shaman, J., Kohn, M., 2009. Absolute humidity modulates influenza survival, transmission, and seasonality. Proc. Natl. Acad. Sci. 106, 3243–3248. https://doi.org/10.1073/PNAS.0806852106

Sieck, K., Nam, C., Bouwer, L.M., Rechid, D., Jacob, D., 2021. Weather extremes over Europe under regional climate ensemble simulations 457–468.

Soares, M.B., Alexander, M., Dessai, S., 2018. Sectoral use of climate information in Europe: A synoptic overview. Clim. Serv. https://doi.org/10.1016/j.cliser.2017.06.001

Tapper, N.J., 1990. Urban influences on boundary layer temperature and humidity: Results from Christchurch, New Zealand. Atmos. Environ. Part B, Urban Atmos. 24, 19–27. https://doi.org/10.1016/0957-1272(90)90005-F

Teichmann, C., Eggert, B., Elizalde, A., Haensler, A., Jacob, D., Kumar, P., Moseley, C., Pfeifer, S., Rechid, D., Remedio, A.R., Ries, H., Petersen, J., Preuschmann, S., Raub, T., Saeed, F., Sieck, K., Weber, T., 2013. How does a regional climate model modify the projected climate change signal of the driving GCM: A study over different CORDEX regions using REMO. Atmosphere (Basel). 4, 214–236. https://doi.org/10.3390/atmos4020214

Trusilova, K., Früh, B., Brienen, S., Walter, A., Masson, V., Pigeon, G., Becker, P., 2013. Implementation of an urban parameterization scheme into the regional climate model COSMO-CLM. J. Appl. Meteorol. Climatol. 52, 2296–2311. https://doi.org/10.1175/JAMC-D-12-0209.1

Trusilova, K., Schubert, S., Wouters, H., Früh, B., Grossman-Clarke, S., Demuzere, M., Becker, P., 2016. The urban land use in the COSMO-CLM model: a comparison of three parameterizations for Berlin. Meteorol. Zeitschrift 25, 231–244. https://doi.org/10.1127/metz/2015/0587

UN-HABITAT, 2016. Urbanization and Development: Emerging Futures World Cities Report 2016, International Journal. https://doi.org/10.1016/S0264-2751(03)00010-6

Unger, J., 1999a. Urban-rural air humidity differences in Szeged, Hungary. Int. J. Climatol. https://doi.org/10.1002/(SICI)1097-0088(19991115)19:13<1509::AID-JOC453>3.0.CO;2-P

Unger, J., 1999b. Urban-rural air humidity differences in Szeged, Hungary. Int. J. Climatol. 19, 1509–1515. https://doi.org/10.1002/(SICI)1097-0088(19991115)19:13<1509::AID-JOC453>3.0.CO;2-P

Union, E., 2015. A European Research and Innovation Roadmap for Climate Services.

Unkašević, M., Jovanović, O., Popović, T., 2001. Urban-suburban/rural vapour pressure and relative humidity differences at fixed hours over the area of Belgrade city. Theor. Appl. Climatol. 68, 67–73. https://doi.org/10.1007/s007040170054

Vanden Broucke, S., Wouters, H., Demuzere, M., van Lipzig, N.P.M., 2019. The influence of convection-permitting regional climate modeling on future projections of extreme precipitation: dependency on topography and timescale. Clim. Dyn. https://doi.org/10.1007/s00382-018-4454-2

Viitanen, H., 2007. Improved Model to Predict Mold Growth in. VTT Tech. Res.

Vincent, K., Daly, M., Scannell, C., Leathes, B., 2018. What can climate services learn from theory and practice of co-production? Clim. Serv. https://doi.org/10.1016/j.cliser.2018.11.001

Welt, 2021. Besonders in den Städten wird es immer heißer. 06.01.2021, by Welt-Wissen, Alice Lanzke, Online https//www.welt.de/wissenschaft/article223847812/Klimawandel-Besonders-in-den-Staedten-wird-es-immer-heisser.html.

Wiesner, S., Bechtel, B., Fischereit, J., Gruetzun, V., Hoffmann, P., Leitl, B., Rechid, D., Schlünzen, K., Thomsen, S., 2018. Is It Possible to Distinguish Global and Regional Climate Change from Urban Land Cover Induced Signals? A Mid-Latitude City Example. Urban Sci. https://doi.org/10.3390/urbansci2010012

Willett, K.M., Gillett, N.P., Jones, P.D., Thorne, P.W., 2007. Attribution of observed surface humidity changes to human influence. Nature 449, 710–712. https://doi.org/10.1038/nature06207

WMO, 2019. Guidance on Integrated Urban Hydro-meteorological, Climate and Environmental Services: Challenges and The Way Forward, Urban Climate Science for Planning Healthy Cities.

Wouters, H., De Ridder, K., Poelmans, L., Willems, P., Brouwers, J., Hosseinzadehtalaei, P., Tabari, H., Vanden Broucke, S., van Lipzig, N.P.M., Demuzere, M., 2017. Heat stress increase under climate change twice as large in cities as in rural areas: A study for a densely populated midlatitude maritime region. Geophys. Res. Lett. https://doi.org/10.1002/2017GL074889

Zhao, L., Oleson, K., Bou-Zeid, E., Krayenhoff, E.S., Bray, A., Zhu, Q., Zheng, Z., Chen, C., Oppenheimer, M., 2021. Global multi-model projections of local urban climates. Nat. Clim. Chang. https://doi.org/10.1038/s41558-020-00958-8

Appendix

A.1. Author contribution statements

The contribution of Gaby S. Langendijk is greater than the individual share of all other co-authors, and is larger than 35% for all three papers presented in this thesis. Therefore, G.S. Langendijk has completed a "predominant contribution", according to the classification of the Leuphana University for a cumulative thesis. G.S. Langendijk's contribution is 100% for the framework paper, therefore, falling within the category "single authorship". Please see the author contributions for each paper detailed below.

Paper 1 // author contributions
Conceptualization, G.S.L., D.R., and D.J.; data curation, G.S.L.; formal analysis, G.S.L.; investigation, G.S.L.; methodology, G.S.L.; project administration, G.S.L.; resources, G.S.L.; software, G.S.L.; supervision, D.R. and D.J.; validation, G.S.L.; visualization, G.S.L.; writing—original draft, G.S.L.; writing—review and editing, G.S.L., D.R., and D.J.

Paper 2 // author contributions
Conceptualization; G.S.L., D.R., K.S., D.J. Data curation; G.S.L. Formal analysis; G.S.L. Investigation; G.S.L. Methodology; G.S.L. Supervision; D.R., K.S., D.J. Validation; G.S.L. Visualization; G.S.L. Writing – original draft; G.S.L. Writing - review & editing; G.S.L., D.R., K.S., D.J..

Paper 3 // author contributions
Conceptualization; G.S.L., D.R., D.J. Data curation; G.S.L. Formal analysis; G.S.L. Investigation; G.S.L. Methodology; G.S.L. Supervision; D.R., D.J. Validation; G.S.L. Visualization; G.S.L. Writing – original draft; G.S.L. Writing - review & editing; G.S.L., D.R., D.J..

A.2. Conferences PhD was presented

Paper 1

8th GEWEX Open Science Conference: extremes and water on the edge
6-11 May 2018 // Canmore, Canada
Conference website: https://www.gewexevents.org/events/2018conference/

CORDEX International Conference on Regional Climate 2019 (CORDEX-ICRC)
14-18 October 2019 // Beijing, China
Conference website: https://icrc-cordex2019.cordex.org/

AGU Fall meeting 2019
9-13 December 2019 // San Francisco, USA
Conference website: https://www.agu.org/fall-meeting-2019

22nd EGU General Assembly 2020
4-8 May 2020 // virtual
Conference website: www.egu2020.eu
Link to abstract: https://ui.adsabs.harvard.edu/abs/2020EGUGA..2220466L/abstract

Paper 2

23rd EGU General Assembly 2021
19-30 April 2021 // virtual
Conference website: www.egu2021.eu
Link to abstract: https://doi.org/10.5194/egusphere-egu21-12054

DKT-12 Germany (Deutsche Klimatagung)
15-18 March 2021 // virtual
Conference website: https://www.dkt-12.de/

Paper 3

AGU Fall meeting 2021
13-17 December 2021 // New Orleans, USA & virtual
Conference website: https://www.agu.org/Fall-Meeting

24rd EGU General Assembly 2022
23-27 May 2022 // Vienna, Austria, & virtual
Conference website: www.egu2022.eu
Link to abstract: https://doi.org/10.5194/egusphere-egu22-1517

A.3. Additional publications

Published within the timeframe of the PhD

Assessing mean climate change signals in the global CORDEX-CORE ensemble
Teichmann, C., Jacob, D., Remedio, A. R., Remke, T., Buntemeyer, L., Hoffmann, P., Kriegsmann, A. Lierhammer, L., Bülow, K., Weber, T., Sieck, K., Rechid, D., **Langendijk, G. S**., Coppola, E., Giorgi, F., Ciarlo, J. M., Raffaele, F., Giuliani, G., Xuejie, G., Sines, T. R., Torres-Alavez, J. A., Das, S., Di Sante, F., Pichelli, E., Glazer, R., Ashfaq, M., Bukovsky, M., Im, E.S. (2020). Climate Dynamics, 1-24.

Three Ways Forward to Improve Regional Information for Extreme Events: An Early Career Perspective
Langendijk, G.S., Aubry-Wake, C., Osman, M., Gulizia, C., Attig-Bahar, F., Behrens, E., Bertoncini, A., Hart, N., Indasi, V.S., Innocenti, S., van der Linden, E.C., Mamnun, N., Rasouli, K., Reed, K.A., Ridder, N., Rivera, J., Ruscica, R., Ukazu, B.U., Walawender, J.P., Walker, D.P., Woodhams, B.J. and Yılmaz, Y.A., 2019. (2019) Frontiers in Environmental Science. 7:6.

Towards a more integrated role for early career researchers in the IPCC process
Gulizia, C., **Langendijk, G. S.,** Huang-Lachmann, JT. de Amorim Borges, P., Flach, R., Githaiga, C., Rahimi, M. (2019) Climatic Change.

Building urgent intergenerational bridges: assessing early career researcher integration in global sustainability initiatives
Jørgensen, P. S., Evoh, C. J., Gerhardinger, L. C., Hughes, A. C., **Langendijk, G. S.**, Moersberger, H., Pocklington, J., Mukherjee, N. (2019) Current Opinion in Environmental Sustainability, 39, 153-159.